TRPM7, Calcium and the cytoskeleton
Langeslag, Michiel

TRPM7, Calcium and the Cytoskeleton

Michiel Langeslag

TRPM7, Calcium and the Cytoskeleton

PROEFSCHRIFT

ter verkrijging van
de graad van Doctor aan de Universiteit Leiden,
op gezag van de Rector Magnificus Dr. D. D. Breimer,
hoogleraar in de faculteit der Wiskunde en
Natuurwetenschappen en die der Geneeskunde,
volgens besluit van het College voor Promoties
te verdedigen op 11 oktober 2006
klokke 13.45 uur

door

Michiel Langeslag

geboren te Vlissingen
in 1976

Promotiecommissie

Promotor   Prof. Dr. W.H. Moolenaar

Co-promotor   Dr. K. Jalink (Nederlands Kanker Instituut, Amsterdam)

Referent   Dr. E.H. Danen

Overige leden   Prof. Dr. J.J. Neefjes
Prof. Dr. T. Schmidt
Dr. F.N. van Leeuwen (NCMLS, Radboud Universiteit, Nijmegen)

Table of Contents

Introduction

Introduction

Every cell responds to external stimuli. Many of these stimuli act through receptors situated at the plasma-membrane that transduce the signal in the cytosol. After receptor activation, the signal propagates via so-called second messengers to cellular responses varying from regulation of gene expression to actomyosin contraction. These second messengers may be proteins, small molecules or ions. An example of the latter is calcium (Ca^{2+}), a universal second messenger in all cells. Other ionic species, e.g. Magnesium (Mg^{2+}) are also important because they regulate the activity of enzymes.

Because various cellular processes depend on the abundance of ions (be it as second messengers or as regulators of enzymes) the cell maintains gradients of ions over the plasma-membrane that are tightly regulated. Potassium (K^+) and Sodium (Na^+) are the main ions controlling the membrane potential of cells: the cell interior is usually negatively charged with regard to the extracellular side. Calcium (Ca^{2+}) and Magnesium (Mg^{2+}) play pivotal roles in the regulation of many cellular reactions and enzymatic activities. The lipid bilayer of the plasma-membrane itself cannot let ions pass through due to its lipophylic nature. Therefore, cells have adapted various mechanisms to control the distribution of ions over the plasma-membrane such as ionic channels and ion exchangers.

Ca^{2+} Homeostasis

The concentration of free cytosolic Ca^{2+} is maintained at extremely low concentrations of 60-100 nM, whereas the concentrations extracellularly and in the endoplasmatic reticulum are higher (~1 and ~3 mM, respectively). Combined with the electrical gradient, there is thus a steep gradient that tends to drive extracellular Ca^{2+} into the cells. Under these conditions, any increase in Ca^{2+} permeability of the membranes (either through release from the ER or through influx via ion channels at the plasma-membrane) causes a sharp rise in intracellular Ca^{2+} (Berridge et al., 2000) Thus, Ca^{2+} is ideally suited to act as a second messenger and many proteins and processes are triggered by local increases in Ca^{2+} concentrations. For these reasons, a strict regulation of intracellular Ca^{2+} is necessary. Cellular Ca^{2+} regulation or Ca^{2+} homeostasis is achieved by

various mechanisms that act at the level of the plasma-membrane as well as at cellular organelles such as the endoplasmatic reticulum (ER) and mitochondria (See Figure 1).

Raising Cytosolic Ca^{2+} Levels

Since the lipid bilayer itself functions as a barrier for ions, passive transmembrane transport is handled by various ion channels with widely different properties. Based on the mode of activation, Ca^{2+} entry through channels can be divided into 4 major classes: receptor-operated (ionotropic) (Shuttleworth, 2004), second-messenger-operated (metabotropic) (Kaupp and Seifert, 2002), voltage-operated (Felix, 2005) and store-operated Ca^{2+} channels (Bolotina, 2004) (Figure 1). Voltage-operated Ca^{2+} channels in excitable cells are best characterized. These channels are capable of generating very fast Ca^{2+} elevations upon membrane depolarization and control fast cellular responses such as exocytosis and muscle contraction. Ionotropic channels are also fast because they are directly controlled through binding of extracellular ligands that open the channels, while gating of metabotropic channels is constrained by cytosolic second-messengers generated upon receptor activation. Yet other Ca^{2+} channels respond to a diverse array of stimuli including emptying of Ca^{2+} stores, temperature and mechanical stress (Voets et al., 2005; Pedersen et al., 2005). Most of these channels belong to the large family of transient receptor potential (TRP) ion channels that will be described in more detail in the sections on TRP ion channels and mammalian TRP channels.

Next to Ca^{2+} entry from the extracellular medium (influx), Ca^{2+} can also be raised by release from intracellular stores (Figure 1), which are primarily located at the ER or in muscle cells at the sarcoplasmic reticulum (SR). Both the ER and SR posses second messenger activated Ca^{2+} channels, the inostol-1,4,5-triphosphate receptors (IP$_3$-R) and ryanodine receptors (RYR) respectively. These channels are activated by IP$_3$ and cADPribose/ NAADP respectively and are controlled by intracellular Ca^{2+} ($[Ca^{2+}]_i$) (Yoshida and Imai, 1997; Guerrero-Hernandez et al., 2002).

Whenever IP$_3$ binds to the IP$_3$-R, it increases the sensitivity of the receptor for Ca^{2+}, which has a biphasic characteristic. At slightly elevated levels, Ca^{2+} acts synergistically with IP$_3$ to open the IP$_3$-R channel, whereas at high concentrations, for example after full Ca^{2+} release, it inhibits the IP$_3$-

R, either directly or indirectly via calmodulin (CaM) (Taylor, 2002).

Cytosolic Ca²⁺ Removal Mechanisms

Cells prevent Ca^{2+} overload and terminate cytosolic Ca^{2+} signals in several ways. First of all, free Ca^{2+} is effectively buffered by different Ca^{2+} binding proteins like parvalbumin, calbindin D-28, calretinin and, to a lesser extent, by Ca^{2+}-effector proteins such as CaM, protein kinase C etc. During Ca^{2+} elevations, these proteins will buffer Ca^{2+}, and subsequently, after termination of the Ca^{2+} signals, the buffers will be regenerated. In this way, the binding kinetics of these buffering proteins helps shaping Ca^{2+} transients in their amplitude and recovery time (John et al., 2001). Secondly, activated Ca^{2+} channels, at the plasma-membrane or internal stores, are closed by various regulatory mechanisms, such as phosphorylation, ionic inhibition, (de-)polarization of the plasma-membrane, or via inhibitory regulators of these channels (Hering et al., 2000). Alternatively, Ca^{2+}-pumps and exchangers located at the plasma-membrane and internal organelles lower elevated cytosolic Ca^{2+} levels to resting levels and ensure that internal stores are refilled with Ca^{2+} (Belkacemi et al., 2005).

Ca^{2+}-pumps and exchangers can be categorized into 4 classes: plasma-membrane Ca^{2+}-ATPases (PMCA), Na^+/Ca^{2+} exchangers (NCX), endo(sarco)plasmatic Ca^{2+} ATPases (SERCA) and the mitochondrial uniporter. Since PMCAs and SERCAs have a high affinity for Ca^{2+}, they detect and respond to even modest changes in cytosolic Ca^{2+}. These proteins have rather low transport rates but are most important to set basal Ca^{2+} levels. In contrast, NCX and the mitochondrial uniporter have a higher transport rate and a wider dynamic range, but they only act optimally at μM Ca^{2+} concentrations ("high capacity, low affinity" pumps).

Kinetics and Spatial Distribution of Ca²⁺ Signals

Ca^{2+} is a very versatile second messenger. The shape and duration of the Ca^{2+} elevation is tailor-suited to fit the spatial and temporal requirements of specific downstream Ca^{2+}-dependent signaling complexes. For example, proteins involved in rapid responses, such as exocytosis, are highly organized and all the downstream effectors are closely associated into a signal complex. These
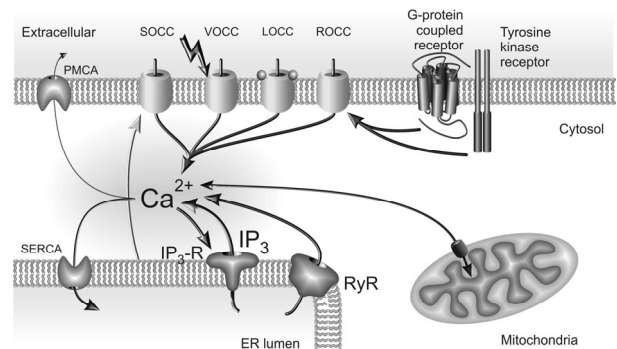

Figure 1: Schematic representation of cellular Ca²⁺ homeostasis.

After receptor activation intracellular Ca^{2+} can be raised from IP_3-sensitive and/or Ryanodine-sensitive stores. Also mitochondria may release Ca^{2+} into the cytosol via the uniporter. At the plasma-membrane various ion channels, non-selective cation or Ca^{2+}-specific, can elevate cellular Ca^{2+} levels after activation by receptors (ROCC), ligand binding (LOCC) or by membrane depolarization (VOCC). Elevated cytosolic Ca^{2+} levels are lowered to resting conditions by Ca^{2+} ATPases located at the plasma-membrane (PMCA) and the endoplasmic reticulum (SERCA). Furthermore, at very high Ca^{2+}_i elevations mitochondria will accumulate cytosolic Ca^{2+} and Na^+/Ca^{2+} exchangers at the plasma-membrane are activated (not shown).

fast responses rely on rapid voltage operated Ca^{2+} channel gating and are spatially restricted to tens of nanometers (Sorensen, 2004). In contrast, muscular actomyosin contractions, as well as other processes, require Ca^{2+} elevations that last from seconds to many minutes (Ebashi and Ogawa, 1988; Fields et al., 2005). Ca^{2+} signals often propagate as waves or oscillations throughout the cell. During prolonged stimulation, the Ca^{2+} concentration may also show repeated oscillations and this phenomenon has been implicated in physiological processes such as growth cone migration and turning, axonal outgrowth and oocyte activation (Berridge et al., 2000). These Ca^{2+}-regulated processes do not require the highly organized, preexisting signaling complex that controls e.g. exocytosis. Cells can interpret Ca^{2+} oscillations using highly sophisticated mechanisms. To date, a number of Ca^{2+} effectors that can decode Ca^{2+} oscillations have been identified, such as Nuclear Factor of Activated T cells (NFAT) (Tomida et al., 2003), Protein Kinase C (PKC) (Oancea and Meyer, 1998) and Calmodulin Kinase II (De Koninck and Schulman, 1998). These decoder proteins use frequency-encoded Ca^{2+} signals to regulate gene transcription, exocytosis and the redox state of mitochondria (Dolmetsch et al., 1997; Li et al., 1998; Dolmetsch et al., 1998).

Replenishment of Intracellular Stores through Store-Operated Calcium Entry

Responses to stimulation of GPCR or tyrosine receptors often are characterized by an initial, rapid Ca^{2+} release from IP_3- or ryanodine-sensitive intracellular stores that is not dependent on the presence of extracellular Ca^{2+}, followed by a second, smaller and more sustained phase that does rely on extracellular Ca^{2+}. Emptying of the intracellular stores is the trigger for this Ca^{2+} influx that is known as Store-Operated Calcium Entry (SOCE). The SOCE conductance is not purely selective for Ca^{2+}, for example Mn^{2+} can also enter the cytosol, as is evident from Fura-2 quenching essays (Jacob, 1990). Thus, depletion of intracellular stores somehow causes opening of a Ca^{2+} entry pathway in the plasma-membrane that is thought to be important for replenishment of intracellular stores. SOCE is proposed to continue as long as the IP_3-sensitive stores are not adequately refilled (Putney, Jr., 1986; Clapham, 1995). This event is observed in many different cell-types but the underlying molecular mechanism is still not understood and under scientific debate.

A major tool to investigate regulation of SOCE is thapsigargin, a naturally occurring sesquiterpene lactone isolated from the umbelliferous plant *Thapsia garganica* (Rasmussen et al., 1978). Thapsigargin specifically binds to and inhibits Ca^{2+} pumps (SERCA) located at the membranes of intracellular stores and thereby prevents Ca^{2+} to be pumped back into the lumen of the store (Thastrup et al., 1990). Under these conditions, basic leakage of Ca^{2+} through the intrinsic IP_3 receptor channels causes depletion of the stores. The rate of store depletion and consequently Ca^{2+} influx via SOCE is highly variable between cell-types, but it may be quite rapid (within 5 s for rat mast cells (Hoth and Penner, 1993)). This indicates that there is high basal Ca^{2+} turnover across the membranes of the Ca^{2+} stores.

The first indications for SOCE were obtained by Fura-2 measurements (Jacob, 1990). Hoth and Penner used electrophysiological recordings to identify ionic currents responsible for SOCE. Using mast cells in whole-cell recordings, they observed ionic currents induced by depletion of intracellular stores as a result of inclusion of IP_3 in the pipette solution (Hoth and Penner, 1992). These store-depletion-mediated currents were described as Calcium Release Activated Current

(I_{CRAC}). In most cells, the current amplitude of I_{CRAC} is much smaller than background currents during patch-clamp, but it can be revealed by increasing extracellular Ca^{2+} to 10mM while intracellular Ca^{2+} is strongly buffered with EGTA or BAPTA. I_{CRAC} selectively permeates Ca^{2+} over monovalent ions, but surprisingly almost no Mn^{2+} entry through CRAC channels was observed (Hoth and Penner, 1992), notwithstanding the fact that Mn^{2+} can efficiently replace Ca^{2+} in SOCE assays with Fura-2 (Jacob, 1990). The amplitude of I_{CRAC} flowing through one channel is very low, a single channel conductance of only ~ 24 fS, which is far below the conductance of any ion channel identified to date (Zweifach and Lewis, 1993). I_{CRAC} can only be measured in a limited number of cells, due to the low current amplitude and the incapability of discriminating between background currents for technical reasons (Zitt et al., 2002). It has not been convincingly demonstrated that SOCE and I_{CRAC} reflect the same process. Until now, the ion channel(s) responsible for conducting I_{CRAC} has remained illusive and scientists all over the world are eager to identify the channel.

Mg^{2+} Homeostasis

Magnesium ions have an undisputable role in regulation of tissue and cell functions. Mg^{2+} is indispensable for the activity of numerous enzymes, e.g. kinases, DNA/RNA polymerases, various ATPases, small and heteromeric G-proteins. In addition, Mg^{2+} might alter transcription by binding to the transcription factor DREAM. Furthermore, regulation of several ion channels, like the IP_3 receptor, TRPM6 and TRPM7, L-type Ca^{2+} channels and ATP-sensitive K^+ channels is mediated by Mg^{2+}.

Given all of these functions, it is not surprising that Mg^{2+} is found in abundance intracellularly. The Mg^{2+} content in cells varies from 17-20 mM (Romani et al., 1995) and it is more or less homogenously distributed over the nucleus, mitochondria, endo(sarco)plasmatic reticulum and cytosol (Griswold and Pace, 1956; Gunther, 1986). Approximately 95% of the cellular Mg^{2+} ions is bound or sequestered. A considerable amount of Mg^{2+} (4-5 mM) found in the cytosol is bound to ATP or other phosphometabolites (Garfinkel et al., 1986) and as a result, in the cytosol only 0.5-1.0 mM ionized Mg^{2+} is free (see table I in Romani and Scarpa, 1992). In mitochondria the free Mg^{2+} levels are estimated to be between 0.5-1.0 mM (Jung et al., 1997) and in

the endo(sarco)plasmatic reticulum ~1mM (Sugiyama and Goldman, 1995).

Because both in the cytosol and the extracellular fluid Mg^{2+} is kept at (sub)millimolar concentrations, the transmembrane Mg^{2+} gradient is small, usually a factor of 2 or less. Therefore, influx or efflux of Mg^{2+} usually results in only small changes in free $[Mg^{2+}]_i$. Despite this small gradient, Mg^{2+} levels in the cells are under control of hormonal signaling: Mg^{2+} can be actively removed and accumulated into the cytosol after hormonal stimulation with e.g. epinephrine, phenylephrine and vasopressin. For details I refer to the box regulation of cellular Mg^{2+} by hormonal signaling.

Plasma-membrane Transport of Mg^{2+}

Data from Mg^{2+} flux-studies indicate the presence of several membrane transporters for Mg^{2+}. An electroneutral, extracellular Na^+-dependent Mg^{2+}/Na^+ exchanger in the plasma-membrane of chicken and turkey erythrocytes was the first characterized Mg^{2+} extruder (Gunther et al., 1984). Over the years, this Mg^{2+}/Na^+ exchanger has been identified in many other cell types (Gunther and Vormann, 1990; Handy et al., 1996; Tashiro and Konishi, 1997; Gunther et al., 1997). This exchanger can be stimulated by receptor-mediated increases in cyclic AMP (cAMP) and is dependent on extracellular Na^+. Removing Na^+ from the extracellular fluid (Romani et al., 1993b) or blocking Na^+ transport (Gunther et al., 1984; Feray and Garay, 1986) inhibits extrusion of Mg^{2+}. However, the data indicate that the mode of activation differs between cell types. Apart from its activation by cAMP (Gunther and Vormann, 1992), the Na^+/Mg^{2+} exchanger can also be turned on by increasing amounts of free cytosolic Mg^{2+} (Gaussin et al., 1997) and Ca^{2+} (Romani et al., 2000). Further more, the exchange stoichiometry varies between cell-types, e.g. in human red blood cells the exchange of Mg^{2+} for Na^+ has a stoichiometry of 1:3 (Ludi and Schatzmann, 1987; Schatzmann, 1993).

In addition, several laboratories have reported a Na^+-independent Mg^{2+} extrusion pathway that exchanges extracellular Ca^{2+} (Romani et al., 1993a), Mn^{2+} (Feray 1987), Cl^- (Gunther et al., 1990) or HCO_3^- (Gunther and Hollriegl, 1993) for Mg^{2+}. Extrusion appears to occur at a one-to-one ratio when Mn^{2+} is used as counter-ion and the exchanger can operate in reverse mode. In line with the presence of a Ca^{2+}/Mg^{2+} exchanger, inhibition of Ca^{2+} channels with nifedipine or verapamil prevents Mg^{2+} extrusion (Romani et al., 1993a).

Both Mg^{2+} extrusion mechanisms may coexist in a single cell. For example, results from the lab of Romani and Scarpa indicate that phenylephrine extrudes Mg^{2+} via a Ca^{2+}-dependent mechanism (accounting for 10-15% of the total Mg^{2+} extrusion) and via a Ca^{2+}-activated Na^+-dependent mechanism that accounts for the majority of extrusion (Romani et al., 2000).

Recently, two channels implicated in Mg^{2+} homeostasis have been cloned and characterized (Runnels et al., 2001; Nadler et al., 2001; Schlingmann et al., 2002; Walder et al., 2002). These highly related channels belong to the TRP family of ion channels and are known as TRPM6 and TRPM7 respectively. Both channels conduct Mg^{2+} and permeability appears to be regulated by the intracellular Mg^{2+} concentration: lowering of intracellular $[Mg^{2+}]$ by washout with Mg^{2+}-free patch pipette solution causes the channels to open, leading to Mg^{2+} influx (Nadler et al., 2001; Voets et al., 2004b). Whereas TRPM6 expression is restricted to the distal tubules of kidney and the intestinal tract (Schlingmann et al., 2002; Walder et al., 2002), TRPM7 is ubiquitously expressed (Runnels et al., 2001; Nadler et al., 2001). Therefore it has been proposed that TRPM7 is the first identified ion channel responsible for cellular Mg^{2+} handling in all cell types (Schmitz et al., 2003). Several mutations in TRPM6 are associated with hypomagnesia with secondary hypocalcaemia, an autosomal-recessive Mg^{2+} handling disorder (Schlingmann et al., 2002; Walder et al., 2002). A more detailed description of both channels can be found in sections on TRPM channels and TRPM7.

BOX 1: Regulation of Cellular Magnesium by Hormonal Signaling

Mg^{2+} Extrusion by Hormone Signaling and ATP Depletion

Stimulation of cardiac (Vormann and Gunther, 1987; Romani et al., 1993b; Howarth et al., 1994) and liver cells (Romani and Scarpa, 1990; Gunther and Vormann, 1991; Keenan et al., 1996) with β-adrenergic receptor agonists results in a marked extrusion of Mg^{2+} evident within 1 minute after application and reaching its maximum after 5-6 minutes. Subsequently, Mg^{2+} levels return towards basal levels, independent of the persistence of the agonist (Keenan et al., 1996; Romani et al., 2000). β-adrenergic receptor agonists act via adenylyl cyclases to increase cAMP levels, which in turn activates Protein Kinase A (PKA) (Huang et al., 1982; Wolf et al., 1997; Rothermel and Parker Botelho, 1988). Besides β-adrenergic receptor mediated extrusion, Cittadini's lab observed Mg^{2+} extrusion in spleen lymphocytes and Ehrlich cells after prostaglandin (PGE1 or PGE2) or arachidonic acid stimulation that is mediated by intracellular cAMP increase (Wolf et al., 1994; Wolf et al., 1996). Mg^{2+} extrusion over the plasma-membrane requires the presence of physiological levels of extracellular Na^+ and Ca^{2+}.

Stimulation with α-adrenergic agonists, such as phenylephrine revealed a second pathway involved in cellular Mg^{2+} regulation (Jakob et al., 1989). Pretreatment of cells with insulin allows discrimination between α- and β-adrenergic receptor-activated Mg^{2+} extrusion. Insulin inactivates β-adrenergic receptors through tyrosine phosphorylation and interferes with intracellular cAMP levels through inhibition of the adenylyl cyclase (Karoor et al., 1995) or activation of phospho-diesterases (Smoake et al., 1995), and thereby prevents Mg^{2+} efflux (Keenan et al., 1996; Romani et al., 2000). In contrast, α-adrenergic receptors are coupled to small G-proteins that activate PhosphoLipase C (PLC) and result in release of Ca^{2+} from IP_3-sensitive stores (Minneman, 1988). Therefore insulin pretreatment does not prevent Mg^{2+} extrusion after α-adrenergic receptor stimulation (Keenan et al., 1996). The release of intracellular Ca^{2+} could directly activate a Ca^{2+}-dependent Mg^{2+} transporter or act as a counter-ion for Mg^{2+} extrusion.

Cellular ATP is the most abundant chelator of Mg^{2+} present in the cytosol. Chemicals that decrease the cellular ATP content, like cyanide, mitocondrial uncouplers (Wolf et al., 1994; Romani and Scarpa, 2000), fructose (Gaussin et al., 1997) or ethanol (Tessman and Romani, 1998), increase the amount of free cytosolic Mg^{2+} that is extruded in a Na^+-dependent fashion. Since there is no evidence that cAMP mediates this extrusion (Tessman and Romani, 1998), it is possible that the elevation of free cytosolic Mg^{2+} due to decreased cellular ATP content is sufficient to activate the Mg^{2+} transporter.

Accumulation of Cellular Mg^{2+}

The Mg^{2+} content of blood plasma and the body is mainly controlled by cells in the renal apparatus and in the intestine. Mg^{2+} uptake from the intestine and reabsorption in the kidney is under hormonal control, although many details of this are still unclear. For a more exhaustive description I refer to reviews of Quamme (Quamme and de Rouffignac, 2000) and Hoenderop (Hoenderop and Bindels, 2005). Here I will focus on Mg^{2+} handling by other cells in the body.

As mentioned before, in liver and cardiac cells adrenergic receptors stimulate Mg^{2+} extrusion, a process that is sensitive to insulin. In contrast, in 3T3 fibroblasts and other cell types insulin causes accumulation of Mg^{2+} (Gylfe, 1990; Ishijima and Tatibana, 1994). Agonists such as vasopressin and angiotensin II also cause accumulation of Mg^{2+} (Okada et al., 1992; Touyz and Schiffrin, 1996; Dai et al., 1998). In hepatocytes, vasopressin-induced Mg^{2+} accumulation is Na^+-dependent and mediated by PKC and Ca^{2+} (Romani et al., 1993a). However the precise mode of action is still obscure.

TRP Ion Channels

TRP channels were identified in 1970 in the phototransduction cascade of *Drosophila melanogaster*. In wildtype fruit flies, continuous illumination of the compound eye produces a long lasting depolarization of photoreceptor cells (Pak et al., 1970). In the *Drosophila trp* mutant, the initial onset of the response to prolonged illumination is identical to wildtype but the depolarization is transiently decaying towards baseline within seconds despite the continuous illumination. This results in a functional loss of sight in bright light (Minke et al., 1975).

Members of the mammalian TRP channel family are involved in a variety of functions, e.g. cation homeostasis and detection of sensory stimuli. I will briefly introduce the activation pathway of *Drosophila* TRP channels and its multiprotein signal complex as it has been extensively studied and is likely to be relevant for regulation of mammalian TRP channels.

TRP Channels in the Drosophila's Eye and Light Perception

Phototransduction in the compound eye of *Drosophila* is a complex signaling cascade that involves G-Protein Coupled Receptors (GPCR), G-proteins, Phospholipase C (PLC), and at least 2 types of channels, TRP and TRPL (Minke and Cook, 2002). Incoming photons isomerize *rhodopsin*, the light-sensitive GPCR, to the active form *metarhodopsin*. *Metarhodopsin* subsequently transduces the signal to a heterotrimeric G-protein (*transducin*) that activates PLC (*norpA*). Consequently, PLC activation leads to TRP and TRPL channel opening resulting in a light-induced current (LIC) via an as yet unknown pathway. Resolving this pathway is difficult and results are controversial, but the key role for PLC is undisputed: in a temperature-sensitive allele of PLC, ts-*norpA*, flies can be rendered fully blind by rapidly switching to the non-responsive temperature, and vice versa (Deland and Pak, 1973). Interestingly, gating of TRP and TRPL channels has long been associated with various PLC-related second messengers, including IP_3, DAG and PIP_2 (Figure 2). As gating of TRPM7 channels by these messengers is the subject of Chapters 2 and 3, I will here review the literature in some detail.
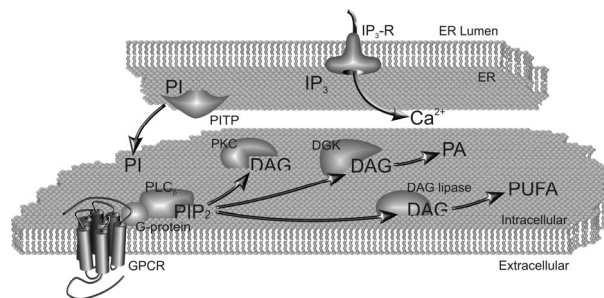

Figure 2: Schematic overview of phosphoinositide signaling cascade.

Upon binding of ligand to G-protein receptors (GPCR), the receptor is activated which in turn activates a heteromeric G-protein. Specific heteromeric G-proteins will activate phospholipase C at the plasma-membrane that catalyzes the hydrolysis of phosphatidylinositol 4,5-biphosphate (PIP_2) into the soluble second messenger inositol 1,4,5-triphosphate (IP_3) and the membrane bound diacylglycerol (DAG). The IP_3 binds to IP_3 receptors (IP_3-R) at the endoplasmasmatic reticulum, which has an internal Ca^{2+} channel that subsequently opens and releases Ca^{2+} into the cytosol. At the plasma-membrane, DAG activates protein kinase C (PKC) which initiates a phosphorylation cascade. DAG can be converted into 2 other potential second messengers: DAG lipases convert DAG to polyunsaturated fatty acids (PUFA) or phosphorylation of DAG by DAG kinases (DGK) it is transformed to phosphatidic acid (PA). Resynthesis of PIP_2 is dependent on the formation of PA that is further processed to CDP-DAG via CD-synthase (not shown). After conversion to PI at the endoplasmatic reticulum, PI is presumably transferred to plasma-membrane by a PI transfer protein (PITP) where 2 sequential phosphorylation steps by PI-kinases and PIP-kinases respectively is converted to PIP_2.

Phototransduction: Roles for IP_3 & Ca^{2+}

In the horseshoe crab *Limulus polyphemus* there is strong evidence that light induces release of Ca^{2+} from intracellular stores via IP_3 receptors localized in the submicrovillar cisternae (Payne et al., 1986). The release of Ca^{2+} precedes LIC by a few milliseconds. Not only PLC activation is required to evoke TRP opening but also the presence of extracellular Ca^{2+} is crucial. When photoreceptor cells are deprived from extracellular Ca^{2+} for prolonged time, this reversibly eliminates excitation (Hardie and Minke, 1992; Cook and Minke, 1999). Nevertheless, photolysis of caged Ca^{2+}, raising intracellular Ca^{2+} from the patch pipette or application of Ca^{2+} ionophores such as ionomycin all fail to activate TRP channels (Hardie, 1996). It has to be emphasized that these

experimental procedures do not mimic the locally very high Ca^{2+} increases found near the pore of IP_3 channels or plasma-membrane channels. This suggests that for example Calmodulin (CaM) may not be activated under these conditions. In Ca^{2+} free conditions, Ca^{2+} release from intracellular stores upon exposure to light was similar in *trp* mutant as in wildtype *Drosophila*. However, genetic elimination of the IP_3 receptor in *Drosophila* surprisingly abolished neither the light responses nor the Ca^{2+} release (Acharya et al., 1997). Furthermore, both caged IP_3 (Raghu et al., 2000) and caged GTPγS (Hardie, 1995) failed to activate phototransduction in *Drosophila*. This may reflect a diffusion barrier that prevents the chemicals from reaching the signaling membrane in the ommatidia. On the other hand, biochemical labeling studies with [³H]-inositol convincingly showed that illumination caused accumulation of IP_3 and IP_2 resulting from PLC activation (Devary et al., 1987). Furthermore, addition of 2,3-diphosphoglycerate (DPG), which prevents hydrolysis of IP_3, prolonged the light response in *Lucillia cuprina* and *Musca domestica* (Devary et al., 1987; Suss et al., 1989). Thus, IP_3 itself can also not be excluded as a second messenger.

Activation by DAG Signaling

Diacylglycerol (DAG) forms the other signal generated by PLC. It is well established that formation of DAG inactivates TRP channels by phosphorylation through PKC (*Drosophila* homolog is called *inaC*). Application of phorbolesters to activate PKC suppresses the light-induced Ca^{2+} release and photon response in *Limulus* (Dabdoub and Payne, 1999). To make things more complicated, a signaling pathway downstream of DAG may lead to TRP and TRPL activation. DAG is a precursor for the generation of polyunsaturated fatty acids (PUFA), although no activity of DAG lipases has been demonstrated in *Drosophila*. However, impaired downstream DAG signaling caused by a mutation in *rdgA* (a *Drosophila* homolog of diacylglycerol kinase) causes light-independent degeneration (Masai et al., 1993; Masai et al., 1997). Thus, it was proposed that accumulation of DAG leads to increased formation of PUFAs that triggers opening of TRP and TRPL channels, leading to toxic intracellular Ca^{2+} levels and retinal degeneration. Exogenous application of PUFA to ommatidia in inside-out patches caused TRP and TRPL channel opening, making PUFA a potential candidate for TRP channel activation in *Drosophila* phototransduction. In line with this notion, a *rdgA/trp* double mutant prevented to a large extend the retinal degeneration (Chyb et al., 1999; Raghu et al., 2000).

PIP₂ Regulating TRP Channel Activity

Finally, it has been suggested that PIP_2 itself could have a role as second messenger in TRP channel activation. Two independent mutations (*rdgB*, a Phospho-Inositide (PI) transfer protein, and *cds*, an enzyme involved in PI resynthesis) in the PIP_2 recycling pathway prevent recovery of TRP channel activity from inactivation (Wu et al., 1995; Hardie et al., 2001). Furthermore, Ca^{2+} influx after illumination is required to maintain PIP_2 levels possibly through termination of PLC activity and/or facilitation of PIP_2 recycling. Hence, removal of extracellular Ca^{2+} results in sustained TRP channel opening after termination of the light exposure (Hardie et al., 2001). Recombinant expressed TRPL channels are activated by application of exogenous PLCβ and are suppressed by PIP_2 application in inside-out patches (Estacion et al., 2001). On the other hand, in *in vivo* experiments in *Drosophila trp* mutants prolonged illumination leads to PIP_2 depletion and closure of TRPL channels, which remain inactivated until PIP_2 is resynthesized (Hardie et al., 2001).

Since DAG/PUFA can activate TRP and PIP_2 regulates these channels, the interesting hypothesis arises that simultaneous generation of DAG and depletion of PIP_2 might trigger TRP channel opening. This suggests that TRP channels may possess domains for DAG/PUFA binding, stabilizing the open state of the channels, as well as for PIP_2 binding to retain the channel in a closed state.

Mammalian TRP Channels

Following the identification of TRP and TRPL channels as Ca^{2+} conducting channels in Drosophila, 28 mammalian genes encoding TRP channels have been cloned and their functions are now beginning to be understood. TRP channels are involved in many different responses such as perception of temperature, touch and pain, smelling odorants and pheromones, but also in regulation of cellular ion homeostasis and uptake of ions in the kidney and intestine. Similarly,

regulation of TRP channels shows a perplexing variety of different mechanisms.

The mammalian TRP channel family can be grouped into 6 subfamilies (Figure 3, Clapham et al., 2003): canonical (TRPC), vanilloid receptor (TRPV) and melastatin-related (TRPM) channels, and the smaller subfamilies mucolipins (TRPML), polycystins (TRPP) and TRPA (an anchorin-repeat containing channel). Whereas the focus of this thesis is on TRPM7, I will here present a brief overview of the current literature on the major subfamilies to provide a background for understanding the regulation and biophysical properties of TRPM7. Emphasis will be on the modes of activation, regulation and the proposed gating mechanisms of TRPC, TRPV and TRPM channels. Information on TRPA, and its Drosophila homologue *NompC*, which have both been implicated in mechanosensation, will be presented in the paragraph on mechanosensation by ion channels.

TRPC Subfamily

The mammalian TRPC subfamily consists of 7 channels, named TRPC1-7. Of all mammalian TRP channels, this subfamily shares the highest homology with *Drosophila* TRP and TRPL channels. TRPC channels can be divided in 3 groups based on phylogeny: first, TRPC1, TRPC4 and TRPC5, second, TRPC3, TRPC6 and TRPC7, and third TRPC2 (Clapham, 2003). All these channels share a structural feature, a so-called TRP box consisting of an invariant amino acid sequence EWKFAR juxtamembrane to the 6th transmembrane domain. Furthermore, these channels possess N-terminal ankyrin repeats and are non-selective cation channels, which selectivity ratio $P_{Ca^{2+}}/P_{Na^+}$ varies from 1.1 for TRPC4 to 9 for TRPC5 (Schaefer et al., 2000). Gating of all TRPC channels is downstream of GPCR- or tyrosine-kinase receptor-mediated PLC activation. In all cases, the exact gating mechanism is still unclear and subject to debate: both store-dependent and -independent mechanisms have been proposed. For example, both TRPC1 and TRPC7 were shown to be activated in a store-dependent manner (Zitt et al., 1996), whereas others have suggested a store-independent mechanism (Lintschinger et al., 2000). Adding to the confusion, a recent paper shows that expression of TRPC1 did not induce any measurable currents at all (Strubing et al., 2001).

Physiological Functions of TRPC Channels

Channels of the first TRPC group regulate a variety of cellular responses. TRPC1, which is expressed in various tissues, is involved in regulating vascular permeability (Bergdahl et al., 2003; Kunichika et al., 2004) and axonal turning upon chemotropic stimulation (Wang and Poo, 2005). The first TRP channel knocked out in mice was TRPC4. These TRPC4-deficient mice revealed that this channel is involved in agonist-induced relaxation of blood vessels and lung microvascular permeability (Freichel et al., 2001; Tiruppathi et al., 2002). TRPC5 is predominantly expressed in the central nervous system and is abundantly present in hippocampal neurons, where it might be an important determinant of axonal growth and growth cone morphology (Greka et al., 2003).

Members of the second group are relatively highly expressed in cardiac and smooth muscle cells. TRPC3 and TRPC6 are shown to be involved in vasoregulation and regulation of tracheal contractility. TRPC3 and TRPC7 are proposed candidates for non-selective cation channels that may regulate Ca^{2+}-dependent contractility. TRPC2 was reported to be a pseudogene in humans, but not in other mammal species (Vannier et al., 1999). This channel is expressed in the vomeronasal organ of the rat (Liman et al., 1999), where it most likely involves pheromone signaling, since TRPC2 deficient mice display abnormal mating behavior (Stowers et al., 2002). Besides, expression of TRPC2 in the head of mouse sperm is involved in the release of hydrolytic enzymes upon egg fertilization (Jungnickel et al., 2001).

Signaling Complex of TRPC Channels

The signaling complex associated with *Drosophila* TRP channels is known as the transducisome or signalplex (Li and Montell, 2000). This protein complex, which consists of TRP channels, the *InaD* scaffold protein and regulatory proteins, has served as a model for possible signaling complexes of TRPC channels. By analogy to this signaling complex, a human homologue of *InaD* protein was cloned that has at least 5 protein-interacting PDZ domains (Philipp and Flockerzi, 1997). Unfortunately, no binding partners have yet been identified. However, several TRPC channels are linked to possible regulatory proteins. For example, TRPC4 and PLCβ₁ form a protein complex with the protein NHERF

(regulatory factor of the Na$^+$/H$^+$ exchanger) that contains 2 PDZ domains and is also linked to the cytoskeleton. To date, still no experimental data are present on the impact of the cytoskeletal interaction on channel functioning (Tang et al., 2000). Like the *Drosophila* TRP channels, all TRPC family members can bind directly to both calmodulin and the IP$_3$-receptor, suggesting that both these proteins are involved in regulation of the channels. As the binding sites of CaM and the IP$_3$-R in TRP channels partially overlap, competition between both proteins may occur (Tang et al., 2001).

Interestingly, PLCs are also involved in trafficking of TRPC channels. TRPC3 contains a partial PH-domain that is complemented by the C-terminal split PH-domain of PLCγ$_1$. The interaction of both domains forms a complete PH-domain capable of interacting with PIP$_2$ and is required for proper trafficking of TRPC3 to the plasma-membrane (Van Rossum et al., 2005)

Hetero-tetramerization of TRPC Channels

TRPC channels are expressed in virtually all tissues, cell types and cell lines and it seems likely that they can co-assemble in hetero-tetrameric complex (Garcia and Schilling, 1997; Hofmann et al., 2000; Riccio et al., 2002). However, to date most data on multimerization of TRPC channels are from heterologous expression studies performed in cancer cell lines. A major drawback of this approach is that overexpression favors formation of TRPC homo-tetramers and cell may lack (sufficient) additional factors that may be involved in channel functioning and regulation. Do these channels exist and function as homo-tetramers *in vivo*?

Increasing evidence suggests that the TRPC channel functioning is far more complex than thought before. Several TRPC family members can bind to each other and form hetero-tetrameric channels with properties different from the individually expressed TRPC channels. Co-immunoprecipitation revealed that TRPC1 can form a hetero-tetrameric channel with TRPC3 (Lintschinger et al., 2000), TRPC4 (Strubing et al., 2003) and TRPC5 (Strubing et al., 2001). Co-expression of TRPC1 with TRPC3 (Lintschinger et al., 2000), TRPC4 or TRPC5 (Strubing et al.,
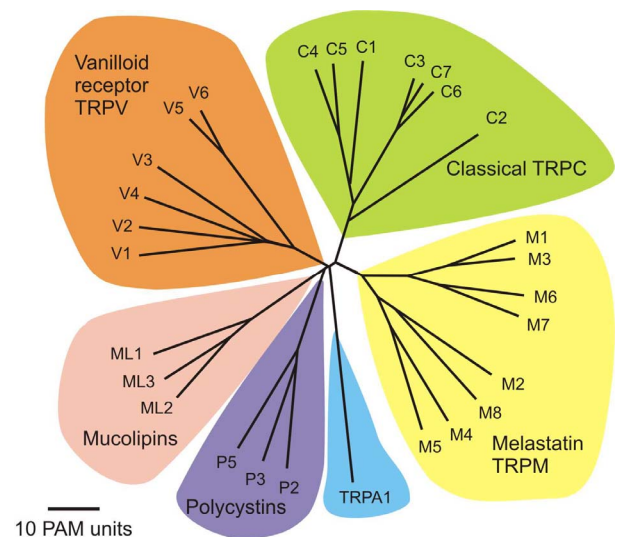

Figure 3: Phylogenetic tree of the mammalian TRP family.
The evolutionary distance is shown by the total branch lengths in point accepted mutations (PAM) units, which is the mean number of substitutions per 100 residues. Adapted by permission from Macmillan Publishers Ltd: Nature, (Clapham 2003) 2003

2001) resulted in currents with properties different of those of individually expressed channels. From studies that use various different approaches such as electrophysiological recording, co-immunoprecipitation and FRET assays, the picture emerges that TRPC1, TRPC4 and TRPC5 can co-assemble together, and that TRPC3, TRPC6 and TRPC7 can interact with each other in both overexpression studies (Hofmann et al., 2002) as well as in native tissues (Goel et al., 2002). In contrast, in both studies, members of one group were unable to cross interact with members of the other group.

The domain responsible for interaction between TRPC proteins has not yet been defined, although recent studies suggest that a conserved coiled-coil domain at the C-terminus of all TRPC channels may be involved (Engelke et al., 2002). Strikingly, alignment of this conserved coiled-coil region reveals that it displays an offset in TRPC3, TRPC6 and TRPC7 compared to TRPC1, TRPC4 and TRPC5, which is consistent with the selective association of the TRPC subunits.

BOX 2: Structure, Ion Selectivity and Gating of TRP Channels

TRP Channels as Tetramers

TRP ion channels possess 6 transmembrane domains and cytosolic N- and C-terminus reside in the cytosol. In analogy to the pore-forming subunits of voltage-gated Ca^{2+}, Na^+ and K^+ channels, which consist of either 4 subunits (Shaker K^+ and IRK channels) or internal 4-fold repeats (Ca^{2+} and Na^+ channels), it is reasonable to assume that TRP channels also consist of 4 subunits.

The TRP Pore Region and Ion Selectivity

A short hydrophobic stretch of amino acids between transmembrane domain 5 and 6 is predicted to be the pore-forming region in analogy to the K^+ channel KscA (Yool and Schwarz, 1991; Yellen et al., 1991). In a tetramer, 4 pore-forming regions together form the channel pore that is a often negatively charged ring that determines the ion selectivity of the channel (Doyle et al., 1998). Overall, the architecture of the selectivity filter of TRP channels is poorly defined. Mutational studies showed that replacing aspartate residues by neutral amino acids in the pore region alters the selectivity for Ca^{2+}, but also the sensitivity for intracellular Mg^{2+}, voltage-dependent gating and sensitivity to channel blockers (Owsianik et al., 2006). The aspartate residues in the proposed selectivity filter of TRPV4, TRPV5 and TRPV6 form a negatively charged ring that to some extent determines

Ca^{2+} selectivity of the channel, analogous to voltage-gated Ca^{2+} channels (Voets et al., 2003). The amino acids involved in cation selectivity in the pore of the other monovalent-selective and non-specific TRP channels have not been identified yet. Alignment of the pore region shows that TRPC and TRPM channels have a relatively high degree of conservation within the subfamilies (Owsianik et al., 2006). There is only marginal homology within the TRPV pore region, and in the absence of further mutational studies, identification of amino acids involved in the selectivity of these channel pores are merely an educated guess.

Proposed Gating Mechanism of TRP Channels

All these channels are involved in sensing and responding to a variety of stimuli. The cytosolic end of the 6th transmembrane domain is suggested to form the gating lever that is situated in line with the selectivity filter of the channel. Upon stimulation, opening and closure of the channel is probably managed by movement of the 4th transmembrane domain. This assumption is based on voltage-gated channels, where this region is positively charged and moves in the extracellular direction in response to cell depolarization, probably pulling the gating lever open.

TRPV Subfamily

TRPV channels, which are also widely expressed, share a high homology with the Osm9 channel in *Caenorhabditis elegans*. Behavioral studies with Osm9-deficient *C. elegans* showed its involvement in response to odorants, osmotic strength and mechanical stimulation (Colbert et al., 1997). The founding member TRPV1 was identified by expression cloning with the hot pepper-derived vanilloid compound capsaicin (Caterina et al., 1997). Like TRPC channels, TRPV family members have a TRP box after the 6th transmembrane domain and N-terminal ankyrin

repeats. TRPV channels non-specifically conduct cations and the Ca^{2+} selectively is set by a single aspartic acid residue in the channel pore (Garcia-Martinez et al., 2000; Voets et al., 2003). The TRPV protein family can be divided in 2 groups based on phylogeny, biophysical properties and cellular function: first, TRPV1-4 and second TRPV5 and TRPV6. Typically, the first group of TRPV channels can be activated and regulated by temperature whereas TRPV5 and TRPV6 are constitutively active.

Temperature Regulated TRPV channels

TRPV1 is activated by temperatures above 43°C and in addition by the chemical compounds 2-APB (Hu et al., 2004), capsaicin and endogenous cannabinoid receptor ligands like anandamide. The binding domain for both ligands is located to an intracellular domain adjacent to the 3rd transmembrane domain (Jordt and Julius, 2002). Heterologous expression of TRPV1 channels displays an outward rectifying current-voltage relationship and reveals anomalous mole fraction behavior as apparent from linearization of the I/V in divalent free medium. TRPV1 currents are activated as well as potentiated by a low pH (< 5.9) (Caterina et al., 1997) and inhibited by PIP$_2$ (Chuang et al., 2001). Release from PIP$_2$ inhibition by receptor mediated PLC activation increases heat-activated TRPV1 currents (Chuang et al., 2001). Furthermore, TRPV1 current are sensitized by PKC and PKA activity, however the mechanisms of action remains to be clarified. A TRPV1 knock-out mouse implicated the involvement of this channel in nociception, inflammation and in the hypothermic effects of vanilloid compounds (Caterina et al., 2000). Moreover this channel is implicated in pancreatitis (Nathan et al., 2002) and asthma (Hwang and Oh, 2002).

TRPV2 shares 50% homology with TRPV1 and is activated by noxious heat (> 52°C) and 2-APB, rather than capsaicin or pH (Caterina et al., 1999; Jordt and Julius, 2002; Hu et al., 2004). Activated TRPV2 channels display moderately outward rectifying I/V characteristics. Activation by growth factors like Insulin Growth Factor-1 (IGF-1) translocates functional TRPV2 channels to the plasma-membrane by incorporation of intracellular vesicles that contain preassembled channels (Kanzaki et al., 1999). Stretch forces can similarly lead to incorporation of the channel in the plasma-membrane in vascular smooth muscle cells (Muraki et al., 2003).

TRPV3 and TRPV4 channels are also activated by heat, but in a more moderate temperature range: raising temperature above 25°C will activate TRPV4 channels (Guler et al., 2002) whereas above 31°C TRPV3 currents are activated (Peier et al., 2002; Smith et al., 2002; Xu et al., 2002). Moreover, TRPV3 channels can be activated by 2-APB while TRPV4 channels are unaffected (Hu et al., 2004). TRPV3 displays an outward rectifying I/V-relationship (Xu et al., 2002) and the I/V-plot of TRPV4 is linear (Watanabe et al., 2002). Unlike TRPV3, TRPV4 currents are enlarged upon osmotic cell swelling

cells (Liedtke et al., 2000; Strotmann et al., 2000). This effect is mediated by phosphorylation of TRPV4 channels, reportedly downstream of the tyrosine kinase Src (Xu et al., 2003). Subsequent cell shrinkage reverses TRPV4 currents to basal values.

Ca^{2+} Gatekeepers TRPV5 and TRPV6

In contrast to the temperature regulated TRPV channels, TRPV5 and TRPV6 can not be activated by temperature changes. Heterologous expression in HEK293 cells showed that both channels are constitutive active (Vennekens et al., 2001) and are highly selective for Ca^{2+} (P$_{Ca}^{2+}$/P$_{Na}^{+}$ > 100). The I/V-relationships of both channels are inward rectifying, with hardly any outward currents at positive voltages (Vennekens et al., 2000; Vennekens et al., 2001). The aspartic residue in the pore defining Ca^{2+} selectivity also influences the Mg^{2+} sensitivity (Nilius et al., 2001). Mg^{2+} ions cause a voltage-dependent block of TRPV5 and TRPV6 currents. TRPV5 channels function as the main gatekeeper of apical Ca^{2+} influx pathway in kidney and TRPV6 fulfils this role in intestine (den Dekker et al., 2003; Nijenhuis et al., 2003)

TRPV5 as well as TRPV6 are controlled by intracellular Ca^{2+} levels through a negative feedback loop with apparent affinity of ~100 nM (Vennekens et al., 2001). The precise mechanism of this feedback loop is still unclear. Interestingly, CaM binds Ca^{2+}-dependently to human TRPV6 and this interaction is regulated by PKC-mediated phosphorylation of the TRPV6 CaM binding domain. Phosphorylation of a threonine residue inhibits CaM binding and thereby attenuates inactivation of human TRPV6 channels (Niemeyer et al., 2001). The CaM-binding domain is poorly conserved between mouse and human, and this mode of regulation thus seems to be restricted to human TRPV6 channels. The human TRPV5 amino-acid sequence also shows poor homology in this binding domain and therefore it is doubtful whether the same Ca^{2+} dependent regulation of TRPV5 channels exists.

Heteromultimeric TRPV Complexes

As covered in the previous paragraph, based on phylogeny, functional and biophysical properties, the TRPV channel family can be divided into 2 subgroups. All TRPV channels do form homo-tetramers (Hellwig et al., 2005) but are they also capable to form hetero-tetramers?

Data from FRET and co-immunoprecipitation assays show that TRPV1 and TRPV2 can interact with each other, although, TRPV2 preferably

associates with other TRPV2 subunits and only to a minor extent with TRPV1 (Hellwig et al., 2005). Smith et. al found that TRPV1 can also co-assemble with TRPV3, based on responses to capsaicin and on immunoprecipitation assays (Smith et al., 2002). In contrast, a very recent study failed to detect functional or physical interactions between these TRPV family members (Hellwig et al., 2005). For this reason, it still remains unclear whether TRPV1 and TRPV3 can form hetero-tetrameric channels. The remaining member of this subgroup, TRPV4 is not able to form hetero-tetrameric channels upon co-expression with all other TRPV family members (Hellwig et al., 2005).

TRPV5 and TRPV6 are endogenously expressed in various epithelial tissues and their co-expression levels affect renal and intestinal Ca^{2+} absorption (van Abel et al., 2005). By various biochemical assays it was shown that TRPV5 and TRPV6 can co-assemble in hetero-tetramers (Hoenderop et al., 2003). In summary, formation of heteromultimeric TRPV channels may occur with some specificity, although the complete picture has not yet emerged.

TRPM Subfamily

TRPM channels show a large variety in cell-biological and biophysical properties. For convenience, members of this subfamily will here be loosely subdivided in 3 groups: TRPM4 and TRPM5, which share significant similarities in both functional and biophysical properties, TRPM6, TRPM7 and TRPM2, which are remarkable combinations of an ion channel and an enzyme, and the remaining channels.

TRPM1, TRPM3 and TRPM8

Melastatin (TRPM1), the founder of the TRPM family, was identified in a screen of human melanoma-correlated mRNAs. In melanocytes, short and full-length TRPM1 mRNA transcripts are present. Decreased expression of the short transcript of TRPM1 correlates with increased invasiveness of malignant melanomas and it is therefore used as a diagnostic marker (Duncan et al., 1998). TRPM1 is widely expressed in different tissues, but functional and electrophysiological properties have not been studied extensively so far. Untill now, the only ion known to be conducted by full-length TRPM1 is Ca^{2+} (Xu et al., 2001). While the precise function of TRPM1 remains unclear, a putative role in cellular differentiation and

proliferation was suggested by Fang et al. (Fang and Setaluri, 2000). The short, cytosolic isoform of TRPM1 may be responsible for correct trafficking of the full length TRPM1 protein to the plasma-membrane (Xu et al., 2001)

The closest relative of TRPM1 is TRPM3, which is primarily expressed in human kidney and brain but not in mouse kidney (Grimm et al., 2003; Lee et al., 2003). Heterologous expression of TRPM3 results in formation of constitutive active, non-selective cation channels. Recently, 5 alternatively spliced TRPM3 variants have been characterized (α1-5). Interestingly, 2 isoforms, TRPM3α1 and TRPM3α2, differ only in their pore region (Oberwinkler et al., 2005). Whereas the TRPM3 was originally reported to have linear I/V characteristics (Grimm et al., 2003), both α1 and α2 splice variants revealed outward rectifying ion currents regulated by intracellular Mg^{2+} (Oberwinkler et al., 2005). However, their ion selectivity is remarkably different: TRPM3α1 channels are poorly permeable for divalent ions whereas TRPM3α2 conduct Ca^{2+} and Mg^{2+} rather well. Furthermore, TRPM3α2 channels are inhibited by extracellular monovalent ions whereas TRPM3α1 mediated currents are unaffected.

TRPM3 is reported to be regulated by osmolarity: in a hypotonic medium, the conductance of TRPM3 increased in amplitude (Grimm et al., 2003). In addition, activation of TRPM3 by store depletion (Lee et al., 2003) and by D-erythro-sphingosin (Grimm et al., 2005) was also reported.

The TRPM8 gene was identified as a prostate-specific gene and it appears to be upregulated in prostate as well as other cancers (Tsavaler et al., 2001). Heterologously expressed TRPM8 channels are activated by low temperatures (8 - 24°C) and by cooling agents such as menthol and icillin (McKemy et al., 2002; Peier et al., 2002; Nealen et al., 2003), which is consistent with a role in thermosensation and nociception. TRPM8 channels permeate both monovalent and divalent ions and they are responsible for the intracellular Ca^{2+} elevations induced by menthol and icillin. TRPM8 currents display strong outward rectification and reverse around 0 mV.

Reponses to cold temperature and icillin depend on a physiological intracellular H^+ concentration: lowering the pH inhibits TRPM8 opening by these stimuli, but menthol-induced activation is unaffected (Andersson et al., 2004). The gating is caused by temperature-dependent

BOX 3: Imaging PIP$_2$ Kinetics in Living Cells

Confocal Imaging of PIP$_2$ Kinetics

The PH-domain of PLCδ1 fused to Green Fluorescent Protein (GFP) detects PIP$_2$ at the plasma-membrane and is widely used to study PIP$_2$ kinetics in living cells by confocal laser scanning microscopy (Figure box 3A, (Stauffer et al., 1998; Varnai and Balla, 1998). Unstimulated cells have high PIP$_2$ levels and GFP-PHd1 is bound to the membrane (Figure box 3A, inset 2). Receptor-activated PLCs hydrolyse PIP$_2$ causing translocation of the PIP$_2$ probe into the cytosol (Figure box 3A, inset 2). During resynthesis of PIP$_2$, the fluorescence recovers at the plasma-membrane.

PIP$_2$ Kinetics Measured by FRET

The principle of measuring PIP$_2$ kinetics by Frequency Resonance Energy Transfer (FRET) is similar as described above. In stead of GFP, the color variants cyan (CFP) or yellow (YFP) are fused to PHδ1 and simultaneously expressed in living cells (Figure box 3B, (van der Wal et al., 2001)). Because the emission spectrum of CFP (donor) overlaps with the excitation spectrum of YFP (acceptor) radiationless transfer of energy occurs. Because of the high plasma-membrane PIP$_2$ levels, the donor and acceptor are in close proximity (< 10 nM) and FRET appears as quenching of the donor and as gain of acceptor fluorescence (Figure box 3B). Upon hydrolysis of PIP$_2$, CFP- and YFP-PHδ1 translocate to the cytosol. Consequently the distance increases between both fluorophores (> 10 nM) and FRET decreases. This leads to a decline in YFP emission and an increased CFP fluorescence (Figure box 3B, graph). When PIP$_2$ levels are recovering, the FRET values increases.
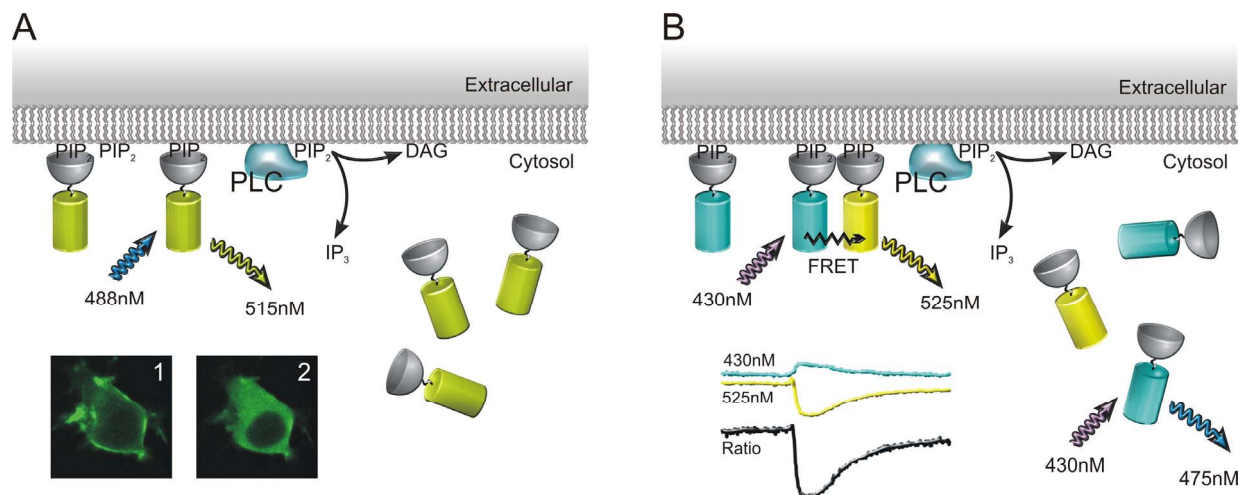

Figure box 3: Principles of imaging PIP2 kinetics in living cells
Cells transfected with FP-PHd1 and PIP2 dynamics are followed in time by either confocal laser scanning or bright field microscopy. During confocal experiments GFP is excited at 488 nM and GFP fluorescence detected at 525 nM. In FRET experiments, excitation occurs at 430 nM and fluorescence CFP and YFP are simultaneously recorded.

shift in voltage-dependence: low temperatures and cooling agents shift the voltage-dependence of TRPM8 negatively towards the physiological range (Voets et al., 2004a). Activity of TRPM8 channels depends on the presence of PIP_2 at the plasma-membrane that binds to the TRP-domain (Rohacs et al., 2005). Whole-cell and inside-out patch experiments produce rundown of TRPM8 channels because of PIP_2 depletion at the plasma-membrane (Rohacs et al., 2005; Liu and Qin, 2005).

TRPM4 and TRPM5: Channels Specific for Monovalent Ions

TRPM4 and TRPM5 are the only TRP channels impermeable to divalent ions: these channels selectively conduct monovalent ions and thereby depolarize the plasma-membrane (Launay et al., 2002; Hofmann et al., 2003; Prawitt et al., 2003). Signaling of GPCRs via PLC and release of Ca^{2+} from the ER will activate these channels, although the precise mechanism is unclear. For activation of the channels relatively high Ca^{2+}_i levels are necessary, $> 0.3\mu M$ for TRPM4 (Launay et al., 2002) and TRPM5 requires over $1\mu M$ of Ca^{2+}_i (Hofmann et al., 2003), suggesting that both channels may be in close proximity to Ca^{2+} release sites of the ER. The I/V plots of both TRPM4 and TRPM5 are non-linear as a result of an intrinsic voltage-sensing mechanism that is independent of divalent cation binding (Launay et al., 2002; Hofmann et al., 2003). Sustained exposure to Ca^{2+} desensitizes both channels, but administration of PIP_2 reverses desensitization partially for TRPM5 (Liu and Liman, 2003) and restores TRPM4 currents fully (Zhang et al., 2005)

TRPM4 is ubiquitously expressed and possibly serves as a negative feedback regulator of Ca^{2+} oscillations (Launay et al., 2002): high Ca^{2+} levels during Ca^{2+} oscillations activate TRPM4, which subsequently depolarizes the plasma-membrane and decreases the driving force for Ca^{2+} entry in non-excitable cells. In addition, in excitable cells TRPM4-mediated depolarization may be important in regulation of Ca^{2+} entry through voltage-gated Ca^{2+} channels, consequently shaping action potential duration and frequency. The TRPM5 gene was originally identified in a chromosomal region that is associated with several tumors (Enklaar et al., 2000), but a later study showed that TRPM5 is primarily found in taste receptor cells (Perez et al., 2002). The taste receptors T1R and T2R both signal via $PLC\beta_2$ to TRPM5. This signaling pathway mediates taste

sensation of sweet, bitter and amino acid (Perez et al., 2002; Zhang et al., 2003).

TRPM Channels with Intrinsic Enzymatic Activity

A separate group of TRPM channels is formed by TRPM2, TRPM6 and TRPM7. These three channels are characterized by a C-terminal enzyme moiety. TRPM2 channels posses a NUDT9 Nudix hydrolase motif (Perraud et al., 2001), whereas TRPM6 (Schlingmann et al., 2002; Walder et al., 2002) and TRPM7 (Runnels et al., 2001) both have a serine/threonine kinase at their C-terminus. Physiological and biophysical properties of TRPM7 will be discussed in detail in the following section.

TRPM2 forms a Ca^{2+} permeant non-selective ion channel that also conducts K^+, Na^+ and Cs^+. It has linear I/V properties and reversal potential around 0 mV (Perraud et al., 2001). The channel is activated by binding of ADP-ribose (~100 μM), cADP-ribose ($> 100\mu M$) or NAD ($> 1mM$) to the Nudix motif, which is an inefficient hydrolase (Perraud et al., 2001; Sano et al., 2001; Kolisek et al., 2005). Interestingly, cADP-ribose ($< 10\mu M$) potentiates ADP-ribose-mediated TRPM2 activation to nM concentrations (Kolisek et al., 2005). Opening of TRPM2 channels is facilitated by intracellular Ca^{2+}, but by itself Ca^{2+} can not activate the channel (Perraud et al., 2001; McHugh et al., 2003).

Furthermore, oxidative stress (hydrogen-peroxide) and tumor necrosis factor α also regulate TRPM2 channel opening. Therefore, Hara and collaborators suggest that TRPM2 may act as an intracellular oxidation-reduction sensor (Hara et al., 2002). Prolonged exposure to oxidative stress concurrently results in increased Ca^{2+} levels and apoptosis of cardiac myocytes and hematopoietic cells (Zhang et al., 2005; Yang et al., 2005).

TRPM6 (also known as ChaK2) channel currents are carried by mono- and divalent cations. TRPM6 currents reverse around 0 mV and their I/V-plot is outward rectifying. Moreover, the current is strongly regulated by internal Mg^{2+} ions (Voets et al., 2004b). TRPM6 expression is predominantly expressed in intestinal epithelia and kidney tubules, and this has lead to the hypothesis that it is involved in uptake of Mg^{2+} in the gut and renal reabsorption of Mg^{2+} and Ca^{2+}. Indeed, several mutations in TRPM6 are linked to a disorder in renal and intestinal Mg^{2+} and Ca^{2+} absorption that is known as familial hypomagnesemia with secondary hypocalcemia (FHSH, Schlingmann et al., 2002; Walder et al., 2002). Transport of TRPM6 to the plasma-

membrane and subsequent incorporation is dependent on hetero-tetramerization with TRPM7. A missense mutation in TRPM6 abrogated oligomerization with TRPM7, providing a possible explanation for the impaired epithelial Mg^{2+} reabsorption in patients diagnosed with FHSH (Chubanov et al., 2004).

TRPM7

Physiological Properties

TRPM7 (also kown as ChaK1, LTRPC7 and TRP-PLIK) shares many properties with TRPM6 but it has been studied much more extensively. Like TRPM6, the TRPM7 currents are carried by cations and, at least in whole-cells, they display an outward rectifying I/V-plot (Runnels et al., 2001; Nadler et al., 2001). Monovalent TRPM7 currents are inhibited by internal Mg^{2+} ions, i.e. the channels display an anomalous mole fraction behavior that has also been termed 'divalent permeation block'. In accordance, the I/V relationship linearizes in divalent-free solutions.

In addition, it was reported that depletion of intracellular Mg^{2+} (Prakriya and Lewis, 2002; Kozak and Cahalan, 2003) or Mg-nucleotides (Nadler et al., 2001; Demeuse et al., 2006) causes full activation of TRPM7 by a mechanism independent of Mg^{2+} permeation block (Kozak and Cahalan, 2003). A current with similar properties had been previously described as Mg-Nucleotide-regulated Metal (MagNuM) ion current (Nadler et al., 2001) or Magnesium Inhibited Current (MIC) (Kerschbaum and Cahalan, 1998). Subsequent inhibitor studies demonstrated that TRPM7 is the carrier of this current (Kerschbaum et al., 2003).

Besides Ca^{2+} and Mg^{2+}, TRPM7 provides a mechanism for entry of trace metal ions as Ni^{2+}, Co^{2+}, Mn^{2+} and Zn^{2+} (Monteilh-Zoller et al., 2003).

Potential Functions of TRPM7 Channels

Whereas it was originally suggested that TRPM7 would be a good candidate to conduct ICRAC (Cahalan, 2001), detailed follow-up studies have now dismissed this idea. It was shown that biophysical and pharmacological properties of TRPM7 differ from those of ICRAC. For example, ICRAC is strongly selective for Ca^{2+} while TRPM7 conducts both Mg^{2+} and Ca^{2+} (Runnels et al., 2001; Nadler et al., 2001). Unlike TRPM7, ICRAC is also impermeant to Mn^{2+} ions and has low Cs^+ permeability. Furthermore, ICRAC displays a rapid desensitization in divalent-free media that is not seen in TRPM7. Inhibitor profiles of ICRAC and TRPM7 show distinct differences as well. In divalent free media, the aspecific Ca^{2+} entry blocker SKF 96365 fully inhibits ICRAC whereas TRPM7 currents are unaffected. Moreover, TRPM7 currents are insensitive to low 2-APB concentrations, while ICRAC is potentiated by this compound (Prakriya and Lewis, 2002).

The TRPM7 protein is ubiquitously expressed and TRPM7 knockout cells are not viable due to Mg^{2+} deficiencies. Therefore this channel was the first protein hypothesized to be directly involved in Mg^{2+} homeostasis (Schmitz et al., 2003). Knocking out the TRPM7 gene in mice is embryonically lethal at a very early stage (E6.5), showing the importance of the channel during development (Kim et al., 2005). A rare point mutation in TRPM7 was identified that increases the sensitivity of the channel to Mg^{2+} inhibition and that may contribute to the pathogenesis of 2 types of neurodegenerative disorders (Hermosura et al., 2005). However, alternative functions for TRPM7 have also been proposed, e.g. in proliferation of retinoblastoma cells (Hanano et al., 2004), anoxic cell death (Aarts et al., 2003) and in zebrafish skeletogenesis (Elizondo et al., 2005).

Regulation of TRPM7 Channel Activity

The α-Kinase Domain and TRPM7 Channel Gating

Since the cloning of TRPM7 it has been debated whether the kinase domain is involved in regulation of the channel gating. Initially it was reported that TRPM7 channel gating requires a functional kinase domain (Runnels et al., 2001). However, subsequent studies and our own data show that the channel gating can be dissociated from kinase activity and TRPM7 autophosphorylation. Whole-cell currents and Ca^{2+} influx through kinase-dead point mutants were indistinguishable from those of wild-type TRPM7 (Schmitz et al., 2003; Matsushita et al., 2005; Clark et al., 2006). Complete deletion of the kinase domain caused a significant, but not complete, decrease in both Ca^{2+} influx and whole-cell currents. According to Matsushita, impaired trafficking to the plasma membrane or assembly of tetramers can not be excluded, since the expression levels of the deletion mutant were similar to the full-length construct (Matsushita et al., 2005). In contrast with observations made by Matsushita,

Schmitz and coworkers found that kinase-dead TRPM7 channels are less sensitive to inhibition by intracellular Mg^{2+}. In their hands, the kinase-deletion mutant did not affect channel conductance but it was more potently inhibited by Mg^{2+}_i (Schmitz et al., 2003). Overall, these reports support the view that the kinase domain is neither required for activation of the TRPM7 channel nor that it contains the internal Mg^{2+} sensor.

TRPM7 Interacts with PLC Isozymes
    The available evidence suggests that TRPM7 contains a number of domains that are involved in PLC-mediated signaling. The channel was originally cloned in the lab of Dr. D. Clapham in a yeast-two-hybrid screen for interactors with PLCβ1. Analysis showed that this interaction involves the kinase domain of TRPM7 and the C2-domain of PLCβ$_l$ (Runnels et al., 2001). Later, it was shown that the kinase domain can also bind to the PLC isoforms β$_2$, β$_3$ and γ$_1$ (Runnels et al., 2002). As PLCγ$_1$ was shown to contain a split PH domain that interacts with a complementary split PH domain in TRPC3 (Van Rossum et al., 2005),
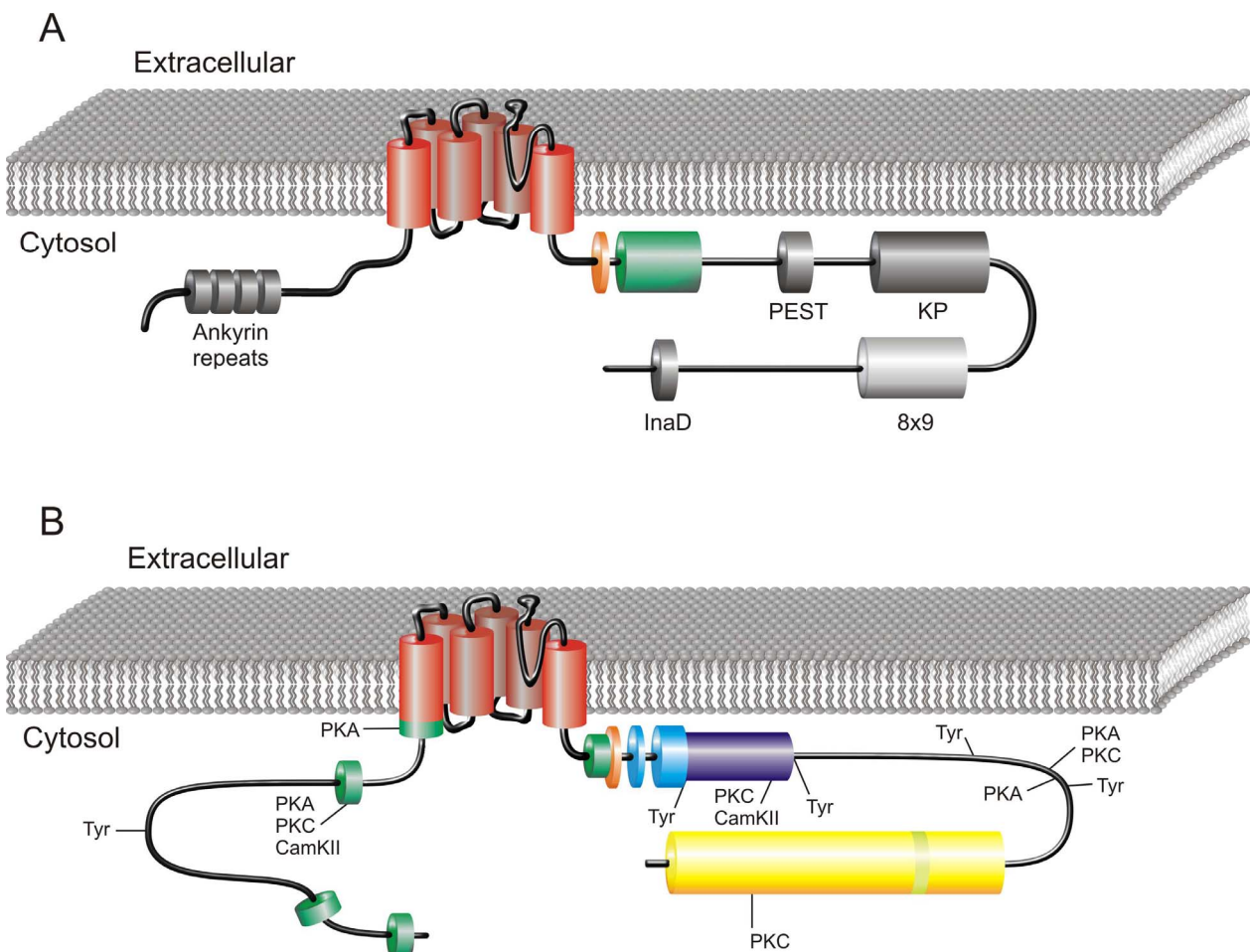

Figure 3: Putative domain structures of *Drosophila* TRP channels and the mammalian TRPM7 channel.
    The protein sequence for both TRP (A) and TRPM7 (B) channels encodes for 6 hydrophobic transmembrane domains (red) and a pore region between the 5th and 6th domain. Downstream of the 6th transmembrane helix the TRP domain is located (orange), characteristic for all TRP channels. In TRP there is one putative Calmodulin-binding motif (green) directly downstream of the TRP domain. *In silico* analysis of the TRPM7 sequences revealed 5 putative CaM motifs and one is topological similar to the one located in TRP. At the end of C-terminus, the TRP channel has an InaD binding and other features of TRP are a PEST sequence, proline-rich region with the dipeptide lysine-proline (KP) repeating 27 times. The TRP domain has a unique and curious hydrophylic sequence (8x9) near the C-terminus. The TRPM7 gene at the C-terminus encodes a unique α-kinase (yellow) with embedded a split PH domain (light green). TRPM7 contains 2 putative PIP$_2$ binding sites at the C-terminal side of the TRP domain (blue, see text for details), which is followed by a coiled-coil region (purple). Amino acid analysis revealed several potential phosphorylation sites for PKA, PKC, CaM kinase II and tyrosine kinases.

we analyzed TRPM7 for the presence of such a split PH domain (van der.Krogt, unpublished). We used a search algorithm that was programmed in our lab to identify split PH domains similar to that of TRPC3. Interestingly, a partial PH-domain complementing the C-terminal half of the PLCγ_1 split PH-domain is located in the TRPM7 kinase (see Figure 3). Therefore we anticipate that the PLCγ_1 interaction with TRPM7 mediates trafficking to the plasma-membrane

TRPM7 Functioning is Dependent on PIP$_2$

The function of many TRP channels, including TRPM4, TRPM5 and TRPM8, depend on the presence of PIP$_2$ at the plasma-membrane. A role for PIP$_2$ in regulating TRPM7 has also been claimed (Runnels et al., 2002). Runnels observed that when TRPM7 channels were pre-activated by depletion of intracellular Mg^{2+} in whole-cells or inside-out patches, agonist-induced PIP$_2$ hydrolysis potently closed the channels. Subsequent addition of PIP$_2$ to the intracellular leaflet of the plasma membrane restored the conductance (Runnels et al., 2002).

This report has been the source of much confusion. First, an inhibitory role for PLC signaling contradicts observations that we had obtained earlier (Chapter 2 & 3, Clark et al., 2006). We found that activation of PLC activates TRPM7 channels, as detected by morphological and electrophysiological methods as well as using Ca^{2+} fluorometry. In Chapter 2 and 3, this issue is addressed in detail.

Second, the results of Runnels were also challenged by Takezawa and colleagues (Takezawa et al., 2004). They observed that upon pretreatment with the "specific" PLC inhibitor U73122 endogenous PLC-activating receptors were still able to inhibit TRPM7 currents and concluded that PLC signaling is not involved. However, Takezawas' data do not justify such as strong conclusion (see Chapter 3) because U73122 is NOT a specific inhibitor for PLC. Rather, it interferes with several GPCR-effector interactions (Balla, 2001) thereby additionally blocking e.g. phospholipase A$_2$ and phospholipase D signaling pathways. U73122 is quite unstable and it rapidly looses its inhibitory potential in solution. Furthermore, in our lab we observed that application of freshly prepared U73122 solution to cells caused a rapid drop in membrane [PIP$_2$], thereby inactivating Mg^{2+} depletion-induced TRPM7 currents (Chapter 3). Horowitz and Hille recently reached a similar conclusion for the effects of U73122 on M-type K$^+$ channels (Horowitz et al., 2005).

A further interesting twist was recently added by Kozak and coauthors (Kozak et al., 2005). These authors reported that cytosolic acidification inhibits both TRPM7 currents and endogenous MIC currents, and they showed that both can be rescued by application of PIP$_2$ in inside-out patches (Kozak et al., 2005). As a mechanism, they proposed that protons might exert this regulatory action by charge-screening of the negatively charged PIP$_2$ moieties. Taken together, most results point out that PIP$_2$ at the plasma-membrane is essential for keeping TRPM7 channels in an open conformation.

Putative Mechanisms of TRPM7 Regulation by PIP$_2$

PIP$_2$ may be important for TRPM7 currents through an interaction with the intermolecular (split) PH-domain, or via interactions independent of this domain. Indeed, sequence analysis identified 2 other putative PIP$_2$ interaction sites in TRPM7 (Dr. T. Balla, NIH, Bethesda, personal communication). Downstream of the TRP domain a short stretch of positively charged amino acids (1147 to 1153) is likely to interact with negatively charged inositol headgroups of PIP$_2$, and at amino acids 1196 to 1218, a stretch including positive residues may form a modular PIP$_2$ binding pocket that is analogous to a PIP$_2$-binding stretch in TRPV1 (Prescott and Julius, 2003). In several other PIP$_2$-regulated TRP channels including TRPM8, TRPM5 and TRPV5, the TRP-domain was reported to be responsible for PIP$_2$ binding and for maintaining the channel in an activated state (Rohacs et al., 2005); this TRP consensus sequence is an additional candidate site of PIP$_2$ interactions in TRPM7. The interaction between PIP$_2$ and TRPM7 at the plasma-membrane most likely reflects an electrostatic interaction (Kozak et al., 2005) rather than the 'key-and-lock' binding observed in PH domains. In conclusion, loss of PIP$_2$ binding to TRPM7 may underlay both cation interferences and PLC-mediated closure of TRPM7 channels.

Regulation of TRPM7 by cAMP Levels

As mentioned above, Takezawa and colleagues challenged a role for PIP$_2$ in regulating TRPM7 based predominantly on inhibitor studies using U73122. Instead, they observed that a decrease in intracellular cAMP levels after muscarinic receptor activation is responsible for TRPM7 current inhibition and that this effect depends on a functional TRPM7 kinase domain.

On the other hand, a raise in intracellular cAMP levels increased Mg^{2+}-depletion-activated TRPM7 currents. Inhibition of PKA prevented carbachol-mediated inhibition of TRPM7 currents (Takezawa 2004). Hence, alterations in cytosolic cAMP levels effects PKA activity and by this means regulate TRPM7 currents. Our *in silico* analysis of the TRPM7 amino acid sequence revealed that it contains several putative PKA phosphorylation sites that may be involved in regulation of TRPM7 function (Figure 3, www.phosite.com, Koenig and Grabe 2004).

Insertion of TRPM7 Containing Vesicles in the Plasma-membrane

A final possible mechanism of TRPM7 current/channel activation must also be mentioned here. By analogy to TRPC3 (Singh et al., 2004) and TRPC5 (Bezzerides et al., 2004), it is conceivable that TRPM7 currents may be activated by fusion of vesicles that contain pre-assembled TRPM7 channels with the plasma-membrane. Whereas the precise signaling steps involved in such regulation are unclear, it is possible that PIP_2-recognizing sequences (including the split PH domain) are involved in this process. Interestingly, Oancea et al (Oancea 2006) recently showed that shear force induced by fluid flow gave rise to some incorporation of native TRPM7 channels in the plasma membrane in vascular smooth mucle cells. How significant the increase is, and whether it is a general mechanism that is also effective in other cells remains to be determined.

Characteristics of the TRPM7 α-Kinase Domain

If the TRPM7 kinase domain does not regulate channel gating, what role does it fulfill in living cells? The majority of the eukaryotic protein kinases belong either the serine/threonine kinase family or to the tyrosine kinase family that together comprise the so-called "conventional protein kinases" or CPKs (Taylor et al., 1992). The human genome further encodes kinases that share sequence homology to this group and are distantly related to CPKs, for example the phosphoinositol-3-kinases (Hunter, 1995). In addition there are kinase known that have no sequence homology to CPKs, although they are structurally similar. The TRPM7 kinase is an example of this group (Yamaguchi et al., 2001). These kinases are known as α-kinases and the name refers to the capability of these kinases to phosphorylate amino acids located within an α-helix (Ryazanov et al., 1999). The TRPM7 kinase domain shares 28% homology to the myosin heavy chain kinase A of *Dictyostelium*, a member of the α-kinase family involved in regulation of myosin stability (Kolman et al., 1996).

Substrates of the TRPM7-Kinase

In vitro characterization of the catalytic domain of TRPM7 showed that it is subject to autophosphorylation and shows kinase activity towards myelin basic protein (MBP), a promiscuous substrate used as a control in many *in vitro* kinase assays. The kinase domain specifically uses ATP as substrate and is unable to use GTP, and it depends on the presence of Mg^{2+} (optimum at 4-10 mM). Importantly, increased Ca^{2+} concentrations up to 1 mM did not alter kinase activity (Ryazanova et al., 2004).

A follow-up study by the group of Ryazanov identified an intriguing substrate for TRPM7-kinase, namely annexin-1, an anti-inflammatory protein that is regulated by Ca^{2+} and can bind actin filaments (Dorovkov and Ryazanov, 2004). An evolutionary conserved serine located in α-helix at the N-terminus of annexin-1 is phosphorylated by the TRPM7 kinase. Phosphorylation of annexin-1 depends on the presence of Ca^{2+} (500µM) and EGTA almost completely prevents annexin-1 phosphorylation.

We have identified non-muscle myosin IIA heavy chain (MHC IIA) as an additional substrate for TRPM7 kinase (chapter 4, Clark et al., 2006). Like all myosin II isoforms, MHC IIA organizes into homo-dimers consisting of a long α-helical domain and a short head domain that interacts with actin filaments. Starting point for this study was the observation of F. van Leeuwen that bradykinin causes MHC IIA phosphorylation in N1E-115 cells, which leads to dissociation of actin filaments from MHC IIA, and consequent loss of contractility that is apparent as a marked cell flattening (van Leeuwen et al., 1999).

TRPM7-Kinase Activity Affects the Actomyosin Organization

The actin cytoskeleton controls many cellular functions, such as intracellular transport, and phagocytosis but also cell adhesion and migration. Actin is organized into filaments, held together by a number of actin bunding proteins. Membrane protrusive activity (force) can be generated by

actin polymerization, which occurs at the leading edge of migrating cells, for instance in response to a chemotactic stimulus (Small, 1981; Burridge et al., 1988; Small et al., 1995). In addition, actin filaments can generate intracellular forces (tension) by associating with myosins. Similar to muscle, also in non-muscle cells myosin II isoforms are the major motor proteins responsible for force generation (Redowicz, 2001). However, important differences exist between muscle and non-muscle myosin II isforms. Whereas in muscle cells, myosin II is assembled in stable, regularly-patterned myofibrils, in non-muscle cells myosin II is part of the dynamic actomyosin cytoskeleton that undergoes continuous remodeling in order to accommodate changes in cell adhesion and cell shape, for instance during cell migration (Burridge and Chrzanowska-Wodnicka, 1996).

As mentioned previously, we find that TRPM7 affects actomyosin function by Ca^{2+}- and kinase-dependent phosphorylation of MHC IIA. Activation of TRPM7 by GPCRs results in cytoskeletal relaxation, leading to increased cell spreading. Simultaneously, cells increase their adhesion to the extracellular matrix accompanied by the formation of large integrin-containing adhesions (Chapter 4, Clark et al., 2006).

We have proposed that TRPM7 may, at least in part, affect actomyosin function by phosphorylation of the myosin II heavy chain. However, additional (kinase-dependent and -independent mechanisms) may contribute to TRPM7-induced cytoskeletal remodeling. For instance, it was shown by Dorokov et al that TRPM7 can phosphorylate annexin-1 (Dorovkov and Ryazanov, 2004), a protein known to bundle actin filaments independent of Ca^{2+} (Campos-Gonzalez et al., 1990; Kusumawati et al., 2000). Furthermore, annexin-1 can interact with profilin and plasma-membrane lipids PIP_2 and phosphatidylserine (Alvarez-Martinez et al., 1996). This suggests that TRPM7-mediated phosphorylation of annexin-1 may regulate cytoskeletal structures. Additionally, we find that some of the effects of TRPM7 on cell spreading appear to be independent of kinase activity (Chapter 4, Clark et al., 2006).

Altogether, the picture emerges that TRPM7 plays a pivotal role in the regulation of the cytoskeleton and that regulation occurs at multiple levels (Chapter 4, Clark et al., 2006).

Actomyosin Regulation by Rho and Rac Proteins

Actomyosin regulation in response to cell surface receptors is controlled by GTP binding proteins of the Rho family. Of particular relevance to this thesis are the small GTPases RhoA and Rac1. Activation of RhoA increases actomyosin contractility by increasing phosphorylation of the myosin II regulatory light chain (MLC) (Chrzanowska-Wodnicka and Burridge, 1996). Increased phosphorylation of the MLC can be achieved via 2 separate Rho signaling pathways; first, activated Rho stimulates MLC kinase and Rho-kinases (ROCK, ROK) to phosphorylate MLC (Amano et al., 1996), and secondly, Rho-like GTPases are also able to inhibit MLC phosphatases (Kimura et al., 1996).

The effects of Rac1 on actomyosin function are often opposite to that of Rho. Rac activation by stimulation of growth factor receptors causes lamellipod formation and membrane ruffling (Ridley et al., 1992). The driving force for lamellipodia formation and membrane ruffling is Rac-induced actin polymerization. Rac can accomplish this through activation of the Arp2/3 complex which associates with members of the conserved WASP family (Miki et al., 2000; Eden et al., 2002). While Rho activity is the major determinant of actomyosin contraction, the small GTPase Rac1 promotes actomyosin relaxation by antagonizing RhoA (van Leeuwen et al., 1997; Kozma et al., 1997). A similar Rho/Rac antagonism was shown to be important during the formation and maintenance of focal adhesions (Rottner et al., 1999). As all of these studies show, myosin II is the endpoint of pathways that control cellular tension.

Regulation of Rho and Rac Activity

In common with other small GTPases, Rho and Rac act as molecular switches. Inactive small GTPases are in a GDP-bound state, and receptor stimulation causes activation by stimulating exchange of GDP for GTP. Hydrolysis of GTP by the intrinsic, low GTPase activity of these proteins terminates the activated state. Three types of regulatory proteins influence this balance: Guanine Nucleotide exchange Factors (GEFs) that speed up the exchange of GDP for GTP, GTPase Activating Proteins (GAPs) that dramatically enhance the low intrinsic GTPase activity, and GTPase Dissociation Inhibitors (GDIs) that stabilize small GTPases in

their inactive conformation (Nobes and Hall, 1995). It is the active conformation of the small GTPases that is located primarily at membranes and that interacts with the target proteins.

The mode of activation of Rho and Rac is complex and involves several signaling pathways. $G\alpha_{12/13}$-coupled receptors such as those for LPA and thrombin can trigger Rho via GAPs (Jalink et al., 1994; Hart et al., 1998; Kozasa et al., 1998). In addition, we found a new PKC mediated signaling pathway that leads to increased Rac activity at the plasma-membrane: elevation of cytosolic Ca^{2+}, originating either from intracellular stores or extracellular Ca^{2+} entry, sufficed to activate a Ca^{2+}-sensitive PKC that in turn enhanced Rac translocation to the plasma-membrane (Chapter 5, (Price et al., 2003).

To add to the regulatory complexity, Rac can bind to and activate both PI(4,5)-kinase and PI(3)-kinase (Tolias et al., 1995). Inhibition of PI(3)-kinase, the kinase that produces PIP_3 from PIP_2 at the membrane, prevented growth factor induced membrane ruffling but could not block ruffling induced by expression of activated Rac (Nobes and Hall, 1995). Many RacGEFs are capable of binding to PIP_2 and PIP_3 with their PH-domain, and recruit Rac GTPases to the plasma-membrane to activate them (Schmidt and Hall, 2002; Mertens et al., 2003). In addition to phosphoinositide dependent activation, binding of the p85 subunit of PI(3)-kinase to RacGEFs also results in activation of Rac (Innocenti et al., 2003).

Rac and Rho Mediated Formation and Maturation of Adhesive Structures

Both Rho and Rac are involved in formation and maturation of focal adhesion structures. Focal adhesions are large multi-protein complexes that anchor cells to the extracellular matrix and function as attachment for stress fibers. Cells can sense mechanical forces through focal adhesions, and the cytoskeleton is strongly influenced by these mechanical forces. I will here review some of the literature on this topic to provide a background for the work presented in Chapter 4 & 5.

Focal complexes arise from nascent integrin containing adhesive contacts that form at the leading edge of migrating cells and can grow out to focal adhesions. The formation of focal complexes depends on Rac, but not Rho (Rottner

et al., 1999), but what triggers their formation is not well understood. When cells attach to the extracellular matrix, translocation of Rac to the plasma-membrane (del Pozo et al., 2000) may trigger the formation of focal complexes by inducing actin polymerization and branching followed by integrin clustering (Kraynov et al., 2000). Different Rac effectors may mediate these effects. Activation of PI(5)P-kinases mediated by Rac increases PIP_2 levels, which results in uncapping of actin filaments (Tolias et al., 2000). Other effectors implicated in focal complex formation are the WAVE/Scar complex (Machesky et al., 1999) and the serine-threonine kinase PAK (Edwards et al., 1999).

The maturation of focal complexes to focal adhesions requires activation of RhoA, although again, the exact mechanism is still poorly understood. It has been shown that the combined action of 2 Rho effectors, Rho kinase ROCK and diaphanous protein Dia1, can substitute for active Rho in the process of focal adhesion assembly (Watanabe et al., 1999). It was suggested, on the based on rather indirect evidence, that Dia promotes actin polymerization by targeting profilin and possibly by enhancing its function (Watanabe et al., 1997). Furthermore, similar to WASP, Dia may directly activate Arp2/3 (Alberts, 2001). On the other hand, formation of focal adhesions relies on increased myosin II-mediated contractility which is due to increased myosin light chain phosphorylation by inactivation of MLC phosphatases and/or activation of MLC kinases (Amano et al., 2000).

Podosomes are a third type of cell-matrix adhesion relevant for this thesis. Podosomes are integrin containing adhesions, clearly distinct from focal adhesions, which are a characteristic feature of cells that have the capacity to cross tissue boundaries. Examples are monocyte-derived cells (Marchisio et al., 1984) but also carcinoma-derived epithelial cells (Spinardi et al., 2004). Podosomes are anchored to the extracellular matrix through integrins and can develop from existing focal adhesions (Moreau et al., 2006) or are *de novo* synthesized by attachment to the matrix (Gaidano et al., 1990). Podosomes have a distinct dense core of F-actin and each podosome is surrounded by ring structure enriched proteins such as vinculin, α-actinin (David-Pfeuty et al., 1980) and regulators of contractility, e.g. myosin II isoforms and TRPM7 (Clark et al., 2006). Podosome structures share similarities with focal adhesion but contrast on several points. First of all, the actin core of podosomes contains proteins that regulate

actin polymerization, such as WASP, Arp2/3 and gelsolin that are absent in focal adhesions (Marchisio et al., 1988). Second, formation of podosomes frequently occurs from rapid and dynamic turnover of pre-existing podosomes (Stickel and Wang, 1987), while focal adhesions are less dynamic and formation requires continuous protein synthesis. At last, podosomes may remodel and tubulate the plasma-membrane (Burgstaller and Gimona, 2005). Furthermore ECM-degrading metalloproteases localize to podosomes (Sato et al. 1997; Delaisse et al. 2000). These observations point out that podosomes are necessary for extracellular matrix degradation.

Cellular Mechanisms Detecting Mechanical Forces

Cells and their cytoskeleton are continuously subjected to mechanical forces due to both physical interactions with the extracellular matrix and their own contractile machinery. Sensing mechanical forces induced by the cells' environment is critical for processes such as motility, adhesion, proliferation and apoptosis (Geiger et al., 2001; Burridge and Wennerberg, 2004). Therefore, cells have developed "force receptors" for mechanosensing that are still poorly characterized. Two types of protein complexes have been proposed to sense these forces, namely focal adhesions and ion channels. As we speculate (Chapter 4) that TRPM7 may act as a mechanosensor, or is involved in mechano-sensation, I will here discuss this topic to provide a background.

Focal Adhesions and Sensing of Mechanical Forces

Several lines of evidence indicate that integrin-mediated adhesion is involved in sensing mechanical stress. Application of forces to cells causes strengthening of their anchorage to the extracellular matrix. This depends on both clustering and occupancy of the integrins that link the cytoskeleton to the extracellular matrix at the adhesion sites (Wang et al., 1993; Choquet et al., 1997; Geiger et al., 2001). Focal adhesions are capable of adjusting their size to the degree of mechanical force applied. Application of force to either the cell (Riveline et al., 2001) or to the (flexible) matrix (Wang et al., 2001) transforms the focal complexes into mature focal adhesions.

The tension that focal adhesions "sense" regulates both their maintenance and growth. Relieve of this tension, by inhibition of myosin-driven contractility, causes rapid disassembly of focal adhesions (Geiger et al., 2001). Furthermore, applied tension also determines the vinculin content in focal adhesions (Opazo et al., 2004). These local effects of force-induced changes in integrin-mediated adhesion indicate that focal adhesions can act as sensors for detection of internal or external forces.

How exactly focal adhesions detect forces is still poorly understood. One possibility is that tension reorganizes the molecular structure of focal adhesions, thus allowing additional cytosolic components to be incorporated. Force-driven maturation of focal complexes to focal adhesions is accompanied by an increase in $\alpha_v\beta_3$ integrins (Ballestrem et al., 2001). Furthermore, β_3 integrins can move into individual focal adhesions in an energy- and myosin II-dependent manner (Tsuruta et al., 2002)). Another possible mechanism relies on intrinsic properties of some of the molecules of the focal adhesion complex. Focal adhesion associated proteins like vinculin, fibronectin and possibly $\alpha\beta$ integrin dimers exist in an active (open) or inactive (closed) conformation (Alberts, 2001; DeMali et al., 2002). Normally, the transition between active and inactive conformation results from signaling involving kinases, phosphatases and changes in membrane lipid composition, but Geiger hypothesized that mechanical forces may similarly expose previously hidden interaction sites (Geiger et al., 2001).

Mechanosensation by Ion Channels

Membrane tension caused by mechanical forces can also be sensed by specialized ion channels (Gustin et al., 1988; Martinac, 2004). A wide variety of mechanosensitive or stretch-activated channels (SAC) are found in all prokaryotic and eukaryotic cells. In eukaryotic cells, 4 different families of ion channels have been implicated in sensing mechanical forces: the mechano-sensitive K^+ channels TREK and TRAAK, Na^+-selective MEC/DEG (for mechanosensory abnormal/degenerins) channels, ClC Cl^- channels and TRP channels.

Other ion channels potentially involved in sensing mechanical forces are linked to the actin cytoskeleton and protein complexes within focal adhesions. In flies it has been demonstrated that the TRP family member TRPN1 (NOMPC), which

binds to actin via the channels N-terminal ankyrin repeats, contributes to bristle mechanosensation (Walker et al., 2000) and the zebrafish homologue mediates mechanoreception in hair cells (Sidi et al., 2003). Mammals do not have a TRPN1 homologue, but recently the TRPA1 channel was implicated in mammalian nociception and hair cell transduction (Nagata et al., 2005).

Two modes of force detection by ion channels have been suggested. First, changes in intrinsic forces (lateral pressure) generated by lipid bilayer composition may regulate channel opening and closure (Kung, 2005). Secondly, mechanical tension may be transduced via either intracellular linkers (mainly the actin cytoskeleton) or external anchors to the channel pore to modulate the intracellular ion concentration (Gillespie, 2002). In this view, Howard hypothesized that the repetitive ankyrin repeats of TRPN1 form a helical turn that can act as a gating spring for channel opening (Howard and Bechstedt, 2004). Mechanosensation is not limited to specialized cells in sensory organs, but all adherent cells can sense mechanical forces. The external environment is probed by cells by applying actomyosin-driven forces to cell-matrix or cell-cell adhesion sites. In turn, the adhesion sites respond to these forces by changes in size, dynamic behavior and by signaling events (Geiger et al., 2001).

In view of the above, it is tempting to speculate that TRPM7 may act as a mechanosensory channel. Interestingly, in endothelial cells it was recently shown that TRPM7 ion channels become embedded into the plasma-membrane in response to fluid flow shear forces (Oancea et al., 2006). This may cause local Ca^{2+} influx at the plasma-membrane through TRPM7 channels located around focal adhesions. Subsequent Ca^{2+}-dependent myosin II phosphorylation or other TRPM7-mediated effects on MHC IIA activity, may induce the transformation of focal adhesions into podosomes as well as contribute to *de novo* formation of podosomal-like adhesions (Clark et al., 2006). Similarly, a recent report of Su et. al. has also implicated TRPM7 in regulation of cell adhesion (Su et al., 2006)

Overview of This Thesis

In this thesis, we address the regulation of TRPM7 channels by receptor-mediated signals and the effects of the ensuing ionic signals on the cytoskeleton. In **Chapter 2** signaling pathways

were investigated that activate TRPM7 channel opening. We show that PLC-activating receptors open TRPM7 channels, leading to influx of extracellular Ca^{2+}. The results presented in this chapter contrast markedly with a report by Runnels et al that appeared during our studies who showed inhibition of TRPM7, rather than activation, by PLC. In **Chapter 3** we present experiments that explain these discrepancies: we explored the differences in PIP$_2$-mediated regulation of TRPM7 measured in perforated-patch and whole-cell configuration after intracellular Mg^{2+} depletion. This leads us to propose that the effects of PLC activation on TRPM7 currents as detected in whole cells can best be viewed as 'accelerated rundown' rather than as bona fide signal transduction.

In **Chapter 4** we examine how agonist-induced TRPM7 activation and subsequent Ca^{2+} influx affect the cytoskeleton. It is shown that TRPM7 phosphorylates the myosin II heavy chain to promote cytoskeletal relaxation and the conversion of focal adhesions to podosomes. Ca^{2+} influx appears crucial for the *in vivo* function of the TRPM7-kinase by triggering the association between the kinase and its substrate. In **Chapter 5**, we report that receptor-mediated Ca^{2+} influx can affect the cytoskeleton by translocating Rac in a PKC-dependent manner to the plasma-membrane, where it induces extensive membrane ruffling.

In conclusion, intracellular Ca^{2+} elevations agonist-induced due to channel activation affects the actin cytoskeleton in multiple ways.

References

Aarts,M., K.Iihara, W.L.Wei, Z.G.Xiong, M.Arundine, W.Cerwinski, J.F.MacDonald, and M.Tymianski. 2003. A key role for TRPM7 channels in anoxic neuronal death. *Cell* 115:863-877.

Acharya,J.K., K.Jalink, R.W.Hardy, V.Hartenstein, and C.S.Zuker. 1997. InsP3 receptor is essential for growth and differentiation but not for vision in Drosophila. *Neuron* 18:881-887.

Alberts,A.S. 2001. Identification of a carboxyl-terminal diaphanous-related formin homology protein autoregulatory domain. *J. Biol. Chem.* 276:2824-2830.

Alvarez-Martinez,M.T., J.C.Mani, F.Porte, C.Faivre-Sarrailh, J.P.Liautard, and W.J.Sri. 1996. Characterization of the interaction between annexin I and profilin. *Eur. J. Biochem.* 238:777-784.

Amano,M., Y.Fukata, and K.Kaibuchi. 2000. Regulation and functions of Rho-associated kinase. *Exp. Cell Res.* 261:44-51.

Amano,M., M.Ito, K.Kimura, Y.Fukata, K.Chihara, T.Nakano, Y.Matsuura, and K.Kaibuchi. 1996. Phosphorylation and activation of myosin by Rho-associated kinase (Rho-kinase). *J. Biol. Chem.* 271:20246-20249.

Andersson,D.A., H.W.Chase, and S.Bevan. 2004. TRPM8 activation by menthol, icilin, and cold is differentially modulated by intracellular pH. *J. Neurosci.* 24:5364-5369.

Balla,T. 2001. Pharmacology of phosphoinositides, regulators of multiple cellular functions. *Curr. Pharm. Des* 7:475-507.

Ballestrem,C., B.Hinz, B.A.Imhof, and B.Wehrle-Haller. 2001. Marching at the front and dragging behind: differential alphaVbeta3-integrin turnover regulates focal adhesion behavior. *J. Cell Biol.* 155:1319-1332.

Belkacemi,L., I.Bedard, L.Simoneau, and J.Lafond. 2005. Calcium channels, transporters and exchangers in placenta: a review. *Cell Calcium* 37:1-8.

Bergdahl,A., M.F.Gomez, K.Dreja, S.Z.Xu, M.Adner, D.J.Beech, J.Broman, P.Hellstrand, and K.Sward. 2003. Cholesterol depletion impairs vascular reactivity to endothelin-1 by reducing store-operated Ca2+ entry dependent on TRPC1. *Circ. Res.* 93:839-847.

Berridge,M.J., P.Lipp, and M.D.Bootman. 2000. The versatility and universality of calcium signalling. *Nat. Rev. Mol. Cell Biol.* 1:11-21.

Bezzerides,V.J., I.S.Ramsey, S.Kotecha, A.Greka, and D.E.Clapham. 2004. Rapid vesicular translocation and insertion of TRP channels. *Nat. Cell Biol.* 6:709-720.

Bolotina,V.M. 2004. Store-operated channels: diversity and activation mechanisms. *Sci. STKE.* 2004:e34.

Burgstaller,G. and M.Gimona. 2005. Podosome-mediated matrix resorption and cell motility in vascular smooth muscle cells. *Am. J. Physiol Heart Circ. Physiol* 288:H3001-H3005.

Burridge,K. and M.Chrzanowska-Wodnicka. 1996. Focal adhesions, contractility, and signaling. *Annu. Rev. Cell Dev. Biol.* 12:463-518.

Burridge,K., K.Fath, T.Kelly, G.Nuckolls, and C.Turner. 1988. Focal adhesions: transmembrane junctions between the extracellular matrix and the cytoskeleton. *Annu. Rev. Cell Biol.* 4:487-525.

Burridge,K. and K.Wennerberg. 2004. Rho and Rac take center stage. *Cell* 116:167-179.

Cahalan,M.D. 2001. Cell biology. Channels as enzymes. *Nature* 411:542-543.

Campos-Gonzalez,R., M.Kanemitsu, and A.L.Boynton. 1990. Epidermal growth factor induces the accumulation of calpactin II on the cell surface during membrane ruffling. *Cell Motil. Cytoskeleton* 15:34-40.

Caterina,M.J., A.Leffler, A.B.Malmberg, W.J.Martin, J.Trafton, K.R.Petersen-Zeitz, M.Koltzenburg, A.I.Basbaum, and D.Julius. 2000. Impaired nociception and pain sensation in mice lacking the capsaicin receptor. *Science* 288:306-313.

Caterina,M.J., T.A.Rosen, M.Tominaga, A.J.Brake, and D.Julius. 1999. A capsaicin-receptor homologue with a high threshold for noxious heat. *Nature* 398:436-441.

Caterina,M.J., M.A.Schumacher, M.Tominaga, T.A.Rosen, J.D.Levine, and D.Julius. 1997. The capsaicin receptor: a heat-activated ion channel in the pain pathway. *Nature* 389:816-824.

Choquet,D., D.P.Felsenfeld, and M.P.Sheetz. 1997. Extracellular matrix rigidity causes strengthening of integrin-cytoskeleton linkages. *Cell* 88:39-48.

Chrzanowska-Wodnicka,M. and K.Burridge. 1996. Rho-stimulated contractility drives the formation of stress fibers and focal adhesions. *J. Cell Biol.* 133:1403-1415.

Chuang,H.H., E.D.Prescott, H.Kong, S.Shields, S.E.Jordt, A.I.Basbaum, M.V.Chao, and D.Julius. 2001. Bradykinin and nerve growth factor release the capsaicin receptor from PtdIns(4,5)P2-mediated inhibition. *Nature* 411:957-962.

Chubanov,V., S.Waldegger, M.Schnitzler, H.Vitzthum, M.C.Sassen, H.W.Seyberth, M.Konrad, and T.Gudermann. 2004. Disruption of TRPM6/TRPM7 complex formation by a mutation in the TRPM6 gene causes hypomagnesemia with secondary hypocalcemia. *Proc. Natl. Acad. Sci. U. S. A* 101:2894-2899.

Chyb,S., P.Raghu, and R.C.Hardie. 1999. Polyunsaturated fatty acids activate the Drosophila light-sensitive channels TRP and TRPL. *Nature* 397:255-259.

Clapham,D.E. 1995. Intracellular calcium. Replenishing the stores. *Nature* 375:634-635.

Clapham,D.E. 2003. TRP channels as cellular sensors. *Nature* 426:517-524.

Clapham,D.E., C.Montell, G.Schultz, and D.Julius. 2003. International Union of Pharmacology. XLIII. Compendium of voltage-gated ion channels: transient receptor potential channels. *Pharmacol. Rev.* 55:591-596.

Clark,K., M.Langeslag, L.B.van, L.Ran, A.G.Ryazanov, C.G.Figdor, W.H.Moolenaar, K.Jalink, and F.N.van Leeuwen. 2006. TRPM7, a novel regulator of actomyosin contractility and cell adhesion. *EMBO J.* 25:290-301.

Colbert,H.A., T.L.Smith, and C.I.Bargmann. 1997. OSM-9, a novel protein with structural similarity to channels, is required for olfaction, mechanosensation, and olfactory adaptation in Caenorhabditis elegans. *J. Neurosci.* 17:8259-8269.

Cook,B. and B.Minke. 1999. TRP and calcium stores in Drosophila phototransduction. *Cell Calcium* 25:161-171.

Dabdoub,A. and R.Payne. 1999. Protein kinase C activators inhibit the visual cascade in Limulus ventral photoreceptors at an early stage. *J. Neurosci.* 19:10262-10269.

Dai,L.J., B.Bapty, G.Ritchie, and G.A.Quamme. 1998. Glucagon and arginine vasopressin stimulate Mg2+

uptake in mouse distal convoluted tubule cells. *Am. J. Physiol* 274:F328-F335.

David-Pfeuty, ., and S.J.Singer. 1980. Altered distributions of the cytoskeletal proteins vinculin and alpha-actinin in cultured fibroblasts transformed by Rous sarcoma virus. *Proc. Natl. Acad. Sci. U. S. A* 77:6687-6691.

De Koninck,K.P. and H.Schulman. 1998. Sensitivity of CaM kinase II to the frequency of Ca2+ oscillations. *Science* 279:227-230.

del Pozo,M.A., L.S.Price, N.B.Alderson, X.D.Ren, and M.A.Schwartz. 2000. Adhesion to the extracellular matrix regulates the coupling of the small GTPase Rac to its effector PAK. *EMBO J.* 19:2008-2014.

Delaisse,J.M., M.T.Engsig, V.Everts, M.del Carmen Ovejero, M.Ferreras, L.Lund, T.H.Vu, Z.Werb, B.Winding, A.Lochter, M.A.Karsdal, T.Troen, T.Kirkegaard, T.Lenhard, A.M.Heegaard, L.Neff, R.Baron, N.T.Foged. 2000. Proteinases in bone resorption: obvious and less obvious roles. *Clin. Chim. Acta* 291, 223–234

Deland,M.C. and W.L.Pak. 1973. Reversibly temperature sensitive phototransduction mutant of Drosophila melanogaster. *Nat. New Biol.* 244:184-186.

DeMali,K.A., C.A.Barlow, and K.Burridge. 2002. Recruitment of the Arp2/3 complex to vinculin: coupling membrane protrusion to matrix adhesion. *J. Cell Biol.* 159:881-891.

Demeuse,P., R.Penner, and A.Fleig. 2006. TRPM7 Channel Is Regulated by Magnesium Nucleotides via its Kinase Domain. *J. Gen. Physiol* 127:421-434.

den Dekker,D.E., J.G.Hoenderop, B.Nilius, and R.J.Bindels. 2003. The epithelial calcium channels, TRPV5 & TRPV6: from identification towards regulation. *Cell Calcium* 33:497-507.

Devary,O., O.Heichal, A.Blumenfeld, D.Cassel, E.Suss, S.Barash, C.T.Rubinstein, B.Minke, and Z.Selinger. 1987. Coupling of photoexcited rhodopsin to inositol phospholipid hydrolysis in fly photoreceptors. *Proc. Natl. Acad. Sci. U. S. A* 84:6939-6943.

Dolmetsch,R.E., R.S.Lewis, C.C.Goodnow, and J.I.Healy. 1997. Differential activation of transcription factors induced by Ca2+ response amplitude and duration. *Nature* 386:855-858.

Dolmetsch,R.E., K.Xu, and R.S.Lewis. 1998. Calcium oscillations increase the efficiency and specificity of gene expression. *Nature* 392:933-936.

Dorovkov,M.V. and A.G.Ryazanov. 2004. Phosphorylation of annexin I by TRPM7 channel-kinase. *J. Biol. Chem.* 279:50643-50646.

Doyle,D.A., C.J.Morais, R.A.Pfuetzner, A.Kuo, J.M.Gulbis, S.L.Cohen, B.T.Chait, and R.MacKinnon. 1998. The structure of the potassium channel: molecular basis of K+ conduction and selectivity. *Science* 280:69-77.

Duncan,L.M., J.Deeds, J.Hunter, J.Shao, L.M.Holmgren, E.A.Woolf, R.I.Tepper, and A.W.Shyjan. 1998. Down-regulation of the novel gene melastatin correlates with potential for melanoma metastasis. *Cancer Res.* 58:1515-1520.

Ebashi,S. and Y.Ogawa. 1988. Ca2+ in contractile processes. *Biophys. Chem.* 29:137-143.

Eden,S., R.Rohatgi, A.V.Podtelejnikov, M.Mann, and M.W.Kirschner. 2002. Mechanism of regulation of WAVE1-induced actin nucleation by Rac1 and Nck. *Nature* 418:790-793.

Edwards,D.C., L.C.Sanders, G.M.Bokoch, and G.N.Gill. 1999. Activation of LIM-kinase by Pak1 couples Rac/Cdc42 GTPase signalling to actin cytoskeletal dynamics. *Nat. Cell Biol.* 1:253-259.

Ehler,E., L.F.van, J.G.Collard, and P.C.Salinas. 1997. Expression of Tiam-1 in the developing brain suggests a role for the Tiam-1-Rac signaling pathway in cell migration and neurite outgrowth. *Mol. Cell Neurosci.* 9:1-12.

Elizondo,M.R., B.L.Arduini, J.Paulsen, E.L.MacDonald, J.L.Sabel, P.D.Henion, R.A.Cornell, and D.M.Parichy. 2005. Defective skeletogenesis with kidney stone formation in dwarf zebrafish mutant for trpm7. *Curr. Biol.* 15:667-671.

Engelke,M., O.Friedrich, P.Budde, C.Schafer, U.Niemann, C.Zitt, E.Jungling, O.Rocks, A.Luckhoff, and J.Frey. 2002. Structural domains required for channel function of the mouse transient receptor potential protein homologue TRP1beta. *FEBS Lett.* 523:193-199.

Enklaar,T., M.Esswein, M.Oswald, K.Hilbert, A.Winterpacht, M.Higgins, B.Zabel, and D.Prawitt. 2000. Mtr1, a novel biallelically expressed gene in the center of the mouse distal chromosome 7 imprinting cluster, is a member of the Trp gene family. *Genomics* 67:179-187.

Estacion,M., W.G.Sinkins, and W.P.Schilling. 2001. Regulation of Drosophila transient receptor potential-like (TrpL) channels by phospholipase C-dependent mechanisms. *J. Physiol* 530:1-19.

Fang,D. and V.Setaluri. 2000. Expression and Up-regulation of alternatively spliced transcripts of melastatin, a melanoma metastasis-related gene, in human melanoma cells. *Biochem. Biophys. Res. Commun.* 279:53-61.

Felix,R. 2005. Molecular regulation of voltage-gated Ca2+ channels. *J. Recept. Signal. Transduct. Res.* 25:57-71.

Feray,J.C. and R.Garay. 1986. An Na+-stimulated Mg2+-transport system in human red blood cells. *Biochim. Biophys. Acta* 856:76-84.

Fields,R.D., P.R.Lee, and J.E.Cohen. 2005. Temporal integration of intracellular Ca2+ signaling networks in regulating gene expression by action potentials. *Cell Calcium* 37:433-442.

Freichel,M., S.H.Suh, A.Pfeifer, U.Schweig, C.Trost, P.Weissgerber, M.Biel, S.Philipp, D.Freise, G.Droogmans, F.Hofmann, V.Flockerzi, and B.Nilius. 2001. Lack of an endothelial store-operated Ca2+ current impairs agonist-dependent vasorelaxation in TRP4-/- mice. *Nat. Cell Biol.* 3:121-127.

Gaidano,G., L.Bergui, M.Schena, M.Gaboli, O.Cremona, P.C.Marchisio, and F.Caligaris-Cappio. 1990. Integrin distribution and cytoskeleton organization in normal and malignant monocytes. *Leukemia* 4:682-687.

Garcia,R.L. and W.P.Schilling. 1997. Differential expression of mammalian TRP homologues across tissues and cell lines. *Biochem. Biophys. Res. Commun.* 239:279-283.

Garcia-Martinez,C., C.Morenilla-Palao, R.Planells-Cases, J.M.Merino, and A.Ferrer-Montiel. 2000. Identification of an aspartic residue in the P-loop of the vanilloid receptor that modulates pore properties. *J. Biol. Chem.* 275:32552-32558.

Garfinkel,L., R.A.Altschuld, and D.Garfinkel. 1986. Magnesium in cardiac energy metabolism. *J. Mol. Cell Cardiol.* 18:1003-1013.

Gaussin,V., P.Gailly, J.M.Gillis, and L.Hue. 1997. Fructose-induced increase in intracellular free Mg2+ ion concentration in rat hepatocytes: relation with the enzymes of glycogen metabolism. *Biochem. J.* 326 (Pt 3):823-827.

Geiger,B., A.Bershadsky, R.Pankov, and K.M.Yamada. 2001. Transmembrane crosstalk between the extracellular matrix--cytoskeleton crosstalk. *Nat. Rev. Mol. Cell Biol.* 2:793-805.

Gillespie,P.G. 2002. Myosin-VIIa and transduction channel tension. *Nat. Neurosci.* 5:3-4.

Goel,M., W.G.Sinkins, and W.P.Schilling. 2002. Selective association of TRPC channel subunits in rat brain synaptosomes. *J. Biol. Chem.* 277:48303-48310.

Greka,A., B.Navarro, E.Oancea, A.Duggan, and D.E.Clapham. 2003. TRPC5 is a regulator of hippocampal neurite length and growth cone morphology. *Nat. Neurosci.* 6:837-845.

Grimm,C., R.Kraft, S.Sauerbruch, G.Schultz, and C.Harteneck. 2003. Molecular and functional characterization of the melastatin-related cation channel TRPM3. *J. Biol. Chem.* 278:21493-21501.

Grimm,C., R.Kraft, G.Schultz, and C.Harteneck. 2005. Activation of the melastatin-related cation channel TRPM3 [corrected] by D-erythro-sphingosine. *Mol. Pharmacol.* 67:798-805.

Griswold,R.L. and N.Pace. 1956. The intracellular distribution of metal ions in rat liver. *Exp. Cell Res.* 11:362-367.

Guerrero-Hernandez,A., L.Gomez-Viquez, G.Guerrero-Serna, and A.Rueda. 2002. Ryanodine receptors in smooth muscle. *Front Biosci.* 7:d1676-d1688.

Guler,A.D., H.Lee, T.Iida, I.Shimizu, M.Tominaga, and M.Caterina. 2002. Heat-evoked activation of the ion channel, TRPV4. *J. Neurosci.* 22:6408-6414.

Gunther,T. 1986. Functional compartmentation of intracellular magnesium. *Magnesium* 5:53-59.

Gunther,T. and V.Hollriegl. 1993. Na(+)- and anion-dependent Mg2+ influx in isolated hepatocytes. *Biochim. Biophys. Acta* 1149:49-54.

Gunther,T., M.Rucker, C.Forster, J.Vormann, and R.Stahlmann. 1997. In vitro evidence for a Donnan distribution of Mg2+ and Ca2+ by chondroitin sulphate in cartilage. *Arch. Toxicol.* 71:471-475.

Gunther,T. and J.Vormann. 1990. Na(+)-dependent Mg2+ efflux from Mg(2+)-loaded rat thymocytes and HL 60 cells. *Magnes. Trace Elem.* 9:279-282.

Gunther,T. and J.Vormann. 1992. Activation of Na+/Mg2+ antiport in thymocytes by cAMP. *FEBS Lett.* 297:132-134.

Gunther,T. and J.Vormann. 1991. Mg2+ influx into Mg(2+)-depleted reticulocytes. *Magnes. Trace Elem.* 10:17-20.

Gunther,T., J.Vormann, and V.Hollriegl. 1990. Characterization of Na(+)-dependent Mg2+ efflux from Mg(2+)-loaded rat erythrocytes. *Biochim. Biophys. Acta* 1023:455-461.

Gunther,T., J.Vormann, and H.J.Merker. 1984. Effect of magnesium injection on foetal development. *J. Clin. Chem. Clin. Biochem.* 22:473-478.

Gustin,M.C., X.L.Zhou, B.Martinac, and C.Kung. 1988. A mechanosensitive ion channel in the yeast plasma membrane. *Science* 242:762-765.

Gylfe,E. 1990. Insulin secretagogues induce Ca(2+)-like changes in cytoplasmic Mg2+ in pancreatic beta-cells. *Biochim. Biophys. Acta* 1055:82-86.

Hanano,T., Y.Hara, J.Shi, H.Morita, C.Umebayashi, E.Mori, H.Sumimoto, Y.Ito, Y.Mori, and R.Inoue. 2004. Involvement of TRPM7 in cell growth as a spontaneously activated Ca2+ entry pathway in human retinoblastoma cells. *J. Pharmacol. Sci.* 95:403-419.

Handy,R.D., I.F.Gow, D.Ellis, and P.W.Flatman. 1996. Na-dependent regulation of intracellular free magnesium concentration in isolated rat ventricular myocytes. *J. Mol. Cell Cardiol.* 28:1641-1651.

Hara,Y., M.Wakamori, M.Ishii, E.Maeno, M.Nishida, T.Yoshida, H.Yamada, S.Shimizu, E.Mori, J.Kudoh, N.Shimizu, H.Kurose, Y.Okada, K.Imoto, and Y.Mori. 2002. LTRPC2 Ca2+-permeable channel activated by changes in redox status confers susceptibility to cell death. *Mol. Cell* 9:163-173.

Hardie,R.C. 1995. Photolysis of caged Ca2+ facilitates and inactivates but does not directly excite light-sensitive channels in Drosophila photoreceptors. *J. Neurosci.* 15:889-902.

Hardie,R.C. 1996. Excitation of Drosophila photoreceptors by BAPTA and ionomycin: evidence for capacitative Ca2+ entry? *Cell Calcium* 20:315-327.

Hardie,R.C. and B.Minke. 1992. The trp gene is essential for a light-activated Ca2+ channel in Drosophila photoreceptors. *Neuron* 8:643-651.

Hardie,R.C., P.Raghu, S.Moore, M.Juusola, R.A.Baines, and S.T.Sweeney. 2001. Calcium influx via TRP channels is required to maintain PIP2 levels in Drosophila photoreceptors. *Neuron* 30:149-159.

Hart,M.J., X.Jiang, T.Kozasa, W.Roscoe, W.D.Singer, A.G.Gilman, P.C.Sternweis, and G.Bollag. 1998. Direct stimulation of the guanine nucleotide exchange activity of p115 RhoGEF by Galpha13. *Science* 280:2112-2114.

Hellwig,N., N.Albrecht, C.Harteneck, G.Schultz, and M.Schaefer. 2005. Homo- and heteromeric assembly of TRPV channel subunits. *J. Cell Sci.* 118:917-928.

Hering,S., S.Berjukow, S.Sokolov, R.Marksteiner, R.G.Weiss, R.Kraus, and E.N.Timin. 2000. Molecular determinants of inactivation in voltage-gated Ca2+ channels. *J. Physiol* 528 Pt 2:237-249.

Hermosura,M.C., H.Nayakanti, M.V.Dorovkov, F.R.Calderon, A.G.Ryazanov, D.S.Haymer, and R.M.Garruto. 2005. A TRPM7 variant shows altered sensitivity to magnesium that may contribute to the pathogenesis of two Guamanian neurodegenerative disorders. *Proc. Natl. Acad. Sci. U. S. A* 102:11510-11515.

Hoenderop,J.G. and R.J.Bindels. 2005. Epithelial Ca2+ and Mg2+ channels in health and disease. *J. Am. Soc. Nephrol.* 16:15-26.

Hoenderop,J.G., T.Voets, S.Hoefs, F.Weidema, J.Prenen, B.Nilius, and R.J.Bindels. 2003. Homo- and heterotetrameric architecture of the epithelial Ca2+ channels TRPV5 and TRPV6. *EMBO J.* 22:776-785.

Hofmann,T., V.Chubanov, T.Gudermann, and C.Montell. 2003. TRPM5 is a voltage-modulated and Ca(2+)-activated monovalent selective cation channel. *Curr. Biol.* 13:1153-1158.

Hofmann,T., M.Schaefer, G.Schultz, and T.Gudermann. 2002. Subunit composition of mammalian transient receptor potential channels in living cells. *Proc. Natl. Acad. Sci. U. S. A* 99:7461-7466.

Hofmann,T., M.Schaefer, G.Schultz, and T.Gudermann. 2000. Cloning, expression and subcellular localization of two novel splice variants of mouse transient receptor potential channel 2. *Biochem. J.* 351:115-122.

Horowitz,L.F., W.Hirdes, B.C.Suh, D.W.Hilgemann, K.Mackie, and B.Hille. 2005. Phospholipase C in living cells: activation, inhibition, Ca2+ requirement, and regulation of M current. *J. Gen. Physiol* 126:243-262.

Hoth,M. and R.Penner. 1992. Depletion of intracellular calcium stores activates a calcium current in mast cells. *Nature* 355:353-356.

Hoth,M. and R.Penner. 1993. Calcium release-activated calcium current in rat mast cells. *J. Physiol* 465:359-386.

Howard,J. and S.Bechstedt. 2004. Hypothesis: a helix of ankyrin repeats of the NOMPC-TRP ion channel is the gating spring of mechanoreceptors. *Curr. Biol.* 14:R224-R226.

Howarth,F.C., J.Waring, B.I.Hustler, and J.Singh. 1994. Effects of extracellular magnesium and beta adrenergic stimulation on contractile force and magnesium mobilization in the isolated rat heart. *Magnes. Res.* 7:187-197.

Hu,H.Z., Q.Gu, C.Wang, C.K.Colton, J.Tang, M.Kinoshita-Kawada, L.Y.Lee, J.D.Wood, and M.X.Zhu. 2004. 2-aminoethoxydiphenyl borate is a common activator of TRPV1, TRPV2, and TRPV3. *J. Biol. Chem.* 279:35741-35748.

Huang,R.D., M.F.Smith, and W.L.Zahler. 1982. Inhibition of forskolin-activated adenylate cyclase by ethanol and other solvents. *J. Cyclic. Nucleotide. Res.* 8:385-394.

Hunter,T. 1995. When is a lipid kinase not a lipid kinase? When it is a protein kinase. *Cell* 83:1-4.

Hwang,S.W. and U.Oh. 2002. Hot channels in airways: pharmacology of the vanilloid receptor. *Curr. Opin. Pharmacol.* 2:235-242.

Innocenti,M., E.Frittoli, I.Ponzanelli, J.R.Falck, S.M.Brachmann, P.P.Di Fiore, and G.Scita. 2003. Phosphoinositide 3-kinase activates Rac by entering in a complex with Eps8, Abi1, and Sos-1. *J. Cell Biol.* 160:17-23.

Ishijima,S. and M.Tatibana. 1994. Rapid mobilization of intracellular Mg2+ by bombesin in Swiss 3T3 cells: mobilization through external Ca(2+)- and tyrosine kinase-dependent mechanisms. *J. Biochem. (Tokyo)* 115:730-737.

Jacob,R. 1990. Agonist-stimulated divalent cation entry into single cultured human umbilical vein endothelial cells. *J. Physiol* 421:55-77.

Jakob,A., J.Becker, G.Schottli, and G.Fritzsch. 1989. Alpha 1-adrenergic stimulation causes Mg2+ release from perfused rat liver. *FEBS Lett.* 246:127-130.

Jalink,K., E.J.van Corven, T.Hengeveld, N.Morii, S.Narumiya, and W.H.Moolenaar. 1994. Inhibition of lysophosphatidate- and thrombin-induced neurite retraction and neuronal cell rounding by ADP ribosylation of the small GTP-binding protein Rho. *J. Cell Biol.* 126:801-810.

John,L.M., M.Mosquera-Caro, P.Camacho, and J.D.Lechleiter. 2001. Control of IP(3)-mediated Ca2+ puffs in Xenopus laevis oocytes by the Ca2+-binding protein parvalbumin. *J. Physiol* 535:3-16.

Jordt,S.E. and D.Julius. 2002. Molecular basis for species-specific sensitivity to "hot" chili peppers. *Cell* 108:421-430.

Jung,D.W., E.Panzeter, K.Baysal, and G.P.Brierley. 1997. On the relationship between matrix free Mg2+ concentration and total Mg2+ in heart mitochondria. *Biochim. Biophys. Acta* 1320:310-320.

Jungnickel,M.K., H.Marrero, L.Birnbaumer, J.R.Lemos, and H.M.Florman. 2001. Trp2 regulates entry of Ca2+ into mouse sperm triggered by egg ZP3. *Nat. Cell Biol.* 3:499-502.

Kanzaki,M., Y.Q.Zhang, H.Mashima, L.Li, H.Shibata, and I.Kojima. 1999. Translocation of a calcium-permeable cation channel induced by insulin-like growth factor-I. *Nat. Cell Biol.* 1:165-170.

Karoor,V., K.Baltensperger, H.Paul, M.P.Czech, and C.C.Malbon. 1995. Phosphorylation of tyrosyl residues 350/354 of the beta-adrenergic receptor is obligatory for counterregulatory effects of insulin. *J. Biol. Chem.* 270:25305-25308.

Kaupp,U.B. and R.Seifert. 2002. Cyclic nucleotide-gated ion channels. *Physiol Rev.* 82:769-824.

Keenan,D., A.Romani, and A.Scarpa. 1996. Regulation of Mg2+ homeostasis by insulin in perfused rat livers and isolated hepatocytes. *FEBS Lett.* 395:241-244.

Kerschbaum,H.H. and M.D.Cahalan. 1998. Monovalent permeability, rectification, and ionic block of store-operated calcium channels in Jurkat T lymphocytes. *J. Gen. Physiol* 111:521-537.

Kerschbaum,H.H., J.A.Kozak, and M.D.Cahalan. 2003. Polyvalent cations as permeant probes of MIC and TRPM7 pores. *Biophys. J.* 84:2293-2305.

Kim,B.J., H.H.Lim, D.K.Yang, J.Y.Jun, I.Y.Chang, C.S.Park, I.So, P.R.Stanfield, and K.W.Kim. 2005. Melastatin-type transient receptor potential channel 7 is required for intestinal pacemaking activity. *Gastroenterology* 129:1504-1517.

Kimura,K., M.Ito, M.Amano, K.Chihara, Y.Fukata, M.Nakafuku, B.Yamamori, J.Feng, T.Nakano, K.Okawa, A.Iwamatsu, and K.Kaibuchi. 1996. Regulation of myosin phosphatase by Rho and Rho-associated kinase (Rho-kinase). *Science* 273:245-248.

Koenig,M. and N.Grabe. 2004. Highly specific prediction of phosphorylation sites in proteins. *Bioinformatics.* 20:3620-3627.

Kolisek,M., A.Beck, A.Fleig, and R.Penner. 2005. Cyclic ADP-ribose and hydrogen peroxide synergize with ADP-ribose in the activation of TRPM2 channels. *Mol. Cell* 18:61-69.

Kolman,M.F., L.M.Futey, and T.T.Egelhoff. 1996. Dictyostelium myosin heavy chain kinase A regulates myosin localization during growth and development. *J. Cell Biol.* 132:101-109.

Kozak,J.A. and M.D.Cahalan. 2003. MIC channels are inhibited by internal divalent cations but not ATP. *Biophys. J.* 84:922-927.

Kozak,J.A., M.Matsushita, A.C.Nairn, and M.D.Cahalan. 2005. Charge screening by internal pH and polyvalent cations as a mechanism for activation, inhibition, and rundown of TRPM7/MIC channels. *J. Gen. Physiol* 126:499-514.

Kozasa,T., X.Jiang, M.J.Hart, P.M.Sternweis, W.D.Singer, A.G.Gilman, G.Bollag, and P.C.Sternweis. 1998. p115 RhoGEF, a GTPase activating protein for Galpha12 and Galpha13. *Science* 280:2109-2111.

Kozma,R., S.Sarner, S.Ahmed, and L.Lim. 1997. Rho family GTPases and neuronal growth cone remodelling: relationship between increased complexity induced by Cdc42Hs, Rac1, and acetylcholine and collapse induced by RhoA and lysophosphatidic acid. *Mol. Cell Biol.* 17:1201-1211.

Kraynov,V.S., C.Chamberlain, G.M.Bokoch, M.A.Schwartz, S.Slabaugh, and K.M.Hahn. 2000. Localized Rac activation dynamics visualized in living cells. *Science* 290:333-337.

Kung,C. 2005. A possible unifying principle for mechanosensation. *Nature* 436:647-654.

Kunichika,N., Y.Yu, C.V.Remillard, O.Platoshyn, S.Zhang, and J.X.Yuan. 2004. Overexpression of TRPC1 enhances pulmonary vasoconstriction induced by capacitative Ca2+ entry. *Am. J. Physiol Lung Cell Mol. Physiol* 287:L962-L969.

Kusumawati,A., C.Cazevieille, F.Porte, S.Bettache, J.P.Liautard, and W.J.Sri. 2000. Early events and implication of F-actin and annexin I associated structures in the phagocytic uptake of Brucella suis by the J-774A.1 murine cell line and human monocytes. *Microb. Pathog.* 28:343-352.

Launay,P., A.Fleig, A.L.Perraud, A.M.Scharenberg, R.Penner, and J.P.Kinet. 2002. TRPM4 is a Ca2+-activated nonselective cation channel mediating cell membrane depolarization. *Cell* 109:397-407.

Lee,N., J.Chen, L.Sun, S.Wu, K.R.Gray, A.Rich, M.Huang, J.H.Lin, J.N.Feder, E.B.Janovitz, P.C.Levesque, and M.A.Blanar. 2003. Expression and characterization of human transient receptor potential melastatin 3 (hTRPM3). *J. Biol. Chem.* 278:20890-20897.

Li,H.S. and C.Montell. 2000. TRP and the PDZ protein, INAD, form the core complex required for retention of the signalplex in Drosophila photoreceptor cells. *J. Cell Biol.* 150:1411-1422.

Li,W., J.Llopis, M.Whitney, G.Zlokarnik, and R.Y.Tsien. 1998. Cell-permeant caged InsP3 ester shows that Ca2+ spike frequency can optimize gene expression. *Nature* 392:936-941.

Liedtke,W., Y.Choe, M.A.Marti-Renom, A.M.Bell, C.S.Denis, A.Sali, A.J.Hudspeth, J.M.Friedman, and S.Heller. 2000. Vanilloid receptor-related osmotically activated channel (VR-OAC), a candidate vertebrate osmoreceptor. *Cell* 103:525-535.

Liman,E.R., D.P.Corey, and C.Dulac. 1999. TRP2: a candidate transduction channel for mammalian pheromone sensory signaling. *Proc. Natl. Acad. Sci. U. S. A* 96:5791-5796.

Lintschinger,B., M.Balzer-Geldsetzer, T.Baskaran, W.F.Graier, C.Romanin, M.X.Zhu, and K.Groschner. 2000. Coassembly of Trp1 and Trp3 proteins generates diacylglycerol- and Ca2+-sensitive cation channels. *J. Biol. Chem.* 275:27799-27805.

Liu,B. and F.Qin. 2005. Functional control of cold- and menthol-sensitive TRPM8 ion channels by phosphatidylinositol 4,5-bisphosphate. *J. Neurosci.* 25:1674-1681.

Liu,D. and E.R.Liman. 2003. Intracellular Ca2+ and the phospholipid PIP2 regulate the taste transduction ion channel TRPM5. *Proc. Natl. Acad. Sci. U. S. A* 100:15160-15165.

Ludi,H. and H.J.Schatzmann. 1987. Some properties of a system for sodium-dependent outward movement of magnesium from metabolizing human red blood cells. *J. Physiol* 390:367-382.

Machesky,L.M., R.D.Mullins, H.N.Higgs, D.A.Kaiser, L.Blanchoin, R.C.May, M.E.Hall, and T.D.Pollard. 1999. Scar, a WASp-related protein, activates nucleation of actin filaments by the Arp2/3 complex. *Proc. Natl. Acad. Sci. U. S. A* 96:3739-3744.

Marchisio,P.C., L.Bergui, G.C.Corbascio, O.Cremona, N.D'Urso, M.Schena, L.Tesio, and F.Caligaris-Cappio. 1988. Vinculin, talin, and integrins are

localized at specific adhesion sites of malignant B lymphocytes. *Blood* 72:830-833.

Marchisio,P.C., D.Cirillo, L.Naldini, M.V.Primavera, A.Teti, and A.Zambonin-Zallone. 1984. Cell-substratum interaction of cultured avian osteoclasts is mediated by specific adhesion structures. *J. Cell Biol.* 99:1696-1705.

Martinac,B. 2004. Mechanosensitive ion channels: molecules of mechanotransduction. *J. Cell Sci.* 117:2449-2460.

Masai,I., A.Okazaki, T.Hosoya, and Y.Hotta. 1993. Drosophila retinal degeneration A gene encodes an eye-specific diacylglycerol kinase with cysteine-rich zinc-finger motifs and ankyrin repeats. *Proc. Natl. Acad. Sci. U. S. A* 90:11157-11161.

Masai,I., E.Suzuki, C.S.Yoon, A.Kohyama, and Y.Hotta. 1997. Immunolocalization of Drosophila eye-specific diacylgylcerol kinase, rdgA, which is essential for the maintenance of the photoreceptor. *J. Neurobiol.* 32:695-706.

Matsushita,M., J.A.Kozak, Y.Shimizu, D.T.McLachlin, H.Yamaguchi, F.Y.Wei, K.Tomizawa, H.Matsui, B.T.Chait, M.D.Cahalan, and A.C.Nairn. 2005. Channel function is dissociated from the intrinsic kinase activity and autophosphorylation of TRPM7/ChaK1. *J. Biol. Chem.* 280:20793-20803.

McHugh,D., R.Flemming, S.Z.Xu, A.L.Perraud, and D.J.Beech. 2003. Critical intracellular Ca2+ dependence of transient receptor potential melastatin 2 (TRPM2) cation channel activation. *J. Biol. Chem.* 278:11002-11006.

McKemy,D.D., W.M.Neuhausser, and D.Julius. 2002. Identification of a cold receptor reveals a general role for TRP channels in thermosensation. *Nature* 416:52-58.

Mertens,A.E., R.C.Roovers, and J.G.Collard. 2003. Regulation of Tiam1-Rac signalling. *FEBS Lett.* 546:11-16.

Miki,H., H.Yamaguchi, S.Suetsugu, and T.Takenawa. 2000. IRSp53 is an essential intermediate between Rac and WAVE in the regulation of membrane ruffling. *Nature* 408:732-735.

Minke,B. and B.Cook. 2002. TRP channel proteins and signal transduction. *Physiol Rev.* 82:429-472.

Minke,B., C.Wu, and W.L.Pak. 1975. Induction of photoreceptor voltage noise in the dark in Drosophila mutant. *Nature* 258:84-87.

Minneman,K.P. 1988. Alpha 1-adrenergic receptor subtypes, inositol phosphates, and sources of cell Ca2+. *Pharmacol. Rev.* 40:87-119.

Monteilh-Zoller,M.K., M.C.Hermosura, M.J.Nadler, A.M.Scharenberg, R.Penner, and A.Fleig. 2003. TRPM7 provides an ion channel mechanism for cellular entry of trace metal ions. *J. Gen. Physiol* 121:49-60.

Moreau,V., F.Tatin, C.Varon, G.Anies, C.Savona-Baron, and E.Genot. 2006. Cdc42-driven podosome formation in endothelial cells. *Eur. J. Cell Biol.* 85:319-325.

Muraki,K., Y.Iwata, Y.Katanosaka, T.Ito, S.Ohya, M.Shigekawa, and Y.Imaizumi. 2003. TRPV2 is a component of osmotically sensitive cation channels in murine aortic myocytes. *Circ. Res.* 93:829-838.

Nadler,M.J., M.C.Hermosura, K.Inabe, A.L.Perraud, Q.Zhu, A.J.Stokes, T.Kurosaki, J.P.Kinet, R.Penner, A.M.Scharenberg, and A.Fleig. 2001. LTRPC7 is a Mg.ATP-regulated divalent cation channel required for cell viability. *Nature* 411:590-595.

Nagata,K., A.Duggan, G.Kumar, and J.Garcia-Anoveros. 2005. Nociceptor and hair cell transducer properties of TRPA1, a channel for pain and hearing. *J. Neurosci.* 25:4052-4061.

Nathan,J.D., R.Y.Peng, Y.Wang, D.C.McVey, S.R.Vigna, and R.A.Liddle. 2002. Primary sensory neurons: a common final pathway for inflammation in experimental pancreatitis in rats. *Am. J. Physiol Gastrointest. Liver Physiol* 283:G938-G946.

Nealen,M.L., M.S.Gold, P.D.Thut, and M.J.Caterina. 2003. TRPM8 mRNA is expressed in a subset of cold-responsive trigeminal neurons from rat. *J. Neurophysiol.* 90:515-520.

Niemeyer,B.A., C.Bergs, U.Wissenbach, V.Flockerzi, and C.Trost. 2001. Competitive regulation of CaT-like-mediated Ca2+ entry by protein kinase C and calmodulin. *Proc. Natl. Acad. Sci. U. S. A* 98:3600-3605.

Nijenhuis,T., J.G.Hoenderop, A.W.van der Kemp, and R.J.Bindels. 2003. Localization and regulation of the epithelial Ca2+ channel TRPV6 in the kidney. *J. Am. Soc. Nephrol.* 14:2731-2740.

Nilius,B., R.Vennekens, J.Prenen, J.G.Hoenderop, G.Droogmans, and R.J.Bindels. 2001. The single pore residue Asp542 determines Ca2+ permeation and Mg2+ block of the epithelial Ca2+ channel. *J. Biol. Chem.* 276:1020-1025.

Nobes,C.D. and A.Hall. 1995. Rho, rac, and cdc42 GTPases regulate the assembly of multimolecular focal complexes associated with actin stress fibers, lamellipodia, and filopodia. *Cell* 81:53-62.

Oancea,E. and T.Meyer. 1998. Protein kinase C as a molecular machine for decoding calcium and diacylglycerol signals. *Cell* 95:307-318.

Oancea,E., J.T.Wolfe, and D.E.Clapham. 2006. Functional TRPM7 channels accumulate at the plasma membrane in response to fluid flow. *Circ. Res.* 98:245-253.

Oberwinkler,J., A.Lis, K.M.Giehl, V.Flockerzi, and S.E.Philipp. 2005. Alternative splicing switches the divalent cation selectivity of TRPM3 channels. *J. Biol. Chem.* 280:22540-22548.

Okada,K., S.Ishikawa, and T.Saito. 1992. Cellular mechanisms of vasopressin and endothelin to mobilize [Mg2+]i in vascular smooth muscle cells. *Am. J. Physiol* 263:C873-C878.

Opazo,S.A., W.Zhang, Y.Wu, C.E.Turner, D.D.Tang, and S.J.Gunst. 2004. Tension development during contractile stimulation of smooth muscle requires recruitment of paxillin and vinculin to the membrane. *Am. J. Physiol Cell Physiol* 286:C433-C447.

Owsianik,G., K.Talavera, T.Voets, and B.Nilius. 2006. Permeation and selectivity of trp channels. *Annu. Rev. Physiol* 68:685-717.

Pak,W.L., J.Grossfield, and K.S.Arnold. 1970. Mutants of the visual pathway of Drosophila melanogaster. *Nature* 227:518-520.

Payne,R., D.W.Corson, A.Fein, and M.J.Berridge. 1986. Excitation and adaptation of Limulus ventral photoreceptors by inositol 1,4,5 triphosphate result from a rise in intracellular calcium. *J. Gen. Physiol* 88:127-142.

Pedersen,S.F., G.Owsianik, and B.Nilius. 2005. TRP channels: an overview. *Cell Calcium* 38:233-252.

Peier,A.M., A.J.Reeve, D.A.Andersson, A.Moqrich, T.J.Earley, A.C.Hergarden, G.M.Story, S.Colley, J.B.Hogenesch, P.McIntyre, S.Bevan, and A.Patapoutian. 2002. A heat-sensitive TRP channel expressed in keratinocytes. *Science* 296:2046-2049.

Perez,C.A., L.Huang, M.Rong, J.A.Kozak, A.K.Preuss, H.Zhang, M.Max, and R.F.Margolskee. 2002. A transient receptor potential channel expressed in taste receptor cells. *Nat. Neurosci.* 5:1169-1176.

Perraud,A.L., A.Fleig, C.A.Dunn, L.A.Bagley, P.Launay, C.Schmitz, A.J.Stokes, Q.Zhu, M.J.Bessman, R.Penner, J.P.Kinet, and A.M.Scharenberg. 2001. ADP-ribose gating of the calcium-permeable LTRPC2 channel revealed by Nudix motif homology. *Nature* 411:595-599.

Philipp,S. and V.Flockerzi. 1997. Molecular characterization of a novel human PDZ domain protein with homology to INAD from Drosophila melanogaster. *FEBS Lett.* 413:243-248.

Prakriya,M. and R.S.Lewis. 2002. Separation and characterization of currents through store-operated CRAC channels and Mg2+-inhibited cation (MIC) channels. *J. Gen. Physiol* 119:487-507.

Prawitt,D., M.K.Monteilh-Zoller, L.Brixel, C.Spangenberg, B.Zabel, A.Fleig, and R.Penner. 2003. TRPM5 is a transient Ca2+-activated cation channel responding to rapid changes in [Ca2+]i. *Proc. Natl. Acad. Sci. U. S. A* 100:15166-15171.

Prescott,E.D. and D.Julius. 2003. A modular PIP2 binding site as a determinant of capsaicin receptor sensitivity. *Science* 300:1284-1288.

Price,L.S., M.Langeslag, J.P.ten Klooster, P.L.Hordijk, K.Jalink, and J.G.Collard. 2003. Calcium signaling regulates translocation and activation of Rac. *J. Biol. Chem.* 278:39413-39421.

Putney,J.W., Jr. 1986. A model for receptor-regulated calcium entry. *Cell Calcium* 7:1-12.

Quamme,G.A. and R.C.de. 2000. Epithelial magnesium transport and regulation by the kidney. *Front Biosci.* 5:D694-D711.

Raghu,P., N.J.Colley, R.Webel, T.James, G.Hasan, M.Danin, Z.Selinger, and R.C.Hardie. 2000. Normal phototransduction in Drosophila photoreceptors lacking an InsP(3) receptor gene. *Mol. Cell Neurosci.* 15:429-445.

Rasmussen,U., C.S.Broogger, and F.Sandberg. 1978. Thapsigargine and thapsigargicine, two new histamine liberators from Thapsia garganica L. *Acta Pharm. Suec.* 15:133-140.

Redowicz,M.J. 2001. Regulation of nonmuscle myosins by heavy chain phosphorylation. *J. Muscle Res. Cell Motil.* 22:163-173.

Riccio,A., C.Mattei, R.E.Kelsell, A.D.Medhurst, A.R.Calver, A.D.Randall, J.B.Davis, C.D.Benham, and M.N.Pangalos. 2002. Cloning and functional expression of human short TRP7, a candidate protein for store-operated Ca2+ influx. *J. Biol. Chem.* 277:12302-12309.

Ridley,A.J., H.F.Paterson, C.L.Johnston, D.Diekmann, and A.Hall. 1992. The small GTP-binding protein rac regulates growth factor-induced membrane ruffling. *Cell* 70:401-410.

Riveline,D., E.Zamir, N.Q.Balaban, U.S.Schwarz, T.Ishizaki, S.Narumiya, Z.Kam, B.Geiger, and A.D.Bershadsky. 2001. Focal contacts as mechanosensors: externally applied local mechanical force induces growth of focal contacts by an mDia1-dependent and ROCK-independent mechanism. *J. Cell Biol.* 153:1175-1186.

Rohacs,T., C.M.Lopes, I.Michailidis, and D.E.Logothetis. 2005. PI(4,5)P2 regulates the activation and desensitization of TRPM8 channels through the TRP domain. *Nat. Neurosci.* 8:626-634.

Romani,A., C.Marfella, and A.Scarpa. 1993a. Hormonal stimulation of Mg2+ uptake in hepatocytes. Regulation by plasma membrane and intracellular organelles. *J. Biol. Chem.* 268:15489-15495.

Romani,A., C.Marfella, and A.Scarpa. 1993b. Regulation of magnesium uptake and release in the heart and in isolated ventricular myocytes. *Circ. Res.* 72:1139-1148.

Romani,A., M.Marfella, and A.Scarpa. 1995. Mg2+ homeostasis in cardiac ventricular myocytes. *In* Biochemistry of cell membranes: A compendium of selected topics. s.papa and j.m.tager, editors. Birkhauser-Verlag, Basel.

Romani,A. and A.Scarpa. 1990. Norepinephrine evokes a marked Mg2+ efflux from liver cells. *FEBS Lett.* 269:37-40.

Romani,A. and A.Scarpa. 1992. Regulation of cell magnesium. *Arch. Biochem. Biophys.* 298:1-12.

Romani,A.M., V.D.Matthews, and A.Scarpa. 2000. Parallel stimulation of glucose and Mg(2+) accumulation by insulin in rat hearts and cardiac ventricular myocytes. *Circ. Res.* 86:326-333.

Romani,A.M. and A.Scarpa. 2000. Regulation of cellular magnesium. *Front Biosci.* 5:D720-D734.

Rothermel,J.D. and L.H.Parker Botelho. 1988. A mechanistic and kinetic analysis of the interactions of the diastereoisomers of adenosine 3',5'-(cyclic)phosphorothioate with purified cyclic AMP-dependent protein kinase. *Biochem. J.* 251:757-762.

Rottner,K., A.Hall, and J.V.Small. 1999. Interplay between Rac and Rho in the control of substrate contact dynamics. *Curr. Biol.* 9:640-648.

Runnels,L.W., L.Yue, and D.E.Clapham. 2002. The TRPM7 channel is inactivated by PIP(2) hydrolysis. *Nat. Cell Biol.* 4:329-336.

Runnels,L.W., L.Yue, and D.E.Clapham. 2001. TRP-PLIK, a bifunctional protein with kinase and ion channel activities. *Science* 291:1043-1047.

Ryazanov,A.G., K.S.Pavur, and M.V.Dorovkov. 1999. Alpha-kinases: a new class of protein kinases with a novel catalytic domain. *Curr. Biol.* 9:R43-R45.

Ryazanova,L.V., M.V.Dorovkov, A.Ansari, and A.G.Ryazanov. 2004. Characterization of the protein kinase activity of TRPM7/ChaK1, a protein kinase fused to the transient receptor potential ion channel. *J. Biol. Chem.* 279:3708-3716.

Sano,Y., K.Inamura, A.Miyake, S.Mochizuki, H.Yokoi, H.Matsushime, and K.Furuichi. 2001. Immunocyte Ca2+ influx system mediated by LTRPC2. *Science* 293:1327-1330.

Sato T, M.del Carmen Ovejero, P.Hou, A.M.Heegaard, M.Kumegawa, N.T.Foged, J.M.Delaisse. 1997 Identification of the membrane-type matrix metalloproteinase MT1-MMP in osteoclasts. *J. Cell Sci.* 110, 589–596

Schaefer,M., T.D.Plant, A.G.Obukhov, T.Hofmann, T.Gudermann, and G.Schultz. 2000. Receptor-mediated regulation of the nonselective cation channels TRPC4 and TRPC5. *J. Biol. Chem.* 275:17517-17526.

Schatzmann,H.J. 1993. Asymmetry of the magnesium sodium exchange across the human red cell membrane. *Biochim. Biophys. Acta* 1148:15-18.

Schlingmann,K.P., S.Weber, M.Peters, L.Niemann Nejsum, H.Vitzthum, K.Klingel, M.Kratz, E.Haddad, E.Ristoff, D.Dinour, M.Syrrou, S.Nielsen, M.Sassen, S.Waldegger, H.W.Seyberth, and M.Konrad. 2002. Hypomagnesemia with secondary hypocalcemia is caused by mutations in TRPM6, a new member of the TRPM gene family. *Nat. Genet.* 31:166-170.

Schmidt,A. and A.Hall. 2002. Guanine nucleotide exchange factors for Rho GTPases: turning on the switch. *Genes Dev.* 16:1587-1609.

Schmitz,C., A.L.Perraud, C.O.Johnson, K.Inabe, M.K.Smith, R.Penner, T.Kurosaki, A.Fleig, and A.M.Scharenberg. 2003. Regulation of vertebrate cellular Mg2+ homeostasis by TRPM7. *Cell* 114:191-200.

Shuttleworth,T.J. 2004. Receptor-activated calcium entry channels--who does what, and when? *Sci. STKE.* 2004:e40.

Sidi,S., R.W.Friedrich, and T.Nicolson. 2003. NompC TRP channel required for vertebrate sensory hair cell mechanotransduction. *Science* 301:96-99.

Singh,B.B., T.P.Lockwich, B.C.Bandyopadhyay, X.Liu, S.Bollimuntha, S.C.Brazer, C.Combs, S.Das, A.G.Leenders, Z.H.Sheng, M.A.Knepper, S.V.Ambudkar, and I.S.Ambudkar. 2004. VAMP2-dependent exocytosis regulates plasma membrane insertion of TRPC3 channels and contributes to agonist-stimulated Ca2+ influx. *Mol. Cell* 15:635-646.

Small,J.V. 1981. Organization of actin in the leading edge of cultured cells: influence of osmium tetroxide and dehydration on the ultrastructure of actin meshworks. *J. Cell Biol.* 91:695-705.

Small,J.V., M.Herzog, and K.Anderson. 1995. Actin filament organization in the fish keratocyte lamellipodium. *J. Cell Biol.* 129:1275-1286.

Smith,G.D., M.J.Gunthorpe, R.E.Kelsell, P.D.Hayes, P.Reilly, P.Facer, J.E.Wright, J.C.Jerman, J.P.Walhin, L.Ooi, J.Egerton, K.J.Charles, D.Smart, A.D.Randall, P.Anand, and J.B.Davis. 2002. TRPV3 is a temperature-sensitive vanilloid receptor-like protein. *Nature* 418:186-190.

Smoake,J.A., G.M.Moy, B.Fang, and S.S.Solomon. 1995. Calmodulin-dependent cyclic AMP phosphodiesterase in liver plasma membranes: stimulated by insulin. *Arch. Biochem. Biophys.* 323:223-232.

Sorensen,J.B. 2004. Formation, stabilisation and fusion of the readily releasable pool of secretory vesicles. *Pflugers Arch.* 448:347-362.

Spinardi,L., J.Rietdorf, L.Nitsch, M.Bono, C.Tacchetti, M.Way, and P.C.Marchisio. 2004. A dynamic podosome-like structure of epithelial cells. *Exp. Cell Res.* 295:360-374.

Stauffer,T.P., S.Ahn, and T.Meyer. 1998. Receptor-induced transient reduction in plasma membrane PtdIns(4,5)P2 concentration monitored in living cells. *Curr. Biol.* 8:343-346.

Stickel,S.K. and Y.L.Wang. 1987. Alpha-actinin-containing aggregates in transformed cells are highly dynamic structures. *J. Cell Biol.* 104:1521-1526.

Stowers,L., T.E.Holy, M.Meister, C.Dulac, and G.Koentges. 2002. Loss of sex discrimination and male-male aggression in mice deficient for TRP2. *Science* 295:1493-1500.

Strotmann,R., C.Harteneck, K.Nunnenmacher, G.Schultz, and T.D.Plant. 2000. OTRPC4, a nonselective cation channel that confers sensitivity to extracellular osmolarity. *Nat. Cell Biol.* 2:695-702.

Strubing,C., G.Krapivinsky, L.Krapivinsky, and D.E.Clapham. 2001. TRPC1 and TRPC5 form a novel cation channel in mammalian brain. *Neuron* 29:645-655.

Strubing,C., G.Krapivinsky, L.Krapivinsky, and D.E.Clapham. 2003. Formation of novel TRPC channels by complex subunit interactions in embryonic brain. *J. Biol. Chem.* 278:39014-39019.

Su,L.T., M.A.Agapito, M.Li, T.N.Simonson, A.Huttenlocher, R.Habas, L.Yue, and L.W.Runnels. 2006. Trpm7 regulates cell adhesion by controlling the calcium dependent protease calpain. *J. Biol. Chem.*

Sugiyama,T. and W.F.Goldman. 1995. Measurement of SR free Ca2+ and Mg2+ in permeabilized smooth muscle cells with use of furaptra. *Am. J. Physiol* 269:C698-C705.

Suss,E., S.Barash, D.G.Stavenga, H.Stieve, Z.Selinger, and B.Minke. 1989. Chemical excitation and

inactivation in photoreceptors of the fly mutants trp and nss. *J. Gen. Physiol* 94:465-491.

Takezawa,R., C.Schmitz, P.Demeuse, A.M.Scharenberg, R.Penner, and A.Fleig. 2004. Receptor-mediated regulation of the TRPM7 channel through its endogenous protein kinase domain. *Proc. Natl. Acad. Sci. U. S. A* 101:6009-6014.

Tang,J., Y.Lin, Z.Zhang, S.Tikunova, L.Birnbaumer, and M.X.Zhu. 2001. Identification of common binding sites for calmodulin and inositol 1,4,5-trisphosphate receptors on the carboxyl termini of trp channels. *J. Biol. Chem.* 276:21303-21310.

Tang,Y., J.Tang, Z.Chen, C.Trost, V.Flockerzi, M.Li, V.Ramesh, and M.X.Zhu. 2000. Association of mammalian trp4 and phospholipase C isozymes with a PDZ domain-containing protein, NHERF. *J. Biol. Chem.* 275:37559-37564.

Tashiro,M. and M.Konishi. 1997. Na+ gradient-dependent Mg2+ transport in smooth muscle cells of guinea pig tenia cecum. *Biophys. J.* 73:3371-3384.

Taylor,S.S., D.R.Knighton, J.Zheng, L.F.Ten Eyck, and J.M.Sowadski. 1992. cAMP-dependent protein kinase and the protein kinase family. *Faraday Discuss.*:143-152.

Taylor,C.W. 2002. Regulation of Ca2+ entry pathways by both limbs of the phosphoinositide pathway. *Novartis. Found. Symp.* 246:91-101.

Tessman,P.A. and A.Romani. 1998. Acute effect of EtOH on Mg2+ homeostasis in liver cells: evidence for the activation of an Na+/Mg2+ exchanger. *Am. J. Physiol* 275:G1106-G1116.

Thastrup,O., P.J.Cullen, B.K.Drobak, M.R.Hanley, and A.P.Dawson. 1990. Thapsigargin, a tumor promoter, discharges intracellular Ca2+ stores by specific inhibition of the endoplasmic reticulum Ca2(+)-ATPase. *Proc. Natl. Acad. Sci. U. S. A* 87:2466-2470.

Tiruppathi,C., M.Freichel, S.M.Vogel, B.C.Paria, D.Mehta, V.Flockerzi, and A.B.Malik. 2002. Impairment of store-operated Ca2+ entry in TRPC4(-/-) mice interferes with increase in lung microvascular permeability. *Circ. Res.* 91:70-76.

Tolias,K.F., L.C.Cantley, and C.L.Carpenter. 1995. Rho family GTPases bind to phosphoinositide kinases. *J. Biol. Chem.* 270:17656-17659.

Tolias,K.F., J.H.Hartwig, H.Ishihara, Y.Shibasaki, L.C.Cantley, and C.L.Carpenter. 2000. Type Ialpha phosphatidylinositol-4-phosphate 5-kinase mediates Rac-dependent actin assembly. *Curr. Biol.* 10:153-156.

Tomida,T., K.Hirose, A.Takizawa, F.Shibasaki, and M.Iino. 2003. NFAT functions as a working memory of Ca2+ signals in decoding Ca2+ oscillation. *EMBO J.* 22:3825-3832.

Touyz,R.M. and E.L.Schiffrin. 1996. Angiotensin II and vasopressin modulate intracellular free magnesium in vascular smooth muscle cells through Na+-dependent protein kinase C pathways. *J. Biol. Chem.* 271:24353-24358.

Tsavaler,L., M.H.Shapero, S.Morkowski, and R.Laus. 2001. Trp-p8, a novel prostate-specific gene, is up-regulated in prostate cancer and other malignancies and shares high homology with transient receptor potential calcium channel proteins. *Cancer Res.* 61:3760-3769.

Tsuruta,D., M.Gonzales, S.B.Hopkinson, C.Otey, S.Khuon, R.D.Goldman, and J.C.Jones. 2002. Microfilament-dependent movement of the beta3 integrin subunit within focal contacts of endothelial cells. *FASEB J.* 16:866-868.

van der Wal,W.J., R.Habets, P.Varnai, T.Balla, and K.Jalink. 2001. Monitoring agonist-induced phospholipase C activation in live cells by fluorescence resonance energy transfer. *J. Biol. Chem.* 276:15337-15344.

van Leeuwen,F.N., D.S.van, H.E.Kain, R.A.van der Kammen, and J.G.Collard. 1999. Rac regulates phosphorylation of the myosin-II heavy chain, actinomyosin disassembly and cell spreading. *Nat. Cell Biol.* 1:242-248.

Van Rossum,D.B., R.L.Patterson, S.Sharma, R.K.Barrow, M.Kornberg, D.L.Gill, and S.H.Snyder. 2005. Phospholipase Cgamma1 controls surface expression of TRPC3 through an intermolecular PH domain. *Nature* 434:99-104.

van Abel,A.M., J.G.Hoenderop, A.W.van der Kemp, M.M.Friedlaender, J.P.van Leeuwen, and R.J.Bindels. 2005. Coordinated control of renal Ca(2+) transport proteins by parathyroid hormone. *Kidney Int.* 68:1708-1721.

Vannier,B., M.Peyton, G.Boulay, D.Brown, N.Qin, M.Jiang, X.Zhu, and L.Birnbaumer. 1999. Mouse trp2, the homologue of the human trpc2 pseudogene, encodes mTrp2, a store depletion-activated capacitative Ca2+ entry channel. *Proc. Natl. Acad. Sci. U. S. A* 96:2060-2064.

Varnai,P. and T.Balla. 1998. Visualization of phosphoinositides that bind pleckstrin homology domains: calcium- and agonist-induced dynamic changes and relationship to myo-[3H]inositol-labeled phosphoinositide pools. *J. Cell Biol.* 143:501-510.

Vennekens,R., J.G.Hoenderop, J.Prenen, M.Stuiver, P.H.Willems, G.Droogmans, B.Nilius, and R.J.Bindels. 2000. Permeation and gating properties of the novel epithelial Ca(2+) channel. *J. Biol. Chem.* 275:3963-3969.

Vennekens,R., J.Prenen, J.G.Hoenderop, R.J.Bindels, G.Droogmans, and B.Nilius. 2001. Pore properties and ionic block of the rabbit epithelial calcium channel expressed in HEK 293 cells. *J. Physiol* 530:183-191.

Voets,T., G.Droogmans, U.Wissenbach, A.Janssens, V.Flockerzi, and B.Nilius. 2004a. The principle of temperature-dependent gating in cold- and heat-sensitive TRP channels. *Nature* 430:748-754.

Voets,T., A.Janssens, J.Prenen, G.Droogmans, and B.Nilius. 2003. Mg2+-dependent gating and strong inward rectification of the cation channel TRPV6. *J. Gen. Physiol* 121:245-260.

Voets,T., B.Nilius, S.Hoefs, A.W.van der Kemp, G.Droogmans, R.J.Bindels, and J.G.Hoenderop. 2004b. TRPM6 forms the Mg2+ influx channel involved in intestinal and renal Mg2+ absorption. *J. Biol. Chem.* 279:19-25.

Voets,T., K.Talavera, G.Owsianik, and B.Nilius. 2005. Sensing with TRP channels. *Nat. Chem. Biol.* 1:85-92.

Vormann,J. and T.Gunther. 1987. Amiloride-sensitive net Mg2+ efflux from isolated perfused rat hearts. *Magnesium* 6:220-224.

Walder,R.Y., D.Landau, P.Meyer, H.Shalev, M.Tsolia, Z.Borochowitz, M.B.Boettger, G.E.Beck, R.K.Englehardt, R.Carmi, and V.C.Sheffield. 2002. Mutation of TRPM6 causes familial hypomagnesemia with secondary hypocalcemia. *Nat. Genet.* 31:171-174.

Walker,R.G., A.T.Willingham, and C.S.Zuker. 2000. A Drosophila mechanosensory transduction channel. *Science* 287:2229-2234.

Wang,G.X. and M.M.Poo. 2005. Requirement of TRPC channels in netrin-1-induced chemotropic turning of nerve growth cones. *Nature* 434:898-904.

Wang,H.B., M.Dembo, S.K.Hanks, and Y.Wang. 2001. Focal adhesion kinase is involved in mechanosensing during fibroblast migration. *Proc. Natl. Acad. Sci. U. S. A* 98:11295-11300.

Wang,N., J.P.Butler, and D.E.Ingber. 1993. Mechanotransduction across the cell surface and through the cytoskeleton. *Science* 260:1124-1127.

Watanabe,H., J.Vriens, S.H.Suh, C.D.Benham, G.Droogmans, and B.Nilius. 2002. Heat-evoked activation of TRPV4 channels in a HEK293 cell expression system and in native mouse aorta endothelial cells. *J. Biol. Chem.* 277:47044-47051.

Watanabe,N., T.Kato, A.Fujita, T.Ishizaki, and S.Narumiya. 1999. Cooperation between mDia1 and ROCK in Rho-induced actin reorganization. *Nat. Cell Biol.* 1:136-143.

Watanabe,N., P.Madaule, T.Reid, T.Ishizaki, G.Watanabe, A.Kakizuka, Y.Saito, K.Nakao, B.M.Jockusch, and S.Narumiya. 1997. p140mDia, a mammalian homolog of Drosophila diaphanous, is a target protein for Rho small GTPase and is a ligand for profilin. *EMBO J.* 16:3044-3056.

Wolf,F.I., F.A.Di, and A.Cittadini. 1994. Characterization of magnesium efflux from Ehrlich ascites tumor cells. *Arch. Biochem. Biophys.* 308:335-341.

Wolf,F.I., F.A.Di, V.Covacci, and A.Cittadini. 1997. Regulation of magnesium efflux from rat spleen lymphocytes. *Arch. Biochem. Biophys.* 344:397-403.

Wolf,F.I., F.A.Di, V.Covacci, D.Corda, and A.Cittadini. 1996. Regulation of intracellular magnesium in ascites cells: involvement of different regulatory pathways. *Arch. Biochem. Biophys.* 331:194-200.

Wu,L., B.Niemeyer, N.Colley, M.Socolich, and C.S.Zuker. 1995. Regulation of PLC-mediated signalling in vivo by CDP-diacylglycerol synthase. *Nature* 373:216-222.

Xu,H., I.S.Ramsey, S.A.Kotecha, M.M.Moran, J.A.Chong, D.Lawson, P.Ge, J.Lilly, I.Silos-Santiago, Y.Xie, P.S.DiStefano, R.Curtis, and D.E.Clapham. 2002. TRPV3 is a calcium-permeable temperature-sensitive cation channel. *Nature* 418:181-186.

Xu,H., H.Zhao, W.Tian, K.Yoshida, J.B.Roullet, and D.M.Cohen. 2003. Regulation of a transient receptor potential (TRP) channel by tyrosine phosphorylation. SRC family kinase-dependent tyrosine phosphorylation of TRPV4 on TYR-253 mediates its response to hypotonic stress. *J. Biol. Chem.* 278:11520-11527.

Xu,X.Z., F.Moebius, D.L.Gill, and C.Montell. 2001. Regulation of melastatin, a TRP-related protein, through interaction with a cytoplasmic isoform. *Proc. Natl. Acad. Sci. U. S. A* 98:10692-10697.

Yamaguchi,H., M.Matsushita, A.C.Nairn, and J.Kuriyan. 2001. Crystal structure of the atypical protein kinase domain of a TRP channel with phosphotransferase activity. *Mol. Cell* 7:1047-1057.

Yang,K.T., W.L.Chang, P.C.Yang, C.L.Chien, M.S.Lai, M.J.Su, and M.L.Wu. 2005. Activation of the transient receptor potential M2 channel and poly(ADP-ribose) polymerase is involved in oxidative stress-induced cardiomyocyte death. *Cell Death. Differ.*

Yellen,G., M.E.Jurman, T.Abramson, and R.MacKinnon. 1991. Mutations affecting internal TEA blockade identify the probable pore-forming region of a K+ channel. *Science* 251:939-942.

Yool,A.J. and T.L.Schwarz. 1991. Alteration of ionic selectivity of a K+ channel by mutation of the H5 region. *Nature* 349:700-704.

Yoshida,Y. and S.Imai. 1997. Structure and function of inositol 1,4,5-trisphosphate receptor. *Jpn. J. Pharmacol.* 74:125-137.

Zhang,Y., M.A.Hoon, J.Chandrashekar, K.L.Mueller, B.Cook, D.Wu, C.S.Zuker, and N.J.Ryba. 2003. Coding of sweet, bitter, and umami tastes: different receptor cells sharing similar signaling pathways. *Cell* 112:293-301.

Zhang,Z., H.Okawa, Y.Wang, and E.R.Liman. 2005. Phosphatidylinositol 4,5-bisphosphate rescues TRPM4 channels from desensitization. *J. Biol. Chem.* 280:39185-39192.

Zitt,C., C.R.Halaszovich, and A.Luckhoff. 2002. The TRP family of cation channels: probing and advancing the concepts on receptor-activated calcium entry. *Prog. Neurobiol.* 66:243-264.

Zitt,C., A.Zobel, A.G.Obukhov, C.Harteneck, F.Kalkbrenner, A.Luckhoff, and G.Schultz. 1996. Cloning and functional expression of a human Ca2+-permeable cation channel activated by calcium store depletion. *Neuron* 16:1189-1196.

Zweifach,A. and R.S.Lewis. 1993. Mitogen-regulated Ca2+ current of T lymphocytes is activated by depletion of intracellular Ca2+ stores. *Proc. Natl. Acad. Sci. U. S. A* 90:6295-6299.

Gq/Phospholipase C-coupled agonists activate TRPM7 channels under physiological conditions

Michiel Langeslag, Kristopher Clark, Wouter H. Moolenaar, Frank N. van Leeuwen, Kees Jalink

Gq/Phospholipase C-coupled Agonists Activate TRPM7 Channels under Physiological Conditions

Michiel Langeslag[*], Kristopher Clark[§], Wouter H. Moolenaar[#], Frank N. van Leeuwen[§,#], Kees Jalink[*]

[*] Division of Cell Biology, and
[#] Division of Cellular Biochemistry, the Netherlands Cancer Institute
Plesmanlaan 121, 1066 CX Amsterdam, the Netherlands, and
[§] Department of Tumor Immunology,
Nijmegen Centre for Molecular Life Sciences, Radboud University Nijmegen Medical Center
PO Box 9101, 6500 HB Nijmegen, the Netherlands

TRPM7 is an ubiquitously expressed non-specific cation channel that has been implicated in cellular Mg^{2+} homeostasis. We recently showed that moderate overexpression of TRMP7 in neuroblastoma N1E-115 cells elevates Ca^{2+} levels and markedly increases cell-matrix adhesion. We also found that activation of TRPM7 by phospholipase C (PLC)-coupled receptors further increased Ca^{2+} levels and augmented cell adhesion and spreading in a Ca^{2+}-dependent manner (Clark et al., 2006).

Regulation of the TRMP7 channel is not well understood, although it has been reported that PIP_2 hydrolysis closes the channel. We here addressed TRPM7 regulation by GPCR agonists. Using FRET assays for second messengers we show that TRPM7-dependent Ca^{2+} increases correlate with PLC activation, but not with other GPCR signaling cascades. In non-invasive "perforated-patch clamp" recordings TRPM7 currents are also activated by PLC agonists. Whereas we could confirm that, under whole-cell conditions, the channels were significantly inhibited by PLC-activating agonists, TRPM7 current inhibition by PIP_2 hydrolysis was only observed when $[Mg^{2+}]_i$ was reduced below physiological levels. Thus, under physiological $[Mg^{2+}]_i$ conditions, TRPM7 currents are activated rather than inhibited by PIP_2-hydrolyzing agonists.

Introduction

TRPM7 is an ubiquitously expressed non-specific cation channel that, intriguingly, contains a C-terminal serine-threonine kinase domain. It belongs to the TRPM (Melastatin-related) subfamily of Transient Receptor Potential (TRP) channels that transduce sensory signals (Clapham, 2003). TRPM7 appears essential for life in that knock-out or overexpression of the channels caused growth arrest, loss of adhesion and rapid cell death (Nadler et al., 2001; Schmitz et al., 2003; Su et al., 2006). We recently discovered that low-level overexpression of TRMP7 induces cell spreading and adhesion and that its′ activation by PIP_2-hydrolyzing receptor agonists leads to the formation of adhesion complexes in a kinase-dependent manner (Clark et al., 2006).

Currents of TRPM7 channels exogenously expressed in mammalian cells have been analysed by several groups. In physiological solutions, the channel conducts mainly Ca^{2+} and Mg^{2+} (Runnels et al., 2001), but in the absence of these divalents K^+ and Na^+ (Nadler et al., 2001; Runnels et al., 2001) are passed efficiently. A characteristic feature is the inhibition of this current by physiological intracellular Mg^{2+} levels: in whole-cell patch clamp experiments, large outward rectifying TRPM7 currents (Runnels et al., 2001; Nadler et al., 2001; Kerschbaum et al., 2003) are revealed by perfusion with Mg^{2+}-free pipette solutions. Furthermore, MgATP and MgGTP also inhibit the channels (Nadler et al., 2001; Demeuse et al., 2006) although some controversy was raised on this topic (Kozak et al., 2002). TRPM7 currents have been termed MagNuM (for Mg^{2+}-Nucleotide sensitive Metal ion (Nadler et al., 2001)) or MIC (for Mg^{2+}-Inhibited Cation (Kozak et al., 2002)) currents. These terms will here be used interchangeably to reflect whole-cell currents evoked by internal Mg^{2+} depletion. MagNuM/MIC currents revert around 0 mV; the inward currents are predominantly carried by divalent cations, whereas outward currents consist mainly of monovalent cations (at low $[Mg^{2+}]_i$). TRPM7 currents lack voltage- and time-dependent

activation (Nadler et al., 2001; Runnels et al., 2001), and outward rectification is most likely due to divalent permeation block of inward currents at negative potentials (Nadler et al., 2001). Accordingly, perfusion with divalent-free extracellular solutions augments inward currents and causes the I/V relationship to become linear. The activation of TRPM7 by internal perfusion with Mg^{2+}-free solutions does not rely on permeation block, but the precise mechanism of action has not been solved yet (Kozak et al., 2002). Several reports document that the setpoint for $[Mg^{2+}]_i$ sensitivity is governed by the kinase domain; however, constructs lacking the entire kinase domain can still be activated by internal Mg^{2+} depletion (Schmitz et al., 2003; Schmitz et al., 2005; Matsushita et al., 2005). Thus, the interactions of TRPM7 with Mg^{2+} are complex: Mg^{2+} is conducted through the channel pore, causes voltage-dependent permeation block, and influences gating at the cytosolic surface.

The exact mechanisms by which receptor agonists regulate TRPM7 are less well characterized and the published data are, at least partly, conflicting. An initially claimed indispensable role for the kinase domain (Runnels et al., 2001) was challenged in subsequent studies (Schmitz et al., 2003; Takezawa et al., 2004; Matsushita et al., 2005; Schmitz et al., 2005). Rather, we recently showed that the TRPM7 α-kinase specifically phosphorylates the heavy chain of myosin-II (Clark et al., 2006) thereby strongly influencing cell adhesion. Importantly, association with- and subsequent phosphorylation of myosin-II depend on prior activation of the channel by PLC-coupled receptors, and influx of extracellular Ca^{2+} constitutes an essential step in this process (Clark et al., 2006). In accordance, TRPM7 binds directly to several PLC isoforms, including PLCγ and PLCβ (Runnels et al., 2002). The stimulatory effect of PLC on TRPM7 observed in intact cells by biochemical-, cell-biological- and live-cell imaging studies contrasts markedly with a report by Runnels et al (Runnels et al., 2002) that in HEK-293 cells whole-cell TRPM7 currents are potently inhibited by carbachol-induced PIP_2 hydrolysis. PIP_2-dependent gating also occurs in other TRP family members, including TRPV1 (Prescott and Julius, 2003), TRPM5 (Liu and Liman, 2003) and TRPM8 (Liu and Qin, 2005; Rohacs et al., 2005). Finally, in a recent study Takezawa and colleagues (Takezawa et al., 2004) reported that in HEK-293 cells (expressing only endogenous muscarinic receptors) carbachol attenuated TRPM7 currents via the G_s-cAMP

signalling pathway, whereas PLC activation was not involved.

As thus regulation of TRPM7 detected in whole-cell experiments appears to differ from our cell-biological studies, we here address the effects of GPCR stimulation by non-invasive techniques in cells retrovirally transduced to overexpress TRPM7 at very low level. We combine FRET assays for second messengers with Ca^{2+} fluorometry and perforated-patch experiments to show that opening of TRPM7 correlates well with PLC, but not with cAMP or cGMP signaling. We also address why in our observations the effect of PLC activation appears opposite to that obtained in whole-cell by comparing both approaches under various ionic conditions. Strikingly, in perforated patches TRPM7 currents can be evoked by treatment with the membrane-permeable Mg^{2+} chelator EDTA-AM, and these currents are inhibited, rather than augmented, by PLC-activating agonists. We conclude that in intact cells TRPM7 currents are enhanced, rather than inhibited, by PLC-coupled agonists.

Methods

Materials

Amphotericin B, MgATP, bradykinin, lysophosphatidic acid, spermin, $La(NO_3)_3$, $Gd_2(CO_3)_3$, sodium nitroprusside, prostaglandin E1, and niflumic acid were from Sigma-Aldrich Co. (St. Louis, MO). Oregon Green 488 BAPTA-1 AM, Fura Red AM, Indo-1 AM, o-nitrophenyl-EGTA AM, pluronic F127 and BAPTA-AM were from Molecular Probes Inc. (Eugene, OR). Ionomycin, 2-APB, SKF 96365, IBMX, forskolin, neurokinin A (NKA) and thapsigargin were from Calbiochem-Novabiochem Corp. (La Jolla, CA). Salts were from Merck (Darmstadt, Germany). Dulbecco's MEM, foetal calf serum, penicillin and streptomycin were obtained from Gibco BRL (Paisley, Scotland). Neomycin was purchased from Invitrogen-Life technologies (Breda, the Netherlands). FuGene 6 transfection reagent was from Roche Diagnostics B.V. (Penzbreg, Germany)

Constructs

Mouse TRPM7 in pTracer-CMV2 was a kind gift from Dr. D. Clapham (Harvard, Boston, Ma). To generate retroviral expression vectors, the TRPM7 cDNA was inserted as an *Xho*I-*Not*I

fragment into the LZRS-ires-neomycin vector. For production of recombinant protein in bacteria a pcr product encoding amino acids 1748 to 1862 of TRPM7 was cloned in frame in pGEX-1N using *Bam*HI and *Eco*RI sites. All constructs were verified by sequencing. The PIP$_2$ FRET sensor (eCFP-PHδ1 and eYFP-PHδ1) was previously generated in our lab as described (van der Wal et al., 2001). The genetically encoded cAMP sensor was a kind gift from Dr. M. Zaccolo (University of Padova, Padova, Italy), the cGMP sensor Cygnet 2.1 was kindly provided by Dr. W. Dostmann (University of Vermont, Burlington, VT), and the Ca^{2+} indicator Yellow Cameleon 2.1 was a gift from Dr. R. Tsien (UCSD, La Jolla, CA).

Cell Culture

Mouse N1E-115 and Phoenix packaging cells were cultured in DMEM supplemented with 10% fetal calf serum, penicillin and streptomycin and kept in a humidified CO$_2$ incubator. Stable cell lines were generated by retroviral transduction as previously described (Clark et al., 2006). Cells were selected by the addition of 0.8 mg/ml G418 to the media and the selection was complete within 7 days. Cells were passaged twice a week and seeded on glass cover slips for experiments.

Generation of Antibodies

To generate anti-TRPM7 antibodies, a GST-fusion protein encoding amino acids 1748 to 1862 was expressed in *Escherichia coli* BL21 and purified on a glutathione-sepharose column. Rabbits were injected with the antigen mixed with Freund's adjuvant and serum was collected 10 days after every vaccination. Serum collected before immunization (preimmune) was used as a control in all experiments (Clark et al., 2006).

In Vitro Kinase Assay

Cells were lysed in RIPA buffer (50 mM Tris pH 7.5, 150 mM NaCl, 0.1% SDS, 0.5% sodium deoxycholate, 1% triton X-100 supplemented with protease inhibitors), incubated on ice for 20 min, and lysates were cleared by centrifugation. Lysates were incubated with anti-TRPM7 antibodies for 3 h at 4°C and immunocomplexes were isolated by the addition of protG-sepharose. The beads were washed 3 times with lysis buffer and subsequently twice with kinase buffer without ATP (50 mM HEPES pH 7.0, 3.5 mM MnCl$_2$, 5 mM DTT). The

kinase reaction was initiated by adding 0.1 mM ATP in combination with 5 μCi γ-^{32}P-ATP and proceeded for 30 min at 30°C. The products of the kinase reaction were resolved by SDS-PAGE on a 6% acrylamide gel and detected using a phosphoimager.

Immunolabeling of N1E-115/TRPM7 Cells

Cells grown for 24 hours on glass coverslips were fixed for 10 minutes at room temperature in phosphate-buffered saline and 4% paraformaldehyde. Subsequently, cells were permeabilized with 0.1% triton X-100 in phosphate-buffered saline. Cells were incubated with rabbit anti-TRPM7 sera (1:200) followed by horse-radish peroxidase-conjugated anti-rabbit Ig (1:1000). Amplification of the signal was by tyramide-conjugated FITC (PerkinElmer, Boston, MA) and images were collected using a Leica SP2 confocal microscope.

Ca^{2+} Determinations and Uncaging Experiments

For Ca^{2+} recordings, cells on glass coverslips were incubated for 30 min with dyes, followed by further incubation in medium for at least 15 min. For pseudoratiometrical determinations (van der Wal et al., 2001; Jalink et al., 1990), a mixture of 1 μg Oregon Green 488 BAPTA-AM and 4 μg Fura Red-AM in 100 μl medium was used. Coverslips were mounted on the inverted microscope and recordings were made at 37°C in HEPES-buffered saline, composed of (in mM): NaCl (140), KCl (5), MgCl$_2$ (1), CaCl$_2$ (1), HEPES (10) and glucose (10), pH 7.2. Single-cell fluorescence recordings were collected with a Nikon inverted microscope fitted with a Biorad MRC600 scanhead (Biorad, Herts, England). Excitation of Oregon Green and Fura-Red was at 488 nm and emission was detected at 522 +/- 16 nm and at >585 nm. All traces were calibrated with respect to maximal ratio (after ionomycin treatment) and minimal ratio (in the presence of excess BAPTA). Calculation of Ca^{2+} concentrations were performed as published (Grynkiewicz et al., 1985). Ca^{2+} experiments were also repeated in large series of ratiometric Indo-1 experiments, as well as using the FRET Ca^{2+} sensor Yellow Cameleon 2.1 (Miyawaki et al., 1997) essentially as published (van der Wal et al., 2001). For Ca^{2+} uncaging experiments, oNP-

EGTA (0.5 µg per 100 µl) was co-loaded with Ca^{2+} dyes into cells. Uncaging of oNP-EGTA was achieved by a sub-second flash of UV light (355 ± 25 nM) from a mercury arc lamp.

Indo-1 Quenching Experiments

N1E-115/TRPM7 cells on rectangular coverslips were grown to near-confluency. Cells were loaded with Indo-1 AM (1.5 µg/100µl) for 30 min and further incubated in fresh medium for at least 30 min. Coverslips were introduced into a photon-counting spectrofluorometer (Quanta-Master, PTI Inc., Lawrenceville, NJ) controlled by the vendors Felix software. Experiments were performed in HEPES-buffered saline; excitation was at 338 nm and emission was detected at 410 nm. Following recording of basal fluorescence changes for ~10 min, 200 µM Mn^{2+} was added and fluorescence was recorded for 10 more min. Autofluorescence, as determined by maximal quenching of Indo-1 with ionomycin + excess Mn^{2+}, was usually less than 10 %. Both the baseline and the initial part of the response after Mn^{2+} addition were fitted linearly, and the Mn^{2+}-induced quench rate was calculated by subtracting the former from the latter. The quench rate is expressed as decrease in detected photons (counts) per second.

Dynamic FRET Essays

Cells grown on coverslips were transfected with FRET constructs (1µg/coverslip) using FuGene 6 according to manufactures' guidelines, and experiments were performed as described previously (van der Wal et al., 2001; Ponsioen et al., 2004). In brief, coverslips were placed on an inverted Nikon microscope and excited at 425nm using an ND3 filter. CFP- and YFP emission were collected simultaneously through 470 ± 20 and 530 ± 25 nm bandpass filters. Data were acquired at 4 samples per second and FRET was expressed as ratio of CFP to YFP signals. This ratio was set to 1.0 at the onset of the experiments, and changes are expressed as per cent deviation from this initial value.

Patch-clamp Experiments

Electrophysiological recordings were collected using an EPC9 amplifier (HEKA electronics, Lambrecht, Germany), connected to a personal computer and controlled by HEKA pulse software. Voltage-clamp protocols were generated using HEKA pulse software, and current recordings were digitized at 100 kHz (ramp and block pulse protocols) or 10 Hz (steady-state whole-cell currents). Borosilicate glass pipettes were pulled on a p-2000 pipette puller (Sutter instruments, Novato, CA) and fire-polished (Narishige Microforge, Tokyo, Japan) to 2-4 MΩ. After establishment of the GΩ seal, the patched membrane was ruptured by gentle suction to obtain whole-cell configuration, or amphotericin B (240 µg/ml) was used to obtain the perforated-patch configuration with typical access resistance of 3-10 MΩ.

Solutions were as follows (in mM): whole-cell pipette solution: K-Glutamate (120), KCl (30), $MgCl_2$ (1), $CaCl_2$ (0.2), EGTA (1), HEPES pH.7.2 (10) and MgATP (1); external solution: NaCl (140), KCl (5), $MgCl_2$ (0-1), $CaCl_2$ (0-10), HEPES (10) and glucose (10), adjusted to pH 7.3 with NaOH; for perforated-patch recordings, the pipette solution was complemented with 240 µg/ml Amphotericin B and MgATP was omitted. For MIC/MagNuM recordings (Fig. 1*c & d*) the pipette solution contained CsCl (120), HEPES (10), MgATP (1) and $MgCl_2$ (0-3), pH adjusted to 7.2 with CsOH, and cells were kept in a solution containing TEACl (100), CsCl (5), $CaCl_2$ (2), $MgCl_2$ (1), HEPES (15), Glucose (10), pH adjusted with TEAOH to 7.3.

Results and Discussion

TRPM7 Expression Causes Increased MIC/MagNuM Currents

Consistent with observations by others (Nadler et al., 2001) we observed that transient overexpression of TRPM7 channels was lethal within 1 to 3 days in N1E-115 cells and all other cell lines tested (data not shown). Furthermore, at early time points after transfection, the protein located primarily to the biosynthetic pathway, with little or no expression detectable at the plasma membrane. To circumvent these problems, we introduced TRPM7 in N1E-115 cells at low expression levels by retroviral transduction. These cells, termed N1E-115/TRPM7 cells, were viable, divided normally and could be routinely kept in culture for several months. Using a TRPM7-specific antibody, the expression level in N1E-115/TRPM7 cells was found to be 2-3 times that of parental cells (Fig. 1*a*). As shown in Fig. 1*b*, the

majority of TRPM7 labeling localized to the plasma membrane.

Initially we analyzed whether TRPM7 overexpression caused in increased MIC/MagNum currents. In whole-cell patch clamp experiments, $[Mg^{2+}]_i$ was lowered by omission of the ion from the pipette solution. With a fluorescent dye in the pipette it was verified by confocal microscopy that intracellular perfusion was near-complete within a few minutes (data not shown). Concomitantly, both in parental and in N1E-115/TRPM7 cells, MIC/MagNuM currents developed. In parental cells, the current density at –60 mV averaged -0.33 +/- 0.08 pA/pF, N = 14 (Fig. 1c, *upper panel*; quantification in Fig. 1d). In N1E-115/TRPM7 cells, MIC/MagNuM current density averaged -0.80 +/- 0.18 pA/pF, N = 9 (Figs. 1c, *middle panel*,

1d), in good agreement with the expression data (Fig. 1a). In both cell lines, currents had all the characteristic hallmarks of MIC/MagNuM currents: first, they were strongly blocked by including 1-3 mM of free Mg^{2+} in the pipette solution (Fig. 1c, *lower panel*). Second, whole-cell currents showed an outward-rectifying I/V relationship in divalent-containing media (Fig. 1e) that became linear upon removal of divalents (Mg^{2+} and Ca^{2+}) from the medium (data not shown). Third, in line with the results from Runnels (Runnels et al., 2001), responses evoked by voltage-step protocols lacked voltage- or time-dependent characteristics (Fig 1e, *right panel*). Furthermore, sensitivity of MIC/MagNuM currents to inhibitors of TRPM7 matches with that reported in the literature (Table 1).

Fig. 1. Expression of TRPM7 in N1E-115 cells by retroviral transduction. *(a)* Retroviral transduction causes moderate overexpression of the TRPM7 channel-kinase as assayed by autophosphorylation of its kinase domain after immunoprecipitation by TRPM7-specific antibodies. *(b)* Confocal image of N1E-115 cell showing localization of the protein to the plasma membrane. TRPM7 was detected using anti-TRPM7 antibodies, followed by tyramide signal amplification. Scale bar, 10 μm. *(c) Upper panel*, MIC/MagNuM detected in whole-cell configuration. MIC/MagNuM currents start to develop immediately after break-in, peak at ~5-10 minutes and then gradually run down. Spikes represent current excursions induced by 1 s pulses to +60 mV from a holding potential of –60 mV. Solutions were chosen so that outward currents are mainly Cs^+, and inward currents are mainly Ca^{2+} by substituting tetraethyl ammonium (TEA^+) for Na^+ in the medium. *Middle panel*, MIC/MagNuM currents in N1E-115/TRPM7 cells are 2- to 3-fold larger in amplitude but display the same kinetics. *Lower panel*, inclusion of 3 mM Mg^{2+} in the pipette completely blocks MIC/MagNuM currents in N1E-115/TRPM7 cell. *(d)* Quantification of MIC/MagNuM currents for N1E-115/TRPM7 and parental cells, detected at –60 mV and at +60 mV. *: p < 0.01. *(e) Left panel*, I/V plots of MIC currents measured in N1E-115/TRPM7 cells by ramps (-100 to +100 mV, grey line) from at 0 mV holding potential and from instantaneous V-steps (20 mV-steps from –80 mV to 80 mV, black squares), corrected for background. Note complete overlap of I/V-plots obtained by these two methods. *Right panel*, individual, uncorrected traces from step-response currents at onset of the experiment (*top panel*) and at maximal activation (*lower panel*) show lack of time-dependent activation. Shown are representative traces from 10 individual experiments.
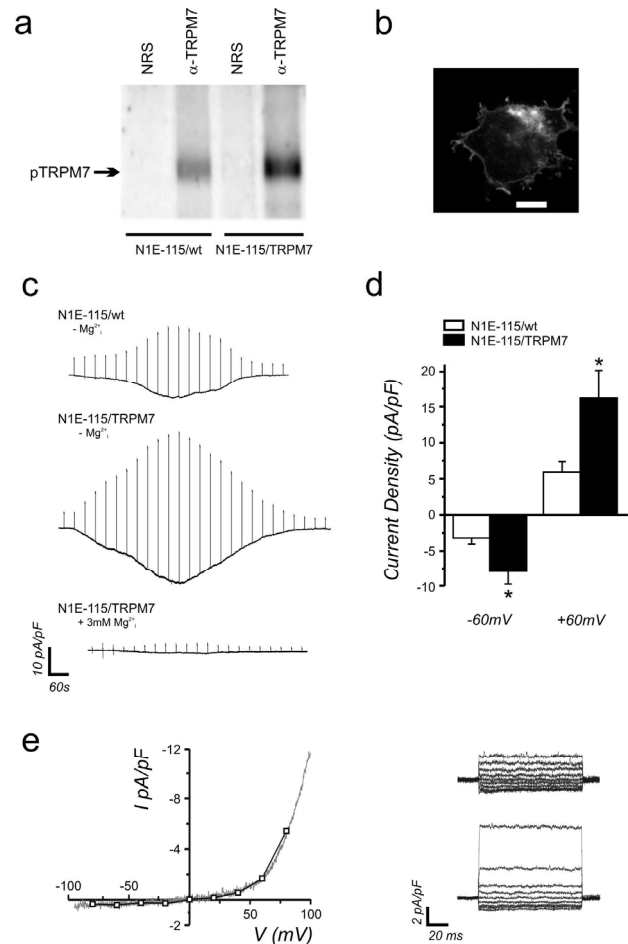
Table 1: Pharmacological characterization of TRPM7 currents as detected by different techniques

	Confocal Calcium	Whole cell	Perforated Patch
La^{3+} / Gd^{3+}	+ (200uM)	+ (5mM)	n.t.
2-APB (100μM)	+	+	+
SKF 96365 (30μM)	+	+	+
Spermin (50μM)	n.a.	+	n.t.
Niflumic acid (100μM)	+	+	+

N1E-115/TRPM7 cells were challenged with 1 μM bradykinin and the sensitivity of the ensuing sustained responses to the indicated blockers was tested. +, response is sensitive to blocker; n.a., not applicable (i.e. spermin works only in divalent-free media); n.t., not tested. All experiments were performed at least in triplicate.

Elevated Basal and Agonist-Induced Cytosolic Ca^{2+} Levels in N1E-115/TRPM7 Cells

Next we analyzed $[Ca^{2+}]_i$ in parental and N1E-115/TRPM7 cells by ratiometrical Ca^{2+} imaging (see Methods). Intracellular Ca^{2+} was elevated significantly in N1E-115/TRPM7 cells (108.9 +/- 6.0 nM, N = 50) as compared to parental cells (85.3 +/- 2.5 nM, N = 50; p < 0.05; Fig. 2a, quantification in *Fig. 2b*). As it has been reported that TRPM7 channels are partly pre-activated (Schmitz et al., 2003; Kozak and Cahalan, 2003; Hanano et al., 2004; Matsushita et al., 2005; Demeuse et al., 2006), this suggests that in N1E-115/TRPM7 cells too, a part of the TRPM7 channel population is open under resting conditions. Thus, low-level overexpression of TRPM7 is well tolerated and contributes to Ca^{2+} homeostasis.

Because cell-biological and biochemical data (Clark et al., 2006) indicate that TRPM7 channels are activated by the GPCR agonist BK, we next monitored the effect of addition of BK on TRPM7-mediated Ca^{2+} influx by comparing N1E-115/TRPM7 to parental cells. In N1E-115 cells, stimulation of endogenous B2 receptors with bradykinin (BK) strongly activates PLC through the G_q pathway (Coggan and Thompson, 1995; Chapter II). In parental cells, 1 μM BK induced a cytosolic Ca^{2+} increase (765.9 +/- 9.7 nM, N = 80) that peaked within seconds and subsequently returned to values close to resting levels (92.9 +/- 2.9 nM) within 60s (Fig. 2a, *left panel*). This corresponds to a mean increase of 7.6 nM from basal levels, which was not statistically significant. In contrast, in N1E-115/TRPM7 cells the BK-induced transient Ca^{2+} increase (peak 843.3 +/-

12.7 nM) was followed by a prominent sustained Ca^{2+} elevation (141.0 +/- 7.0 nM, N = 120) that lasted for several minutes before returning to resting levels rather abruptly (Fig. 2a, *right panel*; quantification in Fig. 2b). Note that, in comparison with wt cells, the magnitude of the mean increase in sustained Ca^{2+} levels in N1E-115/TRPM7 cells (32.1 nM; p < 0.001, paired t-test) corresponds reasonably well with the 2 to 3-fold higher TRPM7 expression levels. Thus, expression of TRPM7 at the plasma membrane elicits a sustained phase in the Ca^{2+} response to BK, in good agreement with
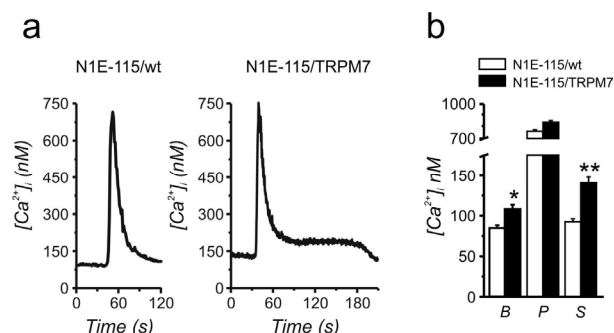

Fig. 2. Sustained Ca^{2+} influx in N1E-115/TRPM7 cells after stimulation of PLC. *(a)* Pseudo-ratiometric single-cell Ca^{2+} traces showing effect of addition of bradykinin (BK, 1 μM) in parental (*left panel*) and TRPM7 transduced cells (*right panel*). Note the characteristic abrupt end of the sustained phase after ~3-5 minutes. Shown are representative traces from hundreds of experiments. Similar results were obtained with Indo-1 as well as with the FRET Ca^{2+} sensor Yellow Cameleon 2.1 (see Methods). *(b)* Effects of retroviral TRPM7 expression on basal (B) and agonist-induced peak (P) and sustained (S, taken 2 minutes after addition of BK) calcium levels. $[Ca^{2+}]_i$ concentrations were calibrated with ionomycin and BAPTA, and data of hundreds of cells were averaged. Shown are mean + s.e.mean of values of the initial Ca^{2+} peak and of the sustained phase, taken 2 minutes after addition of BK. *: p < 0.001.

our cell-biological data (Clark et al., 2006).

BK-Induced Sustained Ca²⁺ Elevation Is Due to Influx Through TRPM7

To address whether the sustained Ca^{2+} phase is due to entry through TRPM7 channels, we investigated several alternatives. First, it is conceivable that expression of TRPM7 could burden the cells with excess Ca^{2+} entry, thereby compromising intracellular Ca^{2+} buffering mechanisms. Therefore we assayed cytosolic Ca^{2+} buffering by quantitating the rate of clearance of UV-released caged Ca^{2+}. Native N1E-115 and N1E-115/TRPM7 cell were loaded with o-nitrophenyl-EGTA and Ca^{2+} dyes (see Methods) and exposed to ~0.2s flashes of UV light (Fig. 3*a*, *left and middle panels*). In wt cells, this caused an instantaneous increase in $[Ca^{2+}]_i$, which was cleared from the cytosol with a time course well fitted by a single exponential. Ca^{2+} drop rates in both cell lines were indistinguishable (21.77 +/- 2.00, N = 15 versus 21.75 +/- 1.76, N = 15, Fig. 3*a*, *right panel*), ruling out different cytosolic buffering as the responsible mechanism. Note that the shape of the BK-induced Ca^{2+} increase, with a prolonged sustained phase that ends rather abruptly after several minutes (Fig. 2*a*, *right panel*), also argues against flawed Ca^{2+} buffering as the responsible mechanism. Rather, sustained elevated Ca^{2+}_i levels are due to influx since they were absent in cells acutely pre-treated with the calcium chelator BAPTA at 3 mM (Fig. 3*b*, *left panel*). Addition of BAPTA during the sustained Ca^{2+} elevation also caused a rapid drop which often proceeded to values below basal level (Fig. 3*b*, *right panel*; 59.9 +/- 8.2 nM), an observation that is in line with the reported pre-activation of TRPM7 channels. Thus, the sustained phase in BK-stimulated N1E-115 cells reflects Ca^{2+} influx over the plasma membrane.

We further ruled out that addition of BK caused depolarization of the cell membrane with consequent Ca^{2+} influx through voltage-sensitive Ca^{2+} channels. Whereas this has been described for N1E-115 cells that were induced to adopt a differentiated neuronal phenotype (Bolsover, 1986) by 2-4 day serum starvation, in non-starved cells Ca^{2+}_i levels were completely insensitive to depolarization by 50-100 mM extracellular K^+ (Fig. 3*c*). Furthermore, resting membrane potentials of non-starved native and TRPM7 overexpressing cells did not differ (-29.9 +/- 3.4 mV and -32.8 +/- 5.3 mV, resp.) and BK

stimulation evoked only minor depolarization of the plasma membrane (wt: 10.0 +/- 4.0 mV, N=6; N1E-115/TRPM7: 11.8 +/- 0.9 mV, N=5). These results rule out activation of a voltage-sensitive Ca^{2+} channel as the responsible mechanism and are in line with the reported lack of voltage sensitivity of TRPM7 at physiological membrane voltage.

Finally, we tested sensitivity of the sustained phase of Ca^{2+} influx to a panel of inhibitors for TRPM7 channels (Table 1). When administered during the sustained Ca^{2+} phase, 2-aminoethoxy-
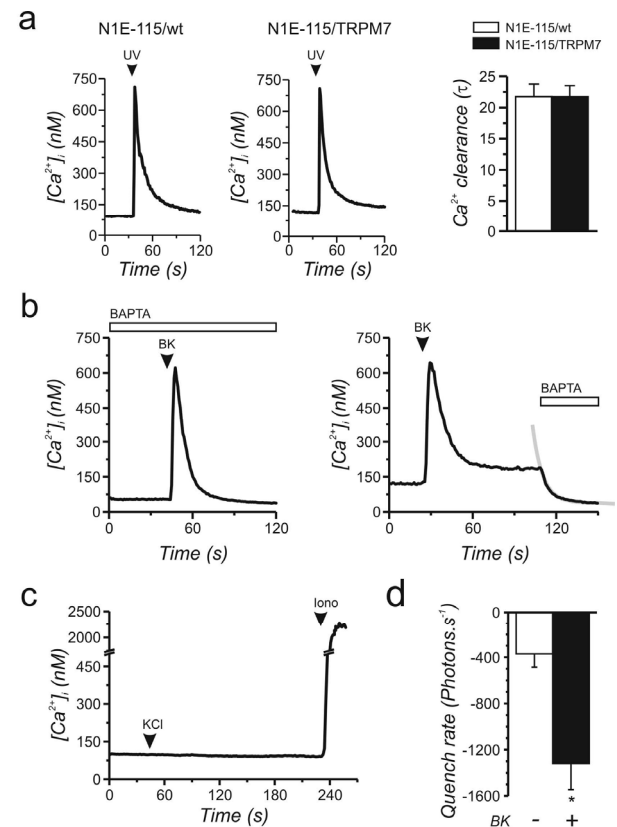

Fig. 3. Sustained Ca²⁺ levels in N1E-115/TRPM7 cells are due to increased membrane permeability. (*a*) *Left and middle panel*, typical traces showing similar Ca^{2+} clearance of caged Ca^{2+} spikes in parental and N1E-115/TRPM7 cells. *Right panel*, quantification (mean + s.e.mean of τ; N = 15) of Ca^{2+} clearance from single-exponential fits. (*b*) *Left panel*, sustained Ca^{2+} elevation after BK stimulation in N1E-115/TRPM7 cells is abolished by brief pre-treatment with extracellular BAPTA. *Right panel*, addition of BAPTA during the sustained Ca^{2+} phase lowers $[Ca^{2+}]_i$ to values below baseline. (*c*) Depolarization of N1E-115/TRPM7 cells by adding extracellular KCl (50mM) does not cause Ca^{2+} influx; iono indicates addition of the Ca^{2+} ionophore ionomycin as a positive control. Note the break in the Y-axis. (*d*) BK (1 μM) stimulation causes increased permeability for Mn^{2+} in N1E-115/TRPM7 cells as measured by an Indo-1 quenching assay (mean + s.e.mean; N = 6; *: $p < 0.025$, single-sided t-test).

diphenyl-borate (2-APB, 50μM) (Jiang et al., 2003) completely blocked BK-induced Ca^{2+} influx. In line with the observation that TRPM7 expression also contributes to basal Ca$^{2+}_i$ levels, the 2-APB-induced drop in Ca^{2+} levels often proceeded to values below baseline (data not shown). Furthermore, we tested SKF 96365 (30μM) (Kozak et al., 2002), and the polyvalent cations Gd^{3+} and La^{3+} (both at 200μM) (Runnels et al., 2001). In all cases, the BK-induced sustained phase, but not the initial Ca^{2+} peak, was strongly inhibited. Note that none of these inhibitors are truly selective for TRPM7, and that this pharmacological profile also fits Icrac. However, unlike Icrac (Hoth and Penner, 1992) TRPM7 permeates Mn^{2+} ions well (Monteilh-Zoller et al., 2003). When tested by Indo-1 quenching assays (see Methods), N1E-115/TRPM7 cells challenged with BK were significantly more permeable to Mn^{2+} than unstimulated cells (Fig. 3d). Taken together, these data strongly suggest that the BK-induced sustained Ca^{2+} elevation in N1E-115/TRPM7 cells is mediated by influx through TRPM7 channels in the plasma membrane.

TRPM7 Activation in Intact N1E-115 Cells Is Downstream of G$_q$/PLC Signaling

In whole-cell patch clamp experiments on HEK-293 cells overexpressing M1 muscarinic receptors, TRPM7 channels were shown to be inhibited by carbachol-induced PIP$_2$ breakdown (Runnels et al., 2002), and this inhibition was reverted by intracellular perfusion with a water-soluble PIP$_2$ analogue. This result was subsequently challenged by Takezawa and colleagues (Takezawa et al., 2004) who found that activating PLC through endogenously expressed M1 receptors had little effect on TRPM7 currents, and used the lack of effect of the inhibitor U-73122 to underscore this point of view. Instead, they reported that whole-cell TRPM7 currents were enhanced or attenuated, respectively, by agonists to receptors that couple to stimulatory (G$_s$) or inhibitory (G$_i$) G proteins to raise or lower intracellular cAMP levels.

We made use of the endogenously expressed B2 bradykinin receptors that couple predominantly to the G$_q$/PLC pathway, but some scattered reports suggest that depending on the cell type the B2 receptor may sometimes either inhibit (Hanke et al., 2001) or stimulate (Albert et al., 1999) production of cAMP. Hence, we set out to identify
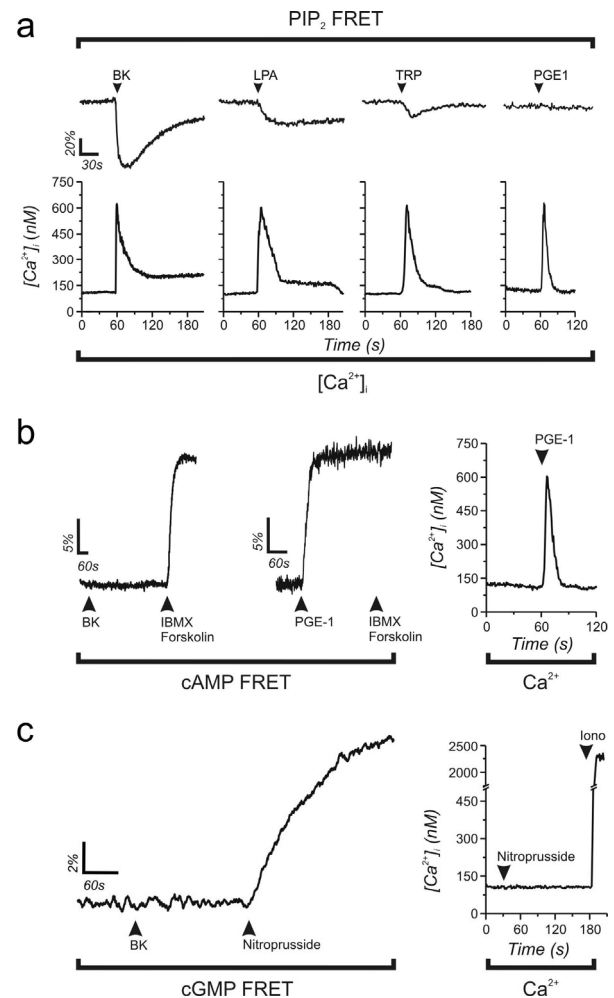

Fig. 4. Activation of TRPM7 by GPCRs: involvement of the G$_q$ / PLC signalling pathway. (*a*) Representative FRET traces showing PIP$_2$ hydrolysis (*upper panel*) induced by BK, LPA and thrombin receptor activating peptide (TRP), and the ensuing sustained Ca^{2+} elevations in N1E-115/TRPM7 cells (*lower panel*). Prostaglandin E1 (PGE-1), a potent activator of cAMP production, does not activate PLC and it fails to evoke sustained Ca^{2+} entry (*rightmost traces*). (*b*) BK receptor activation does not alter cAMP levels in N1E-115/TRPM7 cells as detected by a PKA-based FRET probe *(left panel)*. Addition of the adenylyl cyclase activator forskolin together with the phosphodiesterase inhibitor IBMX serve as a positive control. Conversely, PGE-1 potently activates the G$_s$ / cAMP pathway through its cognate GPCR *(middle panel)* but fails to elicit the sustained Ca^{2+} elevation *(right panel)* that is typically seen after G$_q$ / PLC activation. (*c*) In N1E-115/TRPM7 cells BK fails to alter cGMP levels, whereas the NO-donor nitroprusside readily activates this pathway, as assessed using Cygnet, a FRET sensor for cGMP (Honda et al., 2001). Addition of nitroprusside had no effect on [Ca^{2+}]$_i$ in these cells *(right panel)*.

the signaling route responsible for BK-induced activation of TRPM7 in intact N1E-115/TRPM7 cells by correlating Ca^{2+} fluorometry with activation of intracellular signaling pathways, as detected by various FRET assays.

We and others have previously reported that stimulation of endogenous B2 receptors with BK causes rapid breakdown of a significant fraction (60-80%) of the membrane PIP_2 pool in N1E-115 cells (van der Wal et al., 2001; Xu et al., 2003). Similarly, addition of BK to N1E-115/TRPM7 cells caused near-complete breakdown of PIP_2, as detected by a FRET assay that reports membrane PIP_2 content (Fig. 4*a, upper panel, first trace* (van der Wal et al., 2001)). In these cells, the G_q-coupled agonists lysophosphatidic acid (LPA) and thrombin receptor activating peptide also activate PLC, albeit to a lesser extent (~20-30% of BK values; N > 200; Fig. 4*a, upper panel, second and third trace* (van der Wal et al., 2001)). Similar to BK, the initial Ca^{2+} peak induced by these agonists was followed by sustained Ca^{2+} influx in N1E-115/TRPM7 cells, although responses were a bit more variable than those to BK (Fig. 4*a, lower panel*). In contrast, sustained Ca^{2+} influx was not seen when cells were stimulated with agonists to receptors that do not couple to PLC (Fig. 4*a, right panel*, and data not shown). Thus, TRPM7 activation correlates well with PLC activation / Ca^{2+} signaling but it does not require near-complete breakdown of the PIP_2 pool.

To address possible involvement of cAMP in the BK-induced opening of TRPM7, we monitored cAMP levels in intact N1E-115/TRPM7 cells using a genetically encoded sensor for cAMP (Zaccolo et al., 2000). Of the available FRET sensors for cAMP, this sensor has the highest affinity (Kd of 300 nM (Bacskai et al., 1993)) and it is well suited to reveal small changes from baseline levels. Addition of BK to N1E-115/TRPM7 cells had absolutely no effect on cAMP levels (N = 8), whereas forskolin (25μM) readily raised cAMP levels in these cells (Fig. 4*b, left panel*). Furthermore, we tested the effects of pre-treatment of cells with pertussis toxin, which specifically inhibits G_i and thereby blocks receptor-induced decreases in cAMP levels, on the response to BK. No effects on kinetics or amplitude of the BK-induced Ca^{2+} influx were observed in N1E-115/TRPM7 cells (data not shown). Thus, we find no evidence that cAMP may mediate BK-induced opening of TRPM7. Conversely, we tested the effect of agonists that do signal potently through G_s and G_i, respectively. Prostaglandin E1 (PGE1) potently activates G_s to
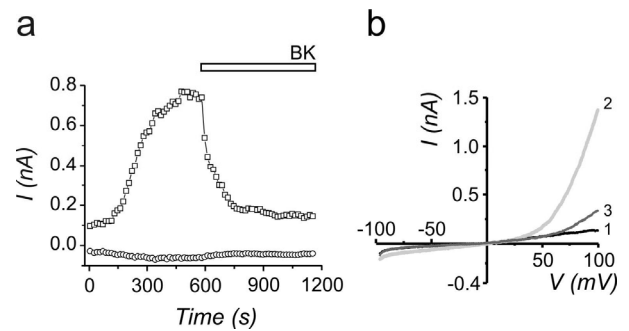

Fig. 5. MIC/MagNuM currents in N1E-115/TRPM7 cells are inhibited by BK. *(a)* TRPM7 currents, evoked with Mg^{2+}-free pipette solution in a N1E-115/TRPM7 cell, are strongly inhibited after activation of PLC. Currents evoked by ±100 mV ramps *(b)* from a holding potential of 0 mV are quantified at –80 mV *(circles)* and +80 mV *(squares)*. Note that the small inward currents are due to divalent-block in Mg^{2+}- and Ca^{2+}-containing extracellular medium. Shown is a representative trace from 10 individual experiments.

cause a rapid and sustained increase in $[cAMP]_i$ (Fig. 4*b, middle panel*) that was not paralleled by sustained Ca^{2+} influx (Fig. 4*b, right panel*). Similarly, activation of G_i by Sphingosine-1-phosphate (S1P) was ineffective. We conclude that there is no evidence for a role of cAMP in BK-mediated Ca^{2+} influx in N1E-115/TRPM7 cells.

We also investigated the role of other well-delineated signaling pathways in N1E-115 cells. In these cells, stimulation with agonists that couple to G_{13} leads to strong activation of the small GTPase Rho, resulting in rapid contraction of the actin cytoskeleton (Postma et al., 1996b). S1P potently activates this signaling cascade (Postma et al., 1996b) but it does not couple to G_q (KJ, unpublished results). In N1E-115/TRPM7 cells, S1P caused rapid cytoskeletal contraction but it had no detectable effect on Ca^{2+} (data not shown). Finally we tested the effects of addition of the NO-donor nitroprusside since NO was reported to activate TRPM7-mediated Ca^{2+} influx in cultured cortical neurons (Aarts et al., 2003). In intact parental and N1E-115/TRPM7 cells, nitroprusside potently triggered production of cGMP (Methods; Fig. 4*c, left panel* (Ponsioen et al., 2004)) but no effect on $[Ca^{2+}]_i$ was observed (Fig. 4*c, right panel*). In conclusion, TRPM7 opening correlates well with G_q / PLC but not with other G-protein mediated signals in our cells.

Activation of PLC Inhibits Whole-cell TRPM7 Currents in N1E-115/TRPM7 Cells.

In whole-cell patch clamp experiments on HEK-293 cells overexpressing M1 muscarinic receptors, TRPM7 channels were shown to be inhibited by carbachol-induced PIP_2 breakdown (Runnels et al., 2002), and this inhibition was reverted by intracellular perfusion with a water-soluble PIP_2 analogue. This result contrasts with our cell-biological, biochemical and Ca^{2+}-data (see above, and (Clark et al., 2006)) that show that PLC activation causes opening rather than closure of TRPM7 channels. We therefore tested whether TRPM7 currents recorded in whole cells with Mg^{2+}-free pipette solution were similarly suppressed in our cells. Upon break-in, channel activation was monitored from outward-rectifying (MIC/MagNuM) currents evoked with voltage ramps. Indeed, challenging the cells with BK after full activation of TRPM7 caused currents to rapidly decrease in both native N1E-115 cells (data not shown) and N1E-115/TRPM7 cells (99.7 % $\pm$

a

b
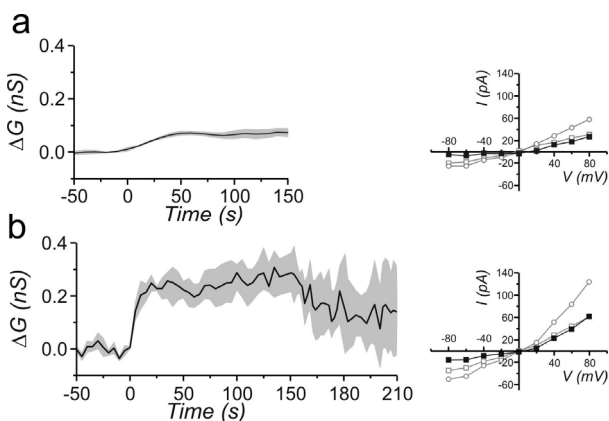
Fig. 6. TRPM7 currents detected using perforated-patch clamping. N1E-115 wt *(a)* and N1E-115/TRPM7 cells *(a)* were kept at a holding potential of −70 mV and membrane conductance changes were determined from current responses to biphasic +10 and −10 mV block pulses. Note the BK-induced sustained activation of an additional conductance (BK, 1 μM). To verify that the small BK-evoked current would suffice to increase $[Ca^{2+}]_i$ significantly, we point out that an influx of just 10 pA of current carried by Ca^{2+} equals 10 x 10^{-12} / F.z = 5 x 10^{-17} mole (F, faraday constant; z, valence of ion), which in a cell of 1 pl volume would raise $[Ca^{2+}]$ by 5 x 10^{-5} M (50 μM) in 1 second, if no buffer systems are in place. Weakly rectifying currents induced by BK in wt (Fig. 6*a*, *left panel*) and N1E-115/TRPM7 (Fig. 6*b*, *left panel*) cells obtained by subtracting unstimulated from stimulated I/Vs.

1.0, N=9, Fig. 5*a*). Whereas inward currents were completely abolished, small outward currents were still observed at high depolarizing potentials (Fig. 5*b*, *trace 3*). Other PLC-coupled agonists, including TRP and LPA, also inhibited the currents, though to a lesser extent. Therefore, it appears that the original observations on PIP_2-dependency of whole-cell TRPM7 currents hold true for N1E-115/TRPM7 cells.

Gq-PLC Coupled Receptor Agonists Activate TRPM7 Currents in Intact Cells

The above observations leave us with a paradox: PLC activation inhibits TRPM7 currents in whole-cell experiments, whereas it opens the channels when assayed by Ca^{2+} fluorometry. What causes this difference? Immediately after breaking the patch membrane to whole-cell, perfusion will start to dilute diffusible signaling molecules, which could influence gating properties. To test this possibility, we analyzed the electrophysiological effects of PLC activation in intact cells using the perforated patch configuration (Rae et al., 1991; Postma et al., 1996a). In this configuration, conventional GΩ seals are obtained, but electrical access to the cell is gained by including selective Na^+/K^+ ionophores in the pipette solution, which incorporate in the patch membrane. Using amphotericin B, we routinely obtained access resistances well below 10 MΩ, allowing reliable recording of total membrane currents without disturbing the cytosolic composition.

Voltage clamped perforated patches were held at −70 mV, and conductance of the membrane was monitored by measuring currents evoked by a biphasic block-pulse protocol (+ 10 and −10 mV from resting potential; Fig. 6*a*). In unstimulated cells, evoked currents were small (0.46 +/- 0.16 pA/pF, N=10), corresponding to a membrane conductance of 23 pS/pF. Note that since Mg^{2+} levels are intact in the perforated-patch configuration, the magnitude of the detected currents should match those of whole-cell experiments with Mg^{2+} included in the pipette (Fig. 1*c*, *lower panel*). Indeed, the currents induced by 120 mV voltage steps in unstimulated whole-cells measured 3.1 +/- 0.4 pA/pF (N=5), which corresponds to ~26 pS/pF, in close agreement with the perforated-patch data. As to be expected, spontaneously developing currents were never observed in perforated patches (Data not shown). Strikingly, stimulation with bradykinin significantly increased the membrane conductance
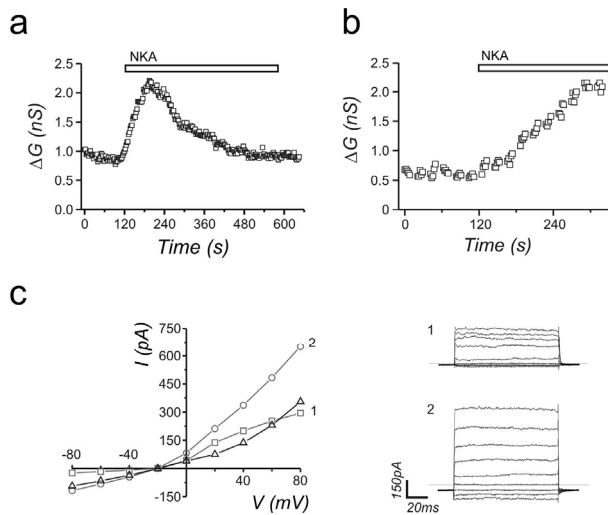
Fig. 7. TRPM7 current activation by NKA in HEK293 overexpressing TRPM7. (*a*) HEK-293 cells transiently expressing TRPM7 as well as NK2 receptors show increased membrane conductance upon stimulation of PLC with NKA (4 μM) in perforated-patch experiments. (*b*) In whole-cells with 1 mM of Mg^{2+} in the pipette solution, addition of NKA stimulates, rather than inhibits, TRPM7 currents. (*c*) *left panel*, I/V-plots from NK2-induced TRPM7 activation in HEK293 cells during whole-cell configuration. I/V-plots obtained before (1) and after (2) NKA stimulation. Black line, NKA-induced increase in currents (i.e., 1 − 2). Individual current responses to voltage steps *(right panel)* show all the hallmarks of TRPM7 currents.

(~250 +/- 53pS, N=6, Fig. 6*b*, *left panel*) in N1E-115/TRPM7 cells. In all cases, currents were transient, reverting to baseline with somewhat variable kinetics (range, 2-8 minutes). Note that whereas these conductance changes are quite small, the magnitude of inward currents, which are carried predominantly by Ca^{2+} (Nadler et al., 2001), is adequate to explain the sustained Ca^{2+} phase observed in fluorometric experiments (for analysis, see legend to Fig. 6). As wildtype N1E-115 cells express some endogenous TRPM7 channels, we next examined whether these are similarly activated after activation of PLC. Indeed, addition of BK increased the membrane conductance slightly, but significantly (Fig 6*a, left panel*). In addition, the same panel of inhibitors blocked the BK-induced currents (see Table 1). I/V plots of BK-induced currents in wt and N1E-115/TRPM7 cells revealed almost linear currents (Fig. 6*a and b*, *right panels*), the magnitude of which correlated with the expression levels. We conclude that bradykinin can activate TRPM7 channels in both native and TRPM7-transduced N1E-115 cells.

We next verified these results in HEK-293 cells. Cells were transiently transfected with TRPM7 (in a GFP-tagged zeocin vector) and the NK2-receptor, a G protein-coupled receptor (GPCR) for neurokinin A (Mau et al., 1990) that signals predominantly through G_q. One day after transfection, healthy cells expressing GFP at low levels were selected. When assayed by whole-cell patch clamping with Mg^{2+}-free pipette solutions, these cells displayed outwardly rectifying currents with all the hallmarks of TRPM7, including spontaneous activation and subsequent run-down (data not shown). In perforated-patch experiments, HEK-293 cells showed small, near-linear currents and no spontaneous developing outward rectifying currents were observed. Challenging HEK-293 cells with neurokinin A (NKA) caused a marked increase in membrane conductance (ΔG 0.79 +/- 0.33 nS; N = 3; Fig.7*a*). Again, conductance increases were transient, reverting to baseline within minutes. Note however, that in HEK-293 cells responses were quite variable, perhaps reflecting more widely diverging TRPM7 expression levels or impaired viability of transiently transfected cells. The inhibitor 2-APB (100 μM) consistently lowered the conductance to below initial values, in line with the notion that part of the channel population is opened under resting conditions (data not shown). Thus, the perforated-patch data obtained from HEK-293 cells transiently expressing TRPM7 match those obtained from N1E-115/TRPM7 cells, demonstrating that the phenotype does not depend on long-term viral transduction. We conclude that the stimulatory effect of PLC on TRPM7 currents in minimally perturbed cells parallels the Ca^{2+} imaging data, but contrasts with the data from Mg^{2+}_i-free whole-cell patch clamping.

The above observations suggest that in whole-cells, loss of $[Mg^{2+}]_i$ or possibly other signaling cofactors is sufficient to cause TRPM7 to become inhibited, rather than activated, by PLC activating agonists. To study this, HEK-293 cells transiently expressing TRPM7 were whole-cell patch-clamped with 1 mM free Mg^{2+} in the pipette. Under these conditions, NKA stimulation (Fig. 7*b*) also caused activation of TRPM7, as observed by the increase in membrane conductance. The I/V-plots obtained are slightly outward-rectifying, suggesting that internal Mg^{2+} partly prevents outward rectification by blocking/obstructing the pore of TRPM7 (Fig. 7*c*, *left panel*). Again, no voltage- or time-dependent components were observed in the current responses to voltage steps (Fig. 7*c*, *right panel*). Thus, stimulatory effects of PLC-activating agonists on TRPM7 currents can also be observed in whole-cells.

Concluding Remarks

In this study we addressed the regulation of TRPM7 channels in intact cells using low-level (2- to 3-fold) overexpression. Transient over-expression of the protein was avoided because this caused mislocalisation of TRPM7 to endo-membranes and cell death within a few days most likely because TRPM7 is to some extent constitutively active. Furthermore, transient overexpression is also more likely to titrate out essential binding partners and thereby influence signaling events. Indeed, Takezawa *et al.* noted that TRPM7 expression abolished activation of PLC by carbachol receptors (Takezawa et al., 2004). Strikingly, in a very recent study by Kim and colleagues (Kim et al., 2005) also concluded that regulation of native TRPM7 channels by PLC appeared different from results published previously from transiently transfected HEK293 cells (Runnels 2002). We furthermore chose to use perforated-patch clamping and Ca^{2+} imaging to avoid disturbing cell signaling due to intracellular perfusion in whole-cell configuration.

Our results revealed that retroviral transduction resulted in the appearance of a conductance with all the properties of TRPM7. The evidence can be summarized as follows. (i) The TRPM7 protein is expressed (Fig. 1*a*) and it resides at the plasma membrane (Fig. 1*b*). (ii) Its expression increases membrane permeability to Ca^{2+}, evident from increased basal Ca^{2+} levels (Fig. 2*a & b,*). (iii) Whole-cell currents in these cells have all the hallmarks of TRPM7 (Fig. 1*d & e*), i.e. activation by omitting Mg^{2+}_i from the pipette solution with subsequent run-down, reversal potential about 0 mV, and outward rectification that becomes linear when extracellular divalents are removed. Moreover, these currents are inhibited upon PLC activation as originally reported. (iv) The sensitivity of sustained Ca^{2+} influx and whole-cell currents to a panel of inhibitors (Table 1) corresponds to that reported earlier for TRPM7. Whereas ICRAC is blocked by the same panel of inhibitors, it differs from TRPM7 in that it is hardly permeable to Mn^{2+} ions (Fig. 3*d*), and shows fast desensitization in divalent-free solutions. (v) The basal currents observed in perforated-patches (which are small due to intracellular Mg^{2+}, data not shown) have the same magnitude as the whole-cell currents in the presence of intracellular Mg^{2+} (Fig. 1*c*, *lower panel*), and BK-evoked additional currents, which are transient and revert to baseline levels within several minutes, have the same properties. (vi) In addition, we can rule out obvious other candidates such as compromised cytosolic Ca^{2+} buffering (Fig. 3*a*) and TRPM2 (which is also widely expressed, and was detected in N1E-115 by RT-PCR) that display linear I/V-relationship and are more Ca^{2+} selective (Perraud et al., 2001).

Of course the phenotype of TRPM7 in Ca^{2+} experiments strongly reminisces of Store-Operated Calcium Entry (SOCE, ICRAC). SOCE is likewise manifested as a sustained plateau phase that depends on Ca^{2+} influx to follow an initial large Ca^{2+} peak from IP$_3$-sensitive internal stores. Unlike SOCE, however, TRPM7 opening was not evoked by depletion of stores with thapsigargin (Prakriya and Lewis, 2002; Hermosura et al., 2002) and data not shown). Moreover, under divalent-free conditions ICRAC inactivates within seconds, whereas MIC/MagNum currents showed no decay for at least a few minutes. Furthermore, the relative permeability of TRPM7 channels to different ions does not fit with ICRAC: TRPM7 channels are permeable to Mg^{2+}, Mn^{2+} (Fig. 3*d*) and Cs^+ (Fig. 1*b & c*) whereas ICRAC is characterized as non-permeable for these ions (Hoth and Penner, 1992; Zweifach and Lewis, 1993; Lepple-Wienhues and Cahalan, 1996). We thus arrive at the same conclusion as previous studies that point out that TRPM7 is not the channel responsible for conducting ICRAC (Kozak et al., 2002; Prakriya and Lewis, 2002; Hermosura et al., 2002).

Two very recent reports strongly support the view that PLC activity augments, rather than inhibits, TRPM7 channels. Kim and colleagues showed that in clusters of interstitial cells of Cajal, which control pacemaking activity in the intestine, pacemaker frequency is determined by endogenous TRPM7 channels. Strikingly, addition of stem cell factor, a stimulus that causes PIP2 breakdown, positively influenced pacemaking, indicative of increased TRPM7 conductance in these cells (Kim et al., 2005). In a second report, we analyzed the role of TRPM7 in regulating actomyosin contractility (Clark et al., 2006). This report showed that upon stimulation of cells with PLC activating agonists such as bradykinin, the TRPM7 kinase domain associates with the actomyosin cytoskeleton in a Ca^{2+} and kinase-dependent manner. Within this complex, TRPM7 inhibits myosin-II function resulting in the transformation of focal adhesions into podosomes. These biochemical and cell biological data unequivocally demonstrate activation of native TRPM7 protein by PLC-activating agonists under physiological conditions.

Strikingly, and at odds with previous reports, we observed that stimulation of PLC-activating receptors caused TRPM7 channel opening rather than closure. This discrepancy is not cell type dependent because similar observations were made in N1E-115 and HEK-293 cells, nor does it depend on TRPM7 expression levels. Rather, it was found that in intact, minimally perturbed cells (Ca^{2+} imaging and perforated-patch) PLC-coupled agonists activated the channel, whereas upon prior channel opening by Mg^{2+}_i depletion (whole-cell) PLC activation potently inhibited MIC/MagNuM currents. Conceivably, Mg^{2+}_i levels act on the TRPM7 protein itself, because it was reported that mutations in the kinase domain altered the channels setpoint for Mg^{2+} inhibition (Schmitz et al., 2003). Alternatively, Mg^{2+} depletion might act by altering interaction with adenosine nucleotides (ATP, cAMP) or by influencing (Nadler et al., 2001; Demeuse et al., 2006) phosphoinositide metabolism, especially since both PIPkinases and PIP_2 phosphatases are strongly Mg^{2+} dependent (Ling et al., 1989). Analysis of the kinetics of BK-mediated stimulatory and inhibitory effects on TRPM7 shows that activation proceeds faster than inactivation. We speculate that this reflects fundamentally different modes of regulation mediating stimulation and inhibition, as opposed to a model whereby Mg^{2+}_i would modulate (flip) the effects of PLC activation on the channel. Rescue of agonist-induced channel inactivation by replenishment of membrane PIP_2 in Mg^{2+}-free inside-out patches (Runnels et al., 2002) shows that PIP_2 is an essential cofactor for channel opening. The precise mechanism of the activation pathway remains elusive, although we can exclude the involvement of the PIP_2-derived messengers DAG (since addition of membrane-permeable analogues did not activate TRPM7, data not shown) and cytosolic Ca^{2+} (Fig. 3*a*). In any case, we find that in unperturbed cells TRPM7 increases Ca^{2+}_i levels upon PLC activation and therefore we propose that this must be the more physiological mode of action.

Takezawa and colleagues recently reported that activation of PLC through endogenous M1-muscarinic receptors had little effect on MIC/MagNuM currents in TRPM7-overexpressing HEK-293 cells (Takezawa et al., 2004). Perhaps the discrepancy between Runnels' and our study on the one hand, and that of Takezawa and colleagues on the other hand, is a difference in potency of the PLC-activating receptors involved as in their (and our) hands endogenous M1 receptors cause only minor PIP_2 breakdown.

Furthermore, unlike in our low-level retroviral overexpression studies, in HEK-293 cells TRPM7 overexpression inhibited carbachol-induced PLC signaling (Takezawa et al., 2004). Their study furthermore relied on the use of the 'PLC inhibitor' U-73122, a compound with many known side effects (Balla, 2001; Horowitz et al., 2005). Rather, Takezawa and colleagues suggested that the modulatory effects of carbachol are mediated by cAMP, as lowering [cAMP]$_i$ attenuated whole-cell TRPM7 currents in HEK-293 cells. However, in N1E-115 cells bradykinin had no effect on cAMP levels, and conversely, potent cAMP-raising agonists did not trigger TRPM7 currents or sustained Ca^{2+} influx.

.Superficially, it could be disturbing that perforated-patch currents reported here are relatively small and lack strong outward rectification, a feature that has been termed 'TRPM7 signature'. However, small amplitude basal and evoked currents are to be expected from the experimental conditions used in this study: first, we expressed the channels at low levels and secondly, we detected currents at negative voltages to assess the inward conductance properties and allow comparison with the Ca^{2+} data. TRPM7 inward currents consist mainly of Ca^{2+} and Mg^{2+} ions that both have low permeation rate (Runnels et al., 2001; Nadler et al., 2001) and in HEK-293 overexpression studies inward currents are also minor. Strong outward rectification is seen under conditions of low [Mg^{2+}]$_i$. Interestingly, like the perforated-patch currents, the currents evoked by PLC activation in TRPM7-transfected HEK-293 cells with 1 mM Mg^{2+} in the pipette show only weak outward rectification (Fig. 6*b*). Perhaps this reflects an anomalous mole fraction effect, whereby Mg^{2+}_i attenuates outward monovalent currents. However, separation of this effect from the inhibitory effect of Mg^{2+}_i on channel gating would require systematic analysis (preferably in inside-out patches) that to our knowledge have not been performed thusfar.

In summary, our experiments reveal a second mode of activation for TRPM7: not only can the channel be activated by depletion of intracellular Mg^{2+}, but also by stimulation of endogenous PLC-activating receptors.

Acknowledgements

References

Aarts,M., K.Iihara, W.L.Wei, Z.G.Xiong, M.Arundine, W.Cerwinski, J.F.MacDonald, and M.Tymianski. 2003. A key role for TRPM7 channels in anoxic neuronal death. *Cell* 115:863-877.

Albert,O., N.Ancellin, L.Preisser, A.Morel, and B.Corman. 1999. Serotonin, bradykinin and endothelin signalling in a sheep choroid plexus cell line. *Life Sci.* 64:859-867.

Bacskai,B.J., B.Hochner, M.Mahaut-Smith, S.R.Adams, B.K.Kaang, E.R.Kandel, and R.Y.Tsien. 1993. Spatially resolved dynamics of cAMP and protein kinase A subunits in Aplysia sensory neurons. *Science* 260:222-226.

Balla,T. 2001. Pharmacology of phosphoinositides, regulators of multiple cellular functions. *Curr. Pharm. Des* 7:475-507.

Bolsover,S.R. 1986. Two components of voltage-dependent calcium influx in mouse neuroblastoma cells. Measurement with arsenazo III. *J. Gen. Physiol* 88:149-165.

Clapham,D.E. 2003. TRP channels as cellular sensors. *Nature* 426:517-524.

Clark,K., M.Langeslag, L.B.van, L.Ran, A.G.Ryazanov, C.G.Figdor, W.H.Moolenaar, K.Jalink, and F.N.van Leeuwen. 2006. TRPM7, a novel regulator of actomyosin contractility and cell adhesion. *EMBO J.* 25:290-301.

Coggan,J.S. and S.H.Thompson. 1995. Intracellular calcium signals in response to bradykinin in individual neuroblastoma cells. *Am. J. Physiol* 269:C841-C848.

Demeuse,P., R.Penner, and A.Fleig. 2006. TRPM7 Channel Is Regulated by Magnesium Nucleotides via its Kinase Domain. *J. Gen. Physiol* 127:421-434.

Grynkiewicz,G., M.Poenie, and R.Y.Tsien. 1985. A new generation of Ca2+ indicators with greatly improved fluorescence properties. *J. Biol. Chem.* 260:3440-3450.

Hanano,T., Y.Hara, J.Shi, H.Morita, C.Umebayashi, E.Mori, H.Sumimoto, Y.Ito, Y.Mori, and R.Inoue. 2004. Involvement of TRPM7 in cell growth as a spontaneously activated Ca2+ entry pathway in human retinoblastoma cells. *J. Pharmacol. Sci.* 95:403-419.

Hanke,S., B.Nurnberg, D.H.Groll, and C.Liebmann. 2001. Cross talk between beta-adrenergic and bradykinin B(2) receptors results in cooperative regulation of cyclic AMP accumulation and mitogen-activated protein kinase activity. *Mol. Cell Biol.* 21:8452-8460.

Hermosura,M.C., M.K.Monteilh-Zoller, A.M.Scharenberg, R.Penner, and A.Fleig. 2002. Dissociation of the store-operated calcium current I(CRAC) and the Mg-nucleotide-regulated metal ion current MagNuM. *J. Physiol* 539:445-458.

Honda,A., S.R.Adams, C.L.Sawyer, V.Lev-Ram, R.Y.Tsien, and W.R.Dostmann. 2001. Spatiotemporal dynamics of guanosine 3',5'-cyclic monophosphate revealed by a genetically encoded, fluorescent indicator. *Proc. Natl. Acad. Sci. U. S. A* 98:2437-2442.

Horowitz,L.F., W.Hirdes, B.C.Suh, D.W.Hilgemann, K.Mackie, and B.Hille. 2005. Phospholipase C in living cells: activation, inhibition, Ca2+ requirement, and regulation of M current. *J. Gen. Physiol* 126:243-262.

Hoth,M. and R.Penner. 1992. Depletion of intracellular calcium stores activates a calcium current in mast cells. *Nature* 355:353-356.

Jalink,K., E.J.van Corven, and W.H.Moolenaar. 1990. Lysophosphatidic acid, but not phosphatidic acid, is a potent Ca2(+)-mobilizing stimulus for fibroblasts. Evidence for an extracellular site of action. *J. Biol. Chem.* 265:12232-12239.

Jiang,X., E.W.Newell, and L.C.Schlichter. 2003. Regulation of a TRPM7-like current in rat brain microglia. *J. Biol. Chem.* 278:42867-42876.

Kerschbaum,H.H., J.A.Kozak, and M.D.Cahalan. 2003. Polyvalent cations as permeant probes of MIC and TRPM7 pores. *Biophys. J.* 84:2293-2305.

Kim,B.J., H.H.Lim, D.K.Yang, J.Y.Jun, I.Y.Chang, C.S.Park, I.So, P.R.Stanfield, and K.W.Kim. 2005. Melastatin-type transient receptor potential channel 7 is required for intestinal pacemaking activity. *Gastroenterology* 129:1504-1517.

Kozak,J.A. and M.D.Cahalan. 2003. MIC channels are inhibited by internal divalent cations but not ATP. *Biophys. J.* 84:922-927.

Kozak,J.A., H.H.Kerschbaum, and M.D.Cahalan. 2002. Distinct properties of CRAC and MIC channels in RBL cells. *J. Gen. Physiol* 120:221-235.

Lepple-Wienhues,A. and M.D.Cahalan. 1996. Conductance and permeation of monovalent cations through depletion-activated Ca2+ channels (ICRAC) in Jurkat T cells. *Biophys. J.* 71:787-794.

Ling,L.E., J.T.Schulz, and L.C.Cantley. 1989. Characterization and purification of membrane-associated phosphatidylinositol-4-phosphate kinase from human red blood cells. *J. Biol. Chem.* 264:5080-5088.

Liu,B. and F.Qin. 2005. Functional control of cold- and menthol-sensitive TRPM8 ion channels by phosphatidylinositol 4,5-bisphosphate. *J. Neurosci.* 25:1674-1681.

Liu,D. and E.R.Liman. 2003. Intracellular Ca2+ and the phospholipid PIP2 regulate the taste transduction

ion channel TRPM5. *Proc. Natl. Acad. Sci. U. S. A* 100:15160-15165.

Matsushita,M., J.A.Kozak, Y.Shimizu, D.T.McLachlin, H.Yamaguchi, F.Y.Wei, K.Tomizawa, H.Matsui, B.T.Chait, M.D.Cahalan, and A.C.Nairn. 2005. Channel function is dissociated from the intrinsic kinase activity and autophosphorylation of TRPM7/ChaK1. *J. Biol. Chem.* 280:20793-20803.

Mau,S.E., P.J.Larsen, J.A.Mikkelsen, and T.Saermark. 1990. Substance P and related tachykinins induce receptor-mediated hydrolysis of polyphosphoinositides in the rat anterior pituitary. *Mol. Cell Endocrinol.* 69:69-78.

Miyawaki,A., J.Llopis, R.Heim, J.M.McCaffery, J.A.Adams, M.Ikura, and R.Y.Tsien. 1997. Fluorescent indicators for Ca2+ based on green fluorescent proteins and calmodulin. *Nature* 388:882-887.

Monteilh-Zoller,M.K., M.C.Hermosura, M.J.Nadler, A.M.Scharenberg, R.Penner, and A.Fleig. 2003. TRPM7 provides an ion channel mechanism for cellular entry of trace metal ions. *J. Gen. Physiol* 121:49-60.

Nadler,M.J., M.C.Hermosura, K.Inabe, A.L.Perraud, Q.Zhu, A.J.Stokes, T.Kurosaki, J.P.Kinet, R.Penner, A.M.Scharenberg, and A.Fleig. 2001. LTRPC7 is a Mg.ATP-regulated divalent cation channel required for cell viability. *Nature* 411:590-595.

Perraud,A.L., A.Fleig, C.A.Dunn, L.A.Bagley, P.Launay, C.Schmitz, A.J.Stokes, Q.Zhu, M.J.Bessman, R.Penner, J.P.Kinet, and A.M.Scharenberg. 2001. ADP-ribose gating of the calcium-permeable LTRPC2 channel revealed by Nudix motif homology. *Nature* 411:595-599.

Ponsioen,B., J.Zhao, J.Riedl, F.Zwartkruis, K.G.van der, M.Zaccolo, W.H.Moolenaar, J.L.Bos, and K.Jalink. 2004. Detecting cAMP-induced Epac activation by fluorescence resonance energy transfer: Epac as a novel cAMP indicator. *EMBO Rep.* 5:1176-1180.

Postma,F.R., K.Jalink, T.Hengeveld, A.G.Bot, J.Alblas, H.R.de Jonge, and W.H.Moolenaar. 1996a. Serum-induced membrane depolarization in quiescent fibroblasts: activation of a chloride conductance through the G protein-coupled LPA receptor. *EMBO J.* 15:63-72.

Postma,F.R., K.Jalink, T.Hengeveld, and W.H.Moolenaar. 1996b. Sphingosine-1-phosphate rapidly induces Rho-dependent neurite retraction: action through a specific cell surface receptor. *EMBO J.* 15:2388-2392.

Prakriya,M. and R.S.Lewis. 2002. Separation and characterization of currents through store-operated CRAC channels and Mg2+-inhibited cation (MIC) channels. *J. Gen. Physiol* 119:487-507.

Prescott,E.D. and D.Julius. 2003. A modular PIP2 binding site as a determinant of capsaicin receptor sensitivity. *Science* 300:1284-1288.

Rae,J., K.Cooper, P.Gates, and M.Watsky. 1991. Low access resistance perforated patch recordings using amphotericin B. *J. Neurosci. Methods* 37:15-26.

Rohacs,T., C.M.Lopes, I.Michailidis, and D.E.Logothetis. 2005. PI(4,5)P2 regulates the activation and desensitization of TRPM8 channels through the TRP domain. *Nat. Neurosci.* 8:626-634.

Runnels,L.W., L.Yue, and D.E.Clapham. 2002. The TRPM7 channel is inactivated by PIP(2) hydrolysis. *Nat. Cell Biol.* 4:329-336.

Runnels,L.W., L.Yue, and D.E.Clapham. 2001. TRP-PLIK, a bifunctional protein with kinase and ion channel activities. *Science* 291:1043-1047.

Schmitz,C., M.V.Dorovkov, X.Zhao, B.J.Davenport, A.G.Ryazanov, and A.L.Perraud. 2005. The channel kinases TRPM6 and TRPM7 are functionally nonredundant. *J. Biol. Chem.* 280:37763-37771.

Schmitz,C., A.L.Perraud, C.O.Johnson, K.Inabe, M.K.Smith, R.Penner, T.Kurosaki, A.Fleig, and A.M.Scharenberg. 2003. Regulation of vertebrate cellular Mg2+ homeostasis by TRPM7. *Cell* 114:191-200.

Su,L.T., M.A.Agapito, M.Li, T.N.Simonson, A.Huttenlocher, R.Habas, L.Yue, and L.W.Runnels. 2006. Trpm7 regulates cell adhesion by controlling the calcium dependent protease calpain. *J. Biol. Chem.*

Takezawa,R., C.Schmitz, P.Demeuse, A.M.Scharenberg, R.Penner, and A.Fleig. 2004. Receptor-mediated regulation of the TRPM7 channel through its endogenous protein kinase domain. *Proc. Natl. Acad. Sci. U. S. A* 101:6009-6014.

van der Wal,W.J., R.Habets, P.Varnai, T.Balla, and K.Jalink. 2001. Monitoring agonist-induced phospholipase C activation in live cells by fluorescence resonance energy transfer. *J. Biol. Chem.* 276:15337-15344.

Voets,T., B.Nilius, S.Hoefs, A.W.van der Kemp, G.Droogmans, R.J.Bindels, and J.G.Hoenderop. 2004. TRPM6 forms the Mg2+ influx channel involved in intestinal and renal Mg2+ absorption. *J. Biol. Chem.* 279:19-25.

Xu,C., J.Watras, and L.M.Loew. 2003. Kinetic analysis of receptor-activated phosphoinositide turnover. *J. Cell Biol.* 161:779-791.

Zaccolo,M., G.F.De, C.Y.Cho, L.Feng, T.Knapp, P.A.Negulescu, S.S.Taylor, R.Y.Tsien, and T.Pozzan. 2000. A genetically encoded, fluorescent indicator for cyclic AMP in living cells. *Nat. Cell Biol.* 2:25-29.

Zweifach,A. and R.S.Lewis. 1993. Mitogen-regulated Ca2+ current of T lymphocytes is activated by depletion of intracellular Ca2+ stores. *Proc. Natl. Acad. Sci. U. S. A* 90:6295-6299.

PIP$_2$ as a Physiological Determinant of TRPM7 Channel Activity

Michiel Langeslag & Kees Jalink

PIP$_2$ as a Physiological Determinant of TRPM7 Channel Activity

Michiel Langeslag & Kees Jalink

Division of Cell Biology
the Netherlands Cancer Institute
Plesmanlaan 121, 1066 CX Amsterdam, the Netherlands

The channel-kinase TRPM7 is of vital importance for cell function, reportedly because it regulates intracellular magnesium homeostasis. TRPM7 channels constitute a Mg^{2+} entry pathway, and their gating is regulated by the free intracellular Mg^{2+} concentration: in whole-cell patch clamp experiments, depletion of Mg^{2+}$_i$ strongly activates TRPM7. Here we show that TRPM7 can also be activated in perforated-patch experiments by treatment with the membrane-permeable Mg^{2+} chelator EDTA-AM. We observed that whereas in whole-cell experiments TRPM7 currents spontaneous inactivate (run-down), in perforated-patch recordings the channel does not inactivate in time. Monitoring of PIP$_2$ at the plasma-membrane by confocal GFP-PHδ1 imaging reveals that PIP$_2$ homeostasis is compromised in whole-cell conditions, as a result of translocation of PI(4)P 5-kinase from the plasma-membrane into the cytosol. This effect is not dependent on intracellular Mg^{2+} since in whole-cells complementation of Mg^{2+} did not prevent translocation, while EDTA-AM loading of intact N1E-115/TRPM7 cells neither caused translocation of PI(4)P 5-kinase nor significantly lowered the PIP$_2$ concentration significantly. Our experiments suggest that whereas depletion of intracellular Mg^{2+} is sufficient to open TRPM7 channels, its activity critically depends on the presence of physiological levels of PIP$_2$ in the plasma membrane.

Introduction

Magnesium is an essential ion involved in many biochemical and physiological processes (Fleig and Penner, 2004; Perraud et al., 2004; Rubin, 2005). Until recently it was remained illusive how Mg^{2+} is taken up by cells, but recently two closely related ion channels were identified that play a vital role in the homeostasis of Mg^{2+} in living cells. These belong to the melastatin subfamily of the transient receptor potential (TRP) channel family (Clapham, 2003) and both channels are known as TRPM6 and TRPM7 respectively. TRPM6 expression is restricted to intestinal epithelial cells and kidney tubules, and this channel was found to be the main ion channel for Mg^{2+} reabsorbtion in these cells (Walder et al., 2002; Schlingmann et al., 2002). On the other hand, TRPM7 is expressed ubiquitously and was the first ion channel to be identified that permeates Mg^{2+} (Runnels et al., 2001; Nadler et al., 2001) and therefore implicated in cellular Mg^{2+} homeostasis (Schmitz et al., 2003). Conditional knock-out of TRPM7 in cells leads to growth arrest and cell death within 48-72 hours (Nadler et al., 2001), reportedly due to deficiency of intracellular Mg^{2+} (Schmitz et al., 2003). Knock-out mice die at a very early stage during embryonic development (E6.5), consistent with a keyrole for TRPM7 during development (Kim et al., 2005).

As both TRPM6 and TRPM7 contribute to the cellular Mg^{2+} homeostasis, it is not surprising that their regulation depends on the concentration of intracellular Mg^{2+} (Kozak and Cahalan, 2003) and Mg^{2+}-nucleotides (Nadler et al., 2001; Demeuse et al., 2006). Free cytosolic Mg^{2+} ions and Mg^{2+}-nucleotides keep the channels in a closed state, but the precise mechanism of this inhibition has not been solved at this time (Nadler et al., 2001; Prakriya and Lewis, 2002; Kozak and Cahalan, 2003; Demeuse et al., 2006). In whole-cell patch-clamp experiments, lowering of intracellular Mg^{2+}/Mg-nucleotides releases this inhibition and consequently currents develop with a strong outward-rectifying IV-relationship. These currents reverse at a membrane potential of about 0 mV (Runnels et al., 2001; Nadler et al., 2001; Kozak and Cahalan, 2003), reflecting little specificity of the pore for cations. TRPM7 inward currents are predominantly carried by the divalent ions Mg^{2+} and Ca^{2+} at negative voltages (Runnels et al., 2001;

Nadler et al., 2001), but rare divalents ions like Zn^{2+}, Co^{2+}, Mn^{2+} and Ni^{2+} are also conducted (Monteilh-Zoller et al., 2003). At positive voltages and in the absence of internal divalent ions, the outward current is mainly carried by monovalent ions, in particular K^+ (Runnels et al., 2001). Following activation, TRPM7 currents gradually and spontaneously decrease in time (Runnels et al., 2001). This phenomenon is known as channel rundown and it is observed in whole-cell or inside-out experiments with many other ion channels.

Remarkably, rundown of ion channels can be often rescued by application of PIP_2. For example, plasma-membrane PIP_2 stabilizes the open state of KNCQ1/KCNE1 K^+ channels (Loussouarn et al., 2003). Also, rundown of other K^+ channels is under control of PIP_2, eg. M-type K^+ channels (Ford et al., 2004), ATP-sensitive K^+ channels (Baukrowitz and Fakler, 2000) and inward rectifying K^+ channels (Huang et al., 1998; Zhang et al., 1999; Logothetis and Zhang, 1999). Furthermore, the inactivation of other ion channels is modulated by PIP_2. For Example, the activity of Cystic Fibrosis Transmembrane conductance Regulator (CFTR) is regulated by PIP_2 and removal of PIP_2 in excised patches results in current decay of CFTR (Himmel and Nagel, 2004). The voltage-gated P/Q- and N-type Ca^{2+} channels are regulated by PIP_2 as well. These authors show that the time-dependent decrease in current activity (rundown) of P/Q and N-type calcium channels following membrane patch excision could be slowed down and partially reversed by the addition of PIP_2, and accelerated with antibodies against PIP_2 (Wu et al., 2002). Note that in all these cases channel activity is inhibited when PIP_2 is hydrolyzed.

Regulation of TRP channels also depends on membrane phospholipids or their metabolites, in particular PIP_2 (Hardie et al., 2001; Su et al., 2006). Of particular interest is PIP_2 that regulates several TRP ion channels. In general, PIP_2 levels are maintained at the plasma-membrane through a metabolic pathway including kinases and phosphatases (Anderson et al., 1999; Tolias and Cantley, 1999). The final step in PIP_2 synthesis is the phosphorylation of phosphatidylinositol 4-phosphate (PI(4)P) by phosphatidylinosistol 4-phosphate 5-kinase (PI(4)P 5-kinase). On the other hand, PIP_2 can be dephosphorylated by inositol phosphatases (Majerus et al., 1999) or hydrolyzed by phospholipases (Rhee, 2001). PIP_2 levels at the plasma-membrane maintain the TRP channels TRPL and TRPV1 in a closed state, whereas TRPM5 and TRPM8 are active in the presence of

PIP_2. With regard to TRPM7, PIP_2 has an ambiguous effect on its' activity. In whole-cell patch-clamp experiments, activated TRPM7 currents are inhibited by Gq-protein coupled receptor stimulation, which is preceded by translocation of the PIP_2-sensor GFP-PHδ1 (Runnels et al., 2002). Under physiological conditions, when Mg^{2+}_i is undisturbed, TRPM7 channels are mainly in a closed (Kozak and Cahalan, 2003; Schmitz et al., 2003; Hanano et al., 2004; Matsushita et al., 2005; Chapter II). Unlike whole-cell experiments, in perforated-patch and Ca^{2+} imaging experiments PLC activation leads to TRPM7 opening, observed as increased membrane conductance and Ca^{2+} influx (Chapter II).

Here we show that whereas rundown of TRPM7 ion channels occurs spontaneously in the whole-cell patch clamp configuration, EDTA-AM activated TRPM7 currents display no channel rundown. As PIP_2 levels regulate TRPM7 activity, we therefore investigated PIP_2 kinetics in both patch configurations. By combining confocal microscopy and patch-clamp we show that loss of PIP_2 at the plasma-membrane is preceded by translocation of GFP-tagged PI(4)P 5-kinase into the cytosol in whole-cell. As a result, inhibition of TRPM7 currents by PLC activity in whole-cell configuration is irreversible. In perforated patches GFP-tagged PI(4)P 5-kinase remains located at the plasma-membrane and therefore EDTA-AM activated currents are transiently inhibited by PLC activation because PIP_2 is resynthesized.

Materials & Methods

Materials

Amphotericin B, MgATP, bradykinin, lysophosphatidic acid and myo-inositol were from Sigma-Aldrich Co. (St. Louis, MO). EDTA-AM was from Molecular Probes Inc. (Eugene, OR). Ionomycin, U73122 was from Calbiochem-Novabiochem Corp. (La Jolla, CA). Salts were from Merck (Darmstadt, Germany). Dulbecco's MEM, foetal calf serum, penicillin and streptomycin were obtained from Gibco BRL (Paisley, Scotland). FuGene 6 transfection reagent was from Roche Diagnostics B.V. (Penzbreg, Germany). DiC8 was purchased from Instruchemie, (Delfzijl, the Netherlands).

Constructs

The PIP$_2$ sensor (eCFP-PHδ1 and eYFP-PHδ1) was previously generated in our lab as described (van der Wal et al., 2001). PI(4)P 5-kinase-GFP was a kind gift from Dr. N. Divecha (NKI, Amsterdam, the Netherlands)

Cell Culture

Mouse N1E-115/TRPM7 cells were cultured in DMEM supplemented with 10% fetal calf serum, penicillin and streptomycin and kept in a humidified CO$_2$ incubator. Cells were passaged twice a week and seeded on glass cover slips for experiments. Transfection of constructs with FuGene6 (1μg DNA/coverslip of each individual construct) was performed according to manufacturers' guidelines (Roche).

Dynamic FRET Essays

Cells grown on coverslips were transfected with FRET constructs (1μg/coverslip) using FuGene 6 according to manufactures' guidelines, and experiments were performed as described previously (van der Wal et al., 2001); (Ponsioen et al., 2004). In brief, coverslips were placed on an inverted Nikon microscope and excited at 425nm using an ND3 filter. CFP- and YFP emission were collected simultaneously through 470 ± 20 and 530 ± 25 nm bandpass filters. Data were acquired at 4 samples per second and FRET was expressed as ratio of CFP to YFP signals. This ratio was set to 1.0 at the onset of the experiments, and changes are expressed as per cent deviation from this initial value.

Patch-clamp Experiments and Confocal Imaging

Electrophysiological recordings were collected using an EPC9 amplifier (HEKA electronics, Lambrecht, Germany), connected to a personal computer and controlled by HEKA pulse software. Voltage-clamp protocols were generated using HEKA pulse software, and current recordings were digitized at 100 kHz (ramp and block pulse protocols) or 10 Hz (steady-state whole-cell currents). Borosilicate glass pipettes were pulled on a p-2000 pipette puller (Sutter instruments, Novato, CA) and fire-polished (Narishige Microforge, Tokyo, Japan) to 2-4 MΩ. After establishment of the GΩ seal, the patched membrane was ruptured by gentle suction to obtain whole-cell configuration, or amphotericin B (240 μg/ml) was used to obtain the perforated-patch configuration with typical access resistance of 3-10 MΩ.

Solutions were as follows (in mM): whole-cell pipette solution: K-Glutamate (120), KCl (30), MgCl$_2$ (1), CaCl$_2$ (0.2), EGTA (1), HEPES pH.7.2 (10) and MgATP (1); external solution: NaCl (140), KCl (5), MgCl$_2$ (0-1), CaCl$_2$ (0-10), HEPES (10) and glucose (10), adjusted to pH 7.3 with NaOH; for perforated-patch recordings, the pipette solution was complemented with 240 μg/ml Amphotericin B and MgATP was omitted.

For Ca^{2+} recordings, cells on glass coverslips were incubated for 30 min with dyes, followed by further incubation in medium for at least 15 min. For pseudoratiometrical determinations (Lipp and Niggli, 1993; Rasmussen et al., 1986), a mixture of 1 μg Oregon Green 488 BAPTA-AM and 4 μg Fura Red-AM in 100 μl medium was used. Coverslips were mounted on the inverted microscope and recordings were made at 37°C in HEPES-buffered saline, composed of (in mM): NaCl (140), KCl (5), MgCl$_2$ (1), CaCl$_2$ (1), HEPES (10) and glucose (10), pH 7.2. Single-cell fluorescence recordings were collected with a Nikon inverted microscope fitted with a Biorad MRC600 scanhead (Biorad, Herts, England). Excitation of Oregon Green and Fura-Red was at 488 nm and emission was detected at 522 +/- 16 nm and at >585 nm. Excitation of eGFP was at 488 nm and emission was detected at 522 +/- 16 nm. All Ca^{2+} recordings were normalized at maximal ratio change after ionomycin treatment. All experiments were calibrated with respect to maximal translocation of eGFP-PHδ1 and eGFP-PI(4)P 5-kinase.

Results

MIC/MagNuM Currents Run Down Spontaneously in Whole Cells But Not in Perforated Patches

To study TRPM7 channels we retrovirally introduced TRPM7 in N1E-115 (N1E-115/TRPM7) cells. Overexpression levels were estimated to be 2-3 times the endogenous TRPM7 channel levels (Chapter II, Clark 2006). TRPM7 currents are activated in whole-cell patch-clamp by depletion of intracellular Mg^{2+} using Mg^{2+}-free pipette solutions (Figure 1A, Kozak and Cahalan, 2003; Chapter II). After full activation of the currents, TRPM7 channels start to inactivate in time with a $t_{1/2}$ of 643 +/- 62 s, N = 3. In contrast, when N1E-115/TRPM7 cells are monitored by perforated-patch clamping, no spontaneous currents are observed (Figure 1B). To activate TRPM7 currents in perforated patches, we sought to lower Mg^{2+}_i by loading the cells with EDTA-AM, a membrane-permeable Mg^{2+} chelator that becomes trapped in the cell. Strikingly, after a short lag-time this treatment caused currents to develop that have all the hallmarks of whole-cell TRPM7 currents, i.e., the IV-plot of the activated currents is outward rectifying and reversal is around 0mV (Figure 1C, *left panel, trace 1*); the IV-plots of these currents become linear when cells are challenged with divalent-free media, and under these circumstances inward currents are completely inhibited by spermin, whereas outward currents are partially blocked (Figure 1C). EDTA-AM activated currents are also blocked by 2-APB, La^{3+} and SKF 96365 (data not shown). All these results are in line with previously reported characteristics of TRPM7 currents (Prakriya and Lewis, 2002; Kozak and Cahalan, 2003; Chapter II). In contrast to whole-cell, perforated-patch recordings of TRPM7 currents in N1E-115/TRPM7 cells never exhibited rundown, even not after 1 hour (Figure 1B). Thus, in perforated patches Mg^{2+}-depletion activates TRPM7 currents with properties similar to whole-cell currents, with the exception that they do not show rundown. This suggests that in the whole-cell configuration, but not in perforated-patch, a factor necessary to keep TRPM7 open is lost over time.
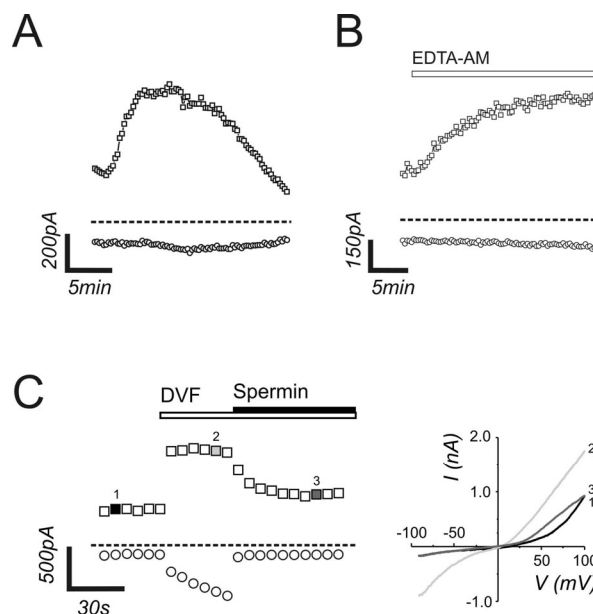

Figure 1: TRPM7 currents measured by 2 different patch clamp techniques. (A) TRPM7 currents measured in whole-cell mode by depletion of intracellular Mg^{2+} depletion show time-dependent inactivation (rundown). (B) N1E-115/TRPM7 cells do not display TRPM7 current activation when recorded by perforated-patch unless intracellular $[Mg^{2+}]$ is chelated by loading the cells with 10μM EDTA-AM. (C) EDTA-AM evoked currents linearize in divalent-free media. Note the inhibition by spermin (50 μM). Open circles depict currents determined at -80mV and open squares at +80mV. dashed line: 0 pA.

GPCR-Induced Suppression of TRPM7 Currents Is Sustained in Whole-cell and Transient in Perforated-patch

In whole-cell experiments in HEK-293, it has been documented that activation of PLC by carbachol inactivates TRPM7 through loss of PIP_2 (Runnels et al., 2002). Similarly, in N115/TRPM7 cells endogenous BK2 receptors (for which we recently showed that they couple exclusively to Gq/PLC; Chapter II) also irreversibly inhibit TRPM7 currents (Figure 2A, *upper panel*). Remarkably, when TRPM7 currents were evoked by EDTA-AM in perforated patches, application of BK resulted in a fast but transient inhibition of the current (Figure 2A, *lower panel*). As compared to the complete inhibition by BK in whole-cell recordings (99.7 +/- 1.0%, N=9), inhibition in perforated-patch is only partial (65.9 +/- 18.7%, N=8, Figure 2A & B). In perforated patches, TRPM7 currents usually fully restored within a few minutes after BK application. Thus, BK causes sustained inhibition in whole cells, whereas

it transiently inhibits EDTA-AM-evoked TRPM7 currents in perforated patches.

Effects of the PLC Inhibition on TRPM7 Currents and PIP₂ Kinetics.

To further address the role of PLC in TRPM7 gating, we used the PLC inhibitor U73122. Pretreatment with U73122 for 15 minutes completely blocked Mg^{2+}_i depletion-induced TRPM7 activation in whole-cell recordings (data not shown), even though PLC is not thought to play a role in this mode of activation. This suggests that U73122 may have side-effects preventing TRPM7 activation by Mg^{2+} depletion. Furthermore, when TRPM7 channels were pre-activated by Mg^{2+} depletion in whole-cell and subsequently challenged with U73122 we observed that the compound caused inactivation of the channels (Figure 3A), reminiscent of that evoked by BK, although the onset was slower

A part of the TRPM7 channel population is already open under resting conditions, resulting in increased basal Ca^{2+} levels as compared to native N1E-115 cells (Chapter II). We therefore tested if U73122 has the same effect on cytosolic Ca^{2+} by fluorometry. Indeed, in N1E-115/TRPM7 cells basal Ca^{2+} levels declined upon addition of U73122. As expected, subsequent BK stimulation

could not trigger any Ca^{2+} release from internal stores (Figure 3B), but remarkably, BK-induced Ca^{2+} influx was also blocked. These results suggest that, in addition to blocking PLC-mediated IP_3 production, U73122 causes TRPM7 channels to close by an unknown mechanism.

To verify that U73122 inhibits PLC activity, we transfected N1E-115/TRPM7 with a PIP_2 FRET sensor (van der Wal et al., 2001). Strikingly, application of U73122 caused a complete translocation of PIP_2 sensor within 5 minutes, observed as loss of FRET (Figure 3C). Stimulation with BK and ionomycin/Ca^{2+} did not lower the FRET signal any further. Similar results were obtained with native N1E-115 and HEK-293 cells. Thus, to our surprise, U73122 elicits complete breakdown of plasma-membrane PIP_2 levels by an unknown mechanism. Therefore we conclude that closure of TRPM7 channels mediated by U73122 correlates with loss of PIP_2 at the plasma-membrane rather than inhibition of PLC.

Whole-cell MIC/MagNuM Rundown Correlates with Hydrolysis of PIP₂

As TRPM7 channel inhibition by both BK and U73122 correlates with loss of PIP_2, we combined patch-clamping and confocal imaging of GFP-PHδ1 (Varnai and Balla, 1998) to study rundown of TRPM7 currents and PIP_2 kinetics simultaneously. During activation of TRPM7 currents in whole-cell, GFP-PHδ1 localized to the plasma-membrane. After a few minutes, GFP-PHδ1 started to gradually translocate into the cytosol (t½ = 983 +/- 131s, N=3), and concurrently TRPM7 currents ran down (t½ = 643 +/- 62, N=3, Figure 4A, *arrowhead*).
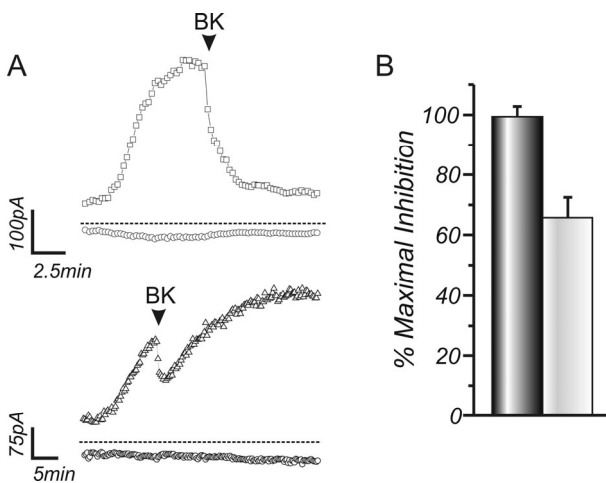

Figure 2: Effects of bradykinin receptor activation on TRPM7 currents. (A) Upper panel, TRPM7 currents measured in whole-cell are irreversibly closed after BK2-R receptor activation. Perforated-patch induced TRPM7 currents are transiently inhibited and in time full TRPM7 activity is restored (lower panel). Open circles depict currents determined at -80mV and open triangles at +80mV. dashed line: 0 pA. (B) Quantification of the degree of inhibition in whole cells (black bar) and perforated-patch (white bar). Data are depicted as mean + SEM**;** * p < 0.001**,** N=8
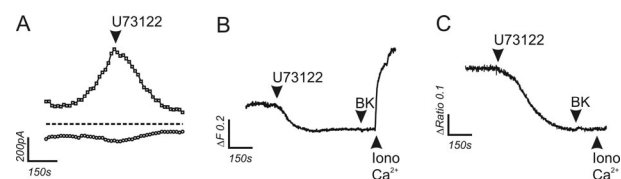

Figure 3: U73122 affects TRPM7 channel functioning and PIP₂ homeostasis. (A) U73122 causes decay of TRPM7 currents in whole-cell patch-clamp. The currents measured at -80mV are depicted by open circles and at +80mV by open squares, dashed line represents 0 pA. (B) U73122 decreased the elevated basal Ca^{2+} levels at resting conditions. (C) The PIP_2 levels at the plasma-membrane, detected by the PIP_2 FRET sensor (van der Wal et al., 2001), decreased upon treatment with U73122. Bradykinin and ionomycin are unable to lower the FRET signal any further .
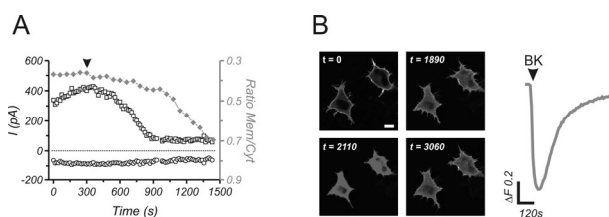
A

B

Figure 4: TRPM7 channel inactivation follows PIP$_2$ depletion in whole-cell. (A) Simultaneous recording of GFP-PHδ1 membrane localization and whole-cell TRPM7 currents reveals that loss of TRPM7 currents and PIP$_2$ coincide. (B) PIP$_2$ kinetics in N1E-115/TRPM7 cells loaded with EDTA-AM. BK stimulation caused a transient translocation of GFP-PHδ1 to the cytosol (left panel). Right panel shows a typical trace of GFP-PHδ1 translocation. Note that the BK-mediated PIP$_2$ kinetics in EDTA-AM treated cells resemble the BK-mediated inhibition of TRPM7 currents in perforated patch recordings (Figure 2A, lower panel).

What happens with PIP$_2$ levels when TRPM7 is activated by EDTA-AM-mediated depletion of Mg^{2+} in intact cells? In confocal time-lapse experiments, GFP-PHδ1 was retained at the plasma-membrane during accumulation of EDTA-AM in the cytosol (Figure 4B, *upper panels*). Subsequent stimulation with BK results in a fast translocation of the PIP$_2$-sensor into the cytosol (Figure 4B, *lower left panel*). GFP-PHδ1 relocated towards the plasma-membrane within several minutes (Figure 4B *lower right panel* & 4C).

In conclusion, rundown of TRPM7 currents correlates with GFP-PHδ1 translocation.

What Determines PIP$_2$-mediated Whole-cell TRPM7 Channel Rundown?

Since breakdown of PIP$_2$, both spontaneous or resulting from PLC activation, correlates with irreversible TRPM7 channel inactivation, we sought to determine which aspect of PIP$_2$ homeostasis is impaired. In whole-cell configuration, diffusable cytosolic components, including proteins of PIP$_2$ homeostasis and PIP$_2$ precursors, will be washed out in time. The first step in phospho-inostide synthesis is attachment of free inositol to cystidine diphosphate diacylglycerol. As free inositol diffuses rapidly, we complemented the intracellular pipette solution with 5 mM inositol in an attempt to prevent loss of plasma-membrane PIP$_2$. In the presence of free inositol, TRPM7 currents activated normally. However, in 3 independent experiments inositol supplementation could not prevent TRPM7

channel rundown (Figure 5A). We also included the water-soluble PIP$_2$ analogue DiC8-PIP$_2$ (24μM) in the pipette solution to directly compensate for the loss of PIP$_2$. Unexpectedly, this also did not rescue spontaneous rundown in whole-cell configuration (Figure 5B). Perhaps the PIP$_2$ hydrolysis rate exceeds the diffusion of DiC8-PIP$_2$ from the pipette. We therefore raised the DiC8-PIP$_2$ concentration to 200μM, but unfortunately this prevented GΩ seal formation.

In another attempt to counteract PIP$_2$ hydrolysis in whole-cell patch clamp, we transfected GFP-PIP(5)-kinase into N1E-115/TRPM7 cells. We combined recordings of GFP-PIP(5)-kinase membrane localization with whole-cell patch-clamping of TRPM7 currents. Remarkably, shortly after breaking the patched membrane, PIP(5)-kinase commences to translocate to the cytosol of N1E-115/TRPM7 cells. The translocation of PIP(5)-kinase preceeds TRPM7 channel inactivation (t½$_{PIP(5)-kinase}$ = 421 +/- 61s vs. t½$_{TRPM7}$ = 643 +/- 62, N=3, Figure 5C). As PIP(5)-kinases are heavily dependent on intracellular Mg^{2+} concentration, we repeated the experiment with 3mM of free Mg^{2+} included in the pipette solution. Even under these conditions, PIP(5)-kinases fall off the membrane during whole-cell patch-clamping (Figure 5C), although TRPM7 currents are not activated under these conditions (Chapter II).

May the translocation of PIP(5)-kinases in whole-cell explain the difference observed in TRPM7 current kinetics between whole-cells and perforated patches? GFP-PIP(5)-kinase expressing N1E-115/TRPM7 cells were challenged with EDTA-AM, comparable to perforated-patch recordings of TRPM7 channel activation. Imaging of GFP-PIP(5)-kinase showed that it remained at the plasma-membrane even after 1 hour of loading with EDTA-AM. Furthermore, the PIP$_2$ concentration also remained stable, as judged from GFP-PHδ1 experiments. Thus, our experiments suggest that in whole-cell recordings loss of PIP(5)-kinase membrane localization underlies TRPM7 channel rundown, whereas in perforated-patch conditions PIP(5)-kinases are unaffected.. The mechanism of this PIP(5)-kinase translocation remains to be addressed.
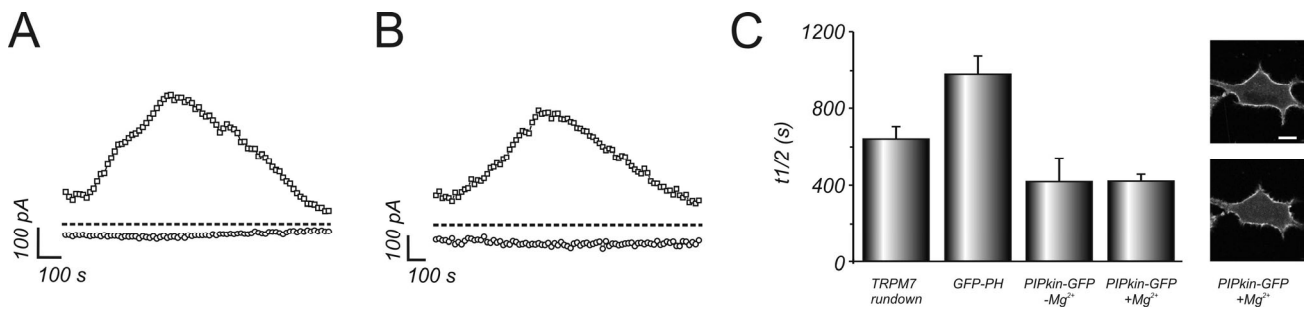
Figure 5: Impaired PIP$_2$ homeostatis due to PIP(5)-kinase translocation in whole-cell, but not in perforated patch
Neither complementation of 5mM free inositol in the pipette solution (A) nor DiC8-PIP$_2$ (B) is able to rescue TRPM7 rundown in whole-cell patch clamping. (C) TRPM7 current decrease is preceeded by GFP-PI(4)P 5-Kinase translocation from the plasma-membrane. Note that GFP-PIP(4) 5-kinase translocation is independent of the presence of intracellular Mg^{2+}. (D) Mg^{2+} depletion by EDTA-AM does not cause translocation of PIP(5)-kinase. All data are depicted as mean + SEM, N = 3, bar equals 10μM

Discussion

In this study we compared TRPM7 channel activation and rundown occurring in whole-cell patch clamp experiments and perforated-patch mode. In close agreement with results published previously for HEK-293 cells {Runnels, 2002 20 /id}, we show that in N1E-115/TRPM7 cells depletion of intracellular Mg^{2+} evokes TRPM7 currents that subsequently gradually decrease and return to resting levels (Figure 1A). Furthermore, activation of PLC-coupled GPCRs inhibited TRPM7 currents permanently in whole cells (Runnels 2002, chapter II). Using a new experimental paradigm to evoke TRPM7 currents in perforated patches, we show that TRPM7 channels do not rundown in this configuration. Moreover, in this configuration bradykinin caused transient, rather than sustained, inhibition of TRPM7 currents (Figure 2A, *lower panel*)

We also show that spontaneous TRPM7 rundown coincides with loss of PIP2, as detected as translocation of GFP-PHδ1 from the plasma-membrane into the cytosol (Figure 4A). Similarly, in HEK-293 cells carbachol-induced loss of PIP$_2$ accompanied TRPM7 inactivation (Runnels et al., 2002). In this study, too, stimulation with bradykinin, which results in massive breakdown of PIP$_2$ at the plasma-membrane (Chapter II), irreversibly closed TRPM7 channels in whole-cell. In contrast, in perforated-patch experiments spontaneously PIP$_2$ depletion does not occur. Furthermore, the effects of BK on PIP$_2$ are transient (Figure 4B). This is in line with an earlier report of Runnels et al., showing that inactivated TRPM7 channels could be reactivated by application of a water-soluble PIP$_2$ analogue,

recorded at single channel level (Runnels et al., 2002). Therefore, it appears that TRPM7 channel function requires the presence of PIP$_2$ at the plasma-membrane. We here propose that the PLC-mediated inhibition of TRPM7 channels in whole-cell is best interpreted as accelerated rundown, and as such an artifact of whole-cell recording.

In contrast, Takezawa et al. reported that not PLC/PIP$_2$ activity but rather the level of cytosolic cyclic AMP, is the major regulator of TRPM7 activity, (Takezawa et al., 2004). However, this notion was rejected in Chaper II. Perhaps the discrepancy between Runnels' and our study on the one hand, and that of Takezawa and colleagues on the other hand, is a difference in potency of the PLC-activating receptors used. In their hands and also in our hands, endogenous M1 receptors cause only minor PIP$_2$ breakdown.. Their study furthermore relied on the use of the 'PLC inhibitor' U-73122, a compound that we here show to have side effects opposite to that of PLC inhibition. For example, we noted that, in addition to blocking PLC, freshly prepared U73122 completely depleted intracellular PIP$_2$ levels, whereas the compound rapidly lost its' potency in solution (KJ, unpublished observation). Horowitz and Hille very recently reported similar findings for this compound {Horowitz, 2005 322 /id}. Furthermore, various side-effects of U73122 on phospho-inositide homeostasis (Vickers, 1993), on G-protein mediated signaling and various phospholipases (A, C and D) activity had been noted before (Balla, 2001).

What causes spontaneous PIP$_2$ breakdown during studies performed in whole-cell and inside-out experiments? Recent studies on the role of PIP$_2$ in TRPM8 function pointed out that inhibition of lipid phosphatases rescued TRPM8 activity

WKYQR   KRRKKDK   RIRVTFERVEQMSIQIKEVGDR
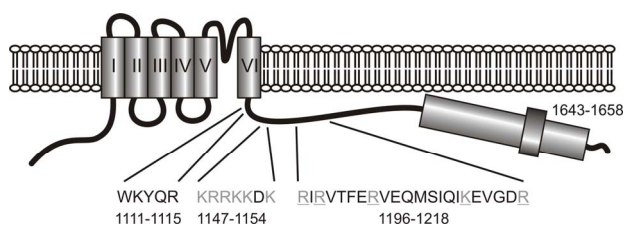1111-1115 1147-1154   1196-1218

Figure 6: Schematic representation of possible PLC/PIP₂ interaction sites in TRPM7. A split PH-domain (dark grey) complementary to a C-terminal split PH-domain of PLCγ1 was predicted in the kinase-domain of TRPM7. Further putative PIP₂ interaction sites in TRPM7 are the TRP-domain, a stretch of positively charged amino-acids (light grey) and modular PIP₂-binding site, similar that of TRPV1.

(Rohacs et al., 2005; Liu and Qin, 2005). This indicates that synthesis of PIP₂ in whole-cell and inside-out patch clamping is impaired. In this study we show that PIP(5)-kinases translocate from the plasma-membrane in whole-cell configuration, resulting in loss off PIP₂. It is well known that PIP-kinases are strongly dependent on free Mg^{2+} and MgATP to function properly (Ling et al., 1989). However, we show that translocation of PIP(5)-kinases is not caused by depletion of intracellular Mg^{2+} (Figure 5C). This may explain why other PIP₂-dependent ion channels inactivate in time, even in the presence of Mg^{2+} and MgATP. In contrast, when intracellular Mg^{2+} is depleted by loading of EDTA-AM, PIP(5)-kinases remain at the plasma-membrane and the PIP₂ homeostasis remains in balance. Hence, whole-cell experiments result in translocation of PIP(5)-kinases by an unknown mechanism. Thus, the same mechanism underlies TRPM7 channel rundown and irreversible inactivation by receptor-mediated PLC activation. This is not observed during perforated-patch experiments.

Does the TRPM7 sequence reveal any indication of PLC and/or PIP₂-binding sites? TRPM7 was identified as an interactor with PLC isozymes, which bind to its kinase domain (Runnels et al., 2001). Recently it has been shown that a C-terminal "split PH-domain" of PLCγ1 can recombine with a split PH-domain found in TRPC3 to form a functional PH-domain (Van Rossum et al., 2005). Therefore, we analyzed the TRPM7 sequence for the presence of split PH-domain by a home-written algorithm (Van Rossum et al., 2005). We identified a complementary split PH-domain located in the kinase-domain of TRPM7 (1643 to 1658). Future biochemical studies are needed to demonstrate this interaction and assess how it may affect TRPM7 regulation.

Additionally, there may be direct binding of PIP₂ to TRPM7 channels analogous to other PIP₂-regulated TRP channels. For example, the TRP-domain of TRPM8 interacts with PIP₂, and this controls channel function (Rohacs et al., 2005). Based on sequence homology between the TRPM subfamily members, this may also be valid for TRPM7. Sequence analysis of TRPM7 further reveals other potential PIP₂-binding sites. Downstream of the TRP-domain, a positive stretch of aminoacids (1111 to 1115, Figure 6) may bind to the negatively charged inositol group of PIP₂. Furthermore, a modular PIP₂-binding domain is predicted at 1147-1218 (T. Balla, Bethesda, personal communication), similar to the capsaicin sensitive TRPV1 channels (Prescott and Julius, 2003). While the TRPM7 protein sequence suggests the presence of PIP₂ and PLC binding motifs, experiments to validate these putative binding sites are needed.

References

Anderson,R.A., I.V.Boronenkov, S.D.Doughman, J.Kunz, and J.C.Loijens. 1999. Phosphatidylinositol phosphate kinases, a multifaceted family of signaling enzymes. *J. Biol. Chem.* 274:9907-9910.

Balla,T. 2001. Pharmacology of phosphoinositides, regulators of multiple cellular functions. *Curr. Pharm. Des* 7:475-507.

Baukrowitz,T. and B.Fakler. 2000. KATP channels gated by intracellular nucleotides and phospholipids. *Eur. J. Biochem.* 267:5842-5848.

Chuang,H.H., E.D.Prescott, H.Kong, S.Shields, S.E.Jordt, A.I.Basbaum, M.V.Chao, and D.Julius. 2001. Bradykinin and nerve growth factor release the capsaicin receptor from PtdIns(4,5)P2-mediated inhibition. *Nature* 411:957-962.

Clapham,D.E. 2003. TRP channels as cellular sensors. *Nature* 426:517-524.

Demeuse,P., R.Penner, and A.Fleig. 2006. TRPM7 Channel Is Regulated by Magnesium Nucleotides via its Kinase Domain. *J. Gen. Physiol* 127:421-434.

Fleig,A. and R.Penner. 2004. The TRPM ion channel subfamily: molecular, biophysical and functional features. *Trends Pharmacol. Sci.* 25:633-639.

Ford,C.P., P.L.Stemkowski, and P.A.Smith. 2004. Possible role of phosphatidylinositol 4,5 bisphosphate in luteinizing hormone releasing hormone-mediated M-current inhibition in bullfrog sympathetic neurons. *Eur. J. Neurosci.* 20:2990-2998.

Hanano,T., Y.Hara, J.Shi, H.Morita, C.Umebayashi, E.Mori, H.Sumimoto, Y.Ito, Y.Mori, and R.Inoue. 2004. Involvement of TRPM7 in cell growth as a spontaneously activated Ca2+ entry pathway in

human retinoblastoma cells. *J. Pharmacol. Sci.* 95:403-419.

Hardie,R.C., P.Raghu, S.Moore, M.Juusola, R.A.Baines, and S.T.Sweeney. 2001. Calcium influx via TRP channels is required to maintain PIP2 levels in Drosophila photoreceptors. *Neuron* 30:149-159.

Himmel,B. and G.Nagel. 2004. Protein kinase-independent activation of CFTR by phosphatidylinositol phosphates. *EMBO Rep.* 5:85-90.

Huang,C.L., S.Feng, and D.W.Hilgemann. 1998. Direct activation of inward rectifier potassium channels by PIP2 and its stabilization by Gbetagamma. *Nature* 391:803-806.

Kim,B.J., H.H.Lim, D.K.Yang, J.Y.Jun, I.Y.Chang, C.S.Park, I.So, P.R.Stanfield, and K.W.Kim. 2005. Melastatin-type transient receptor potential channel 7 is required for intestinal pacemaking activity. *Gastroenterology* 129:1504-1517.

Kozak,J.A. and M.D.Cahalan. 2003. MIC channels are inhibited by internal divalent cations but not ATP. *Biophys. J.* 84:922-927.

Ling,L.E., J.T.Schulz, and L.C.Cantley. 1989. Characterization and purification of membrane-associated phosphatidylinositol-4-phosphate kinase from human red blood cells. *J. Biol. Chem.* 264:5080-5088.

Lipp,P. and E.Niggli. 1993. Microscopic spiral waves reveal positive feedback in subcellular calcium signaling. *Biophys. J.* 65:2272-2276.

Liu,B. and F.Qin. 2005. Functional control of cold- and menthol-sensitive TRPM8 ion channels by phosphatidylinositol 4,5-bisphosphate. *J. Neurosci.* 25:1674-1681.

Logothetis,D.E. and H.Zhang. 1999. Gating of G protein-sensitive inwardly rectifying K+ channels through phosphatidylinositol 4,5-bisphosphate. *J. Physiol* 520 Pt 3:630.

Loussouarn,G., K.H.Park, C.Bellocq, I.Baro, F.Charpentier, and D.Escande. 2003. Phosphatidylinositol-4,5-bisphosphate, PIP2, controls KCNQ1/KCNE1 voltage-gated potassium channels: a functional homology between voltage-gated and inward rectifier K+ channels. *EMBO J.* 22:5412-5421.

Majerus,P.W., M.V.Kisseleva, and F.A.Norris. 1999. The role of phosphatases in inositol signaling reactions. *J. Biol. Chem.* 274:10669-10672.

Matsushita,M., J.A.Kozak, Y.Shimizu, D.T.McLachlin, H.Yamaguchi, F.Y.Wei, K.Tomizawa, H.Matsui, B.T.Chait, M.D.Cahalan, and A.C.Nairn. 2005. Channel function is dissociated from the intrinsic kinase activity and autophosphorylation of TRPM7/ChaK1. *J. Biol. Chem.* 280:20793-20803.

Monteilh-Zoller,M.K., M.C.Hermosura, M.J.Nadler, A.M.Scharenberg, R.Penner, and A.Fleig. 2003. TRPM7 provides an ion channel mechanism for cellular entry of trace metal ions. *J. Gen. Physiol* 121:49-60.

Nadler,M.J., M.C.Hermosura, K.Inabe, A.L.Perraud, Q.Zhu, A.J.Stokes, T.Kurosaki, J.P.Kinet, R.Penner, A.M.Scharenberg, and A.Fleig. 2001. LTRPC7 is a Mg.ATP-regulated divalent cation channel required for cell viability. *Nature* 411:590-595.

Perraud,A.L., H.M.Knowles, and C.Schmitz. 2004. Novel aspects of signaling and ion-homeostasis regulation in immunocytes. The TRPM ion channels and their potential role in modulating the immune response. *Mol. Immunol.* 41:657-673.

Ponsioen,B., J.Zhao, J.Riedl, F.Zwartkruis, K.G.van der, M.Zaccolo, W.H.Moolenaar, J.L.Bos, and K.Jalink. 2004. Detecting cAMP-induced Epac activation by fluorescence resonance energy transfer: Epac as a novel cAMP indicator. *EMBO Rep.* 5:1176-1180.

Prakriya,M. and R.S.Lewis. 2002. Separation and characterization of currents through store-operated CRAC channels and Mg2+-inhibited cation (MIC) channels. *J. Gen. Physiol* 119:487-507.

Prescott,E.D. and D.Julius. 2003. A modular PIP2 binding site as a determinant of capsaicin receptor sensitivity. *Science* 300:1284-1288.

Rasmussen,H., I.Kojima, W.Apfeldorf, and P.Barrett. 1986. Cellular mechanism of hormone action in the kidney: messenger function of calcium and cyclic AMP. *Kidney Int.* 29:90-97.

Rhee,S.G. 2001. Regulation of phosphoinositide-specific phospholipase C. *Annu. Rev. Biochem.* 70:281-312.

Rohacs,T., C.M.Lopes, I.Michailidis, and D.E.Logothetis. 2005. PI(4,5)P2 regulates the activation and desensitization of TRPM8 channels through the TRP domain. *Nat. Neurosci.* 8:626-634.

Rubin,H. 2005. The membrane, magnesium, mitosis (MMM) model of cell proliferation control. *Magnes. Res.* 18:268-274.

Runnels,L.W., L.Yue, and D.E.Clapham. 2002. The TRPM7 channel is inactivated by PIP(2) hydrolysis. *Nat. Cell Biol.* 4:329-336.

Runnels,L.W., L.Yue, and D.E.Clapham. 2001. TRP-PLIK, a bifunctional protein with kinase and ion channel activities. *Science* 291:1043-1047.

Schlingmann,K.P., S.Weber, M.Peters, L.Niemann Nejsum, H.Vitzthum, K.Klingel, M.Kratz, E.Haddad, E.Ristoff, D.Dinour, M.Syrrou, S.Nielsen, M.Sassen, S.Waldegger, H.W.Seyberth, and M.Konrad. 2002. Hypomagnesemia with secondary hypocalcemia is caused by mutations in TRPM6, a new member of the TRPM gene family. *Nat. Genet.* 31:166-170.

Schmitz,C., A.L.Perraud, C.O.Johnson, K.Inabe, M.K.Smith, R.Penner, T.Kurosaki, A.Fleig, and A.M.Scharenberg. 2003. Regulation of vertebrate cellular Mg2+ homeostasis by TRPM7. *Cell* 114:191-200.

Su,L.T., M.A.Agapito, M.Li, T.N.Simonson, A.Huttenlocher, R.Habas, L.Yue, and L.W.Runnels. 2006. Trpm7 regulates cell adhesion

by controlling the calcium dependent protease calpain. *J. Biol. Chem.*

Takezawa,R., C.Schmitz, P.Demeuse, A.M.Scharenberg, R.Penner, and A.Fleig. 2004. Receptor-mediated regulation of the TRPM7 channel through its endogenous protein kinase domain. *Proc. Natl. Acad. Sci. U. S. A* 101:6009-6014.

Tolias,K.F. and L.C.Cantley. 1999. Pathways for phosphoinositide synthesis. *Chem. Phys. Lipids* 98:69-77.

van der Wal,J., R.Habets, P.Varnai, T.Balla, and K.Jalink. 2001. Monitoring agonist-induced phospholipase C activation in live cells by fluorescence resonance energy transfer. *J Biol Chem* 276:15337-15344.

Van Rossum,D.B., R.L.Patterson, S.Sharma, R.K.Barrow, M.Kornberg, D.L.Gill, and S.H.Snyder. 2005. Phospholipase Cgamma1 controls surface expression of TRPC3 through an intermolecular PH domain. *Nature* 434:99-104.

Varnai,P. and T.Balla. 1998. Visualization of phosphoinositides that bind pleckstrin homology domains: calcium- and agonist-induced dynamic changes and relationship to myo-[3H]inositol-labeled phosphoinositide pools. *J. Cell Biol.* 143:501-510.

Vickers,J.D. 1993. U73122 affects the equilibria between the phosphoinositides as well as phospholipase C activity in unstimulated and thrombin-stimulated human and rabbit platelets. *J. Pharmacol. Exp. Ther.* 266:1156-1163.

Walder,R.Y., D.Landau, P.Meyer, H.Shalev, M.Tsolia, Z.Borochowitz, M.B.Boettger, G.E.Beck, R.K.Englehardt, R.Carmi, and V.C.Sheffield. 2002. Mutation of TRPM6 causes familial hypomagnesemia with secondary hypocalcemia. *Nat. Genet.* 31:171-174.

Wu,L., C.S.Bauer, X.G.Zhen, C.Xie, and J.Yang. 2002. Dual regulation of voltage-gated calcium channels by PtdIns(4,5)P2. *Nature* 419:947-952.

Zhang,H., C.He, X.Yan, T.Mirshahi, and D.E.Logothetis. 1999. Activation of inwardly rectifying K+ channels by distinct PtdIns(4,5)P2 interactions. *Nat. Cell Biol.* 1:183-188.

TRPM7, a Novel Regulator of Actomyosin Contractility and Cell Adhesion

Kristopher Clark, Michiel Langeslag, Bart van Leeuwen, Leonie Ran, Alexey G. Ryazanov, Carl G. Figdor, Wouter H. Moolenaar, Kees Jalink and Frank N. van Leeuwen

TRPM7, a Novel Regulator of Actomyosin Contractility and Cell Adhesion

Kristopher Clark[1], Michiel Langeslag[2], Bart van Leeuwen[3], Leonie Ran[3], Alexey G. Ryazanov[4], Carl G. Figdor[1], Wouter H. Moolenaar[3], Kees Jalink[2] and Frank N. van Leeuwen[1].

[1]Department of Tumor Immunology, Nijmegen Centre for Molecular Life Sciences, Radboud University Nijmegen Medical Centre, PO Box 9101, 6500 HB Nijmegen, The Netherlands
[2]Division of Cell Biology, [3]Division of Cellular Biochemistry and Center for Biomedical Genetics, the Netherlands Cancer Institute, Plesmanlaan 121, 1066 CX Amsterdam, The Netherlands
[4]Department of Pharmacology, University of Medicine and Dentistry of New Jersey, Robert Wood Johnson Medical School, 675 Hoes lane, Piscataway, NJ, 08854, USA

Actomyosin contractility regulates various cell biological processes including cytokinesis, adhesion and migration. While in lower eukaryotes α-kinases control actomyosin relaxation, a similar role for mammalian α-kinases has yet to be established. Here, we examined whether TRPM7, a cation channel fused to an α-kinase, can affect actomyosin function. We demonstrate that activation of TRPM7 by bradykinin leads to a Ca^{2+}- and kinase-dependent interaction with the actomyosin cytoskeleton. Moreover, TRPM7 phosphorylates the myosin IIA heavy chain. Accordingly, low overexpression of TRPM7 increases intracellular Ca^{2+} levels accompanied by cell spreading, adhesion and the formation of focal adhesions. Activation of TRPM7 induces the transformation of these focal adhesions into podosomes by a kinase-dependent mechanism, an effect that can be mimicked by pharmacological inhibition of myosin II. Collectively, our results demonstrate that regulation of cell adhesion by TRPM7 is the combined effect of kinase-dependent and -independent pathways on actomyosin contractility.

Introduction

Actomyosin contractility in nonmuscle cells plays a fundamental role in regulating basic cellular functions such as cell shape, cytokinesis, adhesion and migration (Burridge and Wennerberg, 2004; De la Roche *et al*, 2002; Geiger and Bershadsky, 2002). Myosin II is the major motor protein driving contractility. Regulators of myosin II-based contractile responses include the Rho GTPase family and their effectors, myosin light chain (MLC) kinases and phosphatases as well as myosin heavy chain (MHC) kinases (Burridge and Wennerberg, 2004; De la Roche *et al*, 2002). The *Dictyostelium* genome encodes several MHC kinases, which are essential for proper localization and assembly of myosin II during cell division and migration (Heid *et al*, 2004; Kolman *et al*, 1996; Rico and Egelhoff, 2003). Myosin II assembles into bipolar thick filaments that generate cortical tension by pulling together oppositely oriented actin filaments. MHC kinases inhibit myosin II function by phosphorylating the MHC tail on threonine residues leading to filament disassembly and consequently, a release in cortical tension (Egelhoff *et al*, 1993). The cell biological effects of overexpression or knockout of these MHC kinases are consistent with this paradigm. Defects in cytokinesis due to overexpression of MHC kinases are reversed by expressing a MHC mutant that cannot be phosphorylated and therefore forms stable myosin filaments (Rico and Egelhoff, 2003). Thus, MHC kinases play a key role in actomyosin remodeling in *Dictyostelium*.

Dictyostelium MHC kinases belong to a rare and novel class of kinases known as α-kinases that, with the exception of the ATP-binding site, show only limited sequence similarity with other members of the protein kinase superfamily (Ryazanov, 2002). Based on *in vivo* substrates identified to date, these kinases preferentially phosphorylate threonine residues presented within the context of an α-helix, hence the name α-kinases (Ryazanov, 2002). Whether mammalian α-kinases also regulate actomyosin contractility has yet to be established.

The mammalian genome encodes several α-kinases whose function, with the exception of elongation factor kinase, is unknown (Drennan and Ryazanov, 2004). Notably, TRPM6 and TRPM7 are two bifunctional proteins encoding a TRP cationic channel fused to a COOH-terminal α-kinase domain. Electrophysiological characterization of TRPM7 has suggested that it forms part of the channel responsible for the Magnesium Inhibited Current (MIC) and is implicated in cellular Mg^{2+} homeostasis (Kozak and Cahalan, 2003; Nadler *et al*, 2001; Schmitz *et al*, 2003). However, TRPM7 may also relay signals by phosphorylating downstream effector molecules. In line with a hypothesized role for TRPM7 as an active component in receptor mediated signal transduction, it was reported that TRPM7 channels are highly permeable to Ca^{2+}, that the TRPM7 COOH-terminus associates with phospholipase C (PLC) isoforms and that PLC activation regulates TRPM7 channel opening (Runnels *et al*, 2001; Runnels *et al*, 2002; Langeslag et al., manuscript in preparation). We have previously found that bradykinin, a Gq-PLC coupled receptor agonist, induces Ca^{2+}-dependent phosphorylation of the MHC and disassembly of myosin IIA at the cell periphery, which correlates with cell spreading and adhesion in mammalian cells (van Leeuwen *et al*, 1999). Thus, we hypothesized that the coupling of a cation channel to an α-kinase in a single polypeptide could explain the close relationship between Ca^{2+} signaling and Ca^{2+}-dependent actomyosin remodeling. Here, we investigated whether TRPM7 could link receptor-mediated signaling to cytoskeletal contractility and cell adhesion.

Results

TRPM7 Mediates Bradykinin-Induced Calcium Influx

To examine a role for TRPM7 in the regulation of actomyosin contractility, an HA-tagged TRPM7 cDNA encoding wild-type (TRPM7-WT) or a kinase-dead mutant (TRPM7-D1775A) were introduced into N1E-115 neuroblastoma cells by retroviral transduction (a technique that allows low, near physiological expression of recombinant proteins; supplementary Fig. S1). Both TRPM7-WT and TRPM7-D1775A were equally expressed at 2-3 times over endogenous TRPM7 levels (Fig. 1A, supplementary S2; Langeslag et al., manuscript in

preparation). Both TRPM7-WT and TRPM7-D1775A run as doublets at 216 kDa due to differential glycosylation (supplementary Fig. S3). Moreover, proper localization of TRPM7-WT and TRPM7-D1775A to the plasma membrane was confirmed by fluorescence microscopy (supplementary Fig. S3; see also Fig. 4).
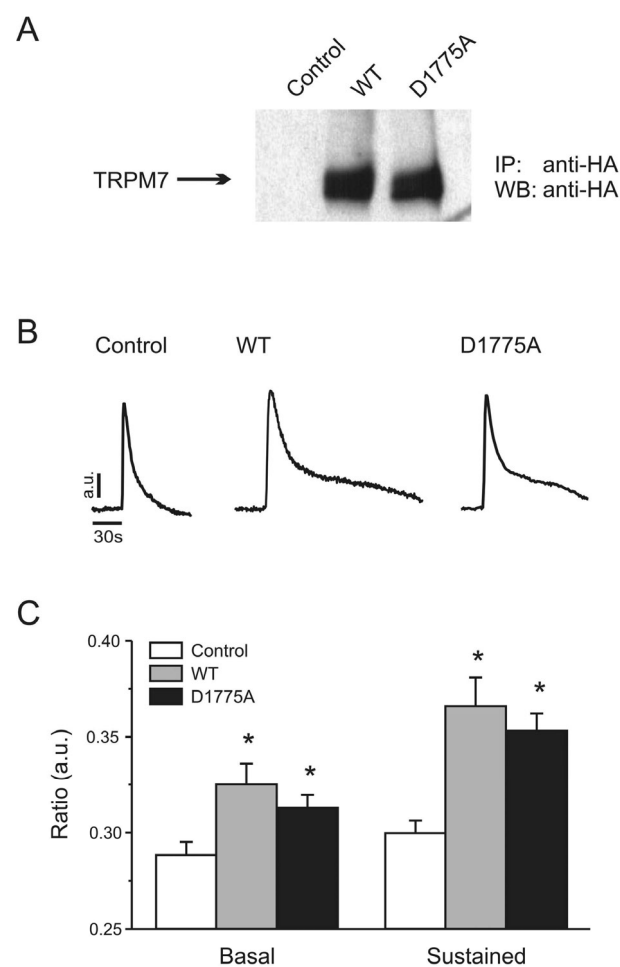

Figure 1 TRPM7 enhances receptor-operated calcium influx. (**A**) Expression of TRPM7-WT and TRPM7-D1775A in N1E-115 neuroblastoma cells was detected by IP-Western blot using antibodies against the HA-tag. Cells containing the empty vector were used as control in all experiments. (**B**) TRPM7 expression causes sustained Ca^{2+} influx following BK stimulation independently of kinase activity. Left panel, typical time course of BK-induced Ca^{2+} changes in control N1E-115 cells; other panels, BK-induced Ca^{2+} mobilizations in N1E-115/TRPM7 cells. The sustained influx depends on Ca^{2+} influx since it is acutely blocked by extracellular La^{3+} and Gd^{3+} (data not shown). (**C**) Quantification of Ca^{2+} data for control and TRPM7-overexpressing cells (mean ± SEM from at least 20 experiments for each condition). Significant differences (*) are $P < 0.01$ from values obtained in control N1E-115 cells.
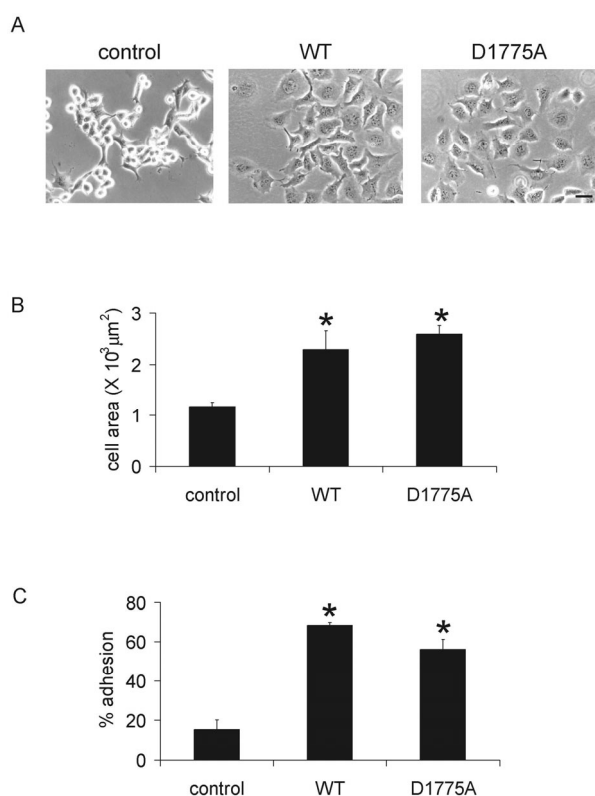
Figure 2 TRPM7 overexpression induces cell spreading and increases cell adhesion. (**A**) Phase contrast images of control, TRPM7-WT and TRPM7-D1775A expressing N1E-115 cells. Scale bar = 50 μm. (**B**) Cell surface area covered by N1E-115 cells expressing WT and kinase-dead TRPM7. Cells were stained for F-actin and cell surface area was calculated by quantifying the amount of pixels that exceeded a threshold (n>5). (**C**) Quantification of cell adhesion of N1E-115 cells expressing WT and kinase-dead TRPM7 (n=3). Significant differences (*) are $P < 0.01$ from values obtained in control N1E-115 cells.

Initially, we investigated by Ca^{2+} fluorometry whether TRPM7 is activated following stimulation with bradykinin (BK), a peptide agonist that promotes actomyosin relaxation in N1E-115 cells (van Leeuwen *et al*, 1999). Low overexpression of TRPM7 in N1E-115 cells resulted in a moderate elevation of the resting Ca^{2+} levels (109 ± 9 nM vs. 85 ± 4 nM). The addition of BK triggered a rapid increase in cytosolic Ca^{2+} from internal stores in both parental and TRPM7 transduced cells. Strikingly in N1E-115/TRPM7 cells, this initial Ca^{2+} transient was followed by a sustained phase of elevated Ca^{2+} that lasted for several minutes before returning to basal levels and was not observed in the parental cells (Fig. 1B). Removal of extracellular Ca^{2+} by BAPTA immediately terminated the

plateau phase (data not shown). Patch-clamp studies and inhibitor profiling identified TRPM7 as the channel responsible for the Ca^{2+} influx (a detailed analysis of TRPM7 channel function will be published elsewhere; Langeslag et al., manuscript in preparation). Finally, channel activation of kinase-dead TRPM7-D1775A by BK was not altered in comparison to TRPM7-WT (Fig. 1B,C), demonstrating that TRPM7 kinase activity is not required for BK-induced Ca^{2+} influx. From these results, we conclude that TRPM7 functions as a BK-regulated Ca^{2+} channel in N1E-115 cells.

TRPM7 Expression Promotes Cell Spreading and Increases Cell-Matrix Adhesion

Mouse N1E-115 neuroblastoma cells are an excellent model system to study the regulation of actomyosin contractility since signals that either activate contraction or promote relaxation are rapidly translated into cell rounding or cell spreading responses, respectively (Jalink *et al*, 1994; van Leeuwen *et al*, 1997; van Leeuwen *et al*, 1999). Consistent with a role for TRPM7 in actomyosin regulation, N1E-115/TRPM7 cells showed enhanced spreading when compared to the parental cells (Fig. 2A,B). In addition to effects on cell spreading, low overexpression of TRPM7 increased cell-matrix adhesion of N1E-115 cells (Fig. 2A,C). Both effects of TRPM7 were independent of kinase activity, suggesting that Ca^{2+}-dependent mechanisms account for the morphological differences between parental and TRPM7-transduced cells.

TRPM7 Activation Leads to Podosome Formation

In light of the effects of TRPM7 on cell morphology and adhesion, we further investigated the effect of low TRPM7 overexpression and activation on the subcellular distribution of F-actin, myosin IIA and vinculin by confocal microscopy (Fig. 3A). Control N1E-115 cells displayed a predominantly cortical distribution of F-actin and myosin IIA, with little or no focal adhesions nor stress fibers. Following BK-induced cell spreading, a part of this peripheral actomyosin was lost while small focal adhesions could now be
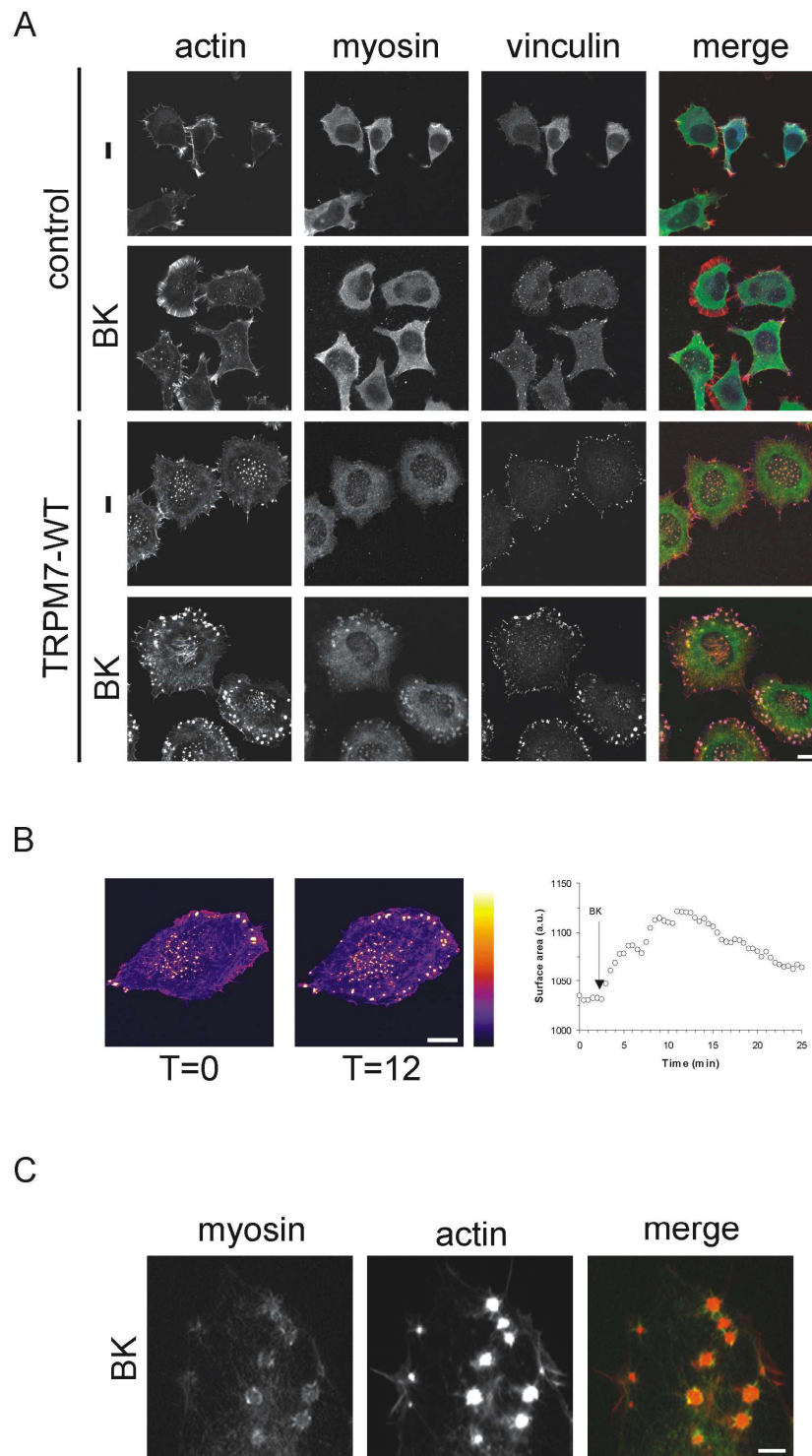
Figure 3 Activation of TRPM7 induces actomyosin reorganization in conjunction with podosome formation. (**A**) TRPM7 activation induces actomyosin reorganization and formation of podosomes in N1E-115/TRPM7 cells. Cells were either serum starved (0.1% FCS) or stimulated with BK (10 nM; 30 min) and stained for actin (red), myosin IIA heavy chain (green) and vinculin (blue). Cells were analyzed by confocal microscopy. Scale bar = 20 μm. (**B**) Increase in cell surface area and production of podosomes occurs within minutes of BK stimulation in N1E-115/TRPM7 cells. N1E-115/TRPM7 cells expressing GFP-β-actin were followed by confocal microscopy before and after BK stimulation. Cell surface area was measured as described in *Materials and Methods*. Grayvalues are displayed using the Fire LookUpTable (LUT) of the public domain software Image J (National Institutes of Health, Bethesda, USA). Left panel, a resting cell; middle panel, the same cell 12 min post-BK stimulation; right panel, kinetics of BK-induced cell spreading. A movie is provided as supplementary data. Scale bar =15 μm. (**C**) High magnification of myosin lattices found in N1E-115/TRPM7 cells following BK stimulation. N1E-115/TRPM7 cells were transfected with GFP-myosin, stimulated with BK and stained for actin. Scale bar = 2 μm.
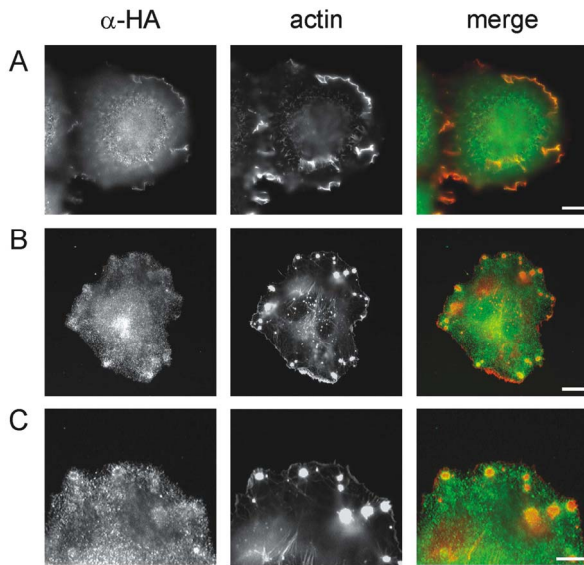
Figure 4 TRPM7 is present at the cell surface and localizes to cell adhesion structures. N1E-115/TRPM7-WT cell were stimulated with BK (10 nM; 30 min). Subsequently, TRPM7 was detected using anti-HA (3F10) antibody followed by alexa 488-conjugated anti-rat IgG. The actin cytoskeleton was visualized using phalloidin-texas red. (A) TRPM7 is found in membrane ruffles. Scale bar = 10 μm. (B) TRPM7 forms a ring surrounding the actin dense core of podosomes. Scale bar = 10 μm. (C) High magnification of TRPM7 rings within podosomes. Scale bar = 5 μm. A rat IgG control antibody did not show any specific staining (data not shown).

observed at the cell periphery by vinculin staining. In N1E-115/TRPM7 cells, a profound redistribution of actomyosin was observed. In contrast to the parental cells, focal adhesions were already present in unstimulated cells, whereas myosin IIA was dispersedly staining the cytoplasm. BK stimulation caused further cell spreading and increased the number and size of adhesion complexes. These responses were noticeable within 2 min and peaked at approximately 10 min after BK stimulation (Fig. 3B and supplementary movie 1). The architecture and size (~1 μm) of these adhesion structures were remarkably different from the focal adhesions observed in unstimulated cells and resembled that of podosomes (Linder and Aepfelbacher, 2003). Similar to podosomes, the TRPM7-induced adhesions, found at the interface of the cell and matrix, had a diameter of approximately 1 μm. Moreover, they consisted of an actin core surrounded by vinculin and conspicuous myosin lattices that were no longer associated with actin stress fibers (Fig. 3C). We conclude therefore, that

TRPM7 activation promotes the formation of podosomes.

TRPM7 is Present at the Cell Surface in Proximity to Cell Adhesion Structures

To examine whether TRPM7 may affect cell adhesion locally, we investigated the cellular distribution of TRPM7 by immunofluorescence. TRPM7 was clearly present within membrane ruffles indicating that the protein is localized at the cell surface (Fig. 4A). In addition, TRPM7 is enriched in cell adhesions where it is found in the podosome ring structure, together with myosin IIA (Fig. 4B,C). Our results suggest that TRPM7 regulates cell adhesion by directly affecting components within these structures.

Induction of Podosomes by TRPM7 Is Mediated by a Kinase-Dependent Mechanism

Although the global effects of TRPM7 on cell spreading and adhesion appear to be independent of kinase activity, we tested whether the TRPM7 kinase domain affects the subcellular organisation of the actomyosin cytoskeleton. By confocal microscopy, we compared N1E-115 cells expressing TRPM7-WT with cells expressing the kinase-dead TRPM7-D1775A mutant. No clear differences were noticed between unstimulated cells (data not shown). However to our surprise, cells expressing kinase-dead TRPM7 failed to induce podosomes in response to BK stimulation (Fig. 5). We conclude that TRPM7 activation
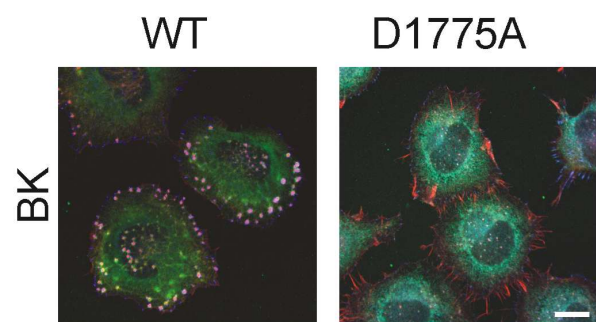

Figure 5 Regulation of podosome formation by TRPM7 is kinase-dependent. N1E-115/TRPM7-WT and N1E-115/TRPM7-D1775A cells were stimulated with BK (10 nM; 30 min) and stained for actin (red), myosin IIA heavy chain (green) and vinculin (blue). Cells were analyzed by confocal microscopy. Scale bar = 20 μm.
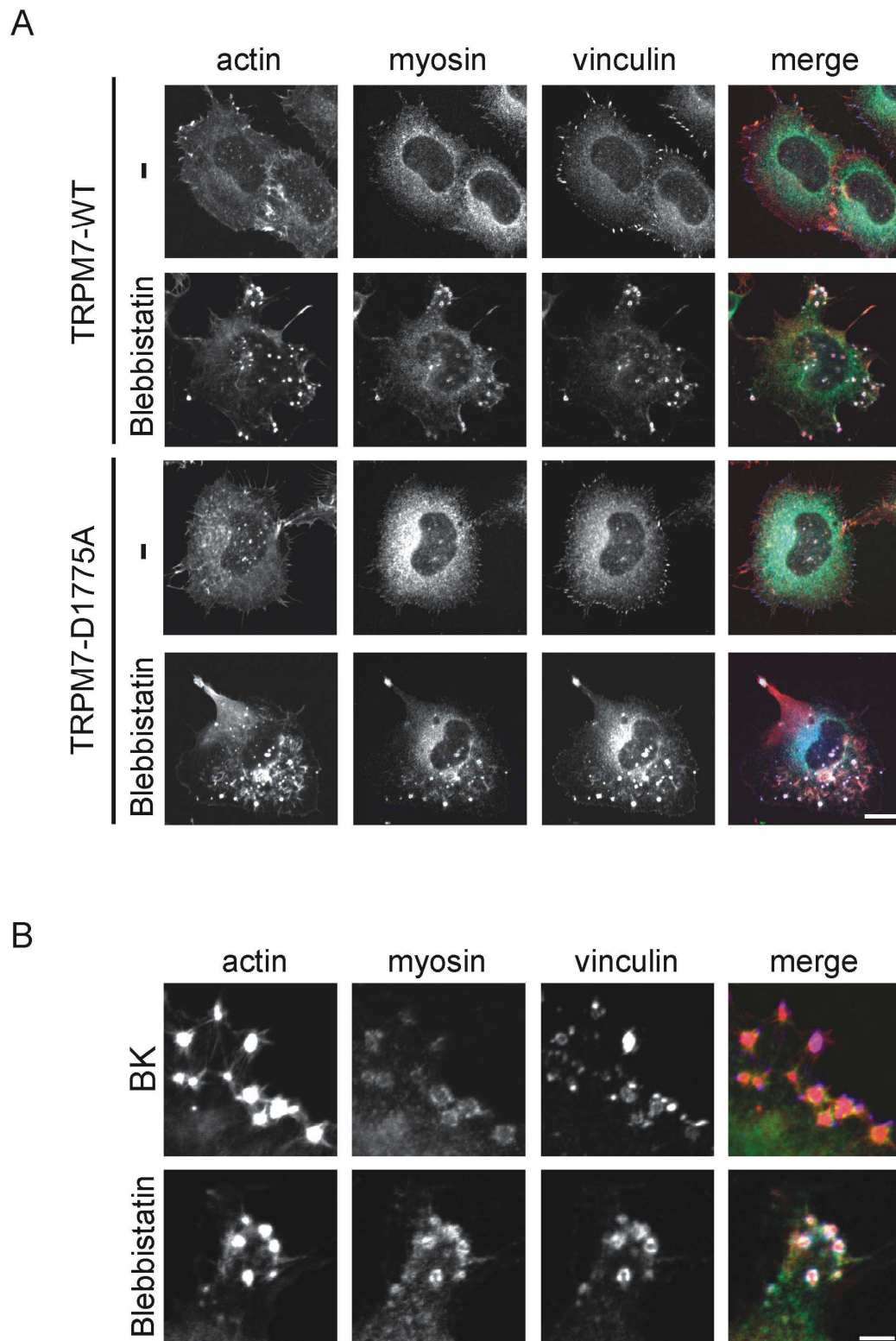
Figure 6 Inhibition of myosin II function in N1E-115 cells expressing TRPM7-WT and TRPM7-D1775A leads to podosome formation. (**A**) N1E-115/TRPM7-WT and N1E-115/TRPM7-D1775A cells were incubated in the presence of vehicle control or 50 μM blebbistatin for 30 min. Cells were stained for actin (red), myosin (green) and vinculin (blue) and visualized by confocal microscopy. Scale bar = 15 μm. (**B**) High magnification view shows that the adhesion complexes induced by BK and blebbistatin in N1E-115/TRPM7-WT cells are architecturally similar since they consist of an actin dense core surrounded by a ring of vinculin and myosin IIA. Scale bar = 5 μm.

results in a kinase-dependent remodeling of the actomyosin cytoskeleton, leading to the assembly of podosomes.

Inhibition of Myosin II Function Leads to Podosome Formation Both in Cells Expressing Wild-type and Kinase–dead TRPM7

Actomyosin contractility plays a central role in regulating the assembly and dissasembly of adhesive contacts (Geiger and Bershadsky, 2002). Notably, the formation of podosomes requires a local inhibition of actomyosin contractility suggesting that TRPM7 may regulate podosome assembly by promoting relaxation of the actomyosin cytoskeleton (Burgstaller and Gimona, 2004). To further test this model, we investigated the effect of directly inhibiting myosin II function on cell adhesion in N1E-115 cells expressing TRPM7-WT and TRPM7-D1775A. Treatment of cells with blebbistatin (a selective inhibitor of myosin II ATPase activity) led to the transformation of focal adhesions into podosomes

Figure 5 Regulation of podosome formation by TRPM7 is kinase-dependent. N1E-115/TRPM7-WT and N1E-115/TRPM7-D1775A cells were stimulated with BK (10 nM; 30 min) and stained for actin (red), myosin IIA heavy chain (green) and vinculin (blue). Cells were analyzed by confocal microscopy. Scale bar = 20 μm.

independently of TRPM7 kinase activity (Fig. 6A). These effects of blebbistatin do not require exogenous TRPM7 as parental N1E-115 cells also produce podosomes in response to myosin II inhibition (supplementary Fig. S4). Notably, the adhesive structures formed upon blebbistatin treatment are remarkably similar to those formed after BK stimulation of N1E-115/TRPM7-WT cells (Fig. 6B). These findings indicate that the transformation of normal focal adhesions into podosomes by BK-mediated activation of TRPM7 is due to a kinase-dependent inhibition of myosin II function.

TRPM7 Interacts with the Actomyosin Cytoskeleton

Since TRPM7 is a member of the α-kinase family, we hypothesized that it may affect actomyosin remodeling and podosome assembly by directly coupling to and potentially phosphorylating components present within the actomyosin cytoskeleton. Therefore, we precipitated TRPM7 complexes with anti-HA antibodies and detected the presence of associated proteins by Western blotting. Both β-actin and the myosin IIA heavy chain were present in a complex with TRPM7 (Fig. 7A). Importantly, endogenous TRPM7 also associates with the actomyosin cytoskeleton (Fig. 7B). This interaction indeed suggests that TRPM7 can affect actomyosin function through a direct association with cytoskeletal proteins.

Bradykinin Causes Calcium and Kinase-dependent Association of the TRPM7 COOH-terminus with Myosin IIA

Since TRPM7 activation by BK results in Ca^{2+}-influx and a kinase-dependent remodeling of the actomyosin cytoskeleton, we investigated whether the interaction between TRPM7 and the actomyosin cytoskeleton is subject to regulation. BK stimulation of N1E-115/TRPM7 cells led to a transient increase in the amount of TRPM7-associated myosin IIA (Fig. 7C,D). Its kinetics closely correlate with those of calcium influx in response to TRPM7 activation (refer to Fig. 1) with maximal association observed at about 2 min after agonist addition. Moreover, chelation of Ca^{2+}, using BAPTA or EDTA, abrogated the association between TRPM7 and myosin IIA (Fig. 7E). These results indicate that the interaction between TRPM7 and myosin IIA is strictly Ca^{2+}-dependent, and suggest that TRPM7-mediated Ca^{2+} influx enhances the TRPM7/myosin IIA interaction. However, in addition to Ca^{2+}, the association of TRPM7 with the cytoskeleton requires an active kinase domain since the kinase-dead TRPM7-D1775A mutant did not interact with myosin IIA (Fig. 7F). A soluble COOH-terminus variant containing the kinase domain of TRPM7 also interacted with myosin IIA (Fig. 7G). We conclude therefore that the interaction between TRPM7 and myosin IIA is mediated by the COOH-terminus and requires an active kinase domain.

TRPM7 Phosphorylates Myosin IIA Heavy Chain

Hitherto, we have shown that TRPM7 associates with myosin IIA in a regulated manner and that both activation of TRPM7-WT (but not TRPM7-D1775A) and inhibition of myosin II
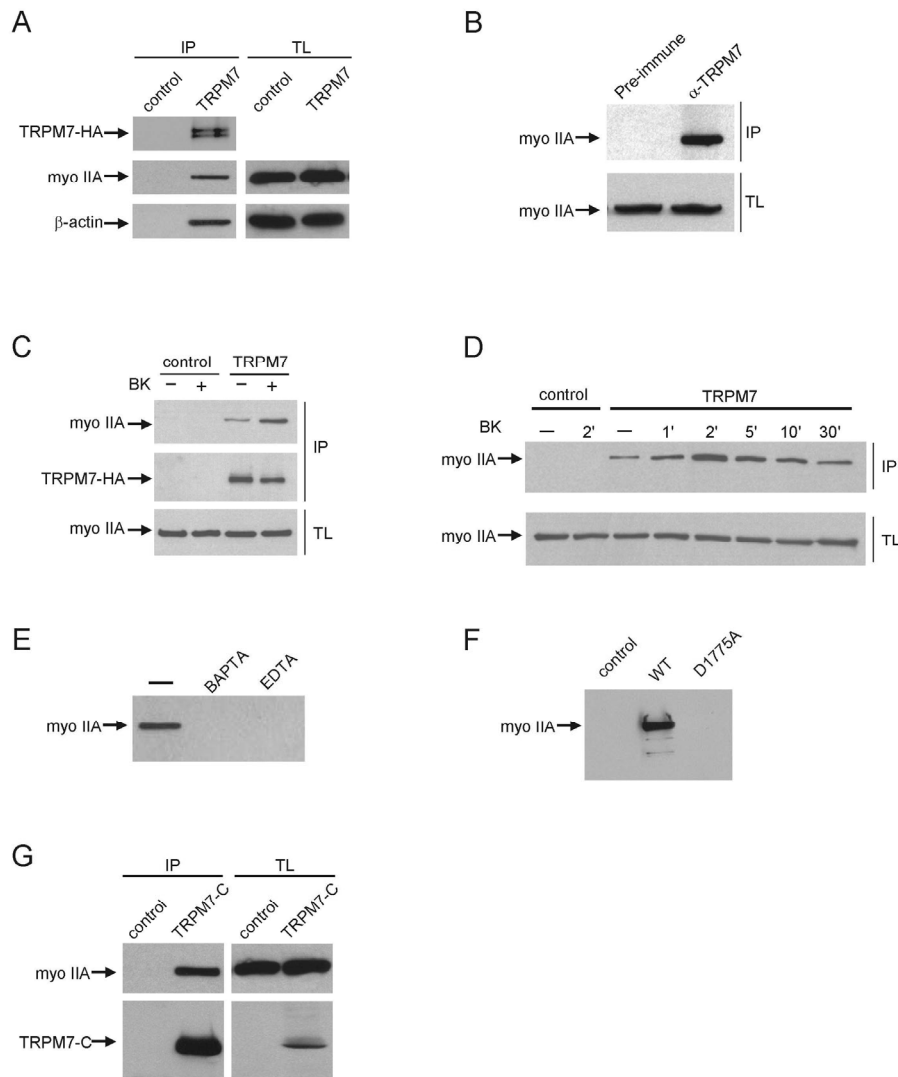
Figure 7 TRPM7 activation promotes its association via the COOH-terminus with the actomyosin cytoskeleton in a calcium- and kinase-dependent manner. In all experiments (except panel B), N1E-115 control or TRPM7-transduced cells were lysed and incubated with anti-HA-coupled protein G beads for 3 h at 4°C. Proteins in the complex were detected by Western blotting. (**A**) Coimmunoprecipitation of TRPM7 with β-actin and myosin IIA. Top, detection of TRPM7 with anti-HA antibodies; middle and bottom, detection of myosin IIA and β-actin, respectively, in the immune complexes (IP, left) and total lysates to control for protein levels (TL, right). (**B**) Endogenous TRPM7 associates with the actomyosin cytoskeleton. PC12 lysates were incubated with pre-immune serum or anti-TRPM7 serum and protein complexes were isolated using protein G-sepharose. The presence of myosin IIA was detected by Western blotting. Top, detection of associated myosin IIA heavy chain in immunoprecipitates; and Bottom, in total lysates. (**C**) Coimmunoprecipitation of TRPM7 with myosin IIA heavy chain in the pre- and post-BK stimulation (10 nM, 1 min). Top, detection of coimmunoprecipitated myosin IIA. Middle, detection of TRPM7 with anti-HA antibodies. Bottom, detection of myosin IIA heavy chain in total lysates to control for protein levels. (**D**) Kinetics of BK induced TRPM7 association with myosin IIA heavy chain. Cells were stimulated with BK (10 nM) for the indicated times and TRPM7 was immunoprecipitated using anti-HA antibodies. Top, Western blot showing coimmunoprecipitated myosin IIA heavy chain. Bottom, detection of myosin IIA heavy chain in total lysates. (**E**) Interaction between TRPM7 and myosin IIA heavy chain is Ca^{2+}-dependent. N1E-115/TRPM7 cells were pre-incubated with 10 mM BAPTA or EDTA for 1 min prior to cell lysis and TRPM7 was immunoprecipitated using anti-HA antibodies. (**F**) TRPM7-D1775A does not interact with myosin IIA heavy chain. TRPM7-WT and –D1775A were immunoprecipitated with anti-HA antibodies and associating myosin IIA heavy chain was detected by Western blotting. (**G**) The COOH-terminus of TRPM7 interacts with myosin IIA. The soluble COOH-terminus of TRPM7 (a.a. 1158-1864) was immunoprecipitated from N1E-115/TRPM7-C cells with anti-HA antibodies and associated myosin IIA was detected by Western blotting. Top, detection of associated myosin IIA heavy chain; bottom, detection of TRPM7-C using anti-HA antibodies in immunoprecipitation (IP, left) and in total lysates (TL, right).

function produce podosomes suggesting that TRPM7 activation promotes actomyosin relaxation. How does TRPM7 mediate the inhibition of myosin II function? By analogy to regulation of *Dictyostelium* myosin II function, we have previously proposed that Ca^{2+}-dependent MHC phosphorylation contributes to cytoskeletal relaxation (van Leeuwen *et al*, 1999). The finding that TRPM7 coprecipitates with myosin IIA, particularly after BK stimulation, enabled us to test whether TRPM7 can phosphorylate myosin IIA heavy chain. Since TRPM7 and myosin IIA heavy chain co-migrate on SDS-PAGE gels, TRPM7 was

immunoprecipitated both under conditions that favor association and dissociation (low vs. high stringency) of the cytoskeletal complex allowing

us to distinguish between TRPM7 autophosphorylation and myosin phosphorylation. By *in vitro* kinase assays, TRPM7 underwent autophosphorylation in agreement with earlier findings (Runnels *et al*, 2001; Ryazanova *et al*, 2004; Schmitz *et al*, 2003) (Fig. 8A; bottom panel). Strikingly, clear phosphorylation of associated myosin IIA heavy chain (which runs slightly faster than TRPM7) was also observed in these kinase reactions (Fig. 8A; bottom panel). In contrast, actin was not phosphorylated (data not shown).

To demonstrate that TRPM7 directly phosphorylates myosin IIA heavy chain, a myosin tail fragment was expressed as a GST-fusion protein in *E. coli* to serve as substrate whereas TRPM7 was immunoaffinity purified from
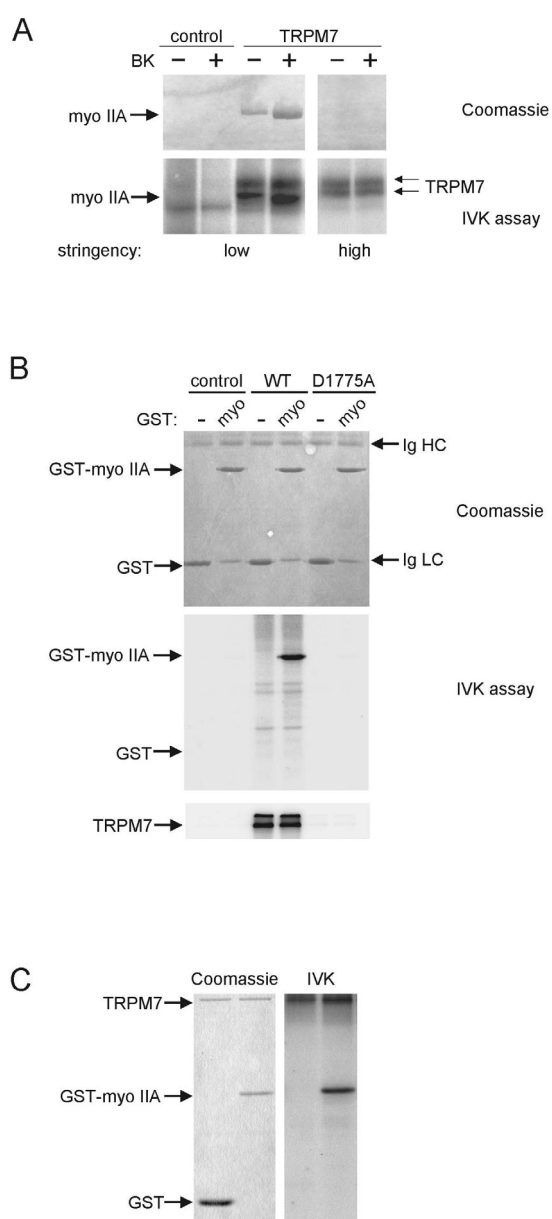
Figure 8 TRPM7 phosphorylates myosin IIA heavy chain. (**A**) *In vitro* kinase assay detecting the phosphorylation of associated myosin IIA heavy chain by TRPM7. TRPM7/myosin IIA heavy chain complexes were isolated before and after stimulation of N1E-115 control and N1E-115/TRPM7 cells with BK (10 nM, 2 min) under low (1% triton X-100) and high (1% triton X-100/ 0.5% deoxycholate/ 0.1% SDS) stringency conditions. Substrates of TRPM7 were detected by labeling proteins with γ-^{32}P-ATP, separating products of the *in vitro* kinase assay by SDS-PAGE (6% gel) followed by autoradiography. Top, Coomassie staining of precipitated proteins. Bottom, autoradiogram of phosphorylated proteins. Note that myosin association is lost under high stringency conditions (1% triton X-100/ 0.5% deoxycholate/ 0.1% SDS) whereas TRPM7 autophosphorylation is unaffected. (**B**) TRPM7 phosphorylates recombinant myosin IIA. TRPM7-WT and –D1775A were immunoaffinity purified from HEK293 cells using anti-HA antibodies under high stringency and mixed with 2 μg of GST or GST-myosin IIA in kinase buffer. To detect phosphorylated myosin IIA, the proteins were separated by SDS-PAGE (12 % gel) followed by autoradiography. Top, Coomassie staining of GST-fusion proteins. Note that GST co-migrates with the antibody light chain (Ig LC). Middle, autoradiogram of phosphorylated GST-fusion proteins. Bottom, autoradiogram showing autophosphorylation of WT but not kinase-dead TRPM7. (**C**) Recombinant TRPM7 kinase phosphorylates myosin IIA. The TRPM7 kinase domain (1403-1864 aa) was produced in *E. coli* as a fusion with maltose binding protein and purified on an amylose column. The purified kinase was incubated with 2 μg of GST or GST-myosin IIA in kinase buffer. The proteins were resolved on a 12% SDS-PAGE gel and detected by coomassie. Phosphorylated proteins were visualized by autoradiography. Left, coomassie staining of gel; right, autoradiogram.

mammalian cells or the COOH-terminus of TRPM7 was purified from *E. coli*. In *in vitro* kinase assays, immunoaffinity purified WT but not kinase-dead TRPM7 efficiently phosphorylated recombinant myosin IIA (Fig. 8B). Notably, GST was not phosphorylated by TRPM7 (Fig. 8B). Similar results were obtained when using the soluble COOH-terminus of TRPM7 (data not shown). Importantly, contaminating actin in the purified TRPM7 fractions is below detection levels and disruption of the actin cytoskeleton prior to TRPM7 purification had no effect on the level of myosin II phosphorylation arguing against the presence of contaminating kinases (supplementary Fig. S5). Finally, recombinant TRPM7 purified from *E. coli* lysates also efficiently phosphorylated myosin IIA, in the absence of other sources of eukaryotic proteins (Fig. 8C). Thus, TRPM7 itself and not an associated kinase is responsible for myosin IIA heavy chain phosphorylation. Collectively, our results demonstrate that TRPM7 associates with the actomyosin cytoskeleton in a Ca^{2+}- and kinase-dependent manner to regulate myosin II activity and consequently, actomyosin contractility. Moreover, our *in vitro* kinase data suggest that phosphorylation of the myosin IIA heavy chain by TRPM7 serves as a regulatory mechanism.

Discussion

In this study, we have tested the hypothesis that TRPM7, by analogy to its α-kinase family members from *Dictyostelium,* affects actomyosin contractility. We provide evidence that TRPM7 promotes relaxation of the actomyosin cytoskeleton via a kinase-dependent inhibition of myosin II, potentially involving myosin IIA heavy chain phosphorylation. The evidence includes: i) electrophysiological measurement of TRPM7 channel opening after BK stimulation; ii) biochemical analyses of the TRPM7 complex showing that TRPM7 interacts in a Ca^{2+}- and kinase-dependent manner with an actomyosin protein complex; iii) *in vitro* kinase reactions demonstrating that TRPM7 phosphorylates myosin IIA heavy chain; and iv) cell biological studies revealing that TRPM7 promotes a loss of cortical tension leading to podosome formation by a kinase-dependent mechanism. Collectively, our data indicate

that TRPM7 plays a role in linking receptor-mediated signals to actomyosin remodeling and cell adhesion. Furthermore, our observations reveal for the first time that TRP channels affect the cytoskeleton by directly associating with cytoskeletal proteins in a highly regulated manner.

What is the relationship between channel opening and the kinase domain? Several studies have suggested that kinase activity regulates TRPM7 channel opening (Runnels *et al*, 2001; Schmitz *et al*, 2003). However, in our model system, TRPM7 channel opening was independent of kinase activity, since the responses to BK stimulation were identical between cells expressing WT and kinase-dead TRPM7. While TRPM7 kinase activity does not directly affect channel opening, it cannot be excluded that actomyosin remodeling serves to regulate TRPM7 function in an indirect manner as reported for other TRP channels (Itagaki *et al*, 2004; Lockwich *et al*, 2001). Based on our observations, rather than the kinase domain regulating TRPM7-channel function, the reverse relationship exists. In this model (Fig. 9), phosphorylation of downstream targets (myosin II, annexin I; (Dorovkov and Ryazanov, 2004)) by the TRPM7-kinase domain is tightly regulated by ion-influx (Ca^{2+}, Mg^{2+}) through the TRPM7-channel. In support of this model, we observed that Ca^{2+} is strictly required for the association of TRPM7 with the cytoskeleton, that increased Ca^{2+}-influx through TRPM7 upon agonist-induced activation enhances its association with myosin IIA and that MHC phosphorylation is strictly Ca^{2+}-dependent (van Leeuwen *et al*, 1999). Recently, Dorovkov and Ryazanov (2004) showed that the kinase activity of TRPM7 is potentiated *in vitro* by the addition of Ca^{2+} and conversely, is inhibited by chelation of Ca^{2+}. Therefore, we propose that ion influx through the channel pore regulates the TRPM7 kinase domain by activating the kinase and controlling the recruitment of its substrates.

Kinases are maintained in an active state by intramolecular and intermolecular protein-protein or protein-lipid interactions (Roskoski, 2004; Van Etten, 2003). Activation of kinases

generally involves autophosphorylation or transphosphorylation at regulatory sites inducing conformational remodeling to expose the catalytic domain to its substrate. We postulate that TRPM7 is similarly regulated, since its kinase activity appears to be essential for its association with the actomyosin cytoskeleton. Autophosphorylation of TRPM7, which occurs on serine and threonine residues (Ryazanova *et al*, 2004; Schmitz *et al*, 2003), may release a cryptic binding site for myosin IIA heavy chain (Fig. 9). Thus, autophosphorylation of TRPM7 may serve as an important regulatory mechanism to modulate the interactions between TRPM7 and its substrates.

A functional consequence of TRPM7 activation is an increase in cell adhesion and spreading, which involves both kinase-dependent and -independent pathways. Expression of a TRPM7 kinase-dead mutant still promotes cell adhesion and spreading but does not lead to the formation of podosomes upon BK stimulation. The fact that the global effects of TRPM7 on cell morphology are independent of kinase activity or its association with the cytoskeleton may reflect the increase in cytosolic Ca^{2+} concentrations observed in TRPM7-transduced cells. Indeed, reducing the internal Ca^{2+} concentration with BAPTA-AM impaired cell spreading (data not shown). Ca^{2+} may act directly at the level of integrin activation or affect the actomyosin cytoskeleton. The activation of integrins can lead to the remodeling of the actomyosin cytoskeleton to promote cell spreading via outside-in signaling pathways (DeMali *et al*, 2003). Alternatively, Ca^{2+} is an important second messenger in actin remodeling including polymerization, severing of filaments and F-actin-membrane interactions (Forscher, 1989; Sun *et al*, 1999). Moreover, since TRPM7 can directly interact with PLC-isoforms, it may influence local concentrations of PIP2, and thus affect actin polymerization (van Rheenen and Jalink, 2002).

The kinase-dependent effects of TRPM7 on cell adhesion are consistent with a role in regulating myosin IIA-dependent contractile responses. Notably, both BK stimulation and myosin II inhibition of N1E-115/TRPM7 cells

induces the formation of large podosomes. Spatial and temporal regulation of actomyosin contractility is central to modulating the assembly and disassembly of focal adhesions and podosomes (Burgstaller and Gimona, 2004; Burridge and Wennerberg, 2004; DeMali *et al*, 2003; Geiger and Bershadsky, 2002; Linder and Aepfelbacher, 2003). While local regulation of contractility appears to be controlled by Rho GTPases (Burgstaller and Gimona, 2004), α-kinases may also fulfill a role in spatial and temporal regulation of myosin II activity. Indeed, TRPM7, which is expressed at the cell surface, was found enriched in cell adhesion structures. By similarity, *Dictyostelium* myosin II function is precisely regulated by a family of MHC kinases with each member possessing a unique spatial distribution (Liang *et al*, 2002). Therefore, we postulate that an increase in TRPM7-mediated MHC phosphorylation contributes to local relaxation of the cortical cytoskeleton causing the transformation of focal adhesions into podosomes. Ablation of TRPM7 kinase activity maintains myosin-based cytoskeletal contractility preventing the reorganization of focal adhesions. Hence, TRPM7 regulates cell adhesion by modulating actomyosin contractility in a kinase-dependent manner and it is tempting to speculate that this phenomenon operates through MHC phosphorylation.

How to reconcile the small increase in TRPM7 expression (2-fold) with dramatic changes in cell morphology and response to BK? Although the kinase activity of TRPM7 is a linear relationship with concentration *in vitro*, it is most likely not linear *in vivo* as the protein will be subject to regulation. In support of this hypothesis, we have found that TRPM7 channels have increased activity as measured by patch-clamp and Ca^{2+} fluorometric experiments in N1E-115/TRPM7 cells. It should be noted that the basal Ca^{2+} levels in the cells are significantly higher upon TRPM7 overexpression, which could influence kinase activity as reported by Dorovkov and Ryazanov (2004). Moreover, TRPM7-mediated Ca^{2+} influx affects the recruitment of substrates for the kinase, by associating with the actomyosin cytoskeleton. Therefore, it can be expected that the activity of the TRPM7 complex in the N1E-115/TRPM7 *in vivo* is significantly more than the two-fold increase in kinase activity that is observed *in vitro*. Finally, if TRPM7 is targeted to a particular part of the cytoskeleton including cell adhesion structures, it is likely that the local activity of TRPM7 kinase increases

significantly more than 2-fold in those areas of the cell.

Bradykinin stimulation of N1E-115 cells leads to cell spreading and focal adhesion formation whereas it promotes the transformation of focal adhesions into podosomes in N1E-115/TRPM7 cells. Although N1E-115 cells express endogenous TRPM7, these cells do not produce podosomes in response to BK. We believe these results reflect the contractile state of the cell and that it is necessary to overexpress TRPM7 to achieve complete relaxation of the actomyosin cytoskeleton required for BK-mediated podosome formation (see supplementary Fig. S6). In parental N1E-115 cells, myosin II is very active leading to a contractile phenotype. BK stimulation of these cells relaxes the cytoskeleton but since focal adhesions are formed, myosin II must be at least partly active as tension is required for focal adhesion biogenesis (Geiger and Bershadsky, 2002). Overexpression of TRPM7 mimics these effects and BK stimulation of these cells leads to further inhibition of myosin II and relaxation of the actomyosin cytoskeleton, which allows for the formation of podosomes (adhesion structures which require an inhibition of myosin II for their formation (Burgstaller and Gimona, 2004)). In support of this model, inhibition of myosin II by blebbistatin in parental N1E-115 cells similarly induces podosomes (supplementary Fig. S4). Thus, since TRPM7 has a basal activity, its expression levels dictate myosin II activity, and thereby cellular phenotype.

Although mammalian nonmuscle actomyosin contractility appears to be primarily regulated by phosphorylation of the myosin regulatory light chain, a role for myosin heavy chain phosphorylation is emerging. Several studies have demonstrated that the MHC tail is phosphorylated on threonine residues upon stimulation of mammalian cells (van Leeuwen *et al*, 1999; Wilson *et al*, 1998). Based on homology to *Dictyostelium* MHC kinases, we hypothesized that TRPM7 may regulate myosin II function by phosphorylating the MHC α-helical tail. Indeed, *in vitro* kinase assays demonstrated that WT but not kinase-dead TRPM7 directly phosphorylates the MHC tail indicating broad evolutionary conservation with respect to both substrate and function. An unexpected result since other α-kinases, α-kinase 1 and EFK-2, regulate protein transport and protein synthesis, respectively (Heine *et al*, 2005; Ryazanov, 2002).

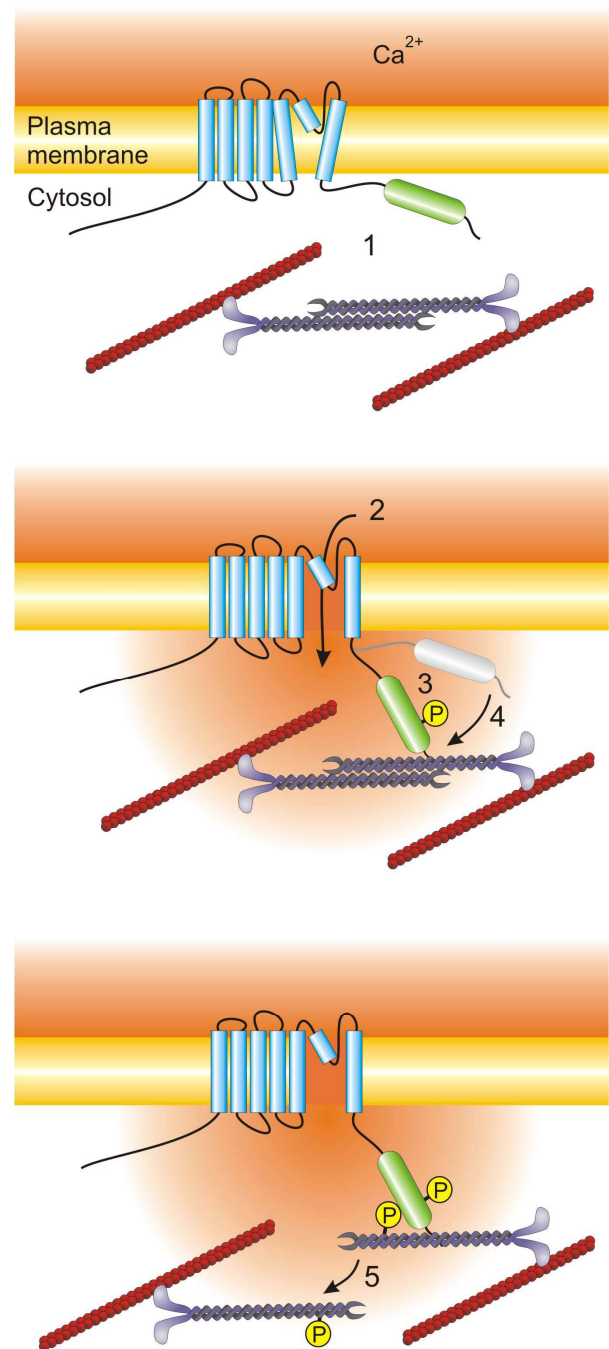Myosin II forms bipolar thick filaments through electrostatic interactions of the MHC tail

Figure 9 Regulation of actomyosin contractility by TRPM7. (**A**) In the resting state, TRPM7 is not associated with the actomyosin cytoskeleton (1). (**B**) Stimulation of cells with PLC-activating agonists induces TRPM7-mediated Ca^{2+} influx (2) as well as TRPM7 kinase activity. Autophosphorylation (3) promotes a conformational change within TRPM7 allowing for Ca^{2+}-dependent association with myosin IIA (4). (**C**) Subsequently, TRPM7 phosphorylates the myosin IIA heavy chain, presumably leading to dissociation of myosin filaments and cytoskeletal remodeling (5).

1 TRPM7 Regulates Actomyosin Contractility

(Hostetter *et al*, 2004). In *Dictyostelium*, phosphorylation of the α-helical MHC tail leads to filament disassembly thereby releasing cortical tension (Egelhoff *et al*, 1993). Whether phosphorylation of mammalian myosin II heavy chain by TRPM7 will have a similar effect on filament assembly remains to be determined (Fig. 9C). Importantly, the region of myosin II phosphorylated by TRPM7 corresponds to the domain responsible for regulating myosin filament assembly (Nakasawa *et al*, 2005). Moreover, phosphorylation by PKC and casein kinase as well as point mutations affecting electrostatic charges (E1841K) within this domain affect myosin II function (Dulyaninova *et al*, 2005; Franke *et al*, 2005). Therefore, we propose that phosphorylation of this region of the myosin IIA tail affects filament formation rather than ATPase activity of myosin II. Future investigations aimed at mapping the TRPM7 target residues within the myosin IIA heavy chain and defining the physiological relevance of MHC phosphorylation will provide further insight into the mechanisms underlying actomyosin contractility in mammalian cells.

In conclusion, we identified TRPM7 as a novel regulator of actomyosin contractility and cell adhesion in response to agonist stimulation. Moreover, we have demonstrated that TRP channels can interact with the actomyosin cytoskeleton to affect cell adhesion. Future experiments will be aimed at defining the role of TRPM7-containing protein assemblies in regulating actomyosin function, and establishing how these cytoskeletal changes affect cell adhesion and/or TRPM7 function.

Materials & Methods

Constructs

Mouse TRPM7 in pTracer-CMV2, and GFP-myosin IIA in pEGFP-C3 were kind gifts from David Clapham (Harvard, Boston, USA) and Robert Adelstein (NIH, Bethesda, USA), respectively. An HA-tag has been inserted at the COOH-terminus of TRPM7 (Runnels *et al*, 2001). To generate retroviral expression vectors, the TRPM7 cDNA was inserted as a *XhoI- NotI* fragment into the LZRS-ires-neomycin vector. The kinase-dead mutant TRPM7-D1775A was produced by site-directed mutagenesis using the Quickchange kit (Stratagene). The soluble TRPM7 COOH-terminus construct encodes for amino acids 1158-1864 and contains a HA-tag at the NH_2-terminus. The cDNA was amplified by PCR and inserted as a *XhoI- NotI* fragment into the LZRS-ires-neomycin vector. GFP-β-actin cDNA was inserted as an *EcoRI- NotI* fragment into the LZRS-ires-neomycin vector. Mouse myosin IIA heavy chain tail (aa 1795-1960) was amplified by RT-PCR from N1E-115 cells and cloned in frame in pGEX-1N using *BamHI- EcoRI* sites. The TRPM7 kinase domain (aa 1403-1864) in pMAL-p2x was described previously (Ryazanova *et al*, 2004). All constructs were verified by DNA sequencing.

Cell Culture

Mouse N1E-115, HEK293 and Phoenix packaging cells were cultured in DMEM medium with 10% FCS while PC12 cells were grown in RPMI medium with 10% horse serum and 5% FCS. Stable cell lines expressing the various TRPM7 constructs and GFP-β-actin were generated by retroviral transduction (van Leeuwen *et al*, 1999). N1E-115 cells transduced with the empty vector served as a control for all experiments. Cells were selected by the addition of 0.8 mg/ml G418 to the media and the selection was complete within 7 days. For transient expression, cells were transfected using Fugene 6 (Roche) according to the manufacturer's recommendations.

Intracellular Calcium Determinations

Calcium measurements were performed by confocal ratiometric imaging of cells loaded with Oregon Green 488 BAPTA-1 AM and Fura Red AM (Molecular Probes) essentially as described (Schild *et al*, 1994). Experiments were performed at 37ºC in a HEPES/bicarbonate-buffered saline under 5% CO_2, pH 7.3 (140 mM NaCl, 23 mM $NaHCO_3$, 5 mM KCl, 2 mM $MgCl_2$, 1 mM $CaCl_2$, 10 mM HEPES and 10 mM glucose), and calibration was with ionomycin (Calbiochem). Shown are representative traces from experiments performed at least in 10-fold; data are presented as mean ± SEM.

Adhesion Assay

Cells (5×10^5) were seeded in a T25 flask and allowed to adhere for 16 h. To quantitate cell adhesion, non-adherent cells were washed away with PBS. The adherent cells were fixed in 3.7% formaldehyde in PBS for 10 min, washed with PBS and subsequently stained with 2% crystal

violet for 50 min. Excess stain was removed by extensive washing in PBS. Cells were lysed in PBS containing 1% NP40 and the absorbance at 570 nm of the lysate was measured. Maximal adhesion as measured on poly-L-lysine coated dishes was set to 100%. Values reported are representative of two independent experiments performed in triplicate.

Microscopy

Cells seeded on glass coverslips, were serum starved (0.1% FCS) overnight prior to stimulation with BK or blebbistatin (Calbiochem). For fixed specimens, cells were stained as previously described (van Leeuwen *et al*, 1997). Antibodies used for immunofluorescence were rat anti-HA (3F10; 1:100; Roche), mouse anti-vinculin (1:400; Sigma), rabbit anti-myosin IIA (1:100; BTI), alexa 488-conjugated anti-rabbit and anti-rat IgG, and alexa 647-conjugated anti-mouse IgG (1:200; Molecular Probes). F-actin was detected using either texas-red or alexa 546-labelled phalloidin (1:50; Molecular Probes). Cells were viewed using either a Zeiss-LSM 510-meta microscope equipped with a Plan-Apochromat 63X, 1.4 NA oil immersion lens or a Leica-DMRA microscope with a 63X, 1.32 NA oil immersion lens. For videomicroscopy, cells were transferred to a bicarbonate-buffered medium as described above and maintained at $37^{o}C$ on a temperature- and CO_2-controlled stage. Cells were imaged with a DM-IRE2 inverted microscope fitted with a TCS-SP2 scanhead and a 63X, 1.32 NA oil immersion lens (Leica). Images were collected at a 30 s time interval and surface area was calculated by quantifying the amount of pixels under a digital mask constructed by using the binary-fill operation after a thresholding step.

Generation of Anti-TRPM7 Antibodies

To generate anti-TRPM7 antibodies, a GST-fusion protein encoding amino acids 1447 to 1555 of TRPM7 was expressed in *E. coli* and purified on a glutathione-sepharose column. Rabbits were injected with the antigen mixed with Freund's adjuvant and serum was collected 10 days after every vaccination. Serum collected prior to immunization (pre-immune) was used as a negative control in all experiments.

Immunoprecipitations

Cells were serum starved (0.1% FCS) overnight prior to stimulation as indicated in the figure legends. After stimulation, cells were lysed on ice for 20 min in lysis buffer (50 mM Tris pH 7.5, 300 mM NaCl, 0.5 mM DTT, 1.5 mM MgCl$_2$, 0.2 mM EDTA, 1% triton x-100 supplemented with protease inhibitors) and the extract was cleared by centrifugation. For the immunoprecipitation of exogenously expressed TRPM7, protein G-sepharose beads, which were blocked with 0.5% BSA and pre-coupled with anti-HA antibody (clone 12CA5), were added to the lysate of N1E-115/ empty vector (control) or N1E-115/TRPM7 cells. The samples were incubated at $4^{o}C$ for 3 h. Endogenous TRPM7 was immunoprecipitated by incubating cellular lysates with anti-TRPM7 antibodies at $4^{o}C$ for 3 h followed by the addition of protein G-sepharose beads at $4^{o}C$ for 15 min. Subsequently, the beads were washed 3 times with lysis buffer, protein complexes were solubilized in Laemmli sample buffer and separated by SDS-PAGE. Proteins were detected by immunoblotting using the following antibodies: anti-HA (clone 3F10; 1:1000), anti-myosin IIA (1:500), anti-β actin (1:20000; Sigma).

In Vitro Kinase Assays

Recombinant TRPM7 kinase domain (amino acids 1402-1864) and myosin tail fragment (amino acids 1795-1960) were expressed, respectively, as a maltose binding protein- and GST-fusion protein in *Escherichia coli* and purified by standard methods. Immunocomplexes containing TRPM7 with or without associated myosin or TRPM7 mixed with 2 μg of GST-myosin were solubilized in kinase buffer (50 mM HEPES pH 7.0, 4 mM MnCl$_2$, 5 mM DTT) without ATP. The kinase reaction was initiated by adding 0.1 mM ATP in combination with 5 μCi γ-^{32}P-ATP and proceeded for 30 min at $30^{o}C$. The products of the kinase reaction were resolved by SDS-PAGE and detected by autoradiography.

Statistical Analysis

All data are representative of at least 3 independent experiments. Quantitative data are presented as the mean ± SEM. Statistical significance of differences between experimental groups was assessed with Student's *t* test.

Differences in means were considered significant if $p < 0.05$.

Supplemental Material

Fig. S1 shows that mutation of aspartate 1775 to alanine abrogates the ability of TRPM7 to undergo autophosphorylation. Fig. S2 shows the relative TRPM7 kinase activity in the different N1E-115 cell lines. Fig. S3 shows that both TRPM7-WT and TRPM7-D1775A are glycosylated and properly localized to the plasma membrane. Fig. S4 depicts the induction of podosomes in parental N1E-115 cells upon blebbistatin treatment. Fig. S5 shows that depletion of actin from TRPM7 immunoprecipitation by latrunculin A treatment has no effect on myosin IIA phosphorylation. Fig. S6 provides a model explaining the correlation between cell phenotype, TRPM7 expression and myosin II activity. Movie 1 depicts the dynamics of cell spreading and focal adhesion formation in N1E-115/TRPM7 cells in response to BK stimulation.

Acknowledgements

References

Burgstaller G, Gimona M (2004) Actin cytoskeleton remodelling via local inhibition of contractility at discrete microdomains. *J Cell Sci* **117:** 223-231

Burridge K, Wennerberg K (2004) Rho and Rac take center stage. *Cell* **116:** 167-179

De la Roche MA, Smith JL, Betapudi V, Egelhoff TT, Cote GP (2002) Signaling pathways regulating Dictyostelium myosin II. *J Muscle Res Cell Motil* **23:** 703-718

DeMali KA, Wennerberg K, Burridge K (2003) Integrin signaling to the actin cytoskeleton. *Curr Opin Cell Biol* **15:** 572-582

Dorovkov MV, Ryazanov AG (2004) Phosphorylation of annexin I by TRPM7 channel-kinase. *J Biol Chem* **279:** 50643-50646

Drennan D, Ryazanov AG (2004) Alpha-kinases: analysis of the family and comparison with conventional protein kinases. *Prog Biophys Mol Biol* **85:** 1-32

Dulyaninova NG, Malashkevich VN, Almo SC, Bresnick AR (2005) Regulation of myosin-IIA assembly and Mts1 binding by heavy chain phosphorylation. *Biochemistry* **44:** 6867-6876

Egelhoff TT, Lee RJ, Spudich JA (1993) Dictyostelium myosin heavy chain phosphorylation sites regulate myosin filament assembly and localization in vivo. *Cell* **75:** 363-371

Forscher P (1989) Calcium and polyphosphoinositide control of cytoskeletal dynamics. *Trends Neurosci* **12:** 468-474

Franke JD, Dong F, Rickoll WL, Kelley MJ, Kiehart DP (2005) Rod mutations associated with MYH9-related disorders disrupt nonmuscle myosin-IIA assembly. *Blood* **105:** 161-169

Geiger B, Bershadsky A (2002) Exploring the neighborhood: adhesion-coupled cell mechanosensors. *Cell* **110:** 139-142

Heid PJ, Wessels D, Daniels KJ, Gibson DP, Zhang H, Voss E, Soll DR (2004) The role of myosin heavy chain phosphorylation in Dictyostelium motility, chemotaxis and F-actin localization. *J Cell Sci* **117:** 4819-4835

Heine M, Cramm-Behrens CI, Ansari A, Chu HP, Ryazanov AG, Naim HY, Jacob R (2005) Alpha-kinase 1, a new component in apical protein transport. *J Biol Chem* **280:** 25637-25643

Hostetter D, Rice S, Dean S, Altman D, McMahon PM, Sutton S, Tripathy A, Spudich JA (2004) Dictyostelium myosin bipolar thick filament formation: importance of charge and specific domains of the myosin rod. *PLoS Biol* **2:** 1880-1892

Itagaki K, Kannan KB, Singh BB, Hauser CJ (2004) Cytoskeletal reorganization internalizes multiple transient receptor potential channels and blocks calcium entry into human neutrophils. *J Immunol* **172:** 601-607

Jalink K, van Corven EJ, Hengeveld T, Morii N, Narumiya S, Moolenaar WH (1994) Inhibition of lysophosphatidate- and thrombin-induced neurite retraction and neuronal cell rounding by ADP ribosylation of the small GTP-binding protein Rho. *J Cell Biol* **126:** 801-810

Kolman MF, Futey LM, Egelhoff TT (1996) Dictyostelium myosin heavy chain kinase A regulates myosin localization during growth and development. *J Cell Biol* **132:** 101-109

Kozak JA, Cahalan MD (2003) MIC channels are inhibited by internal divalent cations but not ATP. *Biophys J* **84:** 922-927

Liang W, Licate L, Warrick H, Spudich J, Egelhoff T (2002) Differential localization in cells of myosin II heavy chain kinases during cytokinesis and polarized migration. *BMC Cell Biol* **3:** 19

Linder S, Aepfelbacher M (2003) Podosomes: adhesion hot-spots of invasive cells. *Trends Cell Biol* **13:** 376-385

Lockwich T, Singh BB, Liu X, Ambudkar IS (2001) Stabilization of cortical actin induces internalization of transient receptor potential 3 (Trp3)-associated caveolar Ca2+ signaling complex and loss of Ca2+ influx without disruption of Trp3-inositol trisphosphate receptor association. *J Biol Chem* **276:** 42401-42408

Nadler MJ, Hermosura MC, Inabe K, Perraud AL, Zhu Q, Stokes AJ, Kurosaki T, Kinet JP, Penner R, Scharenberg AM, Fleig A (2001) LTRPC7 is a Mg.ATP-regulated divalent cation channel required for cell viability. *Nature* **411:** 590-595

Nakasawa T, Takahashi M, Matsuzawa F, Aikawa S, Togashi Y, Saitoh T, Yamagishi A, Yazawa M (2005) Critical regions for assembly of vertebrate nonmuscle myosin II. *Biochemistry* **44:** 174-183

Rico M, Egelhoff TT (2003) Myosin heavy chain kinase B participates in the regulation of myosin assembly into the cytoskeleton. *J Cell Biochem* **88:** 521-532

Roskoski R, Jr. (2004) Src protein-tyrosine kinase structure and regulation. *Biochem Biophys Res Commun* **324:** 1155-1164

Runnels LW, Yue L, Clapham DE (2001) TRP-PLIK, a bifunctional protein with kinase and ion channel activities. *Science* **291:** 1043-1047

Runnels LW, Yue L, Clapham DE (2002) The TRPM7 channel is inactivated by PIP(2) hydrolysis. *Nat Cell Biol* **4:** 329-336

Ryazanov AG (2002) Elongation factor-2 kinase and its newly discovered relatives. *FEBS Lett* **514:** 26-29

Ryazanova LV, Dorovkov MV, Ansari A, Ryazanov AG (2004) Characterization of the protein kinase activity of TRPM7/ChaK1, a protein kinase fused to TRP ion channel. *J Biol Chem* **279:** 3708-3716

Schild D, Jung A, Schultens HA (1994) Localization of calcium entry through calcium channels in olfactory receptor neurones using a laser scanning microscope and the calcium indicator dyes Fluo-3 and Fura-Red. *Cell Calcium* **15:** 341-348

Schmitz C, Perraud AL, Johnson CO, Inabe K, Smith MK, Penner R, Kurosaki T, Fleig A, Scharenberg AM (2003) Regulation of vertebrate cellular Mg2+ homeostasis by TRPM7. *Cell* **114:** 191-200

Sun HQ, Yamamoto M, Mejillano M, Yin HL (1999) Gelsolin, a multifunctional actin regulatory protein. *J Biol Chem* **274:** 33179-33182

Van Etten RA (2003) c-Abl regulation: a tail of two lipids. *Curr Biol* **13:** R608-610

van Leeuwen FN, Kain HE, Kammen RA, Michiels F, Kranenburg OW, Collard JG (1997) The guanine nucleotide exchange factor Tiam1 affects neuronal morphology; opposing roles for the small GTPases Rac and Rho. *J Cell Biol* **139:** 797-807

van Leeuwen FN, van Delft S, Kain HE, van der Kammen RA, Collard JG (1999) Rac regulates phosphorylation of the myosin-II heavy chain, actinomyosin disassembly and cell spreading. *Nat Cell Biol* **1:** 242-248

van Rheenen J, Jalink K (2002) Agonist-induced PIP(2) hydrolysis inhibits cortical actin dynamics: regulation at a global but not at a micrometer scale. *Mol Biol Cell* **13:** 3257-3267

Wilson JR, Ludowyke RI, Biden TJ (1998) Nutrient stimulation results in a rapid Ca2+-dependent threonine phosphorylation of myosin heavy chain in rat pancreatic islets and RINm5F cells. *J Biol Chem* **273:** 22729-22737
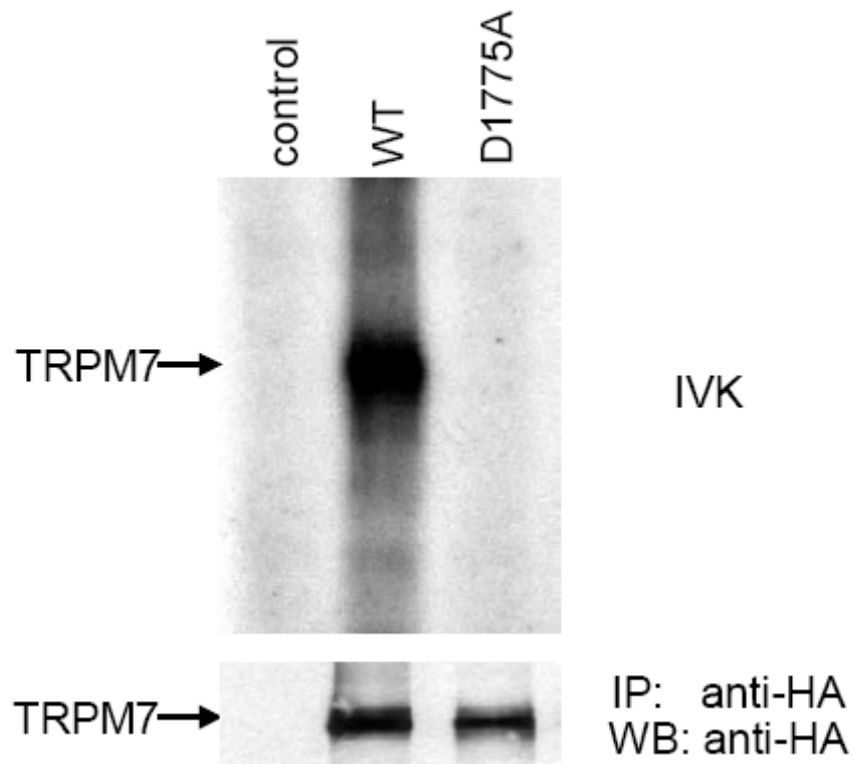
Supplemental Material

Figure S1 Characterization of TRPM7 kinase-dead mutant. Mutation of aspartate 1775 to alanine abrogates the ability of TRPM7 to undergo autophosphorylation. WT and kinase-dead TRPM7 constructs were transiently transfected into HEK293 cells and immuno-affinity purified complexes were subjected to *in vitro* kinase assays. Top, *In vitro* autophosphorylation of TRPM7 detected by 32P labeling and autoradiography. Bottom, expression levels of TRPM7 constructs in HEK293 cells detected using anti-HA antibodies.
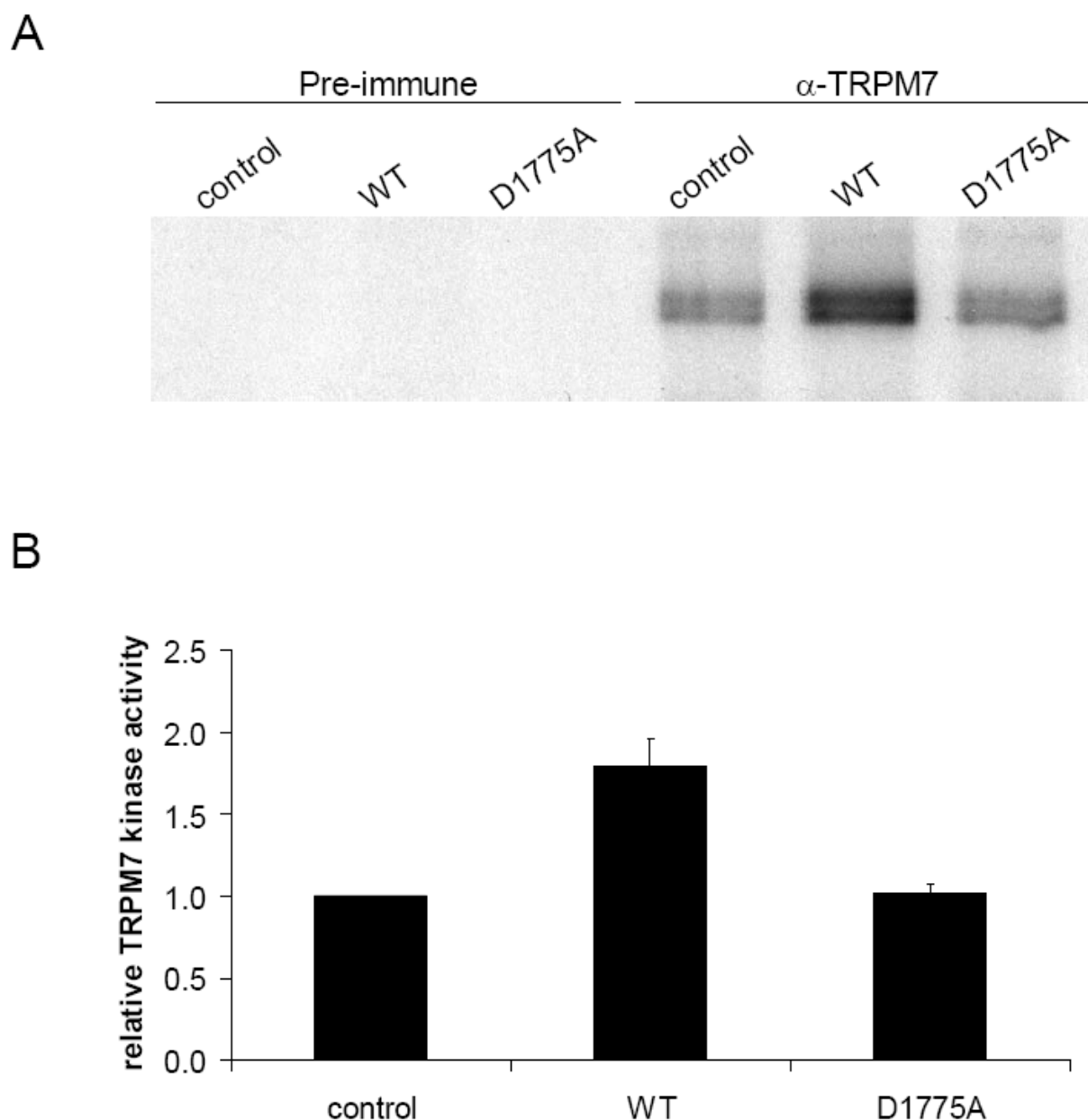
A

B

Figure S2 Quantification of TRPM7 kinase activity in the different N1E-115 cell lines. (**A**) Autoradiogram of TRPM7 autophosphorylation levels in the different N1E-115 cell lines. N1E- 115 cells transduced with either the empty vector, TRPM7-WT or TRPM7-D1775A were lysed in RIPA buffer. Protein concentration was determined using the BCA kit and equal amounts of protein (400 μg) were transferred to each tube. TRPM7 was immunoprecipitated using a rabbit polyclonal TRPM7 antibody or rabbit pre-immune serum as a negative control. To assess the level of kinase activity, TRPM7 was autophosphorylated in the presence of 5 μCi of γ-32P-ATP, separated on an 8% SDS-PAGE gel and detected by autoradiography. (**B**) Quantification of TRPM7 kinase activity. Autophosphorylation of TRPM7 was quantified using phospho-imager analysis. The level of kinase activity in control N1E-115 cells was set to 1 and the data from the other cell lines is expressed as the kinase activity in relation to control cells (n=6).
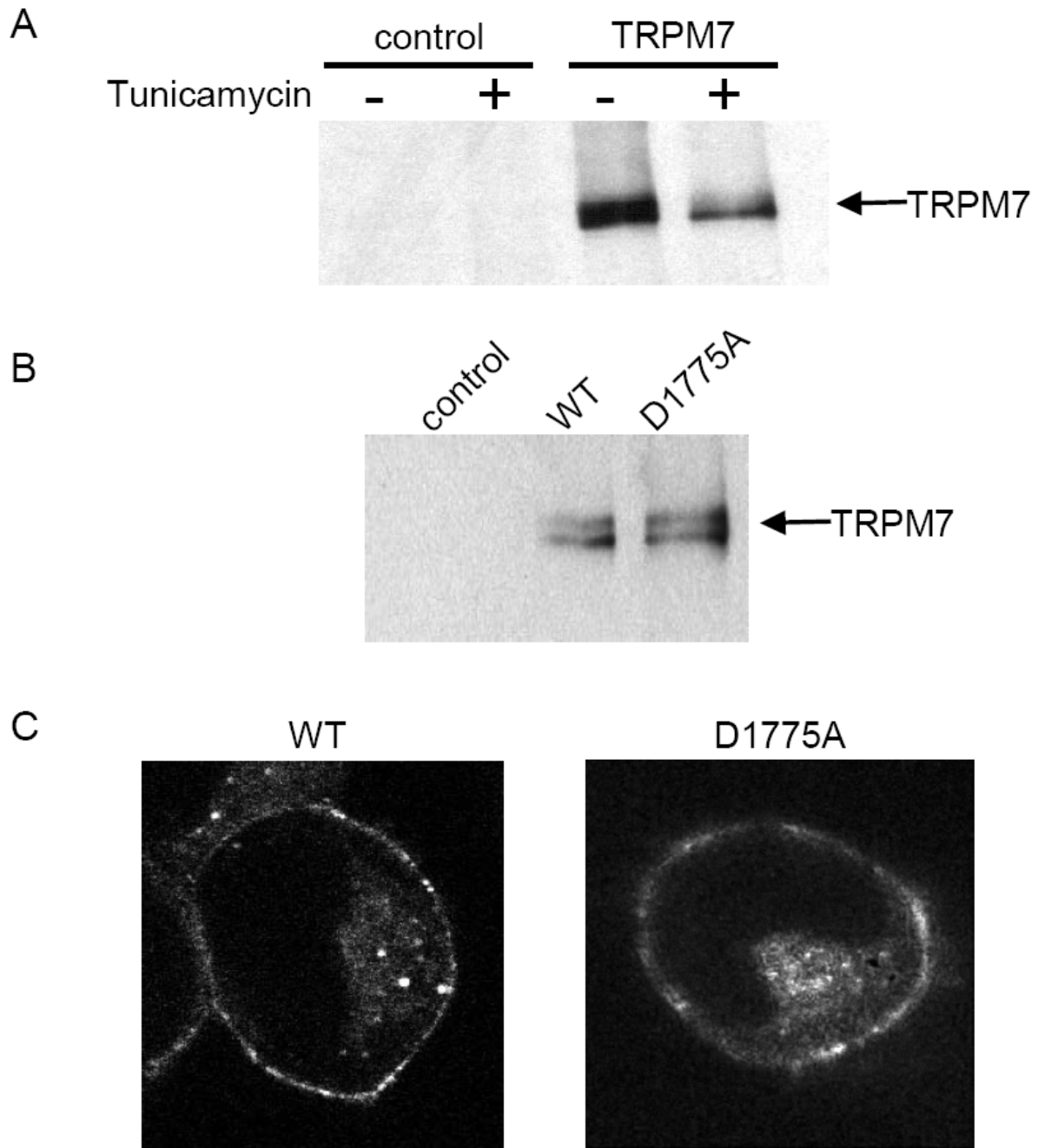
Figure S3 TRPM7 is glycosylated. (**A**) Cells were treated with vehicle control or 2 μg/ml tunicamycin for 24 h. TRPM7 was immunoprecipitated and detected by Western blotting using anti-HA antibodies. Note that while TRPM7 runs as a doublet at 216 kDa, only the fast migrating band is observed upon treatment with tunicamycin. (**B**) Glycosylation is independent of kinase activity. TRPM7-WT and TRPM7-D1775A were detected by immunoprecipitation followed by Western blotting using anti-HA antibodies. Note that both TRPM7-WT and TRPM7-D1775A migrate as doublets on SDS-PAGE gels indicative of glycosylation. (**C**) Expression of TRPM7-WT and TRPM7-D1775A at the cell surface. N1E-115 cells were transfected with YFP-TRPM7-WT or CFP-TRPM7-D1775A. Live cells were visualized by confocal microscopy 48 h post-transfection. Cell surface expression was also detected in N1E-115/TRPM7-WT and N1E-115/TRPM7-D1775A using anti-HA antibodies (Fig. 4 and data not shown).
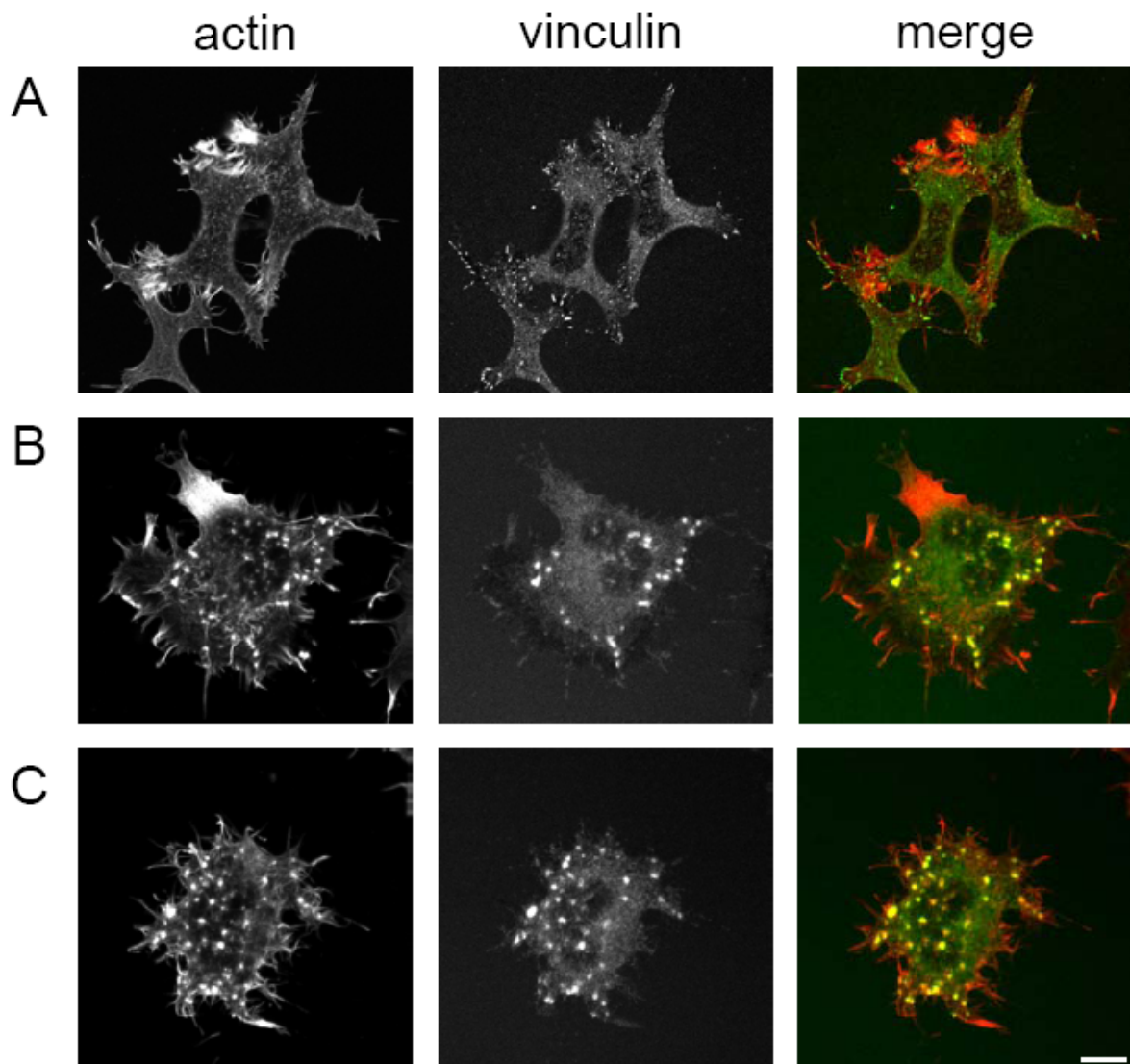
Figure S4 Inhibition of myosin II function in N1E-115 cells leads to cell spreading and podosome formation. N1E-115 cells were seeded on fibronectin-coated coverslips to increase their adherence. Cells were treated with 50 μM blebbistatin for 30 min, fixed and stained for vinculin (green) and F-actin (red). (A) Untreated N1E-115 cells. Note the appearance of focal adhesions. (B) and (C) Blebbistatin treated N1E-115 parental cells. Scale bar =10 μm.
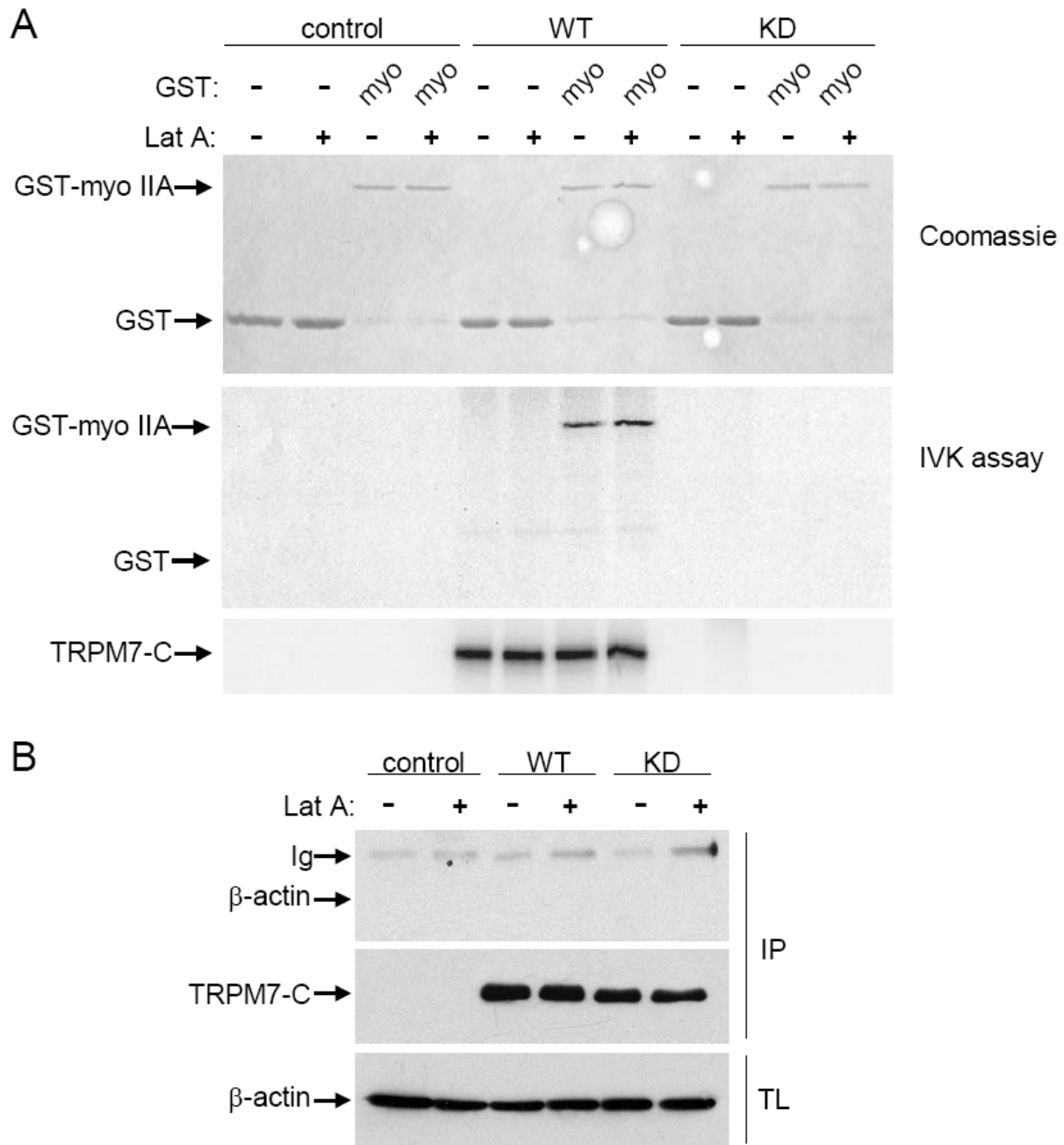
Figure S5 Disruption of the actin cytoskeleton prior to TRPM7 purification does not affect the phosphorylation of myosin IIA. (**A**) Effect of latrunculin A on the phosphorylation of myosin IIA by TRPM7. TRPM7-C WT and KD were immunopurified using anti-HA antibodies under high stringency conditions before and after latrunculin A treatment (1 µM; 30 min). The kinase was incubated with 2 µg of GST or GST-myosin IIA in kinase buffer. Phosphorylated proteins were detected by SDS-PAGE followed by autoradiography. Top, coomassie staining of GST-fusion proteins; Middle, autoradiogram showing that phosphorylation of GST-myosin IIA is unaffected by prior treament with latrunculin A; Bottom, autophosphorylation of TRPM7-C constructs. (**B**) Contaminating actin is below detection levels. An aliquot of the purified TRPM7-C WT and KD from experiment in section A was run on gel and probed for β-actin (Top) or HA-tagged proteins (Middle). The bottom panel shows β-actin in total lysates as a control for protein levels.
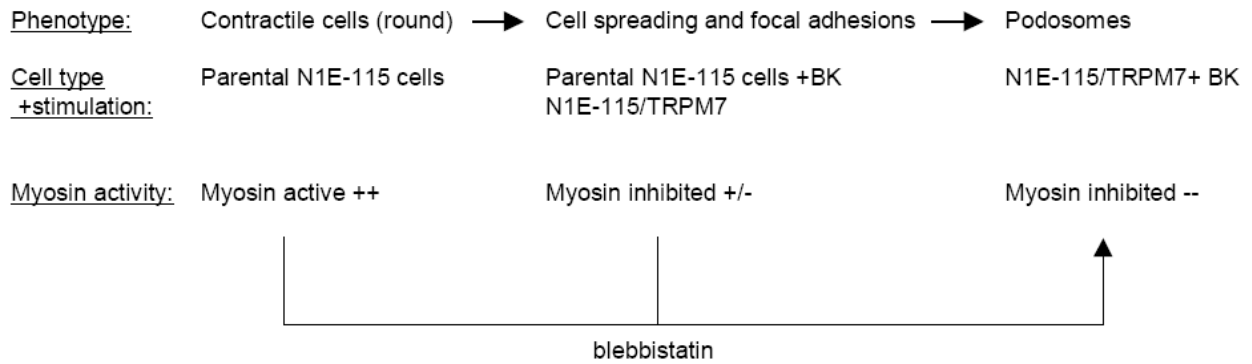
Phenotype:	Contractile cells (round) →	Cell spreading and focal adhesions →	Podosomes
Cell type +stimulation:	Parental N1E-115 cells	Parental N1E-115 cells +BK N1E-115/TRPM7	N1E-115/TRPM7+ BK
Myosin activity:	Myosin active ++	Myosin inhibited +/-	Myosin inhibited --

blebbistatin

Figure S6 Relationship between TRPM7 expression, myosin activity and cellular phenotype. Parental N1E-115 cells have high myosin II activity which is translated into a contractile phenotype where cells are round and poorly adherent. Stimulation of these cells with BK leads to a loss of contractility as observed by the spreading of cells. However, myosin II is not fully inhibited as focal adhesions form at the periphery of the cell. Overexpression of TRPM7 mimics the effect of BK on N1E-115 cells as it has basal activity. Stimulation of N1E-115/TRPM7 cells leads to a further inhibition of myosin II activity leading to the formation of podosomes. Directly inhibiting all myosin II activity leads to the formation of podosomes regardless of whether TRPM7 is present or not. Thus, the level of TRPM7 expression and activation dictates the extent of myosin II activity and thereby the phenotype of N1E-115 cells.

Calcium Signaling Regulates Translocation and Activation of Rac

Leo S. Price, Michiel Langeslag, Jean Paul ten Klooster, Peter L. Hordijk, Kees Jalink, and John G. Collard

Calcium Signaling Regulates Translocation and Activation of Rac

Leo S. Price‡§, Michiel Langeslag‡, Jean Paul ten Klooster¶, Peter L. Hordijk¶, Kees Jalink‡, and John G. Collard‡

From the ‡Division of Cell Biology, The Netherlands Cancer Institute, Plesmanlaan 121, Amsterdam 1066 CX, The Netherlands and ¶Department of Experimental Immunohematology, Sanquin Research at CLB, Plesmanlaan 125, Amsterdam 1066 CX, The Netherlands

Rac is activated in response to various stimuli including growth factors and by adhesion to the extracellular matrix. However, how these stimuli ultimately result in Rac activation is poorly understood. The increase in intracellular calcium $[Ca^{2+}]_i$ represents a ubiquitous second messenger system in cells, linking receptor activation to downstream signaling pathways. Here we show that elevation of $[Ca^{2+}]_i$, either artificially or by thrombin receptor activation, potently induces Rac activation. Lamellipodia formation induced by artificial elevation of $[Ca^{2+}]_i$ is blocked by inhibition of Rac signaling, indicating that calcium-induced cytoskeletal changes are controlled by the activation of Rac. Calcium-dependent Rac activation was dependent on the activation of a conventional protein kinase C. Furthermore, both increased $[Ca^{2+}]_i$ and protein kinase C activation induce phosphorylation of RhoGDIα and induce the translocation of cytosolic Rac to the plasma membrane. Intracellular calcium signaling may thus contribute to the intracellular localization and activation of Rac to regulate the cytoskeletal changes in response to receptor stimulation.

Introduction

The Rho family of small GTPases, including Rho, Rac, and Cdc42 isoforms, regulates different aspects of cytoskeletal organization, which are coordinated in the process of cell migration (1). Of these, Rac is involved in the protrusion of lamellipodia, which occur principally at the leading edge of migrating cells but also emerge from around newly adherent cells to mediate cell spreading (2, 3). Rac also regulates gene transcription, cell cycle progression, and transformation *in vitro* (4–6) and is implicated in tumor initiation and progression *in vivo* (7). Rac is activated in response to various stimuli, including growth factors and adhesion to the extracellular matrix. However, how these stimuli ultimately result in Rac activation is poorly understood. The principal regulators of Rac activation are the guanine nucleotide exchange factors (GEFs)1 and GTPase activating proteins. GEFs induce activation by exchanging GDP for GTP, whereas GTPase activating proteins enhance the intrinsic rate of hydrolysis of bound GTP to GDP, resulting in inactivation. In cells, Rac exists predominantly in its inactive GDP-bound form in a complex with RhoGDI (8). RhoGDI binds and masks the hydrophobic C-terminal region of Rac, the same region that is responsible for targeting Rac to the plasma membrane (9). Thus RhoGDI maintains Rac in the cytoplasm and must dissociate to allow Rac to translocate to the membrane and interact with membrane-associated activators (10–12). It was shown recently (13, 14) that integrin signals disrupt the Rac-RhoGDI interaction, enabling Rac to target to regions of cell-matrix interaction and activate an adhesion-dependent signaling pathway. Thus appropriate localization, as well as activation, is necessary for Rac to carry out its functions. Increased intracellular calcium $[Ca^{2+}]_i$ represents a ubiquitous second messenger system in cells, linking receptor activation to downstream signaling pathways. Previous studies (15–18) have described relationships between intracellular calcium and the activation and function of Rho family GTPases in processes including muscle contraction and the exocytic response. Intracellular calcium is also required for thrombin- and collagen-induced Rac activation in platelets (19). In neutrophils, however, chemoattractant-induced Rac activation is independent of intracellular calcium (20), suggesting that the relationship between calcium and Rac signaling is dependent on the cell type and/or the growth factor receptor involved. Ras-GRF 1 and 2, exchange factors

specific for both Ras and Rac (21, 22), harbor a calcium-calmodulin binding site (23) whereas the Rac exchange factor, Tiam1, is phosphorylated by calcium-calmodulin-dependent protein kinase II, which leads to increased nucleotide exchange on Rac (24). These findings suggest that nucleotide exchange on Rac may be regulated by changes in intracellular calcium. Various studies have implicated protein kinase C (PKC) in the activation of Rac. In Swiss 3T3 cells, phorbol ester treatment induces membrane ruffling, which is indicative of Rac activation (2), whereas PKC is required for PDGF-induce Rac activation in NIH 3T3 cells (25). However, how PKC affects Rac activity is unclear. Here we have examined the effect of intracellular calcium transients on Rac signaling. We find that intracellular calcium transients induce the membrane translocation and activation of Rac. We propose an additional mechanism of regulation of Rac by calcium whereby calcium induces a PKC-dependent disruption of the Rac-Rho GDI complex. This promotes the translocation of Rac to the plasma membrane where it can be activated by membrane-associated or membrane-translocated guanine nucleotide exchange factors.

Experimental Procedures

Materials

To generate the biotinylated CRIB peptide the amino acid sequence n-KERPEISLPSDFEH-TIHVGFDAVTGEFTGMPEQWARLLQTSNIT-c was used and biotinylated during synthesis at the N-terminus. The TAT-CRIB peptide contained the additional N-terminal sequence GCGYGRKK-RRQRRR and was not biotinylated. Thrombin related peptide (TRP) was synthesized as described previously (26). Fura red, Oregon green, BAPTA-AM, and Alexa 568-phalloidin were from Molecular Probes. Thapsigargin, ionomycin, GF109203X (Gö 6850), U73122, calmidazolium chloride, and KN-93 were from Calbiochem. Streptavidin-agarose and PMA were from Sigma, and cytochalasin B was from Roche Applied Science.

Cells and Generation of Stable Cell Lines by Retroviral Transduction

PC3 human prostate carcinoma cells (27) were cultured in DMEM supplemented with 10% fetal calf serum in a humidified incubator at 37 °C and with 5% CO2. NIH 3T3-Tiam1 cells (28) were cultured in DMEM + 10% bovine calf serum. Cells were seeded in tissue culture dishes 24 h before use to obtain a final density of ~70% confluence. For microscopy, cells were seeded at lower density on glass coverslips and grown for 24 h. PC3 cells expressing EGFP-Rac1 were generated by infection with a retrovirus containing EGFP-Rac1 (29, 30). Western blotting showed that EGFP-Rac1 was expressed at approximately the same level as endogenous Rac (not shown). EGFP-Rac1 was also functionally active as determined by Rac activation assays using thapsigargin as a stimulus (not shown).

GTPase Activity Assays

Rac activity was assayed essentially as described previously (28), with the exception that instead of GST-Pak-CRIB a biotinylated peptide corresponding to the CRIB domain of Pak (see above) was used to precipitate active Rac. Briefly, after treatment of cells with the relevant inhibitors and stimuli, cells were washed and then lysed with a 1% Nonidet P-40 buffer containing 2 μg/ml CRIB peptide. Cell lysates were cleared by centrifugation, and active Rac-CRIB complexes were precipitated with streptavidin-agarose and solubilized in SDS sample buffer. Rac was detected following Western blotting with anti-Rac antibodies (clone 23A8; Upstate Biotechnology, Inc.).

Live Cell Imaging of Calcium, PLC Activation, and GFP-tagged Rac

Changes in cytosolic Ca^{2+} in PC3 cells were monitored ratiometrically by simultaneous confocal imaging of the Ca^{2+} indicators Oregon green 488, BAPTA-1AM, and Fura red-AM (31). Cells were loaded for 30 min by incubation in DMEM with 10 μM of the AM-esters of these dyes in the presence of pluronic and incubated in fresh DMEM for 15 min prior to the experiment. Excitation was at 488 nm, and the emission was detected using a 522 ± 17-nm bandpass filter (green) and a 585-nm longpass filter (red). Measurements were performed at 37 °C in a buffer containing, in mM, 140 NaCl, 23 NaHCO₃, 5 KCl, 2 MgCl₂, 1CaCl₂, 10 HEPES, and 10 glucose under 5% CO_2. All measurements were calibrated using ionomycin. For simultaneous detection of phospholipase C activation and $[Ca^{2+}]_i$, PC3 cells

were transfected overnight with pcDNA3-EGFP-PH (32) and subsequently loaded with Fura red-AM and imaged as described above. PLC activation was visualized as translocation of the GFP-tagged, phosphatidylinositol 4,5-biphosphate-binding PH domain from the membrane to the cytosol and quantitated by taking the ratio of membrane to cytosolic fluorescence as described (32). To determine the membrane association of GFP-tagged Rac1, medial sections ~2 μm above the plane of the coverslip were imaged by confocal microscopy. These were captured at 10-s intervals and stored on disk for offline analysis. The mean fluorescence intensity at the membrane and at the cytosol was determined, and the ratio of those was plotted *versus* time, essentially as described (32).

Immunofluorescence Microscopy

PC3 cells or NIH 3T3 cells expressing Tiam1 were seeded on glass coverslips 24 h before use. Following treatment/stimulation, cells were fixed with 3.7% formaldehyde for 10 min and then permeabilized with 0.2% Triton X-100 for 5 min. Filamentous actin was labeled with 0.2 μM Alexa 568-phalloidin (Molecular Probes) for 30 min. Tiam1 was visualized with a polyclonal antibody (33). Where cells were treated with TAT-CRIB peptide, peptide (0.2 mg/ml) was added for 15 min prior to stimulation.

Calcium-dependent Phosphorylation by PKC

To visualize calcium-dependent phosphorylation of cellular proteins, PC3 cells were lysed in buffer containing 0.5% Nonidet P-40, and lysates cleared by centrifugation and resolved by SDS-PAGE. Cellular proteins were resolved by SDS-PAGE transferred to nitrocellulose and probed with Phospho(ser)-PKC substrate antibody (Cell Signaling Technology). GDI phosphorylation was detected as described previously (34). Briefly, PC3 cells were starved of phosphate for 2 h and then metabolically labeled with 0.5 mCi/ml [32P]orthophosphate for 2 h. Cells were treated with or without GF109203X and stimulated with thapsigargin (1 μM) or PMA (100 nM). Cells were washed in cold phosphate-buffered saline and lysed (0.5% Nonidet P-40, 20 mM Tris, pH 7.6, 250 mM NaCl, 5 mM EDTA, 3 mM EGTA, 20 mM $NaPO_4$, 3 mM β-glycerophosphate, 1 mM $NaVO_4$, 100 nM calyculin A, 10 mM NaF, and a protease inhibitor mixture). RhoGDI was precipitated with polyclonal anti-RhoGDIα (Santa Cruz Biotechnology, Inc.) and protein G-Sepharose. Precipitated RhoGDI and RhoGDI from total cell lysates was resolved by SDS-PAGE and Western blots probed with a monoclonal anti-RhoGDIα antibody (Transduction Laboratories).

Cell Fractionation

After treatment/stimulation, PC3 cells in 2-cm dishes were washed once with ice-cold phosphate-buffered saline and then washed again with permeabilization buffer (20 mM Na-PIPES, 137 mM NaCl, 2mM $MgCl_2$, 2.7mM KCl, 0.05% bovine serum albumin). Cells were then permeabilized with 25 μM digitonin in permeabilization buffer for 20 min to allow leakage of cytosolic proteins. Maximal leakage of Rac and complete leakage of the cytosolic markers mitogen-activated protein kinase and RhoGDIα was found to take place within 10 min. No E-cadherin, chosen as a representative transmembrane protein, was extracted by digitonin treatment (not shown). The cytosol-depleted cells were then washed twice with digitonin-containing buffer and lysed with radioimmune precipitation assay buffer. Lysates were cleared by centrifugation at 4 °C for 5 min at $15,000 \times g$, and 5× SDS sample buffer was added to the supernatants. Proteins were resolved on 4–20% gradient gels (Novex), and following Western blotting, membranes were cut and probed with antibodies against Rac, anti-PKCα (Transduction Laboratories), and anti-pan-cadherin (Sigma) for normalization of (membrane) protein loading.

Results

Intracellular Calcium and Receptor-mediated Rac Activation

To study the relationship between intracellular calcium signaling and Rac function, we stimulated PC3 cells with the thrombin receptor agonist TRP and measured the effects on intracellular calcium concentration ($[Ca^{2+}]_i$) and on activation of Rac. Stimulation of the thrombin receptor with TRP results in release of calcium from inositol 1,4,5-trisphosphate-sensitive intracellular stores. As expected, stimulation of PC3 cells with TRP induced a rapid and transient increase in intracellular calcium $[Ca^{2+}]_i$ (Fig. 1*A*). To assay Rac activity, we used a modified Rac
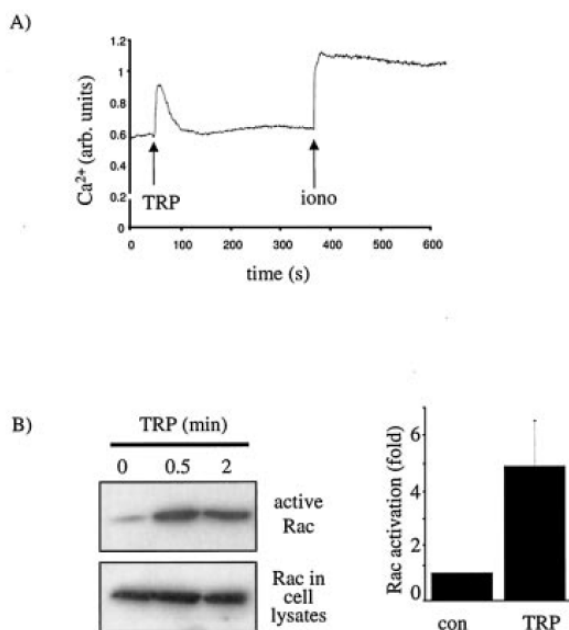
FIG. 1. **Thrombin-related peptide induces Rac activation and increased intracellular calcium.** *A*, TRP (12.5 μM) induces an increase in intracellular calcium in PC3 cells. Intracellular calcium levels were detected by ratiometric imaging of Oregon green and Fura red calcium indicators. The trace represents an average of six individual cells captured from one image field. A representative trace from a single cell is shown and is representative of at least 10 quantifications and three independent experiments. *iono*, ionomycin. *B*, Rac activation in PC3 cells following stimulation with 12.5 mM TRP. Active Rac was precipitated with biotin-CRIB peptide and detected following Western blotting with anti-Rac antibodies (as described under "Experimental Procedures"). Rac (both active and inactive) present in whole cell lysates are shown in the *lower panel* to demonstrate equal amounts of protein in samples. -Fold induction of Rac activation after 1 min of TRP stimulation is shown ($n = 6 \pm$ S.D.; $p = 0.002$). *con*, control.

pull-down assay, which utilizes a synthetic biotinylated peptide corresponding to a region of the Rac-interacting (CRIB) domain of the Rac effector, Pak (see "Experimental Procedures"). This region specifically binds to Rac when it is in its active conformation. The biotinylated CRIB peptide works equally efficiently as the GST-Pak fusion protein used in earlier studies (35, 36) but is more stable and less susceptible to batch-to-batch variation. Stimulating the thrombin receptor with TRP induced a rapid activation of Rac in PC3 cells (Fig. 1*B*). Rac activation was transient, returning to baseline levels after ~10 min (not shown). Treatment with TRP also induced extensive lamellipodia formation and membrane ruffling

(Fig. 2*A*, *upper panels*), which is consistent with an increase in Rac-GTP levels.

To examine whether a causal relationship exists between increased $[Ca^{2+}]_i$ and activation of Rac and lamellipodia formation by TRP, we first examined the effects of calcium chelation on TRP-induced morphological changes. Pre-treatment of PC3 cells with the membrane-permeable calcium chelator, BAPTA-AM, strongly inhibited TRP-induced extension of lamellipodia (Fig. 2*A*), suggesting that lamellipodia formation was calcium-dependent. BAPTA-AM also inhibited TRP-induced Rac activation (Fig. 2*B*), suggesting that increased $[Ca^{2+}]_i$ was required for Rac activation. To ensure that the effects of BAPTA-AM were not because of disrupted receptor signaling, we examined the effect of BAPTA-AM on TRP-induced PLC activation. For this, PC3 cells were transfected with a GFP chimera of the PH domain of PLCδ1, which translocates from plasma membrane to cytosol upon activation with TRP (37). Confocal imaging of living cells showed that TRP induced the translocation of GFP-PH from membrane to cytosol, confirming previous findings that thrombin receptor activation leads to the activation of PLC. TRP induced GFP-PH translocation equally well in the presence or absence of BAPTA-AM (Fig. 2*C*, *lower traces*). However, concomitant measurement of $[Ca^{2+}]_i$ confirmed that BAPTA-AM treatment effectively blocked TRP-induced calcium transients (*upper traces*). This demonstrates that thrombin receptor-Gq-PLC signaling, which ultimately leads to release of intracellular calcium, is not disrupted by BAPTA-AM treatment. From these data we conclude that intracellular calcium is required for thrombin receptor-mediated Rac activation and lamellipodia formation.

Increased $[Ca^{2+}]_i$ Is Sufficient to Activate Rac

To examine further the dependence of Rac activation on calcium signaling, we used pharmacological modulators of $[Ca^{2+}]_i$. Treatment of PC3 cells with thapsigargin, which liberates calcium from intracellular stores by blocking re-uptake from the cytosol by Ca^{2+}-ATPases, led to a transient elevation of $[Ca^{2+}]_i$ that remained somewhat above baseline levels (Fig. 3*A*). Analysis of the time course of Rac activation showed that thapsigargin treatment induced a strong activation of Rac that was maximal at ~5 min (Fig. 3*B*). Similarly, treatment of cells with
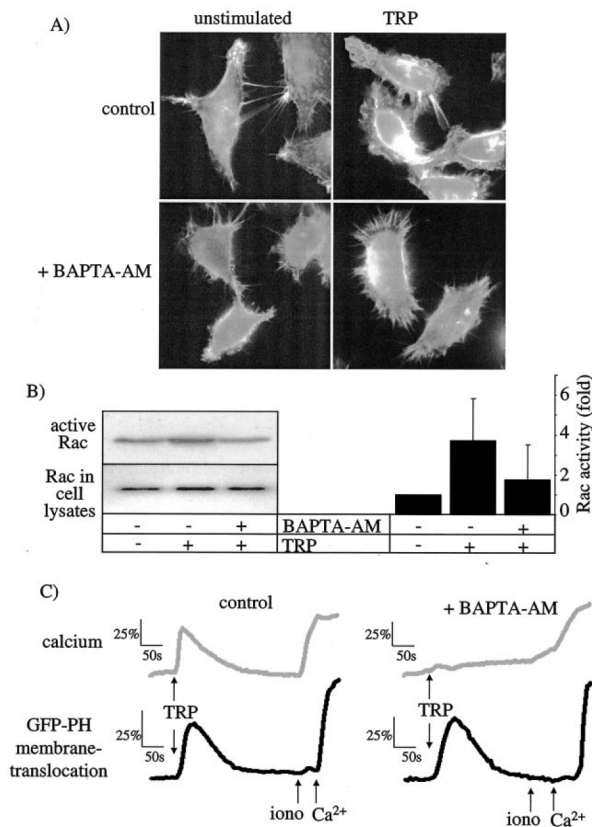
FIG. 2. **Intracellular calcium is required for thrombin receptor dependent Rac activation.** *A*, chelation of calcium with BAPTA-AM inhibits TRP-induced lamellipodia formation. BAPTA-AM (15 μM) was added to PC3 cells on glass coverslips for 10 min before stimulation with TRP for 5 min. Cells were then fixed, and F-actin was stained with rhodamine-phalloidin as described under "Experimental Procedures." *B*, calcium chelation inhibits thrombin peptide-induced Rac activity. To chelate intracellular calcium, cells were treated with 15 μM BAPTA-AM for 10 min. Cells were then stimulated with 12.5 μM TRP for 5 min, and Rac activity was analyzed by pull-down assays. Average -fold induction of Rac activation +S.D. is also shown (*n* = 4, BAPTA-AM significantly inhibited TRP-induced Rac activation; *p* = 0.04). *C*, calcium chelation does not disrupt receptor-phospholipase C signaling. Cells transiently expressing a GFP chimera of the PH domain of phospholipase Cδ were pre-treated with and without BAPTA-AM as above and stimulated with 12.5 μM TRP. Calcium traces (*upper graphs*) show the intracellular calcium concentration as reflected by changes in Fura-red intensity. GFP-PH relocalization from membrane to cytosol (*lower graphs*) reflects activation of PLC and was imaged simultaneously with calcium in the same cell. BAPTA-AM abolishes the TRP-induced calcium transient (*upper right trace*) but not translocation of GFP-PH (*lower right trace*). At the end of the experiment, ionomycin (*iono*) and excess extracellular calcium were added to the medium to give maximal (100%) responses. The *scale bar* indicates percent change of basal fluorescence.

$[Ca^{2+}]_i$ because of influx of extracellular calcium, also induced rapid activation of Rac (Fig. 3, *C* and *D*). Interestingly, we observed consistently that the kinetics of calcium elevation appeared to correlate with that of Rac activation; thus, the prolonged elevation of $[Ca^{2+}]_i$ induced by thapsigargin and ionomycin correlated with prolonged elevation of Rac activity, whereas TRP stimulation produced more transient increases in $[Ca^{2+}]_i$ and Rac activation. Activation of Rac was not because of calcium-induced changes in spreading or other actin-dependent changes, because thapsigargin-induced Rac activity was not inhibited by cytochalasin treatment (not shown). From these results we conclude that elevation of intracellular calcium is sufficient to activate Rac in the absence of receptor stimulation.

Our results also suggest that intracellular calcium mediates TRP-induced activation of Rac via the classical Gq-PLC-inositol 1,4,5-trisphosphate pathway. To test this hypothesis, we examined the effects of PLC inhibition, which is predicted to inhibit receptor-induced intracellular calcium increase but not calcium transients induced directly by thapsigargin. Pre-treatment of cells with the PLC inhibitor U73122 (38, 39) inhibited TRP-induced Rac activation but not thapsigargin-induced Rac activation (Fig. 3*E*). Although we can not exclude the possibility that U73122 inhibited TRP-induced Rac activation non-specifically, our results are consistent with the hypothesis that TRP-induced Rac activation is mediated by PLC-$[Ca^{2+}]_i$ signaling and that direct elevation of $[Ca^{2+}]_i$ can bypass the requirement for receptor-PLC signaling.

We also examined the effects of increased $[Ca^{2+}]_i$ on Rac activation in other cell types. In addition to PC3 cells, thapsigargin also induced Rac activation in T47D mammary carcinoma cells and Madin-Darby canine kidney cells but not in NIH 3T3 fibroblasts or lymphocytes (data not shown). This suggests that Ca^{2+}-dependent Rac activation is cell type-specific and may be restricted to cells of epithelial origin.

Calcium-induced Cytoskeletal Changes Are Mediated by Rac

Plasmid-based expression of the CRIB domain of Pak has been used previously (3, 40) to inhibit the signaling of Rac to endogenous CRIB-containing targets. To examine the role of Rac in cell responses, we inhibited Rac signaling using a peptide corresponding to the CRIB domain of Pak
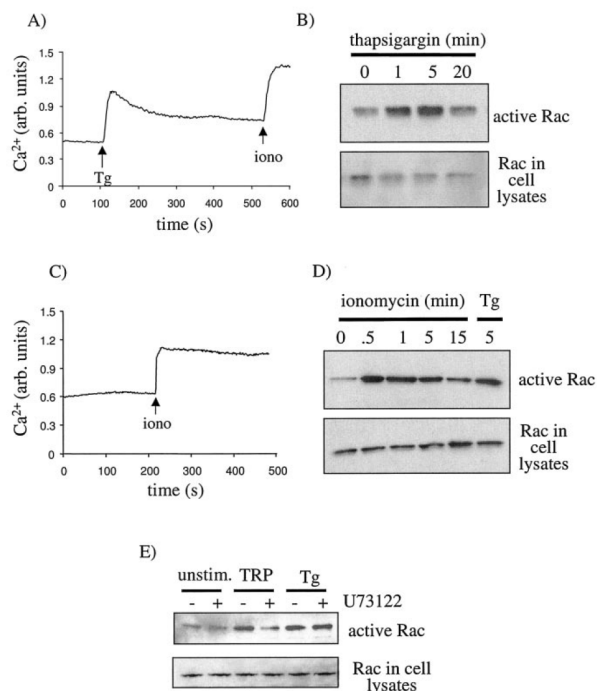
FIG. 3. **Increased intracellular calcium induces Rac activation.** The effect of thapsigargin treatment (100 nM) on intracellular calcium levels (*A*) and Rac activity (*B*) in PC3 cells measured as described for Fig. 1 is shown. The effect of ionomycin (*iono*) treatment (1 μM) on intracellular calcium levels (*C*) and Rac activity (*D*) in PC3 cells is shown. *D* also shows Rac activity in response to thapsigargin for comparison. *E*, effect of the PLC inhibitor U73122 (2.5 μM for 1 h) on Rac activation induced by activation of the thrombin receptor with TRP or by direct elevation of calcium with thapsigargin (*Tg*). PLC inhibition blocks TRP-induced Rac activation but not Rac activation induced by direct elevation of $[Ca^{2+}]_i$ by thapsigargin.

combined with a TAT sequence to confer membrane permeability (see Ref. 41 and "Experimental Procedures"). We first tested the ability of the TAT-CRIB peptide to inhibit Rac signaling using NIH 3T3 cells overexpressing the Rac exchange factor Tiam1, which shows high levels of activated Rac and as a consequence extensive membrane ruffling (28). Addition of TAT-CRIB peptide to the medium for 30 min dramatically attenuated Tiam1-mediated membrane ruffling in these cells, indicating that the peptide inhibits Rac downstream signaling (Fig. 4*A*). Control TAT peptides did not inhibit membrane ruffling (not shown). Treatment of cells with TAT-CRIB peptide for 30 min prior to thapsigargin stimulation also completely inhibited the subsequent detection of active Rac in cells (Fig. 4*B*), most likely because the TAT-CRIB blocked the binding of the biotinylated CRIB

peptide used in the pull-down assay. The TAT-CRIB peptide can therefore be used as a tool to inhibit Rac function in living cells and avoids potential long-term effects of CRIB expression.

We then used the TAT-CRIB peptide to examine the role of Rac in calcium-induced effects in PC3 cells. Thapsigargin and TRP induced extensive membrane ruffling and lamellipodia formation at the cell cortex, which is indicative of Rac activation. This was strongly inhibited by pre-treatment with TATCRIB. From these results we conclude that the induction of lamellipodia by intracellular calcium is Rac-dependent.

PKC Mediates Calcium-dependent Rac Activation and Phosphorylation of RhoGDI

In considering the mechanism by which intracellular calcium transients could mediate Rac activation, we first examined the possible role of GEFs. The GEFs GRF and Tiam1 both promote nucleotide exchange on Rac and are potential targets for regulation by calmodulin and calmodulin-dependent protein kinase II. However, thapsigargin-induced Rac activity in PC3 cells was not blocked by calmidazolium chloride or KN-93, inhibitors of calmodulin and calmodulin-dependent protein kinase II, respectively (data not shown). Furthermore, thapsigargin failed to induce Rac activation in BW5146 T-lymphoma cells, despite the very high level of Tiam1 in these cells but did induce Rac activation in Madin-Darby canine kidney-f3 cells, which have undetectable levels of Tiam1 (not shown). Apparently, these particular exchange factors are most likely not directly involved in calcium-induced Rac activation, and we therefore investigated other potential mechanisms.

Various PKC isoforms have been implicated in the activation of Rho family GTPases. A subclass of these, the conventional PKCs, are also regulated by calcium (42). To determine whether PKC mediates calcium-induced Rac activation, we first inhibited PKC, both by long-term treatment of cells with the phorbol ester PMA, which down-regulates novel and conventional PKC proteins, and with the PKC inhibitor GF109203X, used at concentrations that preferentially inhibit conventional and novel PKCs (43). Both treatments potently inhibited thapsigargin-induced Rac activation (Fig. 5*A*). On the other hand, activation of PKC by short-term PMA treatment transiently activated Rac (Fig. 5*B*). To investigate

whether intracellular calcium transients are sufficient to induce PKC activation in PC3 cells, we used an antibody that recognizes phosphorylated substrates of PKC. Western blot analysis of cell lysates revealed multiple PKC-phosphorylated proteins in response to thapsigargin treatment, which were reduced by GF109203X treatment (Fig. 5*C*). TRP stimulation induced a similar profile of phosphorylation that was also blocked by the PKC inhibitor. These results suggest that intracellular calcium activates a calcium-dependent PKC in PC3 cells, which leads to activation of Rac. Although we cannot exclude the possibility that activation of PKC by calcium is indirect, our data suggest that a conventional PKC mediates calcium-induced Rac activation.

RhoGDIα possesses several potential PKC phosphorylation sites and has been shown to be a substrate for PKCα *in vitro*. Furthermore, it was shown that that phosphorylation of RhoGDI induces translocation of RhoA to the plasma membrane (34). We therefore examined whether calcium induced the phosphorylation of RhoGDI and if so, whether this was PKC-dependent. To do this, [32P] metabolically labeled PC3 cells were stimulated with thapsigargin or PMA in the presence and absence of PKC inhibitor, and RhoGDI phosphorylation was analyzed. We found that both PMA and thapsigargin treatments induced the phosphorylation of RhoGDI and that this phosphorylation was inhibited by GF109203X (Fig. 5*D*). These results demonstrate that elevation of intracellular calcium induces the PKC-dependent phosphorylation of RhoGDI.

Membrane Translocation of Rac

To examine whether calcium and PKC regulate membrane translocation of Rac, we examined the localization of Rac in single living cells. For this we used real-time confocal imaging of PC3 cells stably expressing low levels of wild type eGFP-Rac1. Prior to stimulation, GFP-Rac was predominantly cytoplasmic, with some regions of enrichment at membrane protrusions. Following stimulation with thapsigargin, fluorescence images of medial sections and corresponding line scan analysis showed that GFP-Rac levels increased in most parts of the plasma membrane (Fig. 6*A*). Enrichment of GFP-Rac occurred in particular at regions of the membrane that were often sites of subsequent membrane protrusion. Quantitative analysis of membrane and cytosolic fluorescence over time showed that GFP-Rac translocation
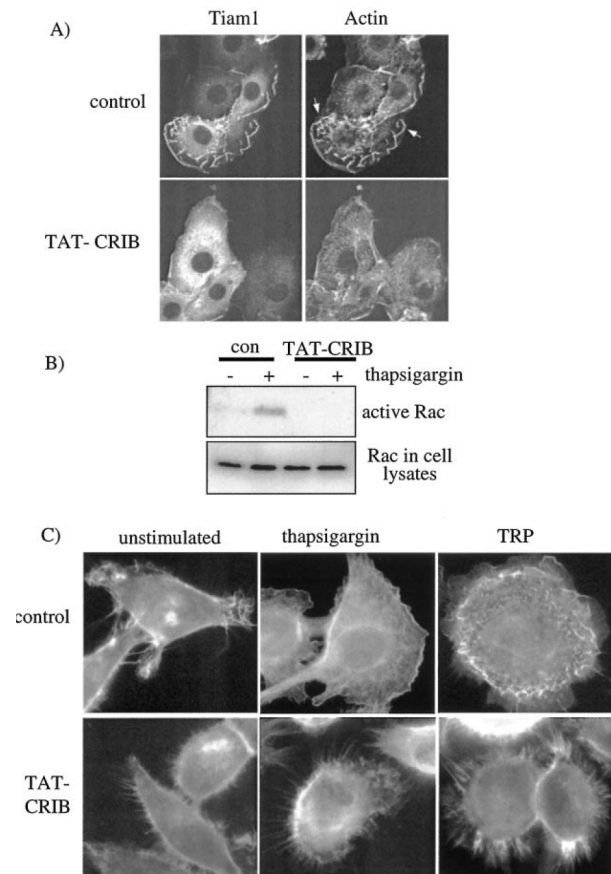

FIG. 4. **Calcium-induced lamellipodia formation is Rac-dependent.** *A*, treatment of NIH 3T3 cells stably overexpressing Tiam1 with or without 0.2 mg/ml TAT-CRIB peptide for 30 min. Cells were stained for Tiam1 expression and F-actin distribution. Note, control cells expressing Tiam1 show extensive actin-rich membrane ruffles (*arrows*), which are absent in TAT-CRIB-treated cells. *B*, treatment of PC3 cells with TAT-CRIB peptide (0.2 mg/ml) inhibits thapsigargin-induced detection of active Rac. *C*, fluorescence micrograph of actin staining of PC3 cells pre-treated with or without TAT-CRIB peptide and stimulated with thapsigargin or TRP. Unlike control cells, TAT-CRIBtreated cells do not extend broad lamellipodia upon stimulation.

peaked at ~2 min and gradually returned to a baseline distribution over 10–30 min (Fig. 6*B*). In addition to an increase of GFP-Rac in the plasma membrane, following stimulation we observed a consistent decrease in cytosolic fluorescence of 10 ± 3% (+S.E.). Although increased labeling in membrane ruffles can sometimes be attributed to increased amounts of membrane (44), simultaneous imaging of GFP-Rac with the membrane dye DiI showed that there is very little increase in membrane in these medial sections (data not shown). Furthermore, a decrease in cytosolic fluorescence support the finding that

translocation to the membrane occurs. Our findings therefore indicate that calcium transients induce a temporary increase in translocation of Rac to the plasma membrane, which precedes the formation of Rac-dependent membrane protrusions. A translocation of 10% of total Rac from cytoplasm to plasma membrane is highly significant in view of the fact that at most 5–10% of total Rac is activated in response to extracellular stimulation as determined by pull-down assays[2].

To further support the live-cell imaging results, we quantified the cytosolic and membrane-bound Rac using a rapid cell fractionation procedure based on cell permeabilization (see "Experimental Procedures"). We found that thapsigargin treatment increased the amount of Rac in the membrane-containing fraction (Fig. 6*C*, compare *lanes 1* and *3*). Densitometry analysis of films from several experiments showed that this represented a mean increase of 2.4-fold ± 0.8 ($n = 4$, $p = 0.05$). To examine the requirement for PKC in calcium-induced translocation of Rac, we inhibited PKC by long-term PMA treatment prior to thapsigargin stimulation. This resulted in inhibition of thapsigargin-induced translocation and also of that induced by TRP (Fig. 6*C*, compare *lanes 3–6*). Moreover, activation of PKC by brief PMA treatment enhanced membrane translocation of Rac (Fig. 6*C*, *lanes 7* and *8*). These results confirm that calcium induces the translocation of Rac to the plasma membrane and further support our conclusion that PKC mediates the membrane translocation and activation of Rac by phosphorylation of RhoGDI.

DISCUSSION

We report here that intracellular calcium transients regulate the activation of Rac. Rac activation could be induced artificially either by releasing calcium from intracellular stores or by inducing the influx of extracellular calcium and was thus not a consequence of store emptying *per se*. Rac activation induced by thrombin receptor stimulation was also calcium-dependent, because it could be blocked by chelation of intracellular calcium. Furthermore, thrombin receptor-mediated Rac activation required phospholipase C activity, whereas thapsigargin-induced Rac activity did not. These findings suggest that calcium transients induced by receptor activation of the canonical Gq-PLCinositol 1,4,5-trisphosphate pathway are sufficient and necessary to activate Rac. Increased
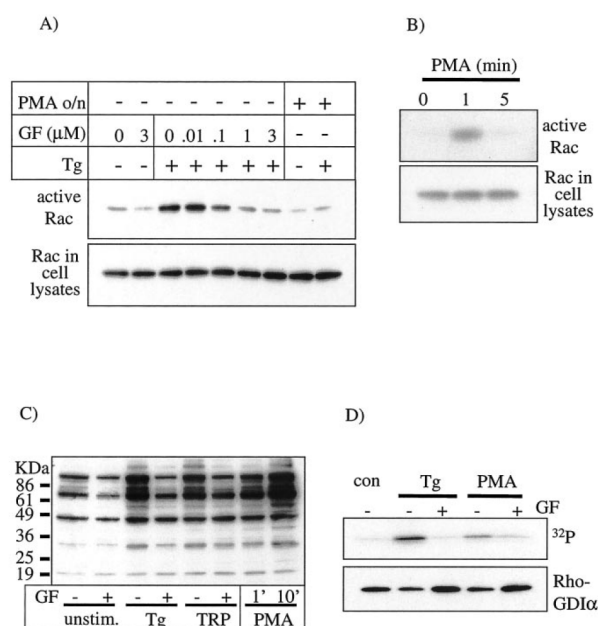
---

[2] L. S. Price and J. G. Collard, unpublished results.

FIG. 5. **PKC-dependent Rac activation and RhoGDI phosphorylation.** *A*, thapsigargin-induced Rac activation is inhibited in a dose-dependent manner by inhibition of PKC with either GF109203X (*GF*) or overnight (16 h overnight (*o/n*)) treatment with PMA (100 nm). The *upper panel* shows active Rac; the *lower panel* shows both active and inactive Rac in original cell lysates. Down-regulation of PKCα was confirmed by Western blotting (not shown). *B*, Rac activation in response to 1- and 5-min treatments with PMA (100 nM). *C*, phosphorylation of cellular proteins by PKC. Cells were stimulated with thapsigargin (5 min; *Tg*) or thrombin peptide (2 min) with or without treatment with GF109203X (*GF*). As a positive control for PKC-induced phosphorylation, cells were also stimulated with PMA for 1 or 10 min. A Western blot of total cell lysates probed with an antibody that recognizes proteins phosphorylated on serine by PKC is shown. Longer exposure of the film revealed multiple additional bands (not shown). *D*, PKC-dependent phosphorylation of RhoGDI. 32-P-labeled PC3 cells were stimulated with thapsigargin (*Tg*) or PMA in the presence or absence of GF109203X (*GF*). Endogenous RhoGDIα was immunoprecipitated, and both 32-Pphosphorylated RhoGDIα and total RhoGDIα were visualized (see "Experimental Procedures"). Note that the PKC inhibitor blocks thapsigargin-induced phosphorylation. *con*, control.

$[Ca^{2+}]_i$ was sufficient to induce Rac activation in several epithelial cell lines, including Madin-Darby canine kidney cells and T47D mammary carcinoma cells, but did not activate Rac in NIH 3T3 fibroblasts or lymphocytes (data not shown). It was reported previously (45, 46) that cell-cell adhesion can regulate Rac activity. However, the differences that we observed between cell types

are unlikely to be because of the formation of adherens junctions in epithelial cells, because PC3 cells do not form cadherin-mediated adhesions. In neutrophils, chemoattractant-induced Rac activation is completely independent of intracellular calcium (20). Cells in which Rac is not activated directly by increased $[Ca^{2+}]_i$ may therefore utilize a calcium-independent mechanism to modulate Rac-RhoGDI interaction or may instead be critically dependent on other receptor-mediated signals, such as those that regulate the activation of specific GEFs.

Intracellular calcium transients also led to increased cell spreading and the formation of lamellipodia, a hallmark of Rac activation. Lamellipodia were inhibited by calcium chelation and also by TAT-CRIB peptide, a membrane-permeable Rac inhibitor, demonstrating that calcium-induced lamellipodia were mediated by Rac. Lamellipodia formation at the leading edge is an important component of the coordinated cytoskeletal reorganization that occurs during cell migration. Oscillations in $[Ca^{2+}]_i$ have been observed during the migration of various cell types and are either essential for or contribute toward migration of cells (47, 48). Rac activation may therefore be coordinated by oscillations in $[Ca^{2+}]_i$ that occur during the migratory process. Previous studies have demonstrated targeting of active Rac to membrane ruffles and the leading edge of migrating cells in response to growth factor and integrin signalling (14, 49). Increases in intracellular calcium can also be highly localized to sites of receptor activation and may therefore be an important factor in the spatial regulation of Rac activation.

In NIH 3T3 cells, PDGF-induced membrane translocation and phosphorylation of the GEF Tiam1 is regulated by calcium-calmodulin kinase II but is independent of PKC (25). However, the Rac activation that we observed in PC3 cells was calmodulin-calmodulin kinase II-independent and strongly dependent on PKC. Furthermore, the capacity of intracellular calcium to regulate Rac activity did not correlate with cellular Tiam1 levels. We conclude therefore that the signaling pathway described in the present study represents an additional mechanism of activation of Rac that is independent of Tiam1 or other calmodulin-regulated Rac exchange factors. Calcium-dependent Rac activation was strongly inhibited by treatments that preferentially inhibit conventional and non-conventional PKCs, whereas stimulation of PKC by transient PMA treatment induced the activation of Rac. Thapsigargin treatment also
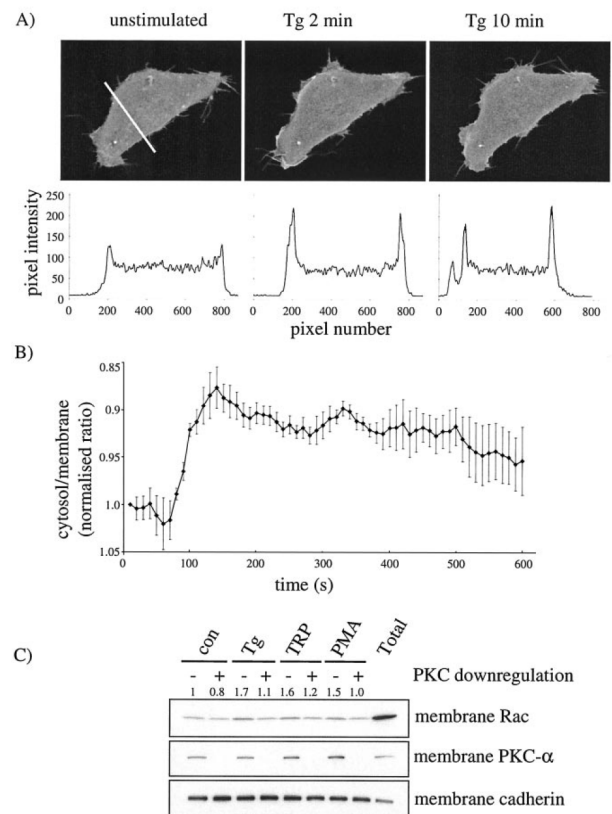

FIG. 6. **Calcium- and PKC-dependent translocation of Rac.** *A*, real-time confocal imaging of GFP-Rac localization (*upper panel*). Cells were stimulated with thapsigargin (*Tg*). Representative images 2 μM above the plane of the coverslip from the same cell were taken at different times after stimulation. The *lower panels* show GFP-Rac fluorescence intensity across the cell at the *line* depicted in the *upper left panel* and demonstrate an increase in cortical fluorescence after stimulation. *B*, time course of the ratio of total cytosol/membrane fluorescence averaged over four representative cells ± S.D. The cytosol/membrane ratio for each cell at *t* = 0 was normalized to 1. *C*, Rac levels in membrane fractions of PC3 cells transiently stimulated with thapsigargin (*Tg*), TRP, or PMA. PKC down-regulation was by overnight PMA treatment. After stimulation, cells were permeabilized to remove cytosolic proteins (see "Experimental Procedures") and then solubilized in radioimmune precipitation assay buffer. These lysates, which contain membraneassociated proteins, were then analyzed for the presence of Rac. -Fold induction of membrane Rac (determined by densitometry) is shown *above* the corresponding *band*. Total Rac content is also shown. Cadherin levels in the membrane fraction, determined using pan-cadherin antibodies, demonstrate equal gel loading. PKCα levels are shown to demonstrate efficient degradation of PKC by overnight PMA treatment. Results are representative of four separate experiments that gave essentially the same results. *con*, control.

resulted in increased PKC kinase activity. From these results we conclude that PKC mediates calcium-induced Rac activation and suggest the involvement of a calcium-dependent conventional PKC isoform. Interestingly, the study by Buchanan *et al.* (25) concluded that PKC was involved in PDGF-induced activation of Rac although this was in a Tiam1-independent manner, which is consistent with our findings. However, increased $[Ca^{2+}]_i$ was not sufficient to induce Rac activation in NIH 3T3 cells. Furthermore, BAPTA-AM did not inhibit PDGF-induced circular ruffle formation, structures that are also associated with Rac activation (data not shown) (50), suggesting that PDGF can induce Rac activation via a pathway that is not dependent on intracellular calcium. Both calcium-dependent and calcium-independent PKCs have been implicated in signaling by Rho family GTPases (25, 43, 51, 52). It is tempting to speculate that calcium-independent PKCs may perform an equivalent function in regulating Rac where intracellular calcium is not critical for activation.

Both increased intracellular calcium and PKC activity induced the translocation of Rac to the plasma membrane. Translocation of Rac has been shown to correlate with activation (53, 54). However, these two events can be uncoupled. Thus, the membrane translocation of a constitutively active Rac mutant (V12Rac) is still regulated by an extracellular stimulus (14), whereas membrane translocation and activation of Tiam1 is not sufficient to activate Rac (25). These findings are consistent with the view that the translocation and activation of Rac are independently regulated events. Our findings show that intracellular calcium- and PKC-dependent targeting of Rac to the plasma membrane may be sufficient to lead to activation of Rac by membrane-associated or membrane translocated exchange factors.

Elevation of $[Ca^{2+}]_i$ resulted in the PKC-dependent phosphorylation of numerous cellular proteins. One of these was RhoGDIα, a protein that binds to the hydrophobic C terminus of Rho family GTPases and maintains them in the cytoplasm (8, 55). These results suggest that calcium- and PKC-dependent phosphorylation of RhoGDI may promote the release of bound Rac and subsequent translocation to the plasma membrane. This hypothesis is supported by previous studies (34, 56), which demonstrated that a conventional PKC, PKCα, induces the phosphorylation of RhoGDI and induces the membrane translocation and activation of RhoA.

RhoGDI preferentially associates with the inactive GDP-bound form of endogenous Rho family GTPases (8, 55, 57). Furthermore, it has been reported that the binding of RhoGDI and Tiam1 to Rac are mutually exclusive (11), a phenomenon that might also hold true for other exchange factors. Together these results suggest that release of Rac from RhoGDI is a prerequisite for the activation of Rac by exchange factors. It was shown recently (14) that integrin signals act on the Rac-RhoGDI interaction inducing release of Rac to sites of cell adhesion. Reduced affinity of RhoGDI for Rac may therefore be a common feature of receptor-mediated Rac activation.

In conclusion, intracellular calcium transients modulate Rac activity through different mechanisms. In addition to regulating guanine nucleotide exchange factors, we show here that calcium also regulates the membrane translocation of Rac. This is mediated by PKC, which we propose acts on the Rac-RhoGDI complex, resulting in translocation of Rac to the plasma membrane, where it is activated by exchange factors, which could be membrane-associated or recruited to the plasma membrane by receptor signaling.

REFERENCES

1. Hall, A., and Nobes, C. D. (2000) *Philos. Trans. R. Soc. Lond. B Biol. Sci.* **355,** 965–970
2. Ridley, A. J., Paterson, H. F., Johnston, C. L., Diekmann, D., and Hall, A. (1992) *Cell* **70,** 401–410
3. Price, L. S., Leng, J., Schwartz, M. A., and Bokoch, G. M. (1998) *Mol. Biol. Cell* **9,** 1863–1871
4. Minden, A., Lin, A., Claret, F. X., Abo, A., and Karin, M. (1995) *Cell* **81,** 1147–1157
5. Zohn, I. M., Campbell, S. L., Khosravi-Far, R., Rossman, K. L., and Der, C. J. (1998) *Oncogene* **17,** 1415–1438
6. Ridley, A. J. (2001) *Dev. Cell* **1,** 160–161
7. Malliri, A., van der Kammen, R. A., Clark, K., van der Valk, M., Michiels, F., and Collard, J. G. (2002) *Nature* **417,** 867–871
8. Olofsson, B. (1999) *Cell. Signal.* **11,** 545–554

9. Scheffzek, K., Stephan, I., Jensen, O. N., Illenberger, D., and Gierschik, P. (2000) *Nat. Struct. Biol.* **7,** 122–126

10. Stam, J. C., Sander, E. E., Michiels, F., van Leeuwen, F. N., Kain, H. E., van der Kammen, R. A., and Collard, J. G. (1997) *J. Biol. Chem.* **272,** 28447–28454

11. Robbe, K., Otto-Bruc, A., Chardin, P., and Antonny, B. (2003) *J. Biol. Chem.* **278,** 4756–4762

12. Schmidt, A., and Hall, A. (2002) *Genes Dev.* **16,** 1587–1609

13. Del Pozo, M. A., Price, L. S., Alderson, N. B., Ren, X. D., and Schwartz, M. A. (2000) *EMBO J.* **19,** 2008–2014

14. Del Pozo, M. A., Kiosses, W. B., Alderson, N. B., Meller, N., Hahn, K. M., and Schwartz, M. A. (2002) *Nat. Cell Biol.* **4,** 232–239

15. Price, L. S., Norman, J. C., Ridley, A. J., and Koffer, A. (1995) *Curr. Biol.* **5,** 68–73

16. van Leeuwen, F. N., van Delft, S., Kain, H. E., van der Kammen, R. A., and Collard, J. G. (1999) *Nat. Cell Biol.* **1,** 242–248

17. Hirata, K., Kikuchi, A., Sasaki, T., Kuroda, S., Kaibuchi, K., Matsuura, Y., Seki, H., Saida, K., and Takai, Y. (1992) *J. Biol. Chem.* **267,** 8719–8722

18. O'Sullivan, A. J., Brown, A. M., Freeman, H. N., and Gomperts, B. D. (1996) *Mol. Biol. Cell* **7,** 397–408

19. Soulet, C., Gendreau, S., Missy, K., Benard, V., Plantavid, M., and Payrastre, B. (2001) *FEBS Lett.* **507,** 253–258

20. Geijsen, N., van Delft, S., Raaijmakers, J. A., Lammers, J. W., Collard, J. G., Koenderman, L., and Coffer, P. J. (1999) *Blood* **94,** 1121–1130

21. Fan, W. T., Koch, C. A., de Hoog, C. L., Fam, N. P., and Moran, M. F. (1998) *Curr. Biol.* **8,** 935–938

22. Kiyono, M., Satoh, T., and Kaziro, Y. (1999) *Proc. Natl. Acad. Sci. U. S. A.* **96,** 4826–4831

23. Farnsworth, C. L., Freshney, N. W., Rosen, L. B., Ghosh, A., Greenberg, M. E., and Feig, L. A. (1995) *Nature* **376,** 524–527

24. Fleming, I. N., Elliott, C. M., Buchanan, F. G., Downes, C. P., and Exton, J. H. (1999) *J. Biol. Chem.* **274,** 12753–12758

25. Buchanan, F. G., Elliot, C. M., Gibbs, M., and Exton, J. H. (2000) *J. Biol. Chem.* **275,** 9742–9748

26. Jalink, K., and Moolenaar, W. H. (1992) *J. Cell Biol.* **118,** 411–419

27. Morton, R. A., Ewing, C. M., Nagafuchi, A., Tsukita, S., and Isaacs, W. B. (1993) *Cancer Res.* **53,** 3585–3590

28. Sander, E. E., ten Klooster, J. P., van Delft, S., van der Kammen, R. A., and Collard, J. G. (1999) *J. Cell Biol.* **147,** 1009–1022

29. Kinsella, T. M., and Nolan, G. P. (1996) *Hum. Gene Ther.* **7,** 1405–1413

30. Michiels, F., van der Kammen, R. A., Janssen, L., Nolan, G., and Collard, J. G. (2000) *Methods Enzymol.* **325,** 295–302

31. Williams, D. A. (1990) *Cell Calcium* **11,** 589–597

32. van der Wal, J., Habets, R., Varnai, P., Balla, T., and Jalink, K. (2001) *J. Biol. Chem.* **276,** 15337–15344

33. Habets, G. G., Scholtes, E. H., Zuydgeest, D., van der Kammen, R. A., Stam, J. C., Berns, A., and Collard, J. G. (1994) *Cell* **77,** 537–549

34. Mehta, D., Rahman, A., and Malik, A. B. (2001) *J. Biol. Chem.* **276,** 22614–22620

35. Sander, E. E., van Delft, S., ten Klooster, J. P., Reid, T., van der Kammen, R. A., Michiels, F., and Collard, J. G. (1998) *J. Cell Biol.* **143,** 1385–1398

36. Zondag, G. C., Evers, E. E., ten Klooster, J. P., Janssen, L., van der Kammen, R. A., and Collard, J. G. (2000) *J. Cell Biol.* **149,** 775–782

37. Varnai, P., and Balla, T. (1998) *J. Cell Biol.* **143,** 501–510

38. Bleasdale, J. E., Thakur, N. R., Gremban, R. S., Bundy, G. L., Fitzpatrick, F. A., Smith, R. J., and Bunting, S. (1990) *J. Pharmacol. Exp. Ther.* **255,** 756–768

39. Glading, A., Chang, P., Lauffenburger, D. A., and Wells, A. (2000) *J. Biol. Chem.* **275,** 2390–2398

40. Sells, M. A., Knaus, U. G., Bagrodia, S., Ambrose, D. M., Bokoch, G. M., and Chernoff, J. (1997) *Curr. Biol.* **7,** 202–210

41. Ho, A., Schwarze, S. R., Mermelstein, S. J., Waksman, G., and Dowdy, S. F. (2001) *Cancer Res.* **61,** 474–477

42. Newton, A. C. (1995) *J. Biol. Chem.* **270,** 28495–28498

43. Uberall, F., Hellbert, K., Kampfer, S., Maly, K., Villunger, A., Spitaler, M., Mwanjewe, J., Baier-Bitterlich, G., Baier, G., and Grunicke, H. H. (1999) *J. Cell Biol.* **144,** 413–425

44. van Rheenen, J., and Jalink, K. (2002) *Mol. Biol. Cell* **13,** 3257–3267

45. Noren, N. K., Niessen, C. M., Gumbiner, B. M., and Burridge, K. (2001) *J. Biol. Chem.* **276,** 33305–33308

46. Betson, M., Lozano, E., Zhang, J., and Braga, V. M. (2002) *J. Biol. Chem.* **277,** 36962–36969

47. Pierini, L. M., Lawson, M. A., Eddy, R. J., Hendey, B., and Maxfield, F. R. (2000) *Blood* **95,** 2471–2480

48. Scherberich, A., Campos-Toimil, M., Ronde, P., Takeda, K., and Beretz, A. (2000) *J. Cell Sci.* **113,** 653–662

49. Kraynov, V. S., Chamberlain, C., Bokoch, G. M., Schwartz, M. A., Slabaugh, S., and Hahn, K. M. (2000) *Science* **290,** 333–337

50. Scaife, R. M., Courtneidge, S. A., and Langdon, W. Y. (2003) *J. Cell Sci.* **116,** 463–473

51. Coghlan, M. P., Chou, M. M., and Carpenter, C. L. (2000) *Mol. Cell. Biol.* **20,** 2880–2889

52. Etienne-Manneville, S., and Hall, A. (2001) *Cell* **106,** 489–498
53. Philips, M. R., Pillinger, M. H., Staud, R., Volker, C., Rosenfeld, M. G., Weissmann, G., and Stock, J. B. (1993) *Science* **259,** 977–980
54. Fleming, I. N., Elliott, C. M., and Exton, J. H. (1996) *J. Biol. Chem.* **271,** 33067–33073
55. Hoffman, G. R., Nassar, N., and Cerione, R. A. (2000) *Cell* **100,** 345–356
56. Meacci, E., Donati, C., Cencetti, F., Romiti, E., and Bruni, P. (2000) *FEBS Lett.* **482,** 97–101
57. Worthylake, D. K., Rossman, K. L., and Sondek, J. (2000) *Nature* **408,** 682–688

Summary

Summary

Ions play an important role in many cellular process. They may act as regulators of enzymes or as second messenger: changes in intracellular ion concentration are induced by stimuli (like hormones) from the outside of the cell. Therefore cells maintain a tightly regulated gradient of ions over the plasma-membrane. Sodium and potassium are the main ions that control the membrane potential of cells whereas calcium (Ca^{2+}) and magnesium (Mg^{2+}) regulate many enzymes and cellular processess. The plasma-membrane consists of various lipids through which ions can not pass. As a result, cells have adopted specialized transporters and channels to control the distribution ions over the plasma-membrane.

TRPM7 channels are widely expressed and play a crucial role in the Mg^{2+} homeostasis of cells. This channel permeates divalent ions, such as Ca^{2+} and Mg^{2+}. Above all, TRPM7 channels have an unique feature at their C-terminus: an α-kinase domain.

It is well established that TRPM7 channels may be activated by depletion of internal Mg^{2+} or magnesium-nucleotides in "whole-cell" patch clamp experiments (a method for measuring ionic currents whereby the contents of the cell is dialyzed). Activation of TRPM7 currents by agonist-induced second messengers was still unknown. In **Chapter II** we describe a receptor-mediated signaling pathway that mediates TRPM7 channel activation in unperturbed cells. In wild-type N1E-115 cells, stimulation of G-Protein Coupled Receptors that couple to PLC cause a single transient intracellular Ca^{2+} elevation through Ca2+ release from the endoplasmatic reticulum, meaured by fluorescent Ca^{2+} dyes. In TRPM7 transduced N1E-115 cells, this single transient Ca^{2+} elevation is followed by a second, sustained Ca^{2+} increase as a result of Ca^{2+} influx through TRPM7 channels. The activation of TRPM7 by PLC activation was validated by perforated-patch experiments (a patch-clamp assay that leaves the contents of the cells unperturbed). Furthermore, in this chapter we show that opening of TRPM7 channels is restricted to PLC-coupled stimuli: using various fluorescent indicators ("FRET assays") we confirmed that TRPM7 opening correlates well with PLC activity, but not other GPCR-derived second messengers such as cyclic AMP and cyclic GMP.

The above described PLC regulation of TRPM7 currents contradicts with results of other groups: they show that activation of PLC leads to closure of TRPM7 cells in "whole-cell" patch-clamp configuration. In **Chapter III** we continued to examine this discrepancy. Here we show that this difference can be ascribed to the difference in the patch-clamp assays. We use minimal invasive techniques like Ca^{2+} experiments and the perforated-patch clamp technique, which both do not interfere with the functioning of the cell. We show that the inhibitory effect of PLC is only observed in "whole-cell" experiments where intracellular Mg^{2+} is artificially clamped at low concentrations. To convincingly proove this, we have developed a method to lower intracellular Mg^{2+} levels in perforated-patch: pretreatment of cells with a membrane-permeable Mg^{2+} buffer. De currents induced in this way are both biohysically and pharmacoligically identical to the TRPM7 currents measured activated by Mg^{2+} depletion measured in whole-cell configuration. Moreover, the data described in this chapter show that a gradual loss of PIP2 at the plasma-membrane probably underlies the artificial whole-cell results.

Mild overexpression of the TRPM7 channel in neuroblastoma cells induces cell spreading, cell adhesion and formation of focal adhesions. In **Chapter IV** we show that all these features are enhanced after PLC-mediated TRPM7 activation. The underlying mechanism is a Ca^{2+}- and kinase-dependent association with the actomyosin cytoskeleton. This association of the kinase domain and the cytoskeleton results in phospho-rylation of myosin IIA and releases the tension of the actomyosin cytoskeleton. Furthermore, podosomes are formed *de novo* or out of existing focal adhesions. Thus, TRPM7 regulates cell adhesion by changing actomyosin contractility.

In **Chapter V** we describe a second Ca^{2+} dependent signaling pathway that regulates the cytoskeleton. In prostate carcinoma cells elevation of intracellular Ca^{2+}, either by receptor stimulation or pharmacologically, activates the small G-protein Rac. This activated protein causes lamellipodia formation: dynamic, flat structures of the plasma-membrane that contain large amounts of actin. The experiments described in this chapter show that the Ca^{2+} increase activates a kinase (a so-called conventional protein kinase C) that phosphorylates an activator of Rac (RhoGDIα) and causes translocation of Rac to the plasma-membrane.

We conclude that TRPM7, which combines a ion channel with a kinase, affects the cytoskeleton in several ways.

Samenvatting

Samenvatting

Ionen spelen een belangrijke rol in tal van cellulaire processen. Ze fungeren o.a. als regulatoren van enzymen of als zogenaamde 'tweede boodschapper': veranderingen in ion concentraties binnen de cel (intracellulair) worden geïnduceerd door stimulansen (zoals een hormoon) aan de buitenkant van de cel. Daarom houden cellen een strikt gereguleerde gradiënt van ionen over de plasma-membraan in stand. Natrium en kalium ionen zijn de belangrijkste ionen in het bepalen van de membraan potentiaal van cellen, terwijl calcium (Ca^{2+}) en magnesium (Mg^{2+}) ionen vele enzymen en cellulaire processen reguleren. De plasma-membraan is opgebouwd uit vetten en ionen kunnen deze barrière niet passeren. Zodoende hebben cellen gespecialiseerde ion transporters en kanalen geëvolueerd om de verdeling van ionen over de plasma-membraan te kunnen reguleren.

TRPM7 ion kanalen worden in elke type cel tot expressie gebracht en hebben een cruciale rol in de interne Mg^{2+} balans van cellen. Dit kanaal laat divalente ionen door, zoals Ca^{2+} en Mg^{2+}. Bovendien heeft het TRPM7 kanaal een unieke eigenschap: het bezit een intrinsiek α-kinase domein aan de C-terminus.

Het is bekend dat TRPM7 kanalen geactiveerd kunnen worden door depletie van intern Mg^{2+} en/of magnesium-nucleotiden in "whole-cell" patch-clamp experimenten (een methode waarbij de inhoud van een cel wordt gedialyseerd). Activatie van TRPM7 stromen door agonist-geïnduceerde 'tweede boodschapper' cascades was nog niet bekend. In **Hoofdstuk II** beschrijven we dat receptor gemedieerde signaal transductie in staat is om TRPM7 kanalen te activeren in intacte cellen. In wildtype N1E-115 neuroblastoma cellen veroorzaakt stimulatie van G-eiwit gekoppelde receptoren die fosfolipase C activeren een enkelvoudige Ca^{2+} verhoging vanuit het endoplasmatisch reticulum, zoals gemeten met fluorescente Ca^{2+} indicatoren. In cellen geïnfecteerd door een virus met TRPM7 wordt deze Ca^{2+} transient gevolgd door een tweede, trage fase van Ca^{2+} verhoging die het resultaat is van Ca^{2+} influx door TRPM7 kanalen. Activatie van TRPM7 door PLC-activerende stimuli is ook te meten in "perforated-patch" experimenten (een meetmethode waarbij de inhoud van de cel intact blijft). In dit hoofdstuk laten we verder zien dat opening van TRPM7 specifiek is voor PLC-gekoppelde stimuli: door gebruik te maken van een aantal verschillende fluorescente indicatoren ("FRET assays") bepalen we dat er een zeer goede correlatie is tussen TRPM7 opening en PLC activatie, maar niet met andere boodschappers zoals cyclisch AMP en cyclisch GMP.

Het hierboven beschreven resultaat is in tegenstelling met resultaten van andere groepen die beschreven dat activatie van PLC juist leidt tot sluiting van TRPM7 in de zogeheten 'whole-cell' patch clamp configuratie. In **Hoofdstuk III** gaan we verder in op deze paradox. We tonen aan dat het verschil is terug te leiden tot een verschil in de meetmethode. Wij gebruiken minimaal invasieve methoden zoals Ca^{2+} metingen en perforated patch clamping, die het normale functioneren van de cel intact laten. We laten zien dat het remmend effect van PLC alleen gevonden wordt in whole-cell metingen waarbij de intracellulaire Mg^{2+} concentratie artificieel laag wordt gehouden. Om dit overtuigend aan te tonen hebben we een methode ontwikkeld om ook in perforated patches de intracellulaire Mg^{2+} concentratie te kunnen verlagen: voorbehandeling met een membraan permeabele Mg^{2+} buffer. De aldus geïnduceerde stromen zijn biofysisch en farmacologisch identiek aan de TRPM7 stromen in whole-cell geactiveerd door Mg^{2+} depletie. De data uit dat hoofdstuk laten verder zien dat het langzaam verloren gaan van het membraan lipide PIP2 waarschijnlijk ten grondslag ligt aan het artificiële whole-cell resultaat.

De milde overexpressie van TRPM7 in neuroblastoma cellen induceert spreiding van cellen, versterkte adhesie van cellen en de formatie van focale adhesie structuren. In **Hoofdstuk IV** laten we zien dat al deze kenmerken worden versterkt na PLC gemedieerde TRPM7 activatie. Het onderliggende mechanisme is een Ca^{2+}- en kinase-afhankelijke associatie met het actomyosine cytoskelet. Deze associatie van het kinase domein en het cytoskelet resulteert in fosforylering van Myosine IIA en verlaagd daardoor de spanning van het actomyosine cytoskelet. Bovendien worden er podosomen gevormd, zowel *de novo* als uit bestaande 'focal adhesion' structuren. TRPM7 reguleert dus cel adhesie door de contractiliteit van het actomyosine cytoskelet te veranderen.

In **Hoofdstuk V,** ten slotte, beschrijven we een tweede, Ca^{2+}-afhankelijk, signaal dat het actine cytoskelet beïnvloedt. In prostaat carcinoma cellen leidt verhoging van de intracellulaire Ca^{2+} concentratie, hetzij door receptor stimulatie hetzij met farmacologische methoden, tot activatie van het kleine G-eiwit Rac. Dit eiwit veroorzaakt uitgroei van zogeheden lamellipodia: dynamische,

platte structuren in de membraan die veel actine bevatten. De experimenten beschreven in dit hoofdstuk laten zien dat Ca^{2+} verhoging een kinase (een zogeheten conventionele PKC) geactiveerdt dat een activator van RAC (RhoGDIα) fosforyleert waardoor Rac naar de plasma membraan transloceert.

We concluderen dat TRPM7, dat een ion kanaal en kinase combineert, het cytoskelet op meerdere manieren beinvloed.

Curriculum Vitae

Curriculum Vitae

Michiel Langeslag werd geboren op 6 maart 1976 te Vlissingen. Na het behalen van zijn Atheneum diploma aan het Bisschoppelijk College Broekhin te Roermond in 1994, begon hij in datzelfde jaar met de studie biologie aan de Katholieke Universiteit van Nijmegen. Tijdens deze studie heeft hij 2 stages doorlopen. In zijn eerste stage van ruim een jaar heeft hij onderzoek gedaan naar verschillen in kinetieken van voltage afhankelijke calcium stromen in actieve en inactieve melanotrope cellen van *Xenopus leavis*. Deze stage vond plaats op het lab Cellulaire Dierfysiologie (K.U.N.) onder begeleiding van Dr. Wim J.J.M Scheenen. Zijn tweede stage heeft hij volbracht bij de medische faculteit van de K.U.N. op de afdeling Biochemie. Hier heeft hij onder begeleiding van Drs. Remco R. Bosch onderzoek gedaan naar de rol van fosfolipase D en regulatie door second messengers in tumor progressie in humane melanoma cellijnen. In 2000 behaalde hij zijn doctoraal examen biologie en begon direct daarna met zijn promotie onderzoek bij de vakgroep celbiologie op het Nederlands Kanker Instituut onder begeleiding van Dr. Kees Jalink. Hier verrichtte hij onderzoek naar de regulatie van het ion kanaal TRPM7 door G-eiwit gekoppelde receptoren en in samenwerking met Kris Clark en Dr. Frank N. van Leeuwen (Tumor Immunologie, NCMLS, Radboud Universiteit Nijmegen) werd de functie van het kinase domein van TRPM7 met betrekking tot het actomyosine cytoskelet opgehelderd. In 2006 werd hij bij dezelfde groep aangesteld als post-doc om het onderzoek met betrekking tot signaal transductie naar TRPM7 en de rol van het kinase domein in podosoom formatie en celadhesie voort te zetten.

List of Publications

List of Publications

Langeslag M., Clark K., Moolenaar W.H., van Leeuwen F.N., Jalink K.
  Gq/Phospholipase C-coupled agonists activate TRPM7 channels under physiological conditions
  Manuscript submitted

Clark K., ***Langeslag M.***, van Leeuwen B., Ran L., Ryazanov A.G., Figdor C.G., Moolenaar W.H.,
  Jalink K., van Leeuwen F.N.
  TRPM7, a novel regulator of actomyosin contractility and cell adhesion.
  EMBO J. 2006 Jan 25; 25(2), pp 290-301.

Zhang H.Y., ***Langeslag M.***, Voncken M., Roubos E.W., Scheenen W.J.
  Melanotrope cells of Xenopus laevis express multiple types of high-voltage-activated Ca2+ channels.
  J Neuroendocrinol. 2005 Jan; 17(1), pp 1-9.

van Rheenen J., ***Langeslag M.***, Jalink K.
  Correcting confocal acquisition to optimize imaging of fluorescence resonance energy transfer by
  sensitized emission.
  Biophys J. 2004 Apr; 86(4), pp. 2517-29.
PMID: 15041688 [PubMed - indexed for MEDLINE]

Price L.S., ***Langeslag M***., ten Klooster J.P., Hordijk P.L., Jalink K., Collard J.G.
  Calcium signaling regulates translocation and activation of Rac.
  J Biol Chem. 2003 Oct 10; 278(41), pp 39413-21.